Studies into the Biosynthesis and Chemical Synthesis of Indolocarbazoles and Related Heterocyclic Compounds. Metalation of Indole-6-Carboxamide.

by

Katherine A. Groom

A thesis submitted to the Department of Chemistry

In conformity with the requirements for

the degree of Doctor of Philosophy

Queen's University

Kingston, Ontario, Canada

February, 2013

Abstract

The electron rich and aromatic character of the indole group allows for a wide range of oxidative and substitution reactions, creating a versatile platform for generating structurally diverse molecules. This thesis explores enzyme and synthetic chemistries that act upon indoles and related molecules. Chapter 1 describes the results of *in vivo* studies of RebC, an enzyme that plays a pivotal role in the biosynthesis of the indolocarbazole alkaloid rebeccamycin. A homologous enzyme, StaC, exists in the biosynthetic pathway for staurosporine, a related indolocarbazole. Structural differences between the RebC and StaC active sites were hypothesized to play a pivotal role in determining the oxidation state in the corresponding natural products. Sequence alignment of RebC and StaC with homologous enzymes from related indolocarbazole biosynthetic pathways revealed six non-conserved residues in the active site. Three RebC variants were generated by replacement of all six, four, or two specific residues with their StaC counterparts. It was demonstrated that only two substitutions, F216V and R239N, are required to convert the specificity of RebC to that of StaC. Analysis of the structure of the RebC bound to a putative reaction intermediate supports the importance of F216 and R239 in catalysis. Based on these results, contrasting mechanisms for RebC and StaC are proposed to account for their differing specificities.

Chapter 2 describes a synthetic approach to primarily heterocyclic analogues of lycogarubin C. Suzuki coupling of appropriately functionalized 3,4-dibromopyrrole or 3,4-bis(trifluoromethanesulfonyl)pyrrole was effective for numerous π-excessive five-membered heterocyclic-3-boronic acids. The optimized conditions were less effective for cross-couplings involving heteroaromatic-2-boronic acids, π-deficient heteroaromatic boronic acids, and heteroaromatic boropinacolate esters. Oxidative cyclization of the 3,4-bis(thiophen-3-yl)pyrrole and 3,4-bis(benzothiophen-3-yl)pyrrole to give analogues of the corresponding indolocarbazoles was demonstrated.

Chapter 3 describes preliminary results on the development of regioselective C-5 and C-7 indole metalation tactics of indole-6-carboxamides, in order to provide new functionalized indoles. The use of an indole C-2 silicon protection strategy in combination with a sterically bulky C-6 *N,N*-di-isopropyl carboxamide directed metalation group overcame undesired side reactions observed with the analogous *N,N*-diethyl indole-6-carboxamide, affording the C-5 and C-7 substituted products in 40% and 13% yields, respectively.

Acknowledgements

I would first like to thank my supervisors Professor Victor Snieckus and Professor David Zechel for providing me with the opportunity to be a part of a rewarding scientific collaboration. Professor Zechel, thank you for spending time with me at the lab-bench in early days, providing a hands-on introduction to molecular biology theory and technique. Your enthusiastic practical and theoretical teachings contributed to my success in a previously unfamiliar area of science, and deepened my intrigue of enzyme chemistry and natural product biosynthesis. I have truly enjoyed being a member of your research group. Professor Snieckus, thank you for the opportunity to work in such a dynamic and supportive research group in which you are so personally engaged. Your individual involvement with my research progress, whether it be from distant places through skype or email, or through discussions at Chernoff or Earl Street gatherings was always valued, as were your teachings at group meetings. I would also like to thank my committee members, Prof. Pratt, Prof. Petitjean, and Prof. Horton, as well as Krista Voigt for her assistance.

I am extremely grateful to Dr. Toni Rantanen for initiating the indole metalation project, and giving me the opportunity to be involved. You have been an inspiring role model and mentor. Many thanks also to Dr. Matthew Kitching and Dr. Timothy Hurst for assistance in working through problems, leading "reaction of the day" exercises, and for your overall guidance.

I am grateful for the many lasting friendships I have made during my time at Queens. Justin, I will never forget the great times we had working together in the VS group, and value our continued friendship. I forgive you for disliking my hedgehogs! Eric, thank you for being such an excellent teacher and friend over the years, I look forward to visiting you in Qc city. Manlio, your passion and dedication to your chemistry, colleagues, and family is admirable, and I thank you and Leanne for your continuing support and friendship. John, whenever I am unsure of a chemical rationale, I can always consider that it may be due to "a delicate balance of steric and electronic effects." To the Germans (Baërbel, Heiko, Claudia, Isabel, Maike, Hendrick, Ricarda, Ellen), Brazilians (Alcides and Vilma), Froggies (Emilie and Cédric) and friends in Scandinavia (Erhad, Josefine, Marianne, Kristopher, Marcus) I enjoyed working with all of you, and will visit you one day. To the entire Snieckus, Snieckus Innovations, and Zechel groups, past and present, I have truly enjoyed working alongside you at the forefront of unchartered scientific frontiers.

Finally I thank my parents Douglas and Maureen Groom, for their personal and financial support, and to my sister Erin and her family for always being there for me. Special thanks to Toni Rantanen for much happiness and support over the years, as well as to Maj-Lis and Pekka Rantanen. I could not have achieved this accomplishment without any of you!

Statement of Originality

I (Katherine Groom) hereby certify that all of the work described within this thesis is the original work of the author under the supervision of Prof. V. Snieckus and Prof. D. Zechel. Any published (or unpublished) ideas and/or techniques from the work of others are fully acknowledged in accordance with the standard referencing practices.

Katherine A. Groom

(February, 2013)

The following is a list of new compounds prepared using new methodology during the course of this work: **2.230**, **2.236**, **2.238**, **2.241**, **2.244**, **2.246**, **2.248**, **2.250**, **2.252**, **2.254**, **2.261**, **2.262**, **2.266**, **2.267**, **3.131**, **3.134**, **3.137**, **3.138**, **3.139**, **3.140**, **3.141**, **3.143**, **3.144**, **3.145**, **3.146**, **3.147**, **3.148**, **3.149**, **3.150**, **3.151, 3.152**.

The following is a list of known compounds prepared using new methodology or existing methods during the course of this work: **2.31**, **2.32**, **2.218**, **2.219**, **2.220**, **2.221**, **2.222**, **2.223**, **2.226**, **2.227**, **2.249**, **2.257**, **2.258**, **2.259**, **2.260**.

To Evelyn Cryan

Table of Contents

Chapter 3. Benzenoid Ring Functionalization of Indoles via Directed *ortho* Metalation (D*o*M) Methodology

List of Figures

List of Tables

Specific Experimental Procedures

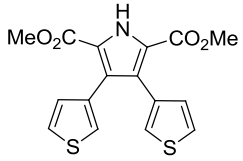

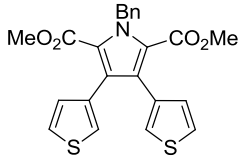

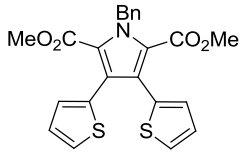

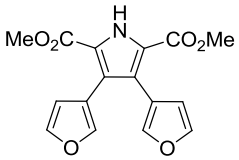

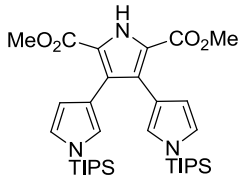

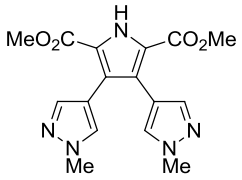

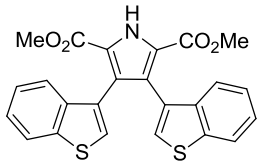

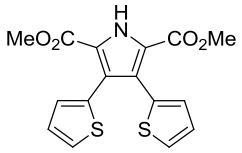

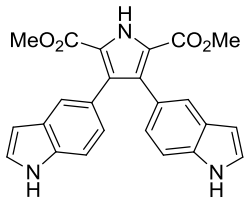

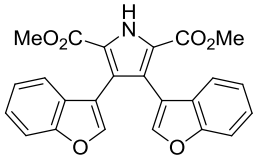

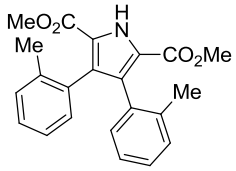

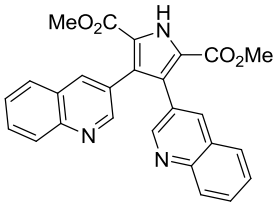

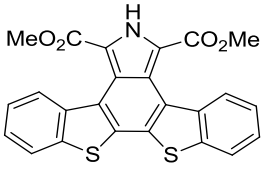

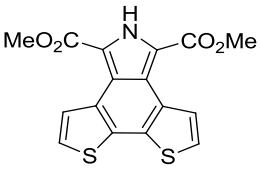

***N*,*N*-di-isopropyl-7-chloro-1-(diethylcarbamoyl)-2-trimethylsilylindole-6-carboxamide (3.151)** **230**

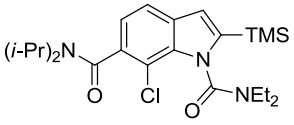

List of Abbreviations

AAO	amino acid oxidase
Ac_2O	acetic anhydride
Arg (R)	arginine
ATP	adenosine triphosphate
B3LYP	Becke, Lee-Yang-Parr
BFCET	bond formation coupled electron-transfer
BLAST	basic local alignment search tool
Boc	*t*-butoxycarbonyl
BBr_3	boron tribromide
CCA	1,11-dichlorochromopyrrolic acid
C*c*P	cytochrome *c* peroxidase
CDK	cyclin-dependent kinase
Chk1	checkpoint kinase I
CIPE	complex induced proximity effect
CMD	concerted metalation-deprotonation
CO_2	carbon dioxide
CPA	chromopyrrolic acid
CSA	camphorsulfonic acid
Cs_2CO_3	cesium carbonate
DDQ	2,3-dichloro-5,6-dicyano-*p*-benzoquinone
DFT	density functional theory
DEB	2,2-diethylbutanoyl
DMB	3,4-dimethoxybenzyl
DMG	directed metalation group

DNA	deoxyribonucleic acid
D*o*M	directed *ortho* metalation
DreM	directed remote metalation
EAS	electrophilic aromatic substitution
E. coli	*Escherichia coli*
EI-MS	electrospray-ionization mass spectrometry
ent	enantiomer
EXSY	exchange spectroscopy
FAD	flavin adenine dinucleotide
FT-IR	fourier transform- infrared spectroscopy
Glu (G)	glutamic acid
HOCl	hypochlorous acid
HOESY	heteronuclear Overhauser enhancement spectroscopy
HPLC	high pressure liquid chromatography
HRMS	high resolution mass spectrometry
HRP	horseradish peroxidase
TMP	2,2,6,6-tetramethylpiperidine
IC	inhibitory concentration
IEDDA	inverse electron-demand Diels Alder
IPA	indole-3-pyruvic acid
K_2CO_3	potassium carbonate
KEM	kinetically enhanced metalation
KIE	kinetic isotope effect
L-AAO	L-amino acid oxidase
LB	lysogeny broth

LDA	lithium diisopropylamide
LTMP	lithium tetramethylpiperidine
L-Trp	L-tryptophan
MALDI-TOF	matrix assisted laser desorption ionization-time of flight
MDR	multi-drug resistance
MIDA	*N*-methyliminodiacetic acid
MeOH	methanol
MLK	mixed-lineage kinase
MM	molecular mechanics
MOM	methoxymethyl
$NaBH_4$	sodium borohydride
NAD	nicotinamide adenine dinucleotide
n-BuLi	*n*-butyllithium
ngt	N-glycosyltransferase
NHC	*N*-heterocyclic carbene
NMR	nuclear magnetic resonance
NOESY	nuclear Overhauser enhancement spectroscopy
ORF	open reading frame
PCET	proton coupled electron-transfer
PCR	polymerase chain reaction
Phe (F)	phenylalanine
PIFA	phenyliodine(III) bis(trifluoroacetate)
PKC	protein kinase C
PPSE	polyphosphoric acid trimethylsilyl ester
QM	quantum mechanics

QSAR	quantitative structure-activity relationship
SAR	structure-activity relationship
S_EAr	electrophilic aromatic substitution
SEM	2-(trimethylsilyl)ethoxymethyl
Ser (S)	serine
SOB	super optimal broth
S-Phos	2-dicyclohexylphosphino-2',6'-dimethoxybiphenyl
TBAHS	tetrabutylammonium sulfate
TBS	*tert*-butyldimethylsilyl
t-BuLi	*tert*-butyllithium
t-BuOH	*tert*-butanol
TEBAC	triethylbenzylammonium chloride
TFA	trifluoroacetic acid
THF	tetrahydrofuran
TIPS	triisopropylsilyl
TMEDA	*N*,*N*,*N*,*N'*-tetramethylethylenediamine
TMHD	2,2,6,6-tetramethyl-3,5-heptanedionate
TMS	tetramethylsilane
Topo I	topoisomerase I
Trp	tryptophan
Ts	*p*-toluenesulfonyl
Thr (X)	threonine
UV-VIS	ultraviolet-visible spectroscopy
Val (V)	valine
WT	wild type

Chapter 1

Investigation of the Chemoselectivity of RebC-Assisted Biosynthesis of Rebeccamycin

1.1 Biological significance of indolocarbazoles

1.1.1 Indolocarbazole natural products

The indolocarbazole alkaloids represent a large and diverse family of natural products that demonstrate important biological activities.[1,2] Representative examples of indolocarbazole alkaloids are presented in Figure 1.1. Rebeccamycin (**1.1**) is produced by the actinomycete *Lechevalieria aerocolonigenes* (ATCC39243, formerly *Saccarothrix aerocolonigenes*), and the genes encoding its biosynthesis were elucidated in 2002.[3] **1.1** has demonstrated significant activity against P388 and L1210 leukemia cell lines, B-16 melanoma cells implanted in mice, as well as growth inhibition of human lung adenocarcinoma cells (GI_{50} = 6 μg/mL *in vivo*),[4] and has also been identified as a potent inhibitor of human DNA topoisomerase I (IC_{50}=1.75 μM).[5] Significant structural features of **1.1** include the regiospecific bis-chlorination pattern of the A and E rings, the single glycosidic linkage connecting the sugar moiety to the D ring of the indolocarbazole, and an oxidation state corresponding to a maleimide ring in the heterocyclic core. AT2433-A1 (**1.2**), produced by the microorganism *Actinomadura melliaura*[6] is an asymmetrically halogenated and *N*-methylated indolocarbazole attached to an unusual disaccharide moiety. The latter contains an aminodideoxypentose sugar moiety that has important implications for the biological activity of **1.2**, as DNA topoisomerase I inhibitory activity is abolished at the expense of enhanced DNA binding ability.[7] Despite having similar biosynthetic pathways, members of the indolocarbazole family of natural products have notable differences in chemical structure and biological activity, a fact which has resulted in the sub-classification of indolocarbazoles into two distinct categories. Owing to their structural resemblance, **1.1** and **1.2** are classified together, whereas staurosporine (**1.3**)[8] and K-252a (**1.4**)[9] having a bis-linked sugar moiety and an oxidation state corresponding to a lactam ring in the heterocyclic core belong to

the second sub-category. **1.3** and **1.4** have been identified as protein kinase inhibitors (with **1.3** having impressive IC_{50} values in the nanomolar range),[10] implying that the biological activities of this sub-category of indolocarbazoles is manifested through a distinct pathway to that of rebeccamycin and related compounds. Consequently, the mechanism of bioactivity of indolocarbazoles is closely related to structural features of the molecules.

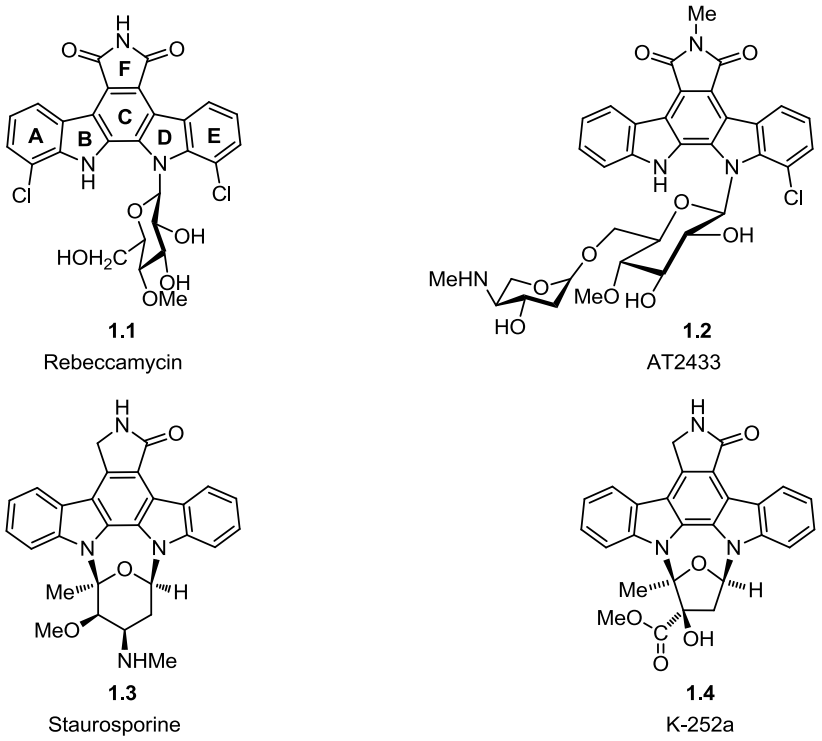

Figure 1.1. Representative members of the indolocarbazole alkaloids

Indolocarbazoles are not the only known inhibitors of DNA topoisomerases, and belong to a broader family of natural products that act either as topoisomerase poisons or suppressors, on the basis of their mechanism of inhibition. Representative examples are shown in Figure 1.2. The specific cellular targets of diverse topoisomerase inhibitors have been investigated in detail,[11] and have culminated in the knowledge that indenoisoquinolines and camptothecins (represented by **1.5** and **1.6**, respectively) target eukaryotic type IB topoisomerases, anthracyclines (such as doxorubicin (**1.7)** and daunorubicin (**1.8**)) target human type IIA topisomerases, and quinolines and aminocoumarins (including novobiocin (**1.9**)) have been shown to target bacterial type II

topoisomerases. Pommier and co-workers have recently reviewed the different types of topoisomerase inhibitors and their associated mechanisms.[5a]

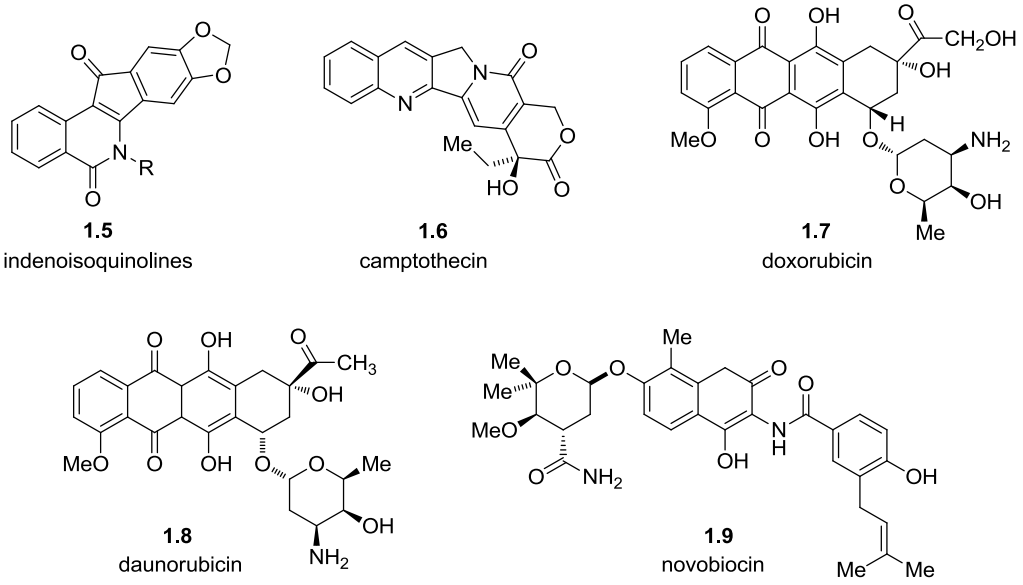

Figure 1.2. Examples of DNA topoisomerase poisons and suppressors

1.1.2 Biological mechanisms of action of indolocarbazoles

The likely primary mechanism of rebeccamycin (**1.1**) is through inhibition of mammalian DNA topoisomerase I (IC_{50} = 1.75 μM *in vitro*).[4] Biological processes such as replication, transcription and mitosis create torsional stress in the DNA helix, and the topological state necessary for normal functioning is restored by the action of topoisomerases. An X-ray crystal structure of a complex containing SA315F,[5a] an analogue of **1.1**, provides a clear explanation of the mechanism of topoisomerase poisoning (Figure 1.3). The mechanism involves the formation of a covalent intermediate between the topoisomerase enzyme and DNA, via trans-esterification of Tyr723 (a conserved active-site Tyr residue in human TopoI) with the backbone of a single strand of DNA, forming a 3'-phosphotyrosine linkage. In the absence of an inhibitor, the resulting cleaved DNA strand rotates around the intact strand, relieving helical strain, and subsequently undergoes re-ligation in a second trans-esterification reaction when the 5'-OH group of the cleaved strand attacks the 3'-phosphotyrosine bond. In the presence of an inhibitor that acts as a DNA topoisomerase poison (as demonstrated for SA315F), interaction with the enzyme-DNA

covalent intermediate is achieved by intercalation of the flat, planar portion of the inhibitor between DNA base pairs at the site of strand cleavage. The result is a rigid complex which is unable to undergo re-ligation to form double stranded DNA. The indolocarbazole sugar moiety plays a role in directing the inhibitor towards its cellular target, as its absence results in a lack of effect on the topoisomerase enzyme activity. Such a mechanism is specific for DNA topoisomerase I poisons, whereas DNA topoisomerase suppressors manifest their bioactive properties through an alternative mechanism of action which prevents binding of the topoisomerase enzymes to DNA (either by interaction of inhibitors with DNA (as intercalating agents, or minor groove ligands)), or the topoisomerase).[12] The potent inhibition of protein kinase C activity by staurosporine[10] (**1.3**) and K-252a[13] (**1.4**) is a consequence of ATP-competitive binding.

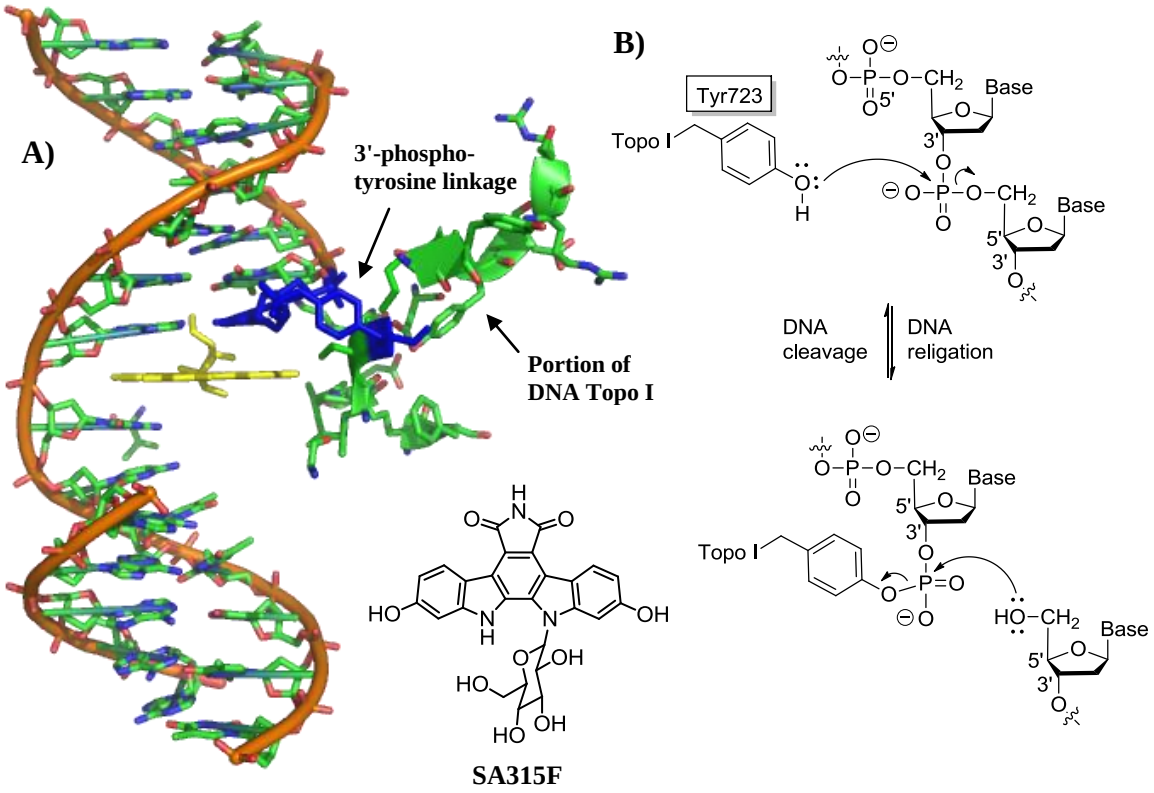

Figure 1.3. Mechanism of action for DNA topoisomerase I poisons. A) X-ray crystal structure of SA315F (yellow structure) bound to the enzyme-DNA "cleavable-complex".[5a] Figure prepared with PyMol (PDB: 1SEU). B) Formation of the 3′-phosphotyrosine linkage between DNA and DNA topo I, necessary for single DNA strand cleavage

1.2 Biosynthesis of indolocarbazoles

1.2.1 Elucidation of the rebeccamycin biosynthetic pathway

The biosynthetic gene cluster encoding the enzymes necessary for rebeccamycin biosynthesis was first reported in 2002.[14] DNA flanking a previously cloned and sequenced *ngt* gene from *Saccarothrix aerocolonigenes* ATCC39243, encoding an *N*-glycosyltransferase known to append D-Glucose to the indolocarbazoles J-10403 and 6-*N*-methylarycriaflavin A,[15] was isolated and introduced into the heterologous host, *Streptomyces albus* J1074. A compound not produced by the host strain was isolated, and identified as rebeccamycin based on observed antibacterial activity (determined in growth inhibition experiments), HPLC analysis, UV-VIS absorption, EI-MS and NMR spectroscopic experiments.[4a] Sequence analysis indicated that the rebeccamycin biosynthetic gene cluster consisted of 16 complete open reading frames (ORF's) and 2 incomplete ORF's (D13 and D12), and the genes believed to be responsible for rebeccamycin biosynthesis were defined in terms of 4 transcriptional units (Figure 1.4).

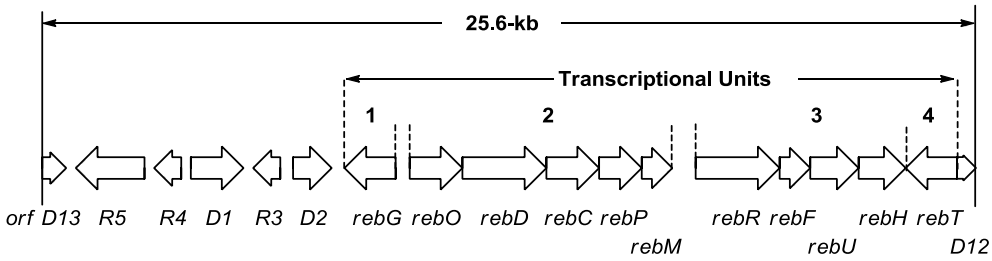

Figure 1.4. Rebeccamycin biosynthetic gene cluster[14]

Elucidation of the rebeccamycin biosynthetic gene cluster greatly advanced our knowledge of the biosynthesis of indolocarbazoles. Use of the Basic Local Alignment Search Tool (BLAST search) allowed for comparison of the amino acid sequences of the identified Reb enzymes with documented proteins whose amino acid sequences have been entered into Genbank (and whose functions were typically known, or proposed). The relationship between enzyme sequence and function was used to assign probable functions to the Reb enzymes in transcriptional units 1-4 (Table 1.1), based upon comparison with the documented protein sharing the highest levels of identity and similarity with the unknown enzyme. The level of

identity is determined by the number of identical amino acid side chains shared between the unknown and documented protein, and can be used to infer similar enzyme function. Sequence similiarity refers to amino acids which have similar properties (e.g. hydrophobicity, polarity, formal charge).

Table 1.1. Deduced functions for genes in the rebeccamycin gene cluster[14]

Gene	Closest Similar Protein (% Identity / Similarity), Accession Number	Proposed Function
rebG	Probable glycosyltransferase from *Deinococcus radiodurans* (45/57), F75587	*N*-glycosyltransferase
rebO	L-amino acid oxidase AIP from *Scomber japonicus* (29/44), CAC00499	L-amino acid oxidase
rebD	VioB from *Chromobacterium violaceum* (34/47), AAD51809	bis-indole formation
rebC	2,4-dihydroxybenzoate monooxygenase from *Sphingomonas* sp. (32/46), CAA51370	FAD-containing monooxygenase
rebP	Cytochrome P450 YjiB from *Bacillus subtilis* (37/53), O34374	P450 heme-thiolate protein
rebM	Methyltransferase from *Amycolatopsis mediterranei* (50/66), AAC01738	Methyltransferase
rebR	Transcriptional activator NysR1 from *Streptomyces noursei* (25/35), BAB50206	Regulatory protein
rebF	Putative FMN:NADH oxidoreductase Gra-orf34 from *S. violaceoruber* (39/52), CAA09661	Flavin reductase
rebU	Putative integral membrane ion antiporter from A. orientalis (40/54), CAB45049	Integral membrane transporter
rebH	Tryptophan halogenase PrnA from Pseudomonas chlororaphis (55/72), AAD46360	$FADH_2$-dependent halogenase
rebT	Putative antibiotic antiporter FrnF from S. roseofulvus (44/62), AAC18101	Integral membrane transporter

Although the ability to propose functions for the enzymes involved in rebeccamycin biosynthesis was a great achievement, the nature of biosynthetic intermediates, as well as specific enzyme substrates, remained largely unknown. Meksuriyen and Cordell demonstrated through feeding studies with radioisotopically labelled tryptophan (Trp) that two Trp molecules with intact side chains were incorporated into the staurosporine aglycon.[16] Pearce and co-workers reached a similar conclusion: experimental results indicated that the biosynthetic precursors of

rebeccamycin consisted of two units of Trp, one methionine, and one glucose molecule, and that the nitrogen atom in the maleimide portion of the aglycon was not derived from the amino group of either Trp precursor.[17] Further evidence that rebeccamycin and staurosporine were metabolites of Trp was provided by studies on the related compound violacein, which showed that this molecule was assembled from two units of Trp.[18] Subsequently, Pearce et al. sought to identify biosynthetic intermediates between Trp and rebeccamycin,[19] and based their experiments on the assumptions that a) incorporation of Trp into the rebeccamycin aglycon was the initial reaction in the biosynthetic pathway, and b) if a tested indole metabolite were a biosynthetic intermediate, then it would competitively inhibit the incorporation of Trp into the rebeccamycin aglycon. Of the five indole metabolites tested, it was found that indole-3-pyruvic acid (IPA (**1.22**), Scheme 1.2) inhibited the incorporation of Trp into rebeccamycin by 79%, and was also introduced into rebeccamycin as effectively as Trp. It was concluded that IPA was an intermediate along the biosynthetic pathway.

Gene disruption experiments carried out by Onaka and co-workers[20] were useful in establishing key biosynthetic intermediates (Scheme 1.1), and allowed the proposal of a rebeccamycin biosynthetic pathway. The proposed role of RebD in formation of the bis-indole intermediate was supported by the inability of the *rebD*-disrupted mutant to produce any indolocarbazole biosynthetic intermediates from **1.10** (Scheme 1.1a). Disruption of the related *vioB* gene (encoding the VioB enzyme known to form a bis-indole intermediate via condensation of 5-hydroxytryptophan with indole-3-pyruvic acid)[21] also failed to produce intermediate indolocarbazoles,[22] providing indirect evidence that RebD and VioB perform similar functions. Given the structural similarities between rebeccamycin (**1.1**) and violacein (**1.19**), shown in Figure 1.5, the results are self-consistent and support the hypothesis that the enzymes RebD and VioB catalyze similar reactions (condensation of two Trp derived units) to form bis-indole intermediates. The structural difference between **1.1** and **1.19** results from occurrence of a 1→2 indole shift during violacein biosynthesis.[23] The *rebP*-disrupted mutant accumulated chloro-chromopyrrolic acid (**1.11**) abbreviated hereafter as CCA (Scheme 1.1b), providing further evidence that formation of a bis-indole intermediate by RebD produced the substrate for the cytochrome P450 enzyme RebP. The *rebC*-disrupted mutant (Scheme 1.1c) accumulated two products, 7-deoxo-7-hydroxyrebeccamycin (**1.12**) and the 4'-*O*-demethyl derivative **1.13**, indicating that the indolocarbazole scaffold could be formed in the absence of RebC. The *rebG*-

disruption experiment (Scheme 1.1d) indicated that indolocarbazole formation preceeded the late stage *N*-glycosylation, and it was concluded that the glycosylated indolocarbazoles **1.12** and **1.13** produced by the *rebC*-disruptant were shunt products resulting from off-pathway reactions. The *rebC* / *rebG* double disruptant experiment (Scheme 1.1e) prevented formation of the shunt

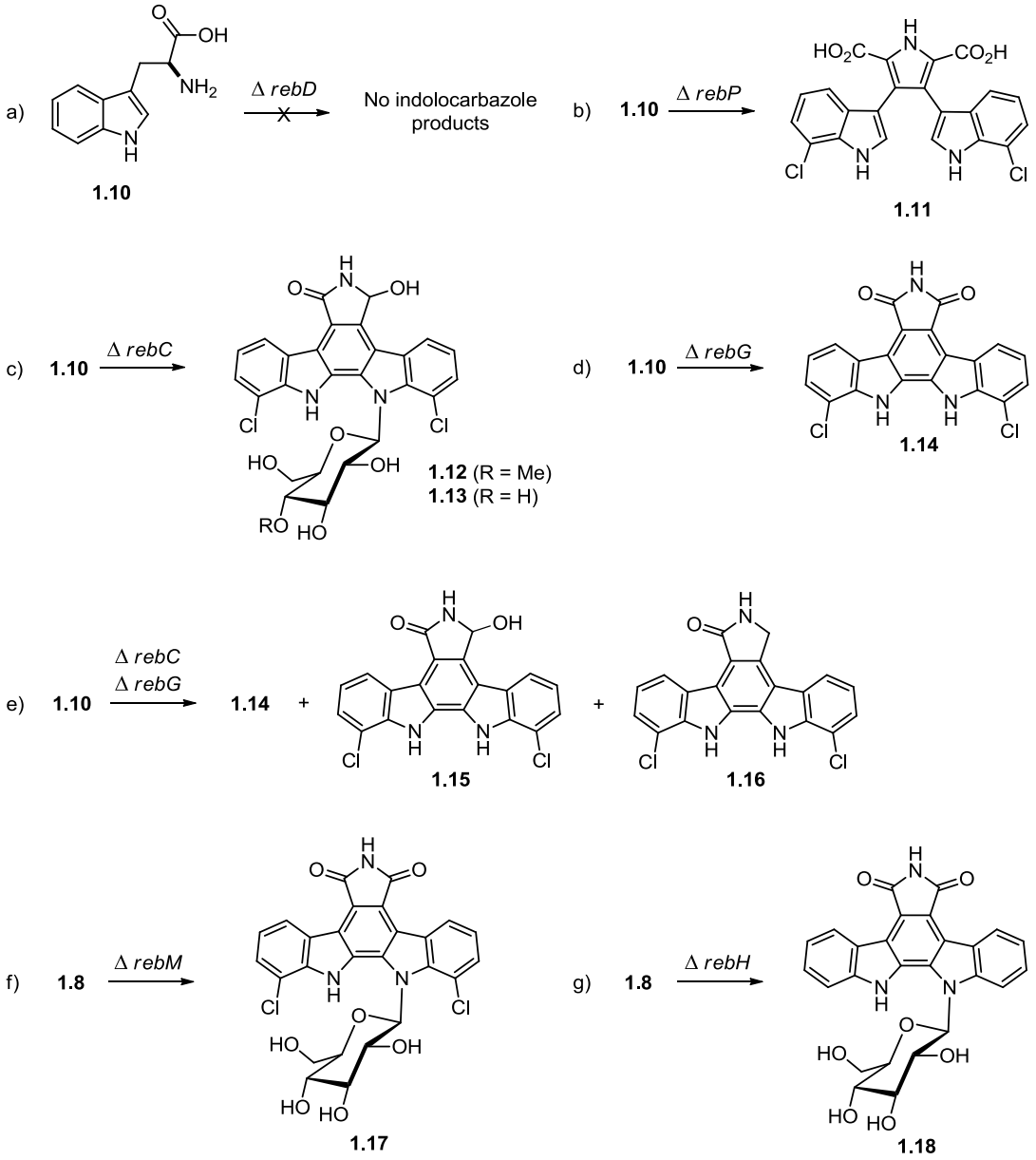

Scheme 1.1. Gene disruption experiments and identification of biosynthetic intermediates.[20] a) *rebD* mutant, b) *rebP* mutant, c) *rebC* mutant, d) *rebG* mutant, e) *rebC*-, *rebG*-double mutant, f) *rebM* mutant, g) *rebH* mutant

products, and **1.14**, **1.15** and **1.16** were identified as fermentation products. Bioconversion experiments indicated that **1.15** and **1.16** were not biosynthetic intermediates, as neither compound could be converted to rebeccamycin. It was suggested that these products arose from oxidation of an unknown intermediate, and that RebP was capable of converting CCA (**1.11**) into

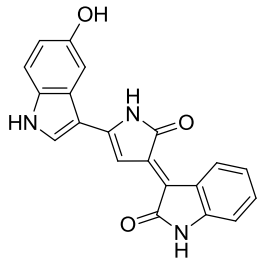

1.19

Figure 1.5. Structure of violacein (**1.19**)[23]

the rebeccamycin aglycon **1.14** in the absence of RebC. The presence of RebC was hypothesized to prevent the formation of non-specific, oxidized indolocarbazoles by controlling the oxidation state at the C-7 site, directing formation of **1.14**. Final stage methylation was demonstrated by the accumulation of glycosylated indolocarbazole **1.17** in the *rebM*-disrupted mutant, and halogenation of L-Trp was shown to occur at the beginning of the pathway, as the *rebH*-disrupted mutant resulted in accumulation of the non-halogenated product **1.18**. The results of gene disruption experiments led to the proposal of a biosynthetic pathway for **1.1** (Scheme 1.2).

1.2.2 Biochemical characterization of individual enzymes involved in indolocarbazole biosynthesis

The significant amount of knowledge obtained from identification of the rebeccamycin and staurosporine biosynthetic gene clusters, as well as the gene deletion studies of rebeccamycin biosynthesis, necessitated further research in order to address subsequent fundamental questions. Specifically, there remained a large gap in the knowledge of the biochemical characterization, structure, function, substrate specificity, and kinetic parameters of the biosynthetic enzymes. The year 2005 witnessed intense research programs directed towards the investigation and characterization of individual enzymes.

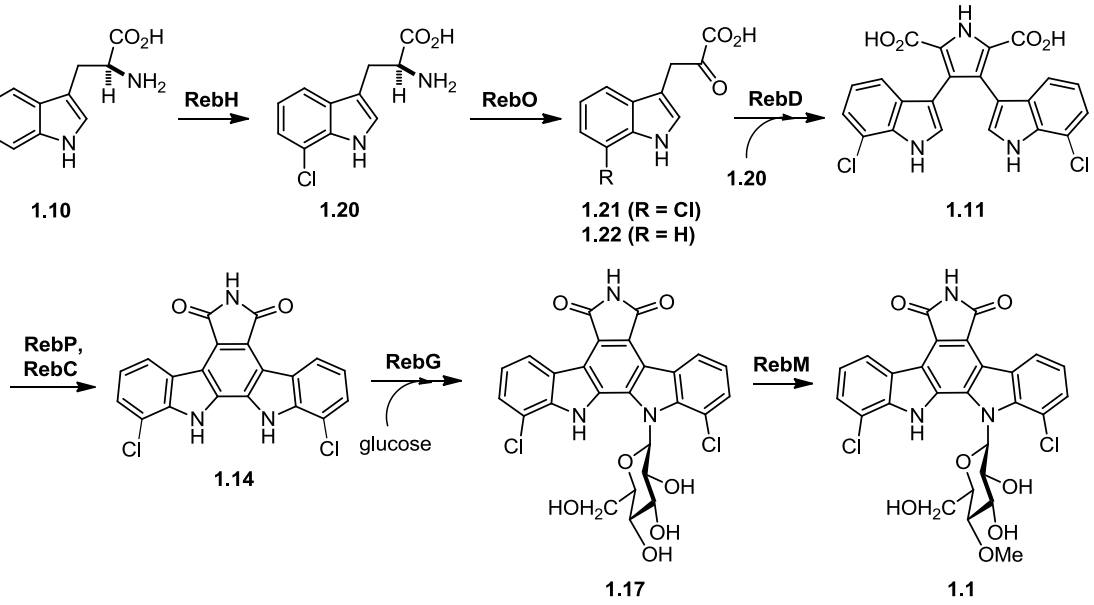

Scheme 1.2. Onaka's proposed biosynthesis of rebeccamycin (**1.1**).[20]

Walsh and co-workers established that RebF and RebH act as a two-component reductase / halogenase system,[24] consistent with the earlier report by van Pée and co-workers that PrnA, the halogenase involved in pyrrolnitrin biosynthesis (which shares 55% similarity with RebH), required an additional flavin reductase as a source of reduced $FADH_2$.[25,26] Both PrnA and RebH have been characterized as regioselective $FADH_2$-dependent halogenase enzymes that require the presence of oxygen. Although several mechanisms have been proposed for the C-7 chlorination of Trp,[27] the most likely mechanism (Scheme 1.3) involves chloramine **1.27** as the active chlorinating species. The catalytic activity of RebF results in the formation of reduced flavin **1.24** ($FADH_2$), which reacts with molecular oxygen to form flavin hydroperoxide **1.25**.[28,29] Bound chloride ion attacks the distal peroxide oxygen, forming hydroxylated flavin **1.26** and hypochlorous acid (HOCl). It is proposed that the HOCl molecule is channeled by RebH to react with an active site lysine residue, forming a chloroamine intermediate **1.27**. This covalently bound, electrophilic form of chlorine undergoes a regioselective reaction with the C-7 position of the indole ring of the substrate,[30] generating **1.20**. The X-ray crystal structure of RebH revealed the presence of an active site Lys79 residue occupying a central position between the flavin and

tryptophan binding sites, at a distance of 4.1 Å from the C-7 position of Trp.[30] These structural features support the plausibility of a chloramine acting as active chlorinating agent.

Structures and mechanisms of halogenating enzymes are remarkably diverse. The flavin-dependent halogenases PrnA and RebH correspond to one class of halogenating enzymes, however nucleophilic and non-heme iron halogenases, as well as peroxidases (heme-iron dependent and vanadium-dependent) are four additional important classes of halogenating enzymes. The relationship between structure and mechanism for these enzymes has been described in a recent excellent review by Blaisak and Drennan.[31]

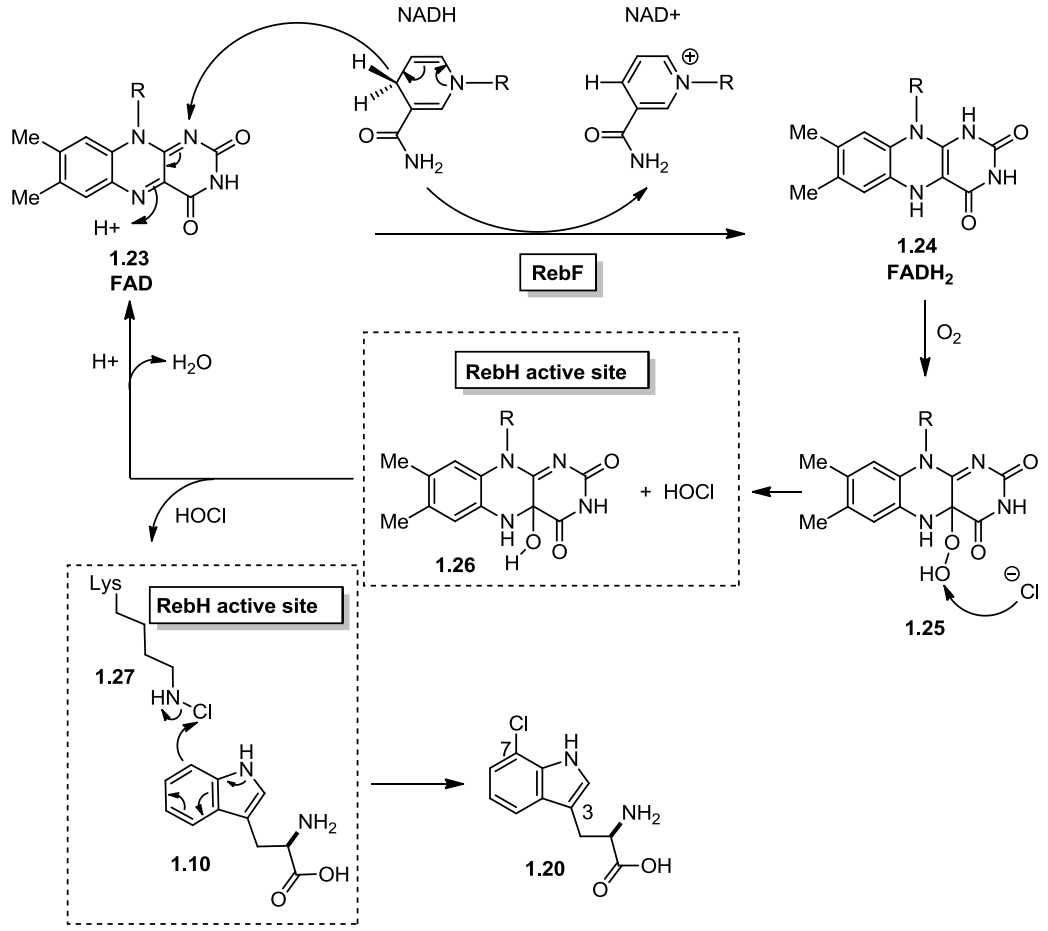

Scheme 1.3. Mechanism of L-Trp halogenation by the RebF/RebH reductase-halogenase system[24]

The work of Sherman and co-workers in 2005 characterized the rebeccamycin biosynthetic enzyme, RebO, and contributed important knowledge about the early stages of the rebeccamycin biosynthesis pathway following initial halogenation.[32] The prediction of RebO as an L-AAO (L-amino acid oxidase) was based on the amino acid sequence which shares 27% sequence identity with the L-amino acid oxidase AIP from *Scomber japonicas*. UV spectroscopic analysis of purified RebO revealed the characteristic absorbance spectrum of a bound FAD molecule (λ_{max} = 385, 460 nm and a shoulder at 480 nm). Flavin dependent L-AAO's typically catalyze the oxidative deamination of L-amino acids to α-imino acids, which hydrolyze to the corresponding α-keto acids. The preferred substrate for RebO was identified as 7-chloro-L-Trp, based on a comparison of kinetic parameters obtained for this substrate with those of selected Trp analogues having variable substitution patterns. The presence of the α-amino and carboxylic acid groups were also required for substrate recognition.

The biochemical characterization of RebD was described by Howard-Jones and Walsh in 2005.[33] RebD purified with a heme prosthetic group, despite the fact that the amino acid sequence contained no apparent heme binding domains. Following halogenation and oxidation of Trp by RebH and RebO, RebD was shown to catalyze an oxidative dimerization of two equivalents of substrate, forming CCA (**1.11**), although unusual oxygen consumption patterns were observed. The rate of CPA production was accelerated with tandem incubations of RebO and RebD, presumably due to efficient shuttling of the unstable RebO product (IPA imine) along the biosynthetic pathway (minimizing the formation of off-pathway oxidative degradation products). The unusual oxygen consumption pattern was rationalized by the catalase activity of RebD, which allows disproportionative scavenging of the H_2O_2 produced as a side product of RebO catalysis.

The Walsh lab performed elegant experiments in order to establish the substrate specificity of RebD leading to the formation of CPA (**1.37**).[33] Two possibilities for catalysis were envisaged: condensation of two molecules of IPA-related substrates would require a net two-electron substrate oxidation, whereas condensation of one molecule of IPA (**1.22**) with one of L-Trp would require a four-electron substrate oxidation. Differential isotopic labeling studies were performed in order to investigate the substrate preference of RebD, by determining the origin of the three nitrogens found in CPA (**1.37**). A RebO / RebD catalytic reaction in the presence of 1 mM (^{15}N)L-Trp, 1 mM (^{14}N)IPA and 10 mM ($^{14}N_2$) ammonium sulfate resulted in the production

of CPA (**1.37**) containing three ^{14}N isotopes. Therefore, neither the indole nitrogen nor the α-amino group of L-Trp were incorporated into CPA, ruling out four-electron oxidation of IPA and L-Trp as the predominant catalytic pathway. Further experiments provided unequivocal evidence that two molecules related to IPA imine were the actual RebD substrates. Incubation of RebO / RebD with a 10:1 ratio of (^{15}N)L-Trp:(^{14}N)IPA and 10 mM ($^{14}N_2$) ammonium sulfate revealed that L-Trp was the origin of the dicarboxypyrrole nitrogen at this substrate ratio, presumably through the imine product of RebO turnover. Consequently, the second indole must be derived from free IPA or the corresponding imine. Finally, perturbation of the IPA ketone-IPA imine equilibrium towards the IPA ketone (by a 100-fold decrease in [$(NH_4)_2SO_4$]) resulted in detection of a single product containing only the ($^{15}N_2$) isotopic labels found in L-Trp. Thus, condensation of two IPA imine molecules (obtained from RebO-mediated L-Trp oxidation) was sufficient to form CPA (**1.37**). As a result of these studies, the preferred substrates for RebD were identified as being two molecules of IPA imine, requiring the enzyme to perform a net two-electron substrate oxidation. Consequently, it was proposed that the mechanism of CPA production by RebD involves the formation of a cross-conjugated imine **1.32** through a trans-imination reaction involving indolepyruvic acid imine **1.28** and indolepyruvic acid enamine **1.29**, followed by radical cyclization to form the resonance stabilized species **1.34** (Scheme 1.4). Subsequent hydrogen abstraction and tautomerization are proposed to complete the biosynthesis of CPA.[33] Particularly noteworthy is the key 5-*endo*-trig radical cyclization of **1.33**, which is an apparent violation of Baldwin's rules.[34]

Investigation of the StaD-mediated synthesis of CPA by Onaka and co-workers revealed that incubation of StaD with two molecules of IPA and ammonium ion generated CPA,[35] suggesting initial formation of IPA imine **1.29** and a subsequent radical coupling process between two molecules of **1.39** to afford an intermediate IPA imine dimer **1.40** (Scheme 1.5a). Subsequent tautomerization to **1.41**, followed by cyclization to **1.42** and aromatization would afford CPA (**1.37**). In 2012, the same researchers provided experimental evidence which supports the occurrence of IPA imine dimerization in *in vivo* indolocarbazole biosynthesis (Scheme 1.5b).[36] NMR spectroscopic studies of the StaD-mediated turnover of IPA (in the absence of ammonium ions) revealed that the enzyme specifically processed the enol tautomer of IPA **1.43**, resulting in the formation of a symmetrical IPA ketone dimer **1.46**. The coupling reaction was suggested to proceed through initial hydrogen abstraction from the IPA enol **1.43**, with the products including

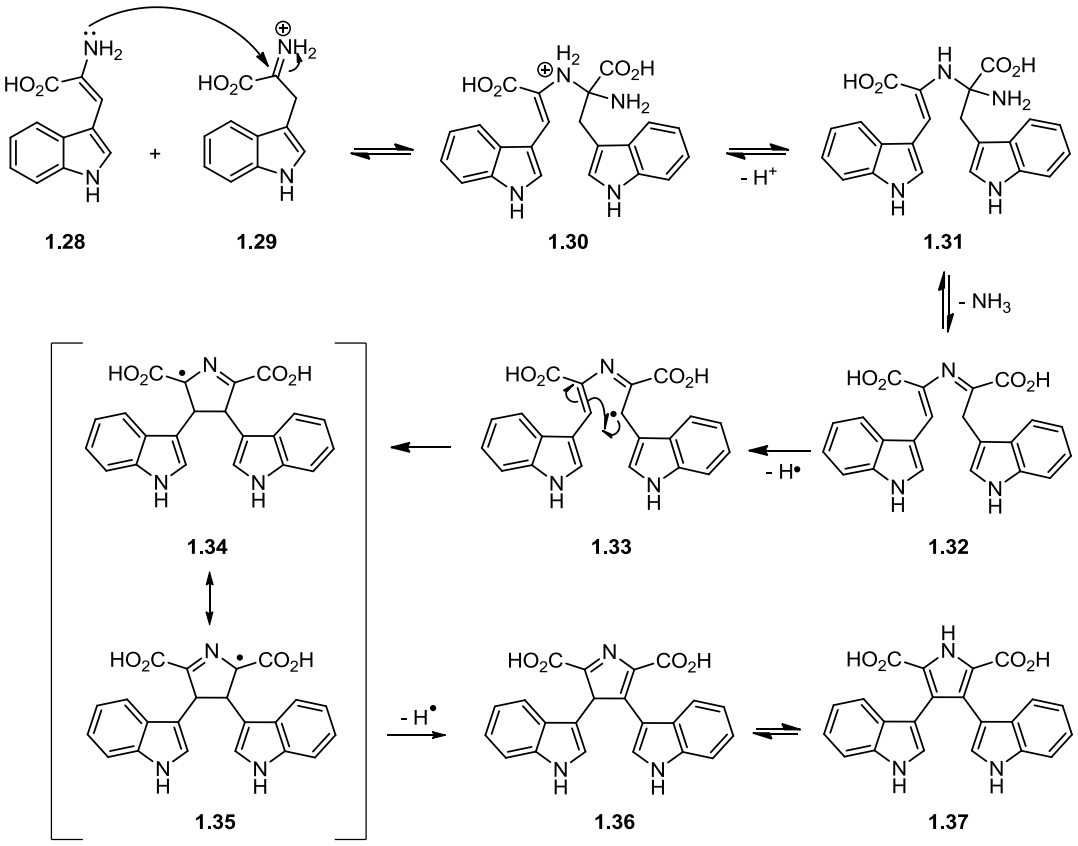

Scheme 1.4. Proposed reaction scheme to form CPA (**1.37**)[33]

O- and C-centered resonance radical structures **1.44** and **1.45** that would combine to form the observed C-C bond in the IPA dimer **1.46**. Similar reactivity has been observed in successive single-electron oxidation of *p*-cresol by horseradish peroxidase.[37] Additional evidence in support of IPA dimer formation was provided by LC-MS and HPLC analysis, the StaD reaction stoichiometry (with an approximate 2:1 yield of IPA enol consumption:product yield), and the observed conversion of **1.46** to CPA in the presence of ammonium ions. By analogy, the conversion of two molecules of IPA enol **1.43** to the IPA dimer **1.46** correlates with the conversion of two molecules of IPA imine **1.29** to the IPA imine dimer **1.40**. Consequently, these recent experimental results support the reaction pathway for CPA production in indolocarbazole biosynthesis shown in Scheme 1.5a, involving initial radical coupling followed by pyrrole ring formation. Significant implications of this recent understanding of CPA formation by StaD includes the potential for synthesis of non-natural indolocarbazoles (generated by addition of

various amines to the IPA ketone dimer **1.46**), as well as the potential development of StaD and homologues as tools for generating diverse pyrrole containing compounds.

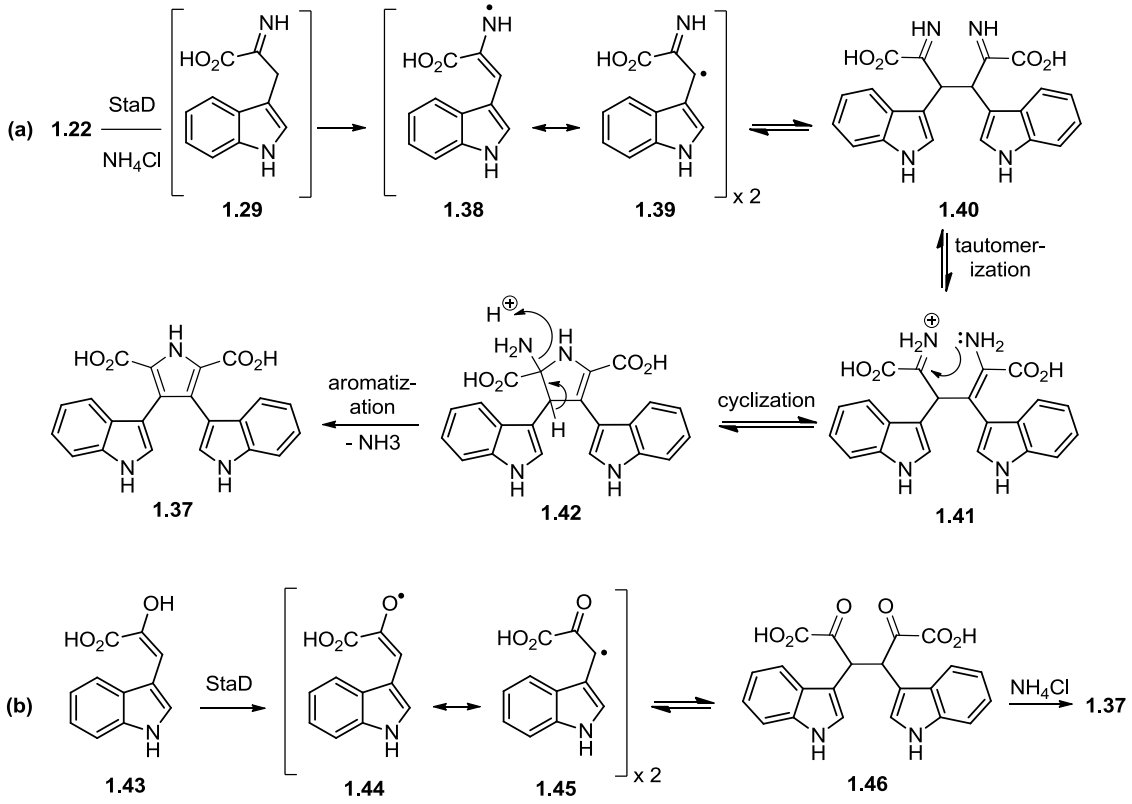

Scheme 1.5. Proposed reaction scheme to form CPA (**1.37**)[35,36]

Results of the first biochemical studies of the enzymes involved in staurosporine or rebeccamycin indolocarbazole aglycon biosynthesis (StaP, StaC and RebC) from CPA were recently described by Howard-Jones and Walsh.[38] RebP and StaP had been annotated as cytochrome P450 enzymes, and were hypothesized to catalyze an aryl-aryl coupling between the C2 and C2' carbon atoms of the indole rings in CPA. Although these types of coupling reactions are known to occur in biosynthetic pathways, detailed investigations of the corresponding enzymes are uncommon.[39-40] RebC and StaC have been annotated as flavin-dependent monooxygenases, and are hypothesized to catalyze oxidative decarboxylation reactions of the RebP/StaP product, with exclusive control over the oxidative chemistry leading to the final indolocarbazole aglycon. The Walsh lab demonstrated that incubation of StaP with CPA (**1.37**) in

the presence of an external redox couple and electron source resulted in the formation of the staurosporine aglycon K-252c (**1.48**), 7-hydroxy-K252c (**1.49**), and arycriaflavin A (**1.50**), in an approximate ratio of 1:7:1, respectively (Scheme 1.6). Combination of StaP and StaC influenced the observed product distribution such that **1.48** was formed exclusively, with the second decarboxylation appearing to proceed along a non-oxidative pathway. Combination of StaP and RebC, however, resulted in the exclusive formation of **1.50**, presumably along an oxidative pathway. This is a remarkable result, as it implies a significant difference in the mechanisms of these homologous flavin-dependent oxidoreductase enzymes.

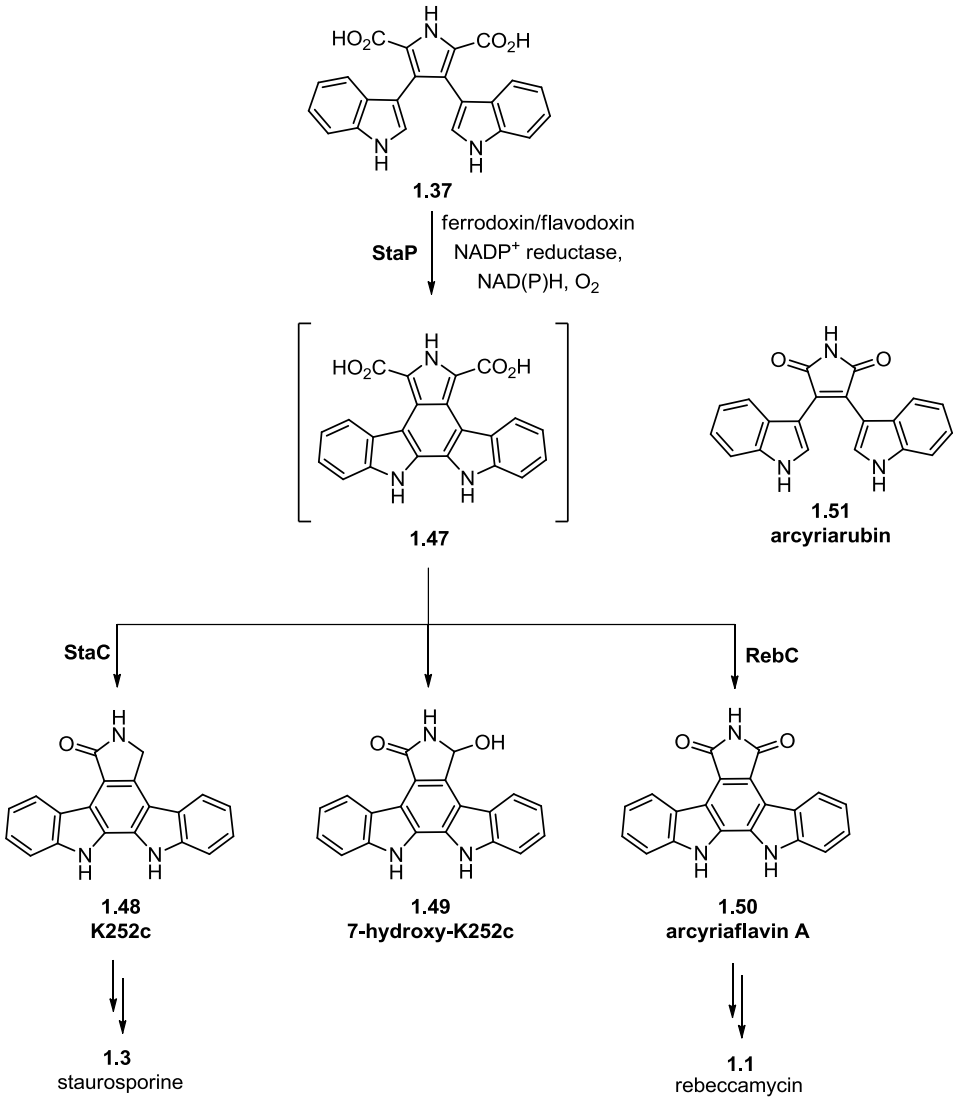

Scheme 1.6. Staurosporine and rebeccamycin aglycone biosynthesis[38]

Important mechanistic features were established as a result of this research. The aryl-aryl coupling reaction producing putative intermediate **1.47** was shown to occur prior to the oxidative decarboxylation chemistry, as incubation of StaP with arcyriarubin (**1.51**) did not result in catalytic turnover. Incubation of RebC or StaC with CPA (**1.37**) also failed to result in catalytic turnover, indicating that CPA was not a substrate for these enzymes. Attempted interconversion of **1.48**, **1.49** and **1.50** was unsuccessful, indicating that these products are not biosynthetic intermediates and must arise from a common biosynthetic precursor. Further significance of StaC incorporation into the rebeccamycin biosynthetic pathway will be discussed in detail in section 1.2.4, as the potential for generation of diverse indolocarbazoles through interchanging enzymes from similar biosynthetic pathways is an intriguing concept.

Isolation of the putative intermediate **1.47** has never been reported, likely due to the susceptibility of this compound towards decarboxylation and autooxidation. In this context, it remains a challenge to ascertain the contributions of enzyme catalysis in controlling product distribution, as formation of the observed products could also occur under aerobic, non-enzymatic conditions. Howard-Jones and Walsh further addressed this issue in 2007.[41] Chemical synthesis of putative intermediate **1.47** from lycogarubin C (**1.52**) was attempted (Scheme 1.7) in order to study the stability of this compound in aqueous, aerobic conditions. However, only 7-carboxy-K252c (**1.54**) and 7-carboxy-7-hydroxy-K252c (**1.55**) could be identified following saponification of the ester groups. This result suggested that intermediate **1.47** was too unstable to be isolated, and spontaneously formed **1.54** and **1.55** under aerobic conditions. These compounds were suspected of representing biosynthetic intermediates resulting from the catalytic turnover of CPA (**1.37**) by StaP or RebP, en route to the staurosporine or rebeccamycin aglycons **1.48** or **1.50**. The stability of **1.55** in an aqueous environment, as well as the inability to convert to an indolocarbazole aglycon in the presence of any combination of StaP, RebC or StaC resulted in determination of **1.55** as an off-pathway oxidative degradation product. In contrast, **1.54** was highly unstable, and spontaneously formed **1.48** and **1.49** (in a 2:1 ratio). Therefore it was proposed that aerobic reaction conditions were sufficient to affect formation of the indolocarbazole mixture of **1.48**, **1.49** and **1.50**, with StaP (or RebP) only being required to perform the initial cross-coupling reaction. Furthermore, no significant kinetic isotope effect was observed, indicating that aryl-aryl bond formation is not the rate-limiting step.

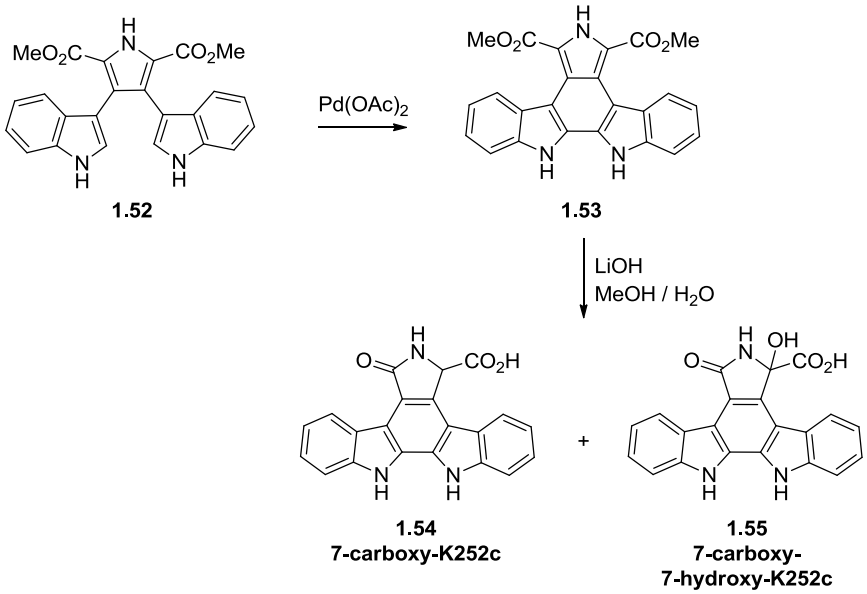

Scheme 1.7. Attempted synthesis of putative intermediate **1.47**[41]

Onaka and co-workers reported an X-ray crystal structure of StaP with CPA bound in the active site (Figure 1.6), which provided an enhanced understanding of the mechanism by which StaP converts CPA to an indolocarbazole.[42] CPA was found to adopt a twisted-butterfly conformation in the active site of StaP, oriented perpendicularly to the heme co-factor, and stabilized in the active site through numerous hydrogen bonding interactions. The CPA carboxylate proximal to the heme group is stabilized by hydrogen bonding with the amide-bond nitrogen of Thr-305, Arg-67 and the 7-propionate of the heme. The distal CPA carboxylate group is stabilized via two hydrogen bonding interactions with Thr-187 (through the side chain hydroxyl group and amide bond nitrogen) and Ser-186. The orientation of the indole rings is maintained through a series of π-π interactions with Trp-97 and Phe-403, as well as hydrophobic interactions with Val-99, Phe-100 and Val-402 (not shown). Evidence supporting the hypothesis that aryl-aryl coupling must preceed oxidative decarboxylation is provided by analysis of the StaP crystal structure shown in Figure 1.6. The carboxylate groups of CPA are positioned far away from the heme iron (> 8 Å), whereas the proximal indole ring is only 4.7 Å away. Experimental results confirmed this hypothesis, as incubation of StaP with arcyriarubin (**1.51**) failed to generate an indolocarbazole.

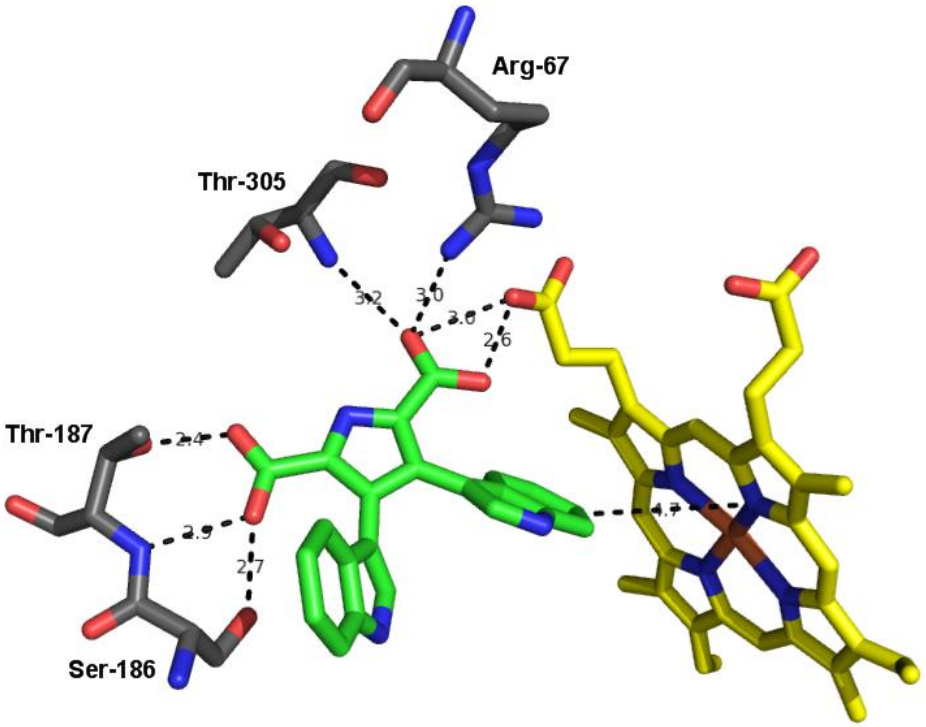

Figure 1.6. X-ray crystal structure of StaP with CPA bound in the active site.[42] Active site residues Ser-186, Thr-187, Thr-305, and Arg-67 are shown in grey. CPA is shown in green and the heme co-factor in yellow. Observed interactions in the active site are shown as dashed lines (distances in Å). Figure prepared with PyMol (PDB: 2Z3U)

As shown in Figure 1.7, cytochrome P450 enzymes use a highly reactive Fe(IV)=O species **1.56** (referred to in the literature as compound I (CpdI)) to oxidize substrates. Reactions involve oxygen insertion into different types of bonds, including C-H bond hydroxylation, alkene epoxidation, and dealkylations, which typically proceed via radical mechanisms. CpdI is formed by reaction of the heme Fe(II) with molecular oxygen, two reducing equivalents, and two protons. Peroxidase enzymes also use Cpd I to oxidize substrates via electron-transfer or proton-coupled electron transfer (PCET) pathways,[43] as observed in the oxidation of ferulic acid by horseradish peroxidase.[44] The ligand in Cpd I of P450's **1.56** is a cysteine thiolate group, whereas peroxidase Cpd I species **1.57** are ligated to the imidazole ring of a histidine residue.

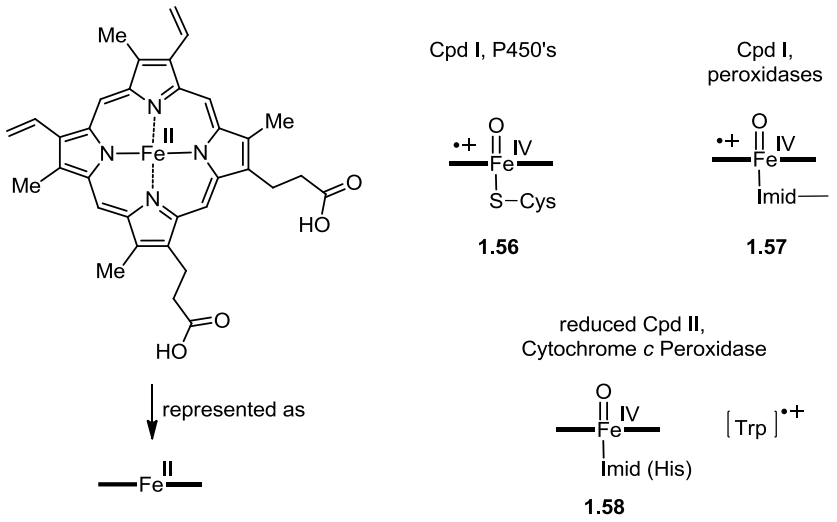

Figure 1.7. Reactive Cpd I species found in mono-oxygenases and peroxidases

The powerful electron-accepting character of peroxidase Cpd I **1.57** has been shown to facilitate a different reaction in the presence of protein Trp residues. Oxidation of Trp-191 in Cytochrome *c* Peroxidase (C*c*P) by **1.57** forms an indole radical cation and the one electron reduced Cpd II **1.58** which subsequently oxidizes C*c*P by radical abstraction.[45] Intermediates like **1.58** have been described as "electronic chameleons," as they are able to adapt their electronic and structural properties to the surrounding protein environment.[46] In the case of C*c*P, for example, the surrounding side chain amino acid residues are good electron donors (M230, M231, and D235), and participate in the electronic structure of Cpd I by donating electron density to the porphyrin radical cation. These residues also function in stabilization of the reactive indole radical cation moiety. In the case of P450 Cpd I **1.56**, the electron-donor thiolate ligand decreases the electron affinity of the porphyrin ring, and normal P450 reactivity is observed.

Analysis of the StaP active site with bound CPA (**1.37**) indicates that electron-donating groups reside in the region surrounding the proximal indole ring of CPA (including the carboxylate groups of CPA, and the heme propionic acid substituents), and the proximal indole ring of CPA resides at a comparable distance and orientation to the heme prosthetic group as Trp-191 in CcP. Furthermore, the extensive hydrogen bonding and aromatic interactions with CPA control the extent of interaction between CPA and CpdI, favoring one-electron oxidation over hydroxylation. The similar protein environments surrounding StaP Cpd I **1.56** and CcP reduced

Cpd II **1.58** resulted in the proposed mechanism of StaP-mediated aryl-aryl coupling of CPA (Scheme 1.8).[42] It was proposed that Cpd I of StaP was capable of initiating a single-electron oxidation of the proximal indole ring of CPA (**1.37**) forming the indole radical cation **1.59** and a reactive Fe(IV)=O species, analogous to the reduced Cpd II of cytochrome *c* peroxidase. Loss of a proton from the acidic radical cation (pK_a = 4.3) in step 2 would form neutral radical **1.60**, and two possible reaction pathways leading to carbon-carbon coupled CPA **1.47** have been proposed. The C-C bond could be created directly from **1.60** (Step 3'), through a one-electron oxidation and deprotonation of **1.60** (Step 4') to form **1.47**. Alternatively, single-electron oxidation of neutral radical **1.60** by the ferryl-oxo heme of StaP would produce di-radical **1.62** (Step 3), which would undergo radical cyclization to form **1.63** (Step 4). Final tautomerization would complete the synthesis of coupled product **1.47** (Step 5). Formation of the indolocarbazole core requires subsequent decarboxylation and oxidation of **1.47**, and it was proposed that formation of **1.48** or **1.50** could occur in a second catalytic turnover of StaP through a three-step enzyme-mediated process,[38] consisting of i) StaP-mediated one-electron oxidation of **1.47**, ii) carboxylate group deprotonation and decarboxylation, and iii) binding of the resulting neutral radical to molecular oxygen. Steric clash between the carboxyl groups and the indolocarbazole core, or electronic repulsion between the carboxyl group and heme propionate groups were suggested as possible triggers of this decarboxylation. The occurrence of decarboxylation and oxidation in the StaP active site is an important consideration, as formation of indolocarbazole aglycons has been shown to occur in the absence of RebC.

Understanding the mechanism of StaP catalysis is significant not only because of the relevance to the study of staurosporine biosynthesis, but the knowledge can also be used for the study of structure, substrate recognition, and mechanism of the related homologous enzymes RebP and AtmP (which share > 50% amino acid sequence identity with StaP). Onaka's proposal of the mechanism of catalytic turnover by StaP inspired studies towards understanding the divergence of StaP from typical cytochrome P450 behavior. Key features of the StaP substrate binding pocket containing CPA^{2-} were modelled using DFT(B3LYP)/MM hybrid calculations.[47] In addition to the extensive hydrogen bonding array stabilizing the carboxylate groups, a triad consisting of two water molecules and His-250 was identified, connecting the oxo group of the heme to the proximal indole ring of the substrate. One of the water molecules was not observed in the X-ray structure, and was included in the model to represent the water molecule that is

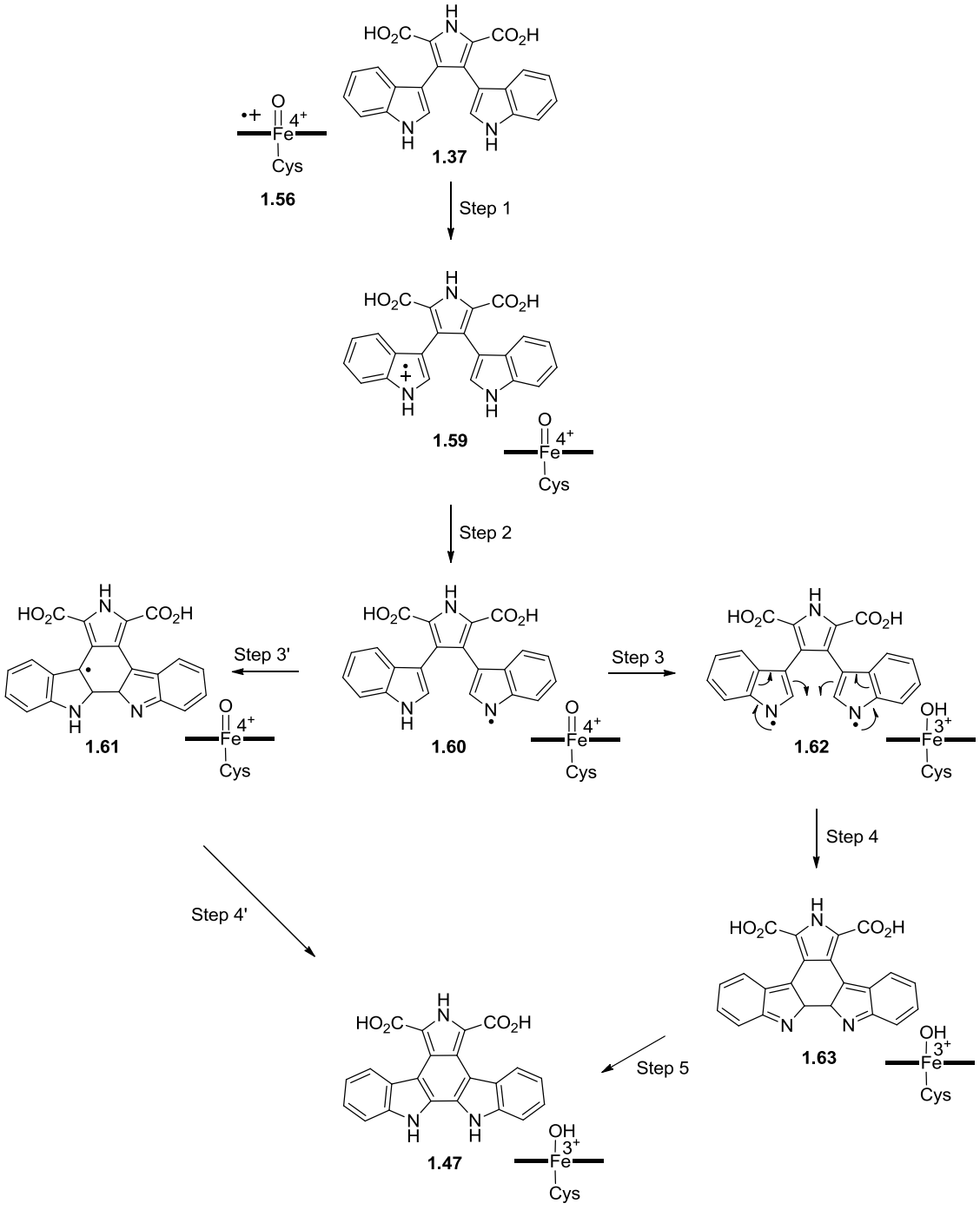

Scheme 1.8. Proposed mechanism of StaP-mediated aryl-aryl coupling of CPA[42]

generated during the formation of Cpd I.[48] The model suggested that the triad facilitated electron transfer from CPA to Cpd I, resulting in generation of the Cpd II species (analogous to C*c*P Cpd II). Transfer of the N-H hydrogen from the proximal indole ring of CPA to the Fe-oxo Cpd II could not be achieved directly due to the 4.7 Å gap (Figure 1.6), and a PCET mechanism involving the water-His250-water triad was suggested. Precedence for a PCET mechanism operating through a proton relay system is typical of peroxides. For example, oxidation of ferulic acid by horseradish peroxidase (HRP) has been demonstrated by QM/MM calculations to proceed via a PCET mechanism through a relay involving an active site proline and water.[49] The mechanism initially proposed by Onaka et al. was revised to include the PCET mechanism shown in Scheme 1.9.

The role of Wat644 and Wat789 was further investigated, and found to extend beyond the initial PCET. QM/MM calculations have shown that they are intricately involved in the aryl-aryl coupling process, which is proposed to occur via a bond-formation coupled electron-transfer (BFCET) mechanism.[50] The water molecules belonging to the wat644-his250-wat789 triad act as mobile "catalytic elements", which facilitate the coupling of electron-transfer processes with group transfer events and bond reorganizations. In particular, the involvement of these molecules in four steps of proton transfer and tautomerization following C-C bond formation was demonstrated in a complete proposal of the StaP catalytic pathway leading to aryl-aryl coupled CPA.[50]

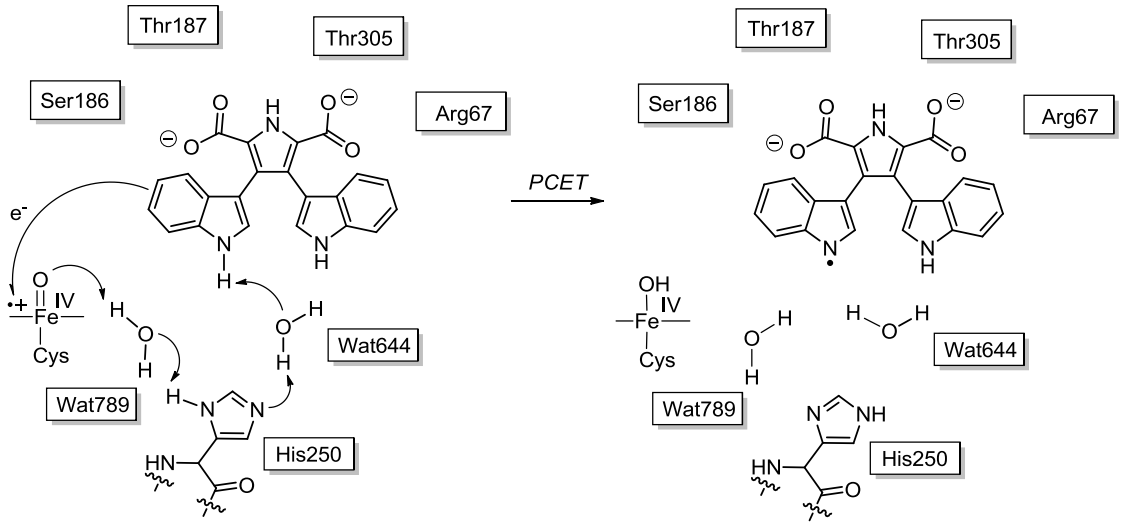

Scheme 1.9. Demonstration of a PCET mechanism activating CPA in the StaP active site[47]

Our research group has been interested in studying the enzymes involved in indolocarbazole biosynthesis for a number of years, particularly the roles of RebC and StaC. This thesis will return to these enzymes as a topic of investigation later in this chapter. As described previously, RebC and StaC channel the RebP / StaP product towards an indolocarbazole product with a specific oxidation state. In 2007 we published the cloning, expression, purification and preliminary X-ray diffraction studies for RebC,[51] only to see the X-ray crystal structure of this enzyme published by a competing lab that same year.[52] The crystals belonged to the primitive monoclinic space group $P2_1$, with one monomer present in each asymmetric unit. This result was consistent with the results from size-exclusion chromatography, which indicated that the protein was monomeric in solution. Three functional domains have been identified in the RebC monomer,[52] and are shown in Figure 1.8. Domain I (red) is involved in binding the FAD co-factor, domain II (blue) contains the substrate binding pocket, and domain III (green) is of unknown function, although it possesses a typical thioredoxin fold.[53]

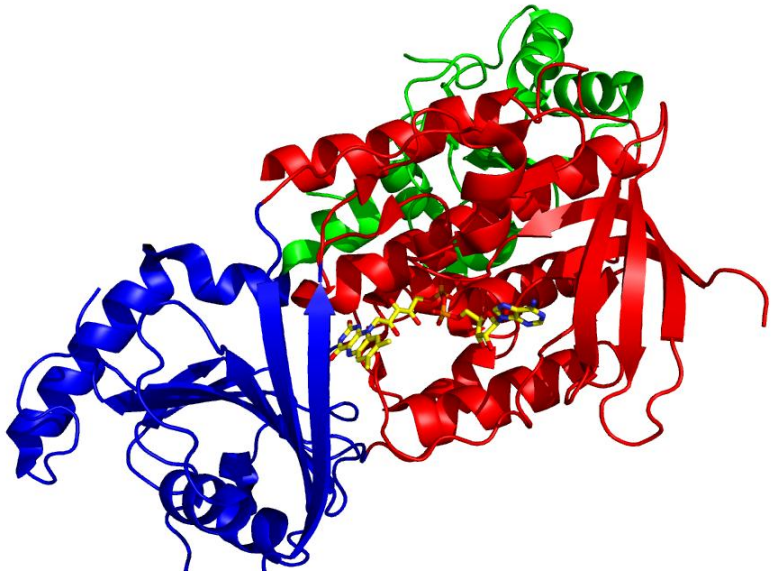

Figure 1.8. X-ray crystal structure of RebC without substrate bound.[52] Domain I is shown in red, Domain II in blue, and Domain III in green. The flavin co-factor is shown as yellow sticks. Figure prepared with PyMol (PDB: 3EPT)

Structural analysis of RebC revealed the presence of a mobile flavin and a "melting helix".[52] Two conformations are possible for the flavin co-factor: bound in the flavin binding pocket (IN) or facing bulk solvent (OUT). When the flavin occupies the OUT conformation as in

Figure 1.9a, the isoalloxazine ring is stacked between residues W276 and R46, and hydrogen bonds with R239. This conformation is adopted when the active site is unoccupied by the substrate, and allows the isoalloxazine ring to be exposed to the solvent where it can be readily reduced by NAD(P)H. Upon substrate binding, the $FADH_2$ pivots on the lowest phosphate of the adenosyl-diphosphate moiety, and adopts a conformation in which the isoalloxazine ring is positioned in close proximity to the substrate (the IN conformation), as shown in Figure 1.9b. A new interaction is formed between R46 and the phosphate group of the FAD, and between Arg-239 and the bound 7-carboxy-K252c. Presumably molecular oxygen reacts with the IN oriented isoalloxazine ring to form the reactive flavin hydroperoxide.

The close homologues of RebC, namely *p*-hydroxybenzoate hydroxylase[54] and phenol hydroxylase[55] also show evidence of a mobile flavin. Interestingly, a third conformation (the OPEN conformation) is exhibited by phenol hydroxylase, which is thought to allow the substrate to enter the active site. RebC catalysis requires a different mechanism for entry into the active site (due to the size of the substrate) in which a "melting helix" is proposed to play a role.[52] This helix spans across the interface of Domain I and Domain II, and is observed in the crystal structure of RebC bound to a putative reaction intermediate. It has been speculated that a mobile loop exists until substrate binds, at which point a helix forms that seals the substrate-binding pocket until product release is required.

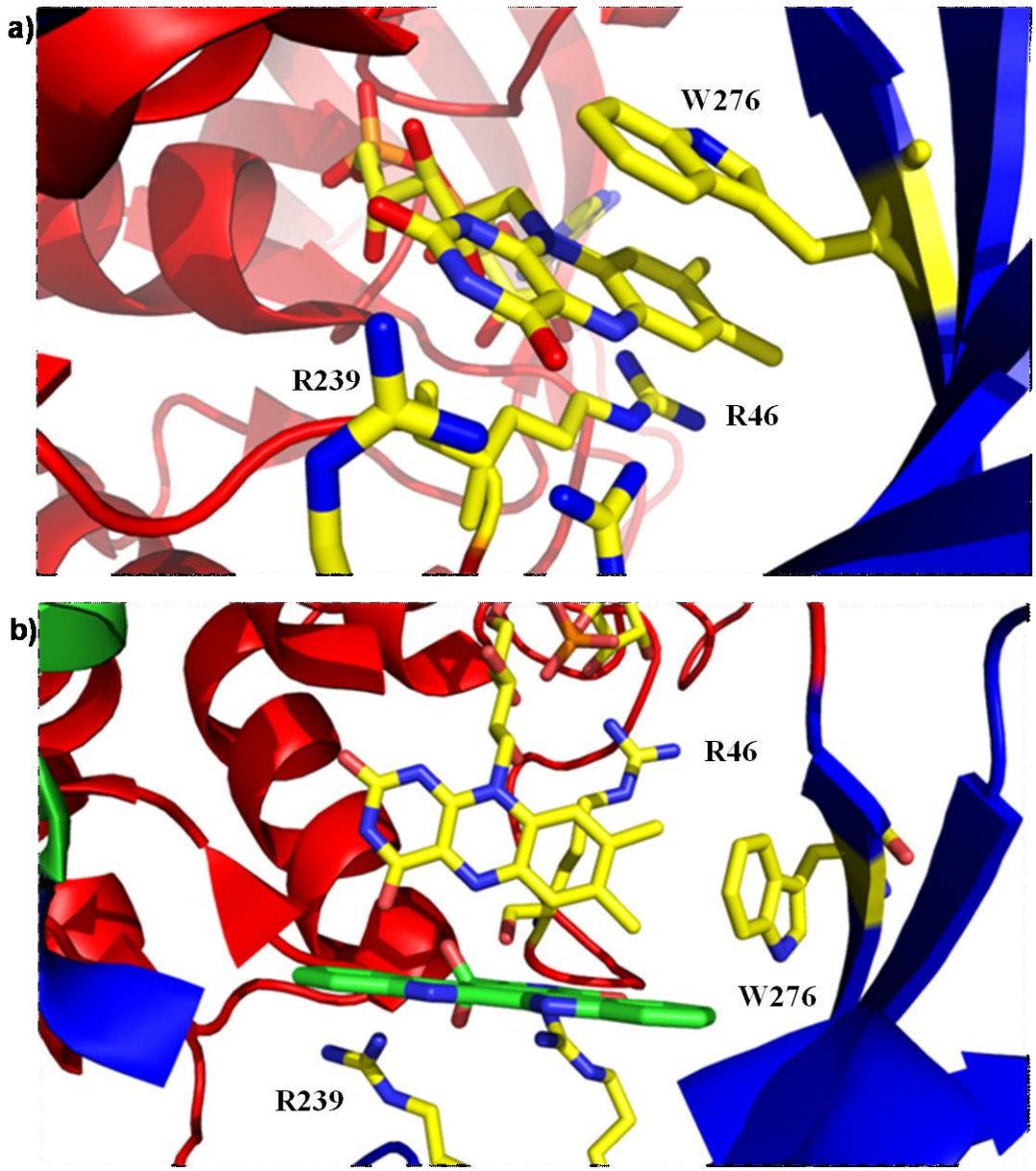

Figure 1.9. The two possible conformations of the FAD co-factor of RebC:[52] a) The OUT conformation in which the isoalloxazine ring is stacked between R46 and W276 b) The IN conformation of the FAD co-factor. The putative reaction intermediate 7-carboxy-K252c is shown as green sticks. Figure prepared with PyMol (PDB: 2R0C and 2R0G)

As noted previously, CPA is not a substrate for RebC. However, it is one C-C bond away from the putative RebC substrate (ie. the RebP product) and thus represents a reasonable substrate mimic for crystallization studies. An X-ray crystal structure of RebC with a bound substrate in the active site (obtained after a week long soak of the RebC crystal with CPA),[52] shown in Figure 1.10, generated a surprising result.

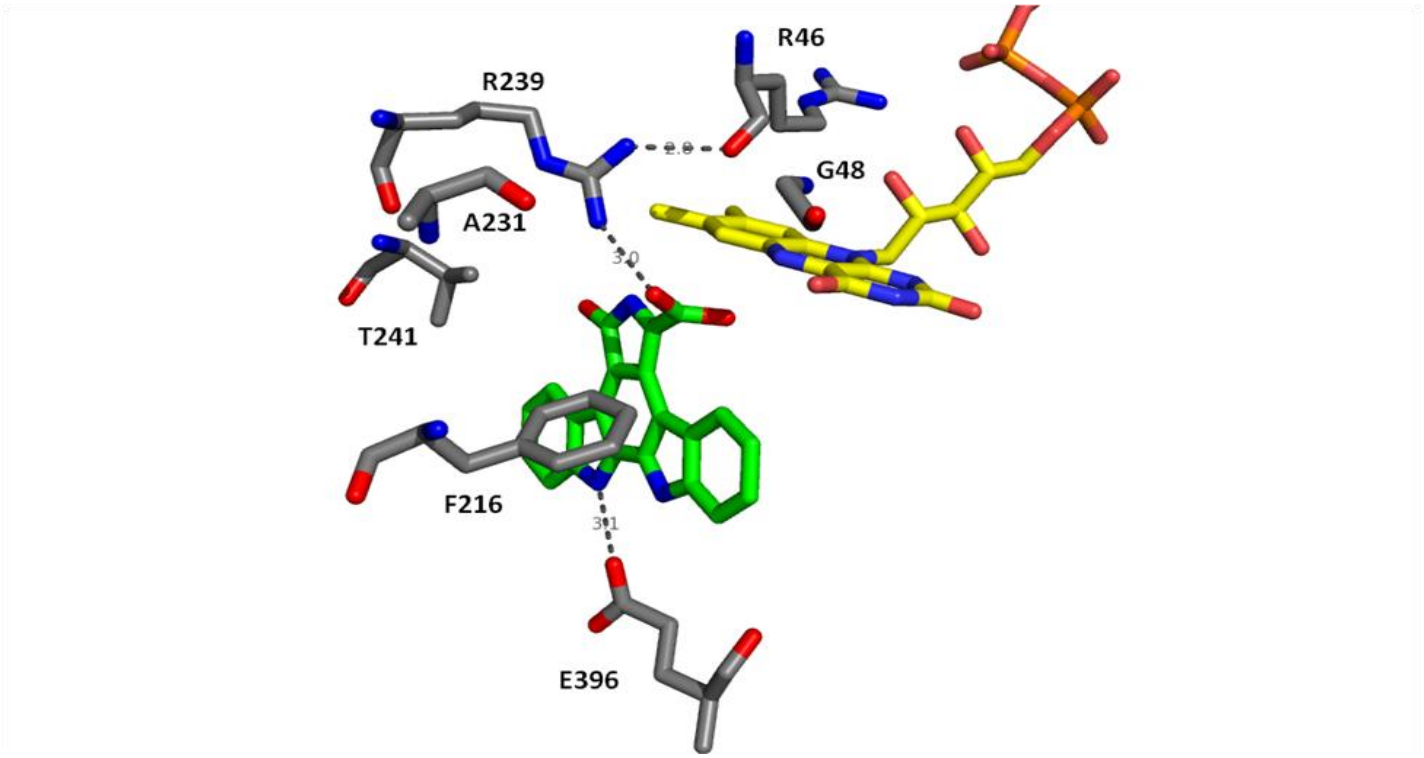

Figure 1.10. X-ray crystal structure of RebC with a putative reaction intermediate contained in the active site.[52] Active site residues are shown in grey, the reactive intermediate in green and the FAD co-factor in yellow. Figure prepared with PyMol (PDB: 2R0G)

Analysis of the experimental electron density map indicated that a planar molecule had been captured by the RebC crystal, and that a covalent bond had likely formed between the C2 and C2' carbon atoms of the indole rings (Figure 1.10). The identity of this molecule as CPA was ruled out on the basis of computational calculations, which indicated that the energy minimized conformation of CPA would have the indole rings oriented away from each other to minimize

unfavourable steric interactions. Instead, the electron density was best fit with an aryl-aryl coupled product. The electron density of the bound ligand also suggested the presence of a carbonyl or hydroxyl group at C-5, and a carboxylate-type moiety at C-7. The most consistent results were obtained when the structure was refined with either tautomer **1.64** or **1.65** (Figure 1.11) trapped in the active site, as the electron density map could readily accommodate either an in-plane or out-of-plane carboxylate group. It was assumed that this compound must have arisen from autooxidation of CPA during the week long experiment.

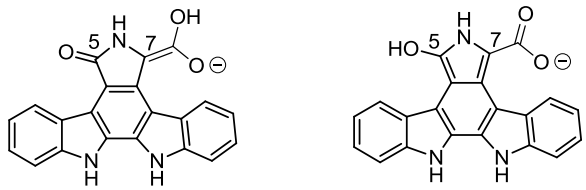

1.64 **1.65**

Figure 1.11. Proposed structures of the putative reaction intermediate observed in the active site of RebC (upon soaking the crystal with CPA)[52]

As shown in Figure 1.10, the RebC active site is suitably designed to stabilize an intermediate such as 7-carboxy-K252c (**1.64**). Glu-396 is positioned to form hydrogen bonds with both indole nitrogen atoms, evidenced by the disordered → ordered transition of the Glu396 side chain upon substrate binding. Arg-239 (and Arg-230, not shown) electrostatically stabilize the negatively charged carboxylate of the bound molecule. Additional stabilization may be obtained from the interaction between the peptide bond carbonyl of Arg-46 and the side chain of Arg-239, which maintains the conformation of Arg-239 required for effective interaction with the substrate. The R46 side chain also interacts with the pyrophosphate moiety of the FAD co-factor, providing additional stabilization of the active site structure. Phe216 exerts steric pressure on the bound substrate, assisting R46, R239 and E396 in maintaining the substrate orientation required for reaction with the FAD co-factor.

A crystal structure of RebC containing the StaC specified product K252c **1.48** in the active site was also obtained.[52] In this structure, the flavin switched to the OUT conformation, suggesting that the presence of a carboxy group in the substrate was required to support the IN conformation, possibly mediated by the electrostatic interaction with R239. This study indicated the remarkable ability of RebC to stabilize a specific reactive intermediate from RebP catalysis,

and direct oxidation to a specific indolocarbazole aglycon. The putative snapshot of the RebC catalytic cycle obtained with 7-carboxy-K252c in the active site suggested that this could be the actual substrate, or a reactive intermediate formed after the product of the StaP or RebP reaction (aryl-aryl coupled CPA).

The Walsh lab carried out further experiments using X-ray crystallography to capture snapshots of the RebC catalytic cycle.[56] The structure of RebC with reduced flavin ($FADH_2$) indicated that a) the flavin had adopted the IN conformation, and b) that the melting helix was ordered, closing the substrate binding pocket. This structure was assumed to represent a catalytically incompetent state of RebC, and was likely obtained as a result of an off-pathway process. Indeed, this structure was very similar to the previous structure of RebC with trapped 7-carboxy-K252c (the reduced flavin had adopted the IN conformation, and the melting helix had sealed off the entrance to the active site). Consequently, the $FADH_2$ structure implied that substrate binding must preceed flavin reduction. Two possible triggers of conformational change by the co-factor could be envisaged: either flavin reduction preceeds the switch from the OUT to IN conformation, or proximity to a substrate molecule containing a carboxylate group was required to induce the change. Preliminary conclusions about the RebC catalytic cycle could be made based on the three crystal structures. The structure of native RebC with the flavin co-factor in the OUT conformation was assumed to correspond to the beginning of the catalytic cycle. Substrate binding triggered flavin reduction and shift to the IN conformation, followed by closure of the binding-pocket by the melting helix (corresponding to the X-ray crystal structure with bound 7-carboxy-K252c). Experimental evidence that substrate binding occurred prior to flavin reduction was provided by kinetic studies: the rate constant for flavin reduction in the presence of substrate was an order of magnitude greater than the reaction without substrate. Rate acceleration was aslo observed when the FAD co-factor of *p*-hydroxybenzoate was reduced by NAD(P)H in the presence of substrate. In the second step, molecular oxygen reacts with the bound $FADH_2$ to form the flavin hydroperoxide **1.25**. This subsequently hydroxylates the substrate **1.47**, affording **1.66** and regenerating oxidized flavin (after loss of water). Finally, the FAD co-factor flips to the OUT conformation, regenerating the resting state of RebC. An overview of one cycle of RebC oxidation suggested by these studies is given in Scheme 1.10.

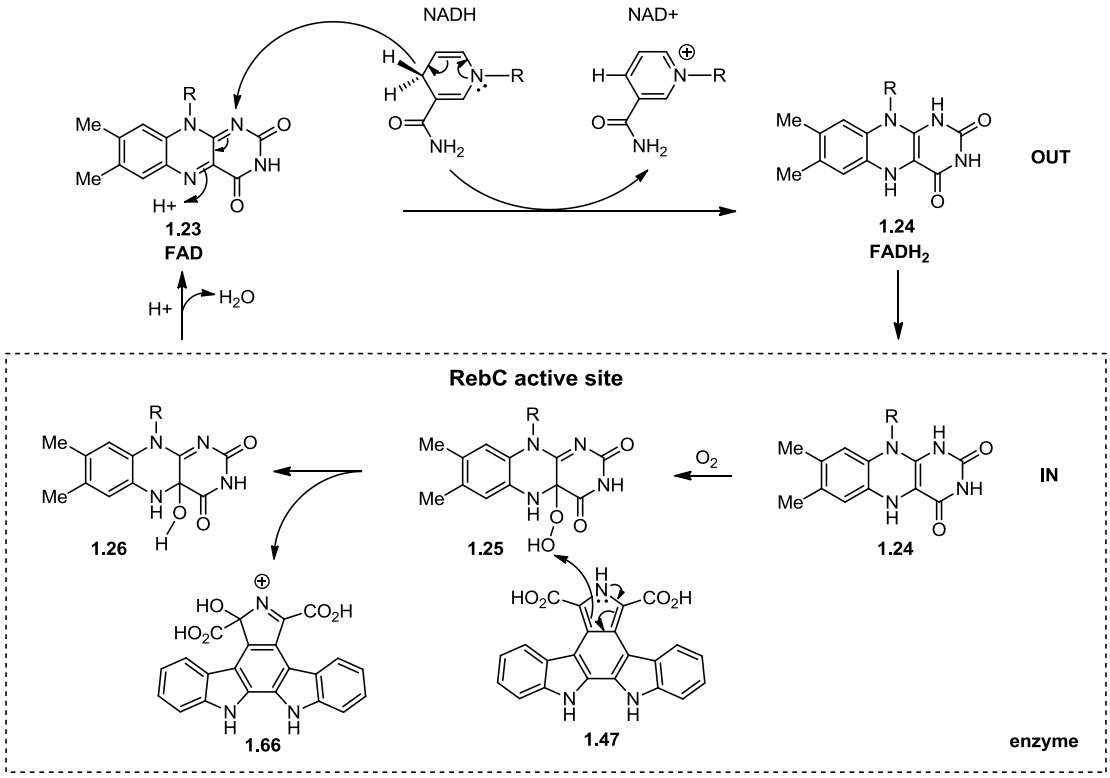

Scheme 1.10. Proposed mechanism for a single catalytic cycle of RebC[56]

Several tailoring enzymes are required for modification of the indolocarbazole aglycon resulting from RebC catalysis. The *N*-glycosyltransferase RebG attaches the glucose sugar moiety to the indolocarbazole aglycon,[57] followed by regioselective methylation of the glucose 5'-hydroxy group by RebM, an *S*-adenosylmethionine dependent methyltransferase.[58] The locations of RebG and RebM in transcriptional units 1 and 2 of the rebeccamycin biosynthetic gene cluster were shown in Figure 1.4.

The overall biosynthetic pathway which has been established as a result of the previously described experimental work is summarized in Scheme 1.11. The biosynthesis begins with the regioselective chlorination of L-Trp (**1.10**) at the 7-position by the combined action of RebF and RebH as a two-component reductase-halogenase system. The halogenated product **1.20** serves as the substrate for the L-AAO RebO that catalyzes the formation of the imine of IPA **1.67**. RebD, a cytochrome P450 enzyme, catalyzes the condensation of **1.67** with the enamine equivalent, forming CCA **1.11**. RebP catalyzes the formation of a C-C bond between the indole C2 and C2'

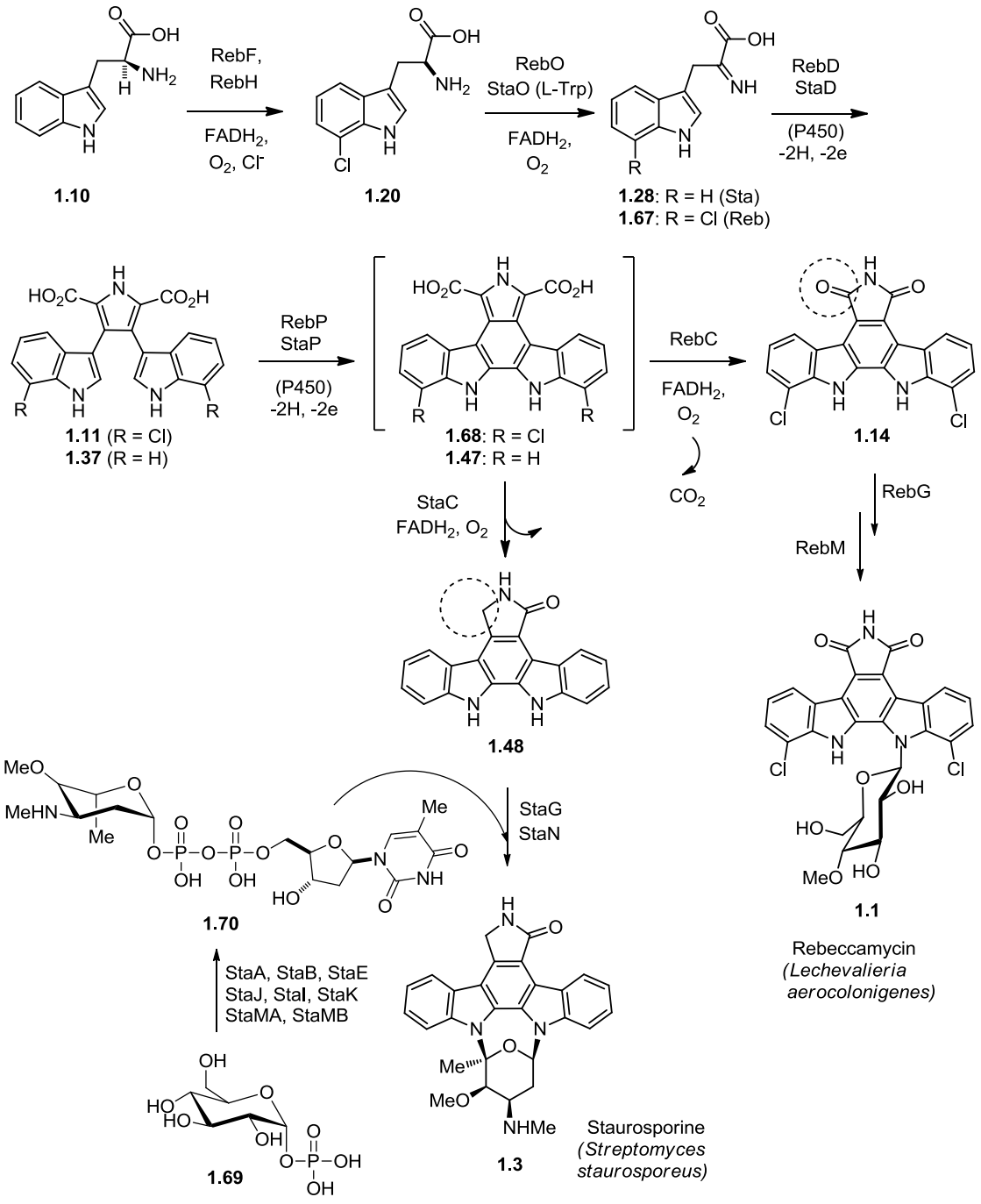

Scheme 1.11. Overall biosynthetic pathways of rebeccamycin and staurosporine

positions of the indole rings, via an initial PCET mechanism involving an iron-oxo porphyrin species (Cpd II), followed by bond-formation coupled electron-transfer (BFCET) process and a series of proton transfers and final tautomerization. The resulting reactive intermediate is rapidly sequestered by the flavin-dependent hydroxylase RebC, where it undergoes oxidative decarboxylation to form the indolocarbazole aglycon of rebeccamycin **1.14**. Finally, RebG and RebM perform glycosylation and methylation, respectively, leading to rebeccamycin (**1.1**). The related staurosporine biosynthetic pathway is essentially analogous up to the formation of **1.47**. Chemoselective oxidation with StaC forms indolocarbazole **1.48**, to which sugar **1.70** is appended in a glycosylation reaction catalyzed by StaG. StaN activity results in the construction of the second sugar linkage, generating staurosporine (**1.3**).

1.2.3 Biosynthesis of structurally diverse indolocarbazoles

The enzymes involved in rebeccamycin and staurosporine biosynthesis perform essentially analogous reactions in converting 7-Cl-L-Trp or L-Trp, respectively, to the corresponding indolocarbazole aglycons. Interestingly, the bioactive properties of these two compounds are very distinct (rebeccamycin is a potent DNA topoisomerase I poison, whereas staurosporine mimics ATP and inhibits protein kinases in the 1-20 nM range).[59, 60] Division of the indolocarbazole natural products into categories based on the relationship between structure and function was addressed in Figure 1.1.

The biosynthetic gene cluster responsible for staurosporine biosynthesis (*Streptomyces longisporoflavus*) was cloned and characterized shortly after that of rebeccamycin.[61] It was found to be strikingly similar to the rebeccamycin biosynthetic gene cluster, containing 14 ORF's spanning 20-kb. Sequence homology comparisons revealed that three of the ORFs (*staO*, *staD*, and *staP*) encoded proteins necessary for indolocarbazole formation, although an ORF corresponding to *staC* was not identified initially. Eight genes were identified that encoded biosynthesis of the deoxysugar **1.70** (as shown in Scheme 1.10), as well as two other genes (*staG* and *staN*) that encode glycosidic bond formation between staurosporine aglycon **1.48** and deoxysugar **1.70** The requirement of a two-enzyme system for attachment of the sugar moiety to **1.48** is further evidenced by the translational coupling of StaN with StaG, which suggests that these two enzymes need to be translated at the same time and in equal amounts. Formation of the

second linkage between the indolocarbazole and dihydrostreptose moiety via an oxidative C-N coupling reaction was supported by the similiarity of StaG to the cytochrome P450 hydroxylase found in the daunorubicin biosynthetic gene cluster.[62] Heterologous expression of the staurosporine cluster in *Streptomyces lividans* TK23 resulted in the production of staurosporine, indicating that the cloned fragment contained all of the genes necessary for staurosporine biosynthesis.[61]

The unique sequence of the RebD gene has proven to be a useful probe to screen for indolocarbazole biosynthetic clusters in other bacterial strains and even metagenomic DNA isolated from soil. Application of this strategy resulted in the discovery of a gene encoding a RebD enzyme homologue in *Nocardiopsis* sp. NRRL15532 chromosomal DNA,[63] and subsequent identification of the biosynthetic cluster for K252a and K252c.[64] The 45-kb DNA sequence was found to contain 35 ORF's, whose functions were predicted based on comparison with known proteins. Four identified genes (*nokA*, *nokB*, *nokC* and *nokD*) displayed significant sequence homology to indolocarbazole biosynthetic genes involved in rebeccamycin, staurosporine, and AT2433 biosynthetic pathways, suggestive of related functions of the corresponding enzymes. Attachment of the sugar unit was presumed to occur through a two-stage process involving a glycosidation reaction catalyzed by NokL, and a subsequent oxidative C-N coupling reaction mediated by NokJ to produce the indolocarbazole metabolite K-252b (**1.71**), in an analogous fashion to the action of StaG and StaN in staurosporine biosynthesis. Subsequent methylation by NokK produces the related metabolite K-252a (**1.4**). The promiscuous glycosyltransferase NokL was demonstrated to accept TDP-L-rhamnose as an alternative substrate to the dihydrostreptose sugar found in K-252a, and resulted in the production of a different indolocarbazole metabolite, K-252d (**1.72**). Variants of K-252d having regioselectively methylated sugar hydroxyl groups (**1.73** and **1.74**) were identified as a result of the methyltransferase activity of NokM. Thus, the versatility of indolocarbazole biosynthetic pathways in *Nocardiopsis* sp. NRRL15532 has been demonstrated by the numerous indolocarbazole metabolites that can be produced (see Figure 1.12).

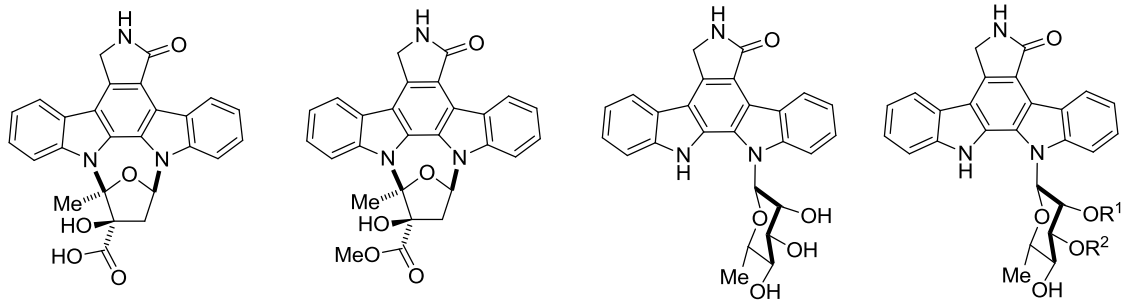

Figure 1.12. Indolocarbazole metabolites produced by *Nocardiopsis* sp. NRRL15532[63,64]

Interesting modifications of indolocarbazole biosynthetic pathways have been observed in the case of the natural products violacein (**1.19**),[22] discussed in 1.2.1, and the indolotryptoline BE-54017 (**1.83**) recently reported by Brady and co-workers,[65] shown in Scheme 1.12a,b. As shown in Scheme 1.12a, VioA and VioB are homologues of RebO and RebD which convert **1.10** into CPA **1.37**, through the intermediate imine of indole-3-pyruvic acid **1.28**. VioE, an enzyme that is absent in the rebeccamycin and staurosporine biosynthetic pathways, catalyzes a unique 1,2-indole migration affording intermediate **1.75**, and further enzymatic chemistry produces violacein **1.19**. The biosynthetic gene cluster for indolotryptoline BE-54017 **1.83** contains some interesting enzymes that have no homologues in rebeccamycin or staurosporine biosynthetic pathways. Brady recently demonstrated that the monooxygenases AbeX1 and AbeX2 are responsible for conversion of the indolocarbazole framework to the indolotryptoline ring system, via epoxidation chemistry. Regioselective epoxidation of **1.76** by AbeX1 and subsequent epoxide opening affords *trans*-diol **1.78**. AbeX2 performs a second epoxidation to form **1.79**, and epoxide opening occurs such that the indolocarbazole ring system is opened, yielding hydroxy product **1.80**. Intramolecular ring closure forms *cis*-diol **1.82**, and further enzymatic chemistry (mediated by AbeM1-M3) affords BE-54017 (**1.83**).

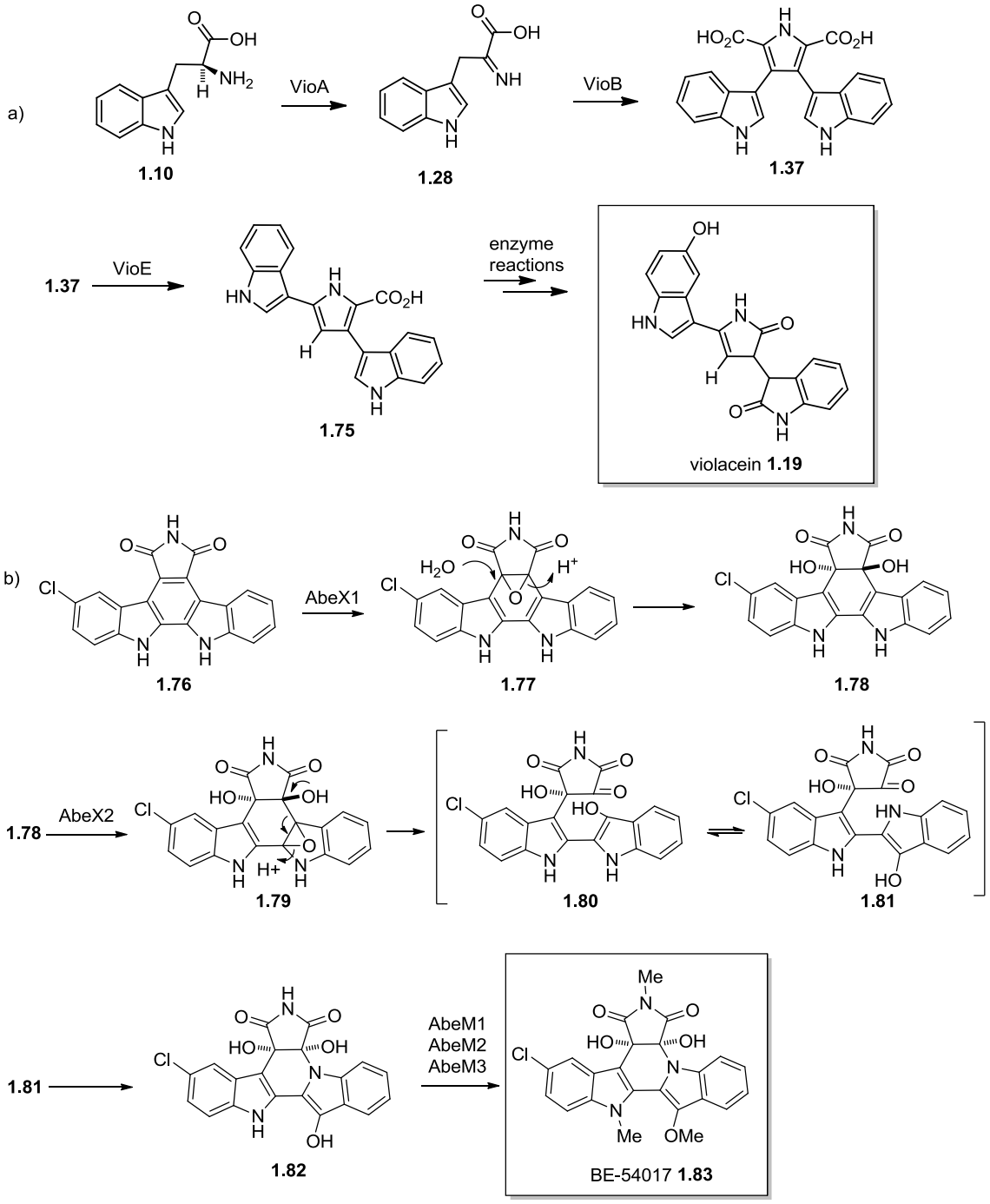

Scheme 1.12. Enzymatic chemistry unique to the indolocarbazole related natural products violacein **1.19** (a)[22] and BE-54017 **1.83** (b)[65] `

Analysis of the biosynthetic pathways responsible for the production of the indolocarbazole alkaloids rebeccamycin, AT2433, staurosporine, and K252a revealed the presence of four homologous enzymes necessary for generation of the respective indolocarbazole aglycons. It is clear from the preceding discussion, that in addition to the standard enzymes involved in formation of the indolocarbazole core, functionally unique enzymes have also evolved and been incorporated into diverse natural product biosynthesis pathways. Consequently, biosynthesis of remarkable natural products such as violacein and BE-54017, having unprecedented structural diversity, are a testament to the needs of producing bacteria to exploit antibacterial and antifungal properties of such complex natural products (in order to ensure survival in an environment in which competing organisms are present).

1.2.4 Combinatorial biosynthesis of indolocarbazoles

The important bioactive properties of rebeccamycin, staurosporine and related indolocarbazoles have resulted in the generation of novel indolocarbazoles using a combinatorial biosynthesis approach.[66] Sanchez et al. have described combinatorial biosynthesis as a "metabolic engineering toolbox by which genes responsible for individual metabolic reactions from different organisms are combined to generate metabolic pathways to biosynthesize products that were previously inaccessible or difficult to obtain."[67]

Structural variation can be achieved in many ways, including precursor feeding (via modified RebO substrates, or downstream modification by glycosidation using non-natural sugar moieties), mutagenesis, or modification of fermentation conditions. Indolocarbazole biosynthetic pathways are particularly suitable for combinatorial biosynthesis, owing to their unique substrate acceptance profiles and the ability to interchange enzymes from similar biosynthetic pathways. For example, incorporation of StaC into the rebeccamycin biosynthetic pathway will produce an indolocarbazole bearing the modified glucose found in rebeccamycin attached to the staurosporine aglycon. Substitution of $FADH_2$ dependent halogenases (such as replacement of RebF by PrnA) can result in interesting halogenation patterns in the indolocarbazole that might be difficult or impossible to access using synthetic or semi-synthetic approaches. The molecules resulting from these processes have significant potential as new bioactive compounds.

Sanchez et al. co-expressed different indolocarbazole biosynthesis genes from either one pathway or a combination of pathways in the heterologous host *Streptomyces albus*, and were able to generate greater than 30 novel indolocarbazole compounds using the recombinant strains.[67] Combinations of thirteen genes from four different organisms were used for the generation of novel compounds. Nine genes required for rebeccamycin biosynthesis in *L. aerocolonigenes* (*rebH*, *rebO*, *rebD*, *rebP*, *rebC*, *rebG*, *rebM*, *rebF*, and *rebT*) allowed dissection and reconstitution of the biosynthetic pathway in the heterologous host, and two genes from the staurosporine biosynthetic pathway in *S. longisporoflavus* (*staC* and *staP*) were also employed in the study. The *rebT* gene (encoding a membrane transporter protein) was required due to the toxicity of rebeccamycin towards the host strain. Variation in halogenation patterns was achieved by incorporation of halogenases found in other biosynthetic pathways, specifically the Trp-5-halogenase *pyrH* (involved in pyrrolomycin biosynthesis in *S. rugosporus* LL-42D005),[68] or the Trp-6-halogenase *thaI* (involved in thienodolin biosynthesis in *S. albogriseolus*).[69]

Specific examples of modified indolocarbazoles that have been obtained using this approach are presented in Figure 1.13. Generation of "hybrid" staurosporine indolocarbazole **1.84** bearing the rebeccamycin sugar moiety was achieved by recombinant strains harbouring either of the gene combinations shown in Figure 1.13a. Unnatural halogenation patterns of the staurosporine and rebeccamycin aglycons have been realized through combination of *reb* and *sta* genes with the *pyrH* or *thaI* genes required for pyrrolomycin or thienodolin biosynthesis, respectively. Consequently, regioselective introduction of chlorine at the C-3 position of the rebeccamycin aglycon (**1.85**, Figure 1.13b) was realized when the *pyrH* gene was used in combination with *rebC* and *staC*, and similarly, C-3 chlorination of the staurosporine aglycon was realized with a *pyrH*, *rebODP* and *staC* combination, affording **1.86** (Figure 1.13c).

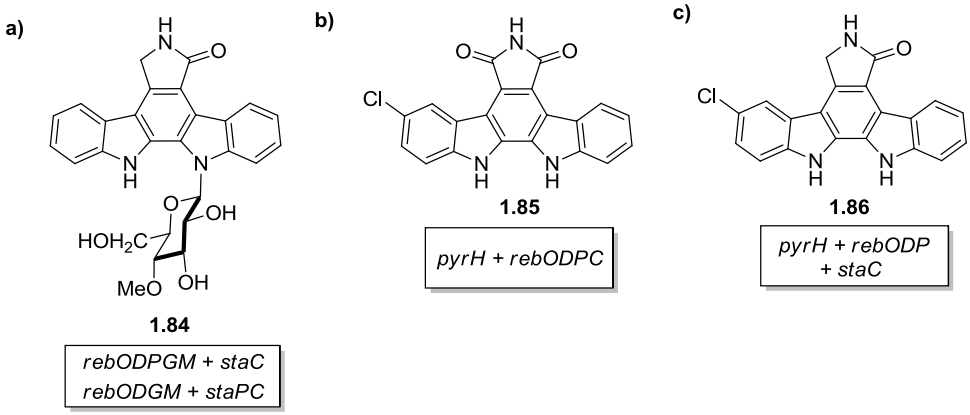

Figure 1.13. Combinatorial biosynthesis of "hybrid" indolocarbazoles;[67] a) staurosporine aglycon bearing rebeccamycin sugar moiety, b) and c) unnaturally halogenated rebeccamycin and staurosporine aglycons

Targeting novel glycosylated indolocarbazoles has also been a focus of combinatorial biosynthesis in recent years. With the knowledge that the glycosyltransferase StaN and cytochrome P450 enzyme StaG are required for introduction of the bis-linked sugar moiety of staurosporine, the ability of these enzymes to attach novel sugars was explored.[70] The flexibility of StaG towards D or L deoxysugars allowed for generation of novel glycosylated compounds, although StaN had more stringent requirements and was only tolerant of L-sugars in generating the second linkage of the sugar to the indolocarbazole framework. Salas and Mendez took advantage of the flexibility of StaG and StaN, as well as the corresponding enzyme RebC required for rebeccamycin biosynthesis and generated a larger library of mono- and bis-glycosylated derivatives of rebeccamycin and staurosporine.[71] The importance of combinatorial biosynthesis of glycosylated indolocarbazoles was also demonstrated by Sanchez and co-workers in 2009,[72] who used this strategy for the development of potent and selective kinase inhibitors.

1.3 Total Synthesis of Indolocarbazoles

The significant biological activity of the indolocarbazole alkaloids has captured the attention of synthetic chemists, and numerous strategies have been used in total synthesis efforts, initially of the indolocarbazole aglycon, and subsequently of the glycosylated natural products. Comprehensive review of the historical synthetic routes used to prepare indolocarbazole aglycons is beyond the scope of this discussion, as these methods have recently been summarized in an

excellent review by Knolker and Reddy,[73] which the reader is encouraged to access for more comprehensive coverage of this topic. Historically, the Fischer indole synthesis has been widely used as a key reaction in the total synthesis of the indolo[2,3-a]carbazole ring system as described initially by Bhide et al. in 1957,[74] and subsequently by Mann and Wilcox in the following year.[75] These procedures involved either Fischer indolization of 1,2,3,4-tetrahydrocarbazole-9H-carbazol-1-one or cyclohexane-1,2-dione monophenylhydrazone (upon reaction with phenylhydrazine), or indolization of the hydrochloride of 1,2,3,4-tetrahydrocarbazole-9H-carbazol-1-one phenylhydrazone. Kirsch further applied this methodology to the synthesis of indolocarbazoles, starting from tricyclic ketones of similar structure to 1,2,3,4-tetrahydrocarbazole-9H-carbazol-1-one.[76] Bergman and Pelcman described an alternative approach involving a double Fischer indolization of bis(phenylhydrazones) **1.90**, realized in the presence of PPSE (Scheme 1.13).[77] Preparation of **1.89** was achieved via cycloaddition of 2,3-bis[(trimethylsilyl)oxy]butadiene **1.87** with maleimides **1.88**, producing the bis(trimethylsilyl)-protected α-hydroxy ketones **1.89** in 90% yield, regardless of the R substituent. Reaction of **1.89** with excess arylhydrazine (3 equiv) afforded 1,2-bis(phenylhydrazones) **1.90** which underwent smooth Fischer indolization to **1.91** in the presence of polyphosphoric acid trimethylsilyl ester (PPSE). Aromatization to generate indolocarbazoles **1.92** was readily achieved upon exposure of the crude Fischer indolization reaction product **1.91** to Pd/C or DDQ dehydrogenation conditions, and proceeded in good to excellent yields without the requirement for intermediate purification.

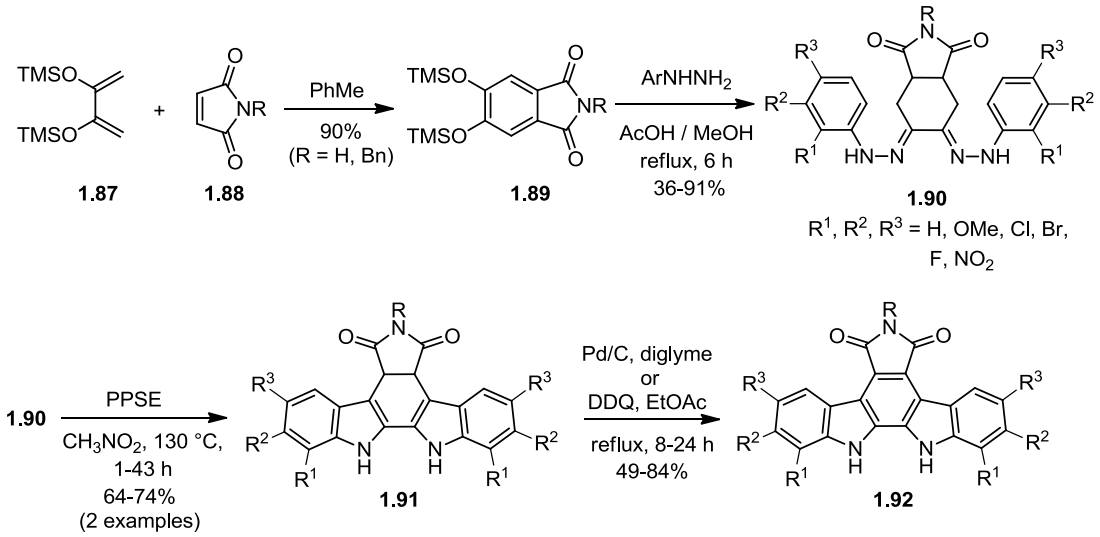

Scheme 1.13. Bergman and Pelcman's synthesis of indolocarbazoles[77]

Sequential palladium-catalyzed Suzuki and Sonogashira cross-coupling reactions were used during the five-step indolocarbazole synthesis described by Merlic and McInnes in 1997 (Scheme 1.14).[78] Treatment of indole (**1.93**) with *n*-BuLi followed by CO_2 electrophile quench of the resulting anion generated an intermediate indole-*N*-carboxylate, known to act as a transient directed metalation group (DMG). Subsequent directed *ortho* metalation (D*o*M) chemistry using *t*-BuLi as the base resulted in regioselective C-2 lithiation, and use of ICH_2CH_2I as the electrophilic quench reagent afforded the desired 2-iodoindole **1.94** in 91% yield.[79] *N*-methylation followed by metal-halogen exchange and subsequent Li→B transmetalation of **1.95** allowed for the in situ generation of boropinacolate ester **1.96**, which underwent Suzuki cross-coupling with 2-iodo indole **1.94** to form the bis-indole intermediate **1.97** in 51% yield. Electrophilic iodination using the procedure of Bocchi and Palla,[80] followed by *N*-methylation, afforded Sonogashira coupling partner **1.98** which, in subsequent Sonogashira coupling and benzannulation reactions, afforded indolocarbazoles **1.99** and **1.100** in respectable yields.

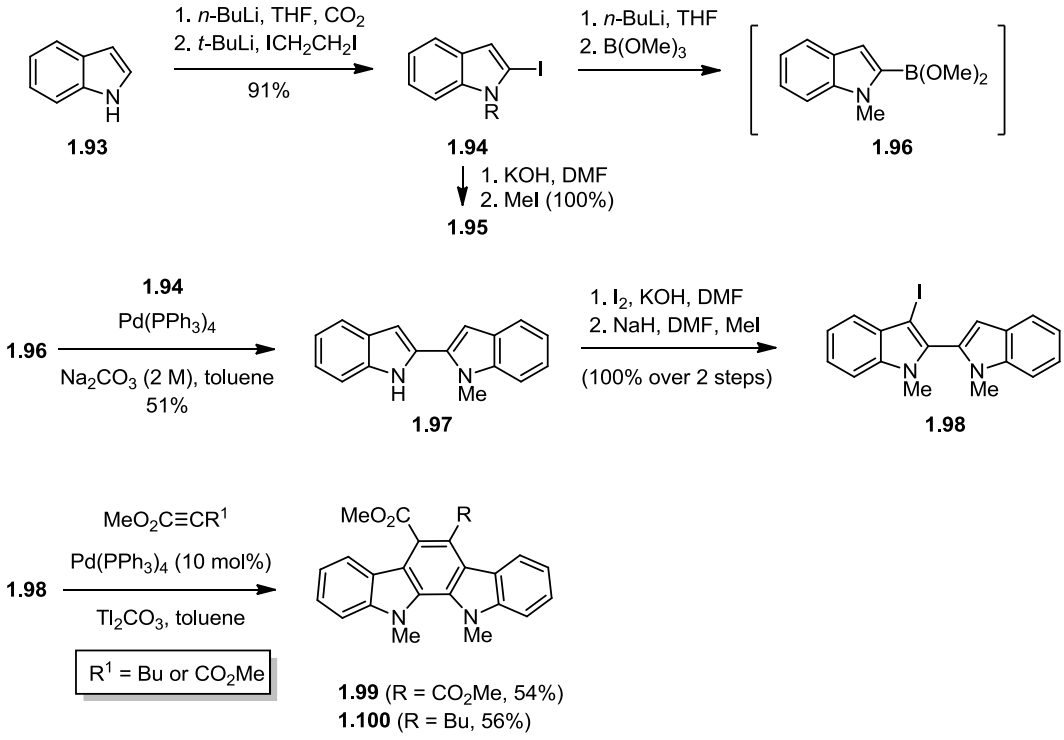

Scheme 1.14. Application of Suzuki and Sonogashira coupling in Merlic and McInnis indolocarbazole synthesis[78]

Rajeshwaran and Mohanakrishnan recently described an 11 step total synthesis of the staurosporine aglycon starting from 2-methyl indole **1.101** with an overall yield of 28-36% (Scheme 1.15).[81] Prominent key steps in the synthesis involved the thermal electrocyclization of divinyl indole **1.102** to afford the carbazole **1.103** which was converted to tetracyclic carbazole **1.105** via allylic bromination and amidation. Intramolecular nitrene insertion of **1.105** completed the synthesis of indolocarbazole **1.106**. Synthesis of the staurosporine aglycon **1.107** was completed upon hydrolytic cleavage of the *N*-benzenesulfonyl protecting group in a refluxing solution of potassium carbonate in a MeOH:THF mixture.

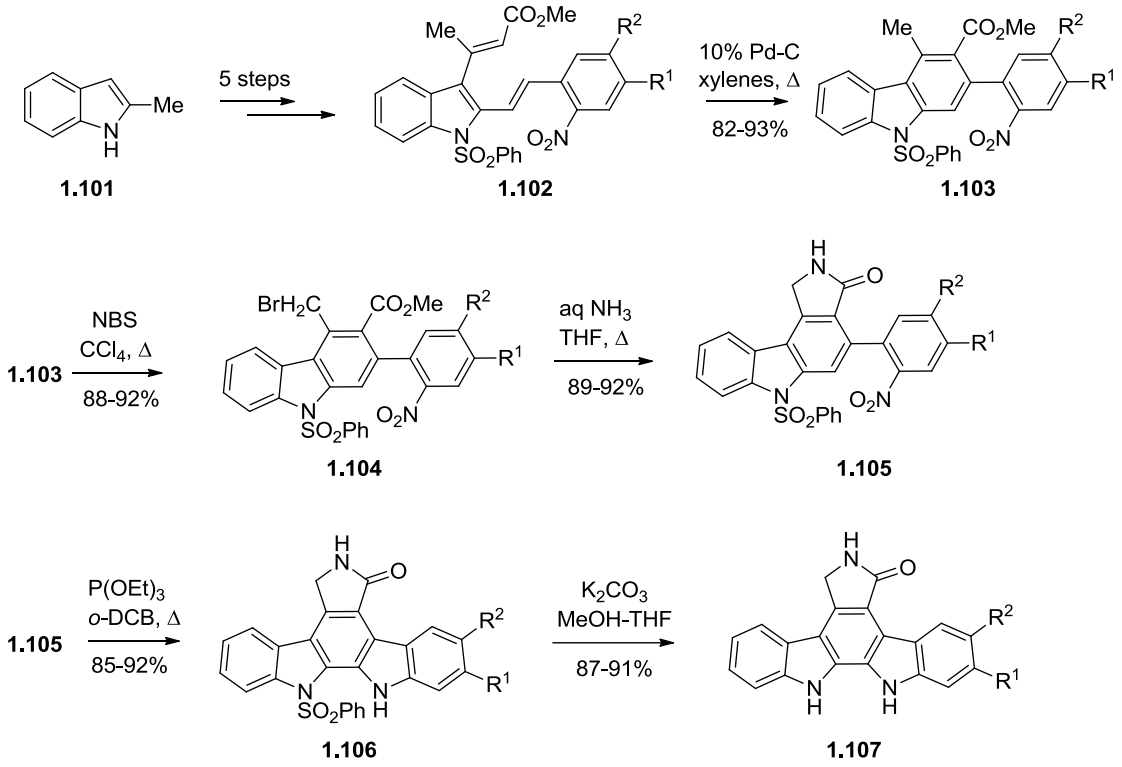

Scheme 1.15. Rajeshwaran and Mohanakrishnan total synthesis of staurosporine aglycon using electrocyclization and nitrene insertion as key steps[81]

Despite the elegant methods for the synthesis of indolocarbazole compounds described thus far, the most straightforward preparative method still involves the oxidative cyclization of a bis-indolylmalemide (prepared either by Suzuki cross-coupling of an indole boronic acid or an indole Grignard reagent with a dihalomaleimide). These facile routes to the indolocarbazole core

have been employed in the synthesis of the rebeccamycin and staurosporine aglycons,[82] as well as synthetic analogues of staurosporine and rebeccamycin having significant biological activities.[83]

Danishefsky and co-workers developed a powerful synthetic method for the stereospecific construction of indole β-*N*-glycosides via intermolecular coupling of indole anion with 1,2-anhydrosugars. This approach was used in the first total synthesis of rebeccamycin reported in 1993 (Scheme 1.16).[84]

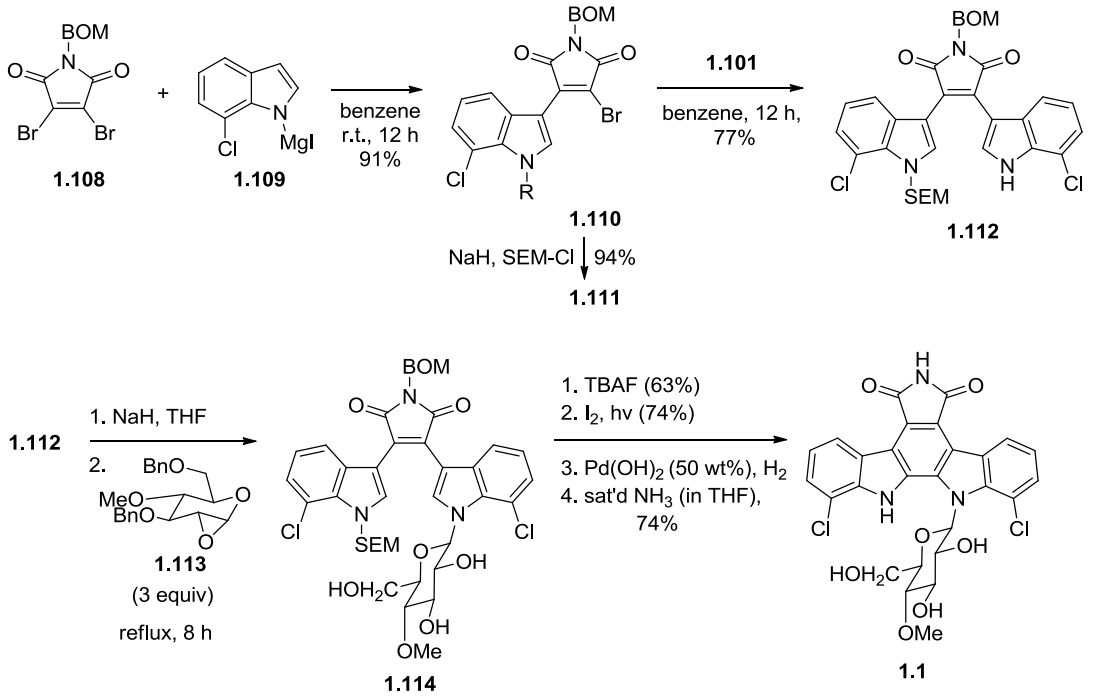

Scheme 1.16. Danishefsky's total synthesis of rebeccamycin via stereospecific glycosidation[84]

The sequence of reactions began with two successive Michael additions of indole Grignard reagent **1.109** onto the *N*-protected dibromomaleimides **1.108** and **1.111**. As shown in Scheme 1.15, the occurrence of bis-glycosylation was avoided by an intermediate SEM-protection of the indolic nitrogen of **1.110**, prior to the second Michael addition. Glycosylation of the unsymmetrical bis-indolylmaleimide **1.112** was achieved by reaction with anhydrosugar **1.113**, followed by SEM group cleavage and photochemical C-C bond formation to form the indolocarbazole core structure. Final deprotection to reveal the rebeccamycin natural product was not trivial, as reduction of the C-Cl bonds was also observed upon prolonged heating in the

presence of metal catalysts. However, the use of Pearlman's catalyst ($Pd(OH)_2$, 50 wt%) followed by ammonolysis completed the benzyloxymethyl deprotection and afforded rebeccamycin (**1.1**) in 72% overall yield, with only 14% suffering from reductive cleavage of the C-Cl bonds. The characterization data of **1.1** (^{1}H-NMR, ^{13}C-NMR, HRMS, optical rotation) was consistent with the data reported for the isolated natural product.

Stoltz and co-workers employed rhodium carbenoid chemistry in the construction of the indolocarbazole aglycon, and, more specifically, in the racemic total synthesis of K-252a, as well as the asymmetric syntheses of (+)-K252a and (-)-K252a, achieved over a decade ago (1997).[85a-b]

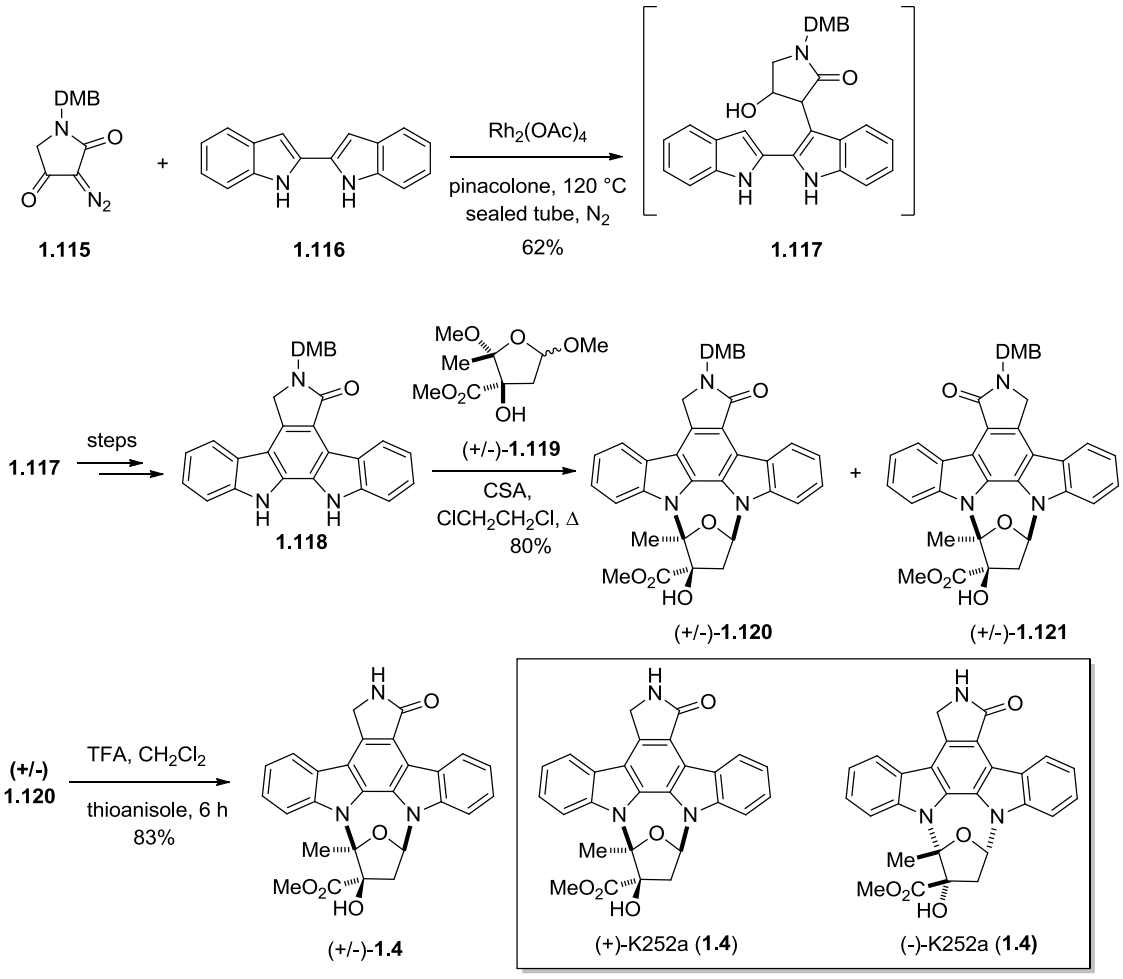

Scheme 1.17. Stoltz and co-workers total synthesis of racemic (±)-K252a (**1.4**) using rhodium-carbenoid chemistry[85a-b]

The racemic synthesis (shown in Scheme 1.17) involved coupling of suitably protected diazolactam **1.115** with 2,2'-bis-indolyl intermediate **1.116** (prepared according to Bergman's procedure involving double Madelung cyclization),[86] followed by cycloaromatization to form the indolocarbazole aglycon **1.118**. The diazolactam coupling reaction was sensitive to numerous parameters, including solvent, presence of oxygen, and protecting group of the diazolactam (which drastically influenced the yield of the coupled product). Optimized conditions required heating the reaction in a sealed tube at 120˚C in rigorously deoxygenated pinacolone. Without protection of the diazolactam, the reaction proceeded in modest 25% yield, but increased to 62% when 3,4-DMB was used as the protecting group. The first racemic synthesis of the K252a carbohydrate was developed,[80a] and produced the two diastereomeric furanose products of **1.119**. Attachment of the bis-linked furanose sugar was achieved through a modified McCombie cycloglycosylation strategy,[87] in the presence of CSA. The reaction proceeded with high stereoselectivity to afford the regioisomeric furanosylated indolocarbazoles (±)-**1.120** and (±)-**1.121**. Deprotection conditions reported by Steglich for the removal of 2,4-DMB groups from peptides (TFA and thioanisole in dichloromethane at room temperature)[88] afforded racemic (±)-K252a (**1.4**). Enantioselective syntheses of the carbohydrate precursors **1.119** required for the asymmetric syntheses of (+)-K252a and (-)-K252a were also achieved and underwent successful cycloglycosidation with **1.118**. Cleavage of the DMB protecting group afforded the desired enantiomerically pure compounds of **1.4** (shown in the inset of Scheme 1.17).

Incorporation of methodology developed for rebeccamycin total synthesis was subsequently applied in Danishefsky's total syntheses of *ent*-staurosporine **1.130** and *ent*-isostaurosporine **1.131** in 1996 (Scheme 1.18).[89] Prior to this time there were limited examples of chemistry in which a carbohydrate moiety could be attached between two indole nitrogens. The pioneering enantioselective total synthesis of (+)-K252c and (-)-K252c by Wood and co-workers (Scheme 1.16)[85b] involving the attachment of a *bis*-linked furanose sugar was perhaps the most relevant of the established chemistry to the advancement of indolocarbazole glycosidation strategies at the time. The complexity of this synthetic endeavour arises from the non-equivalence of the C-5 and C-7 carbons, and the need for control over the order of sequential glycosylation events. Although the syntheses were very challenging, many important problems were addressed and solved along the way. The final route to **1.130** and **1.131** is presented in Scheme 1.18.

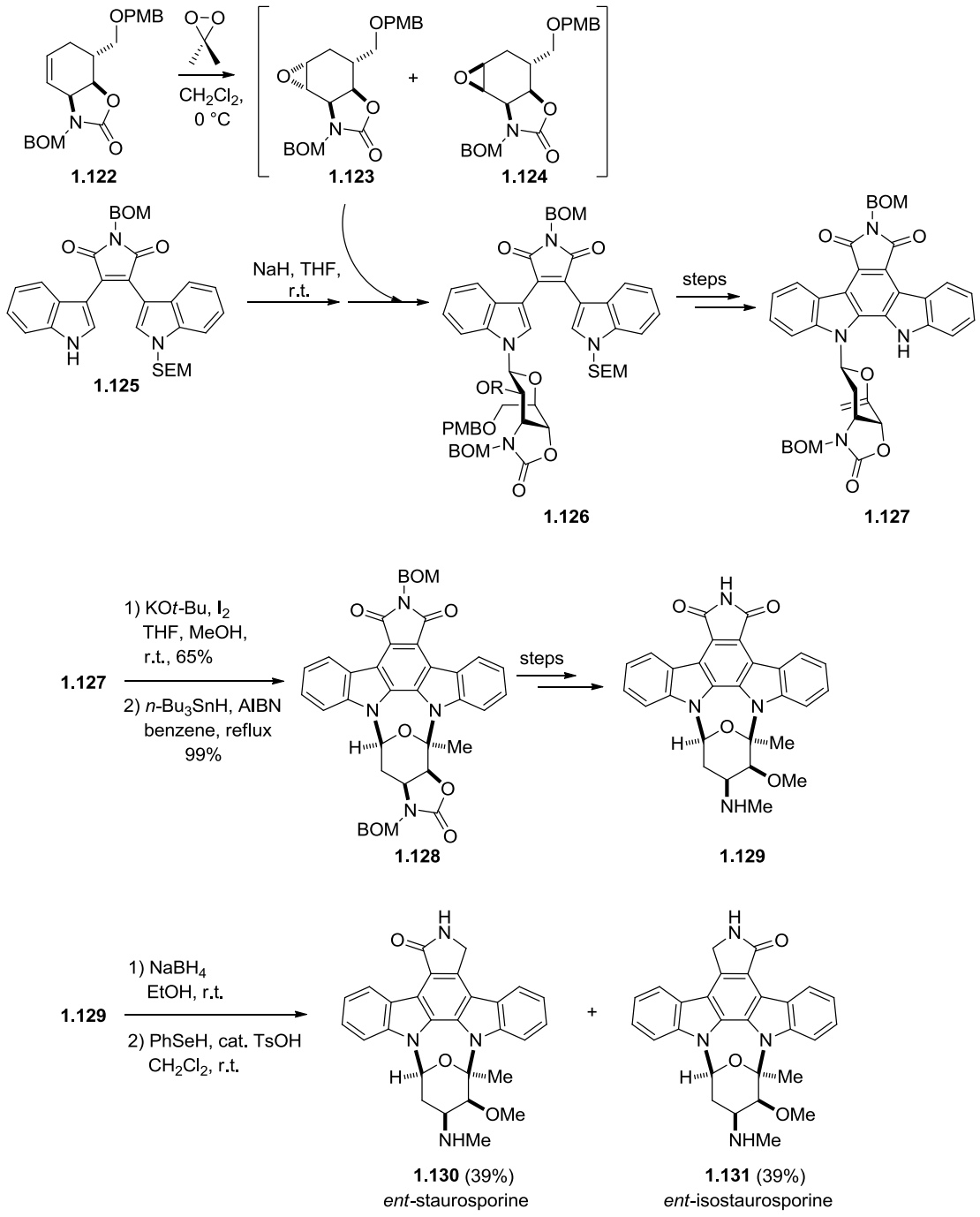

Scheme 1.18. Danishefsky's total synthesis of *ent*-staurosporine and *ent*-isostaurosporine[89]

The sequence of reactions involved initial epoxidation of oxazolidinone glycal **1.122**, followed by preferential reaction of epoxide **1.123** with the bisindolylmaleimide **1.125**. Subsequent chemical modifications of **1.126** afforded indolocarbazole glycoside **1.127**. Deprotonation of **1.127** with potassium *tert*-butoxide and reaction with iodine, followed by subsequent deiodination afforded cyclized product **1.128** in 65% isolated yield. A series of reactions involving oxazolidinone ring opening and protecting group manipulations afforded **1.129**, which produced *ent*-staurosporine **1.130** and *ent*-isostaurosporine **1.131** upon $NaBH_4$ mediated reduction. A similar sequence of reactions was employed in the total synthesis of staurosporine (**1.3**), commencing from the enantiomeric glycosyl donor **1.132** (Scheme 1.19).[89]

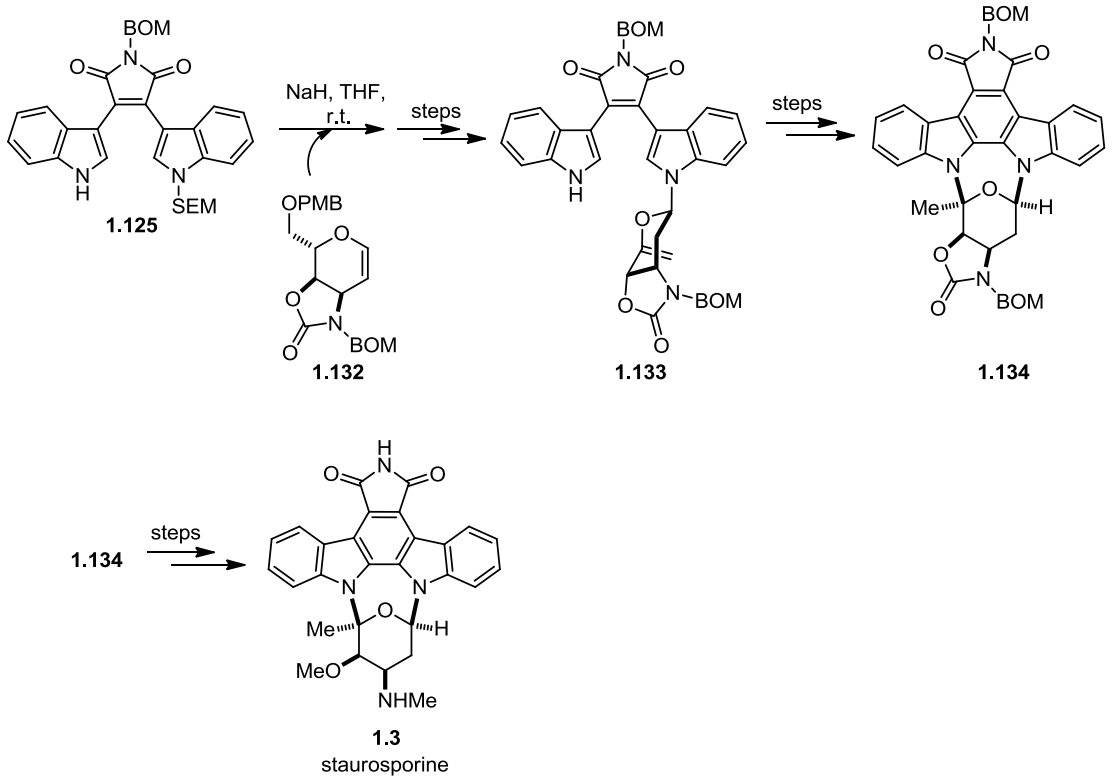

Scheme 1.19. Danishefsky's total synthesis of staurosporine (**1.3**)[89]

The same year that Danishefsky published the total synthesis of staurosporine and *ent*-staurosporine (1996), Stoltz and co-workers reported the total syntheses of pyranosylated indolocarbazoles (+)-staurosporine and its congeners ((+)-RK286c and (+)-MLR-52),[90] from

common intermediate **1.137** (Scheme 1.20), previously employed in the successful total syntheses of (+)-K252c.[85b]

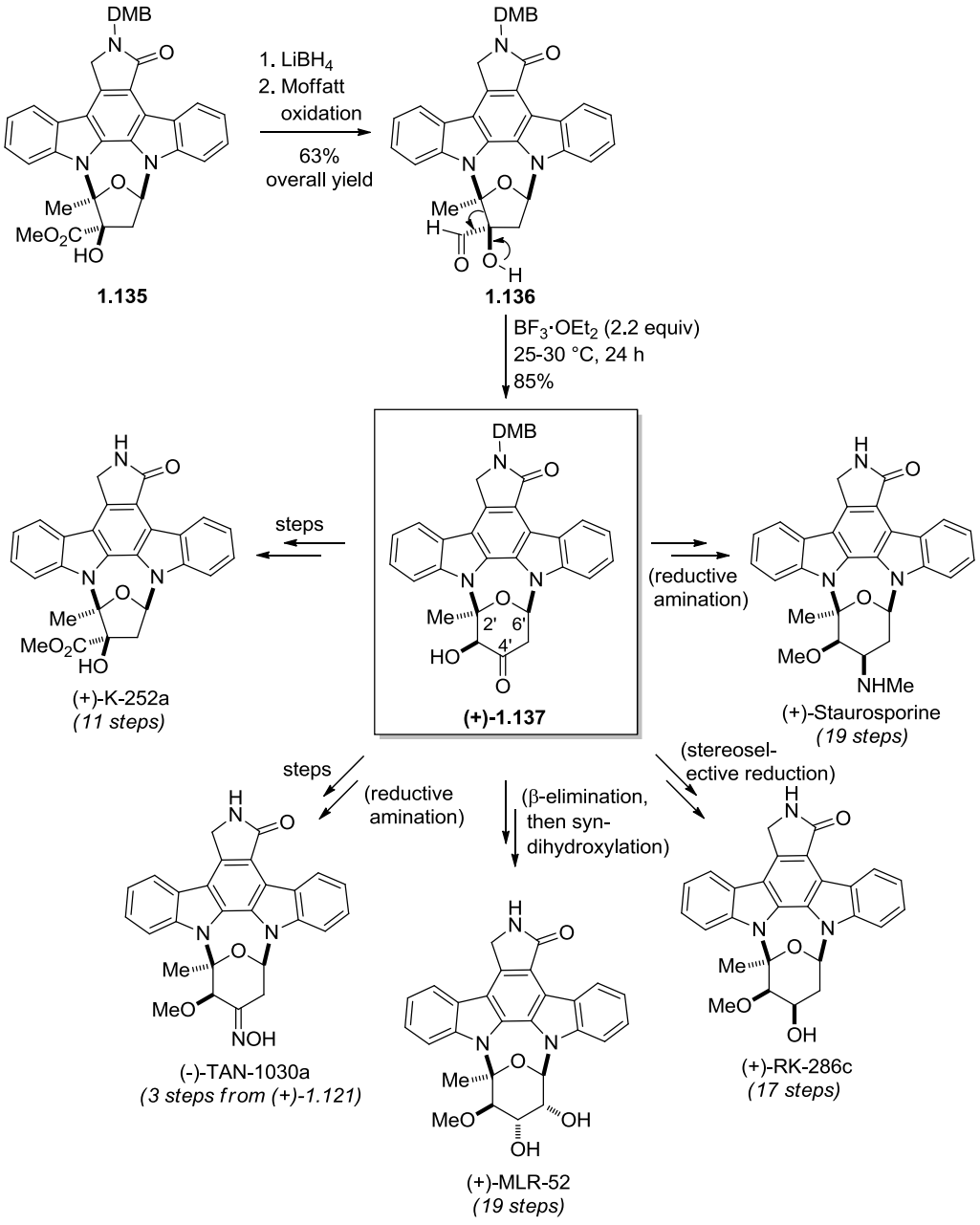

Scheme 1.20. Stoltz methodology for total synthesis of indolocarbazoles from (+)-**1.137**[85,90]

Subsequent application of this methodology to the total synthesis of (-)-Tan-1030a was reported by Stoltz and co-workers in 1997.[91] As shown in Scheme 1.20, **1.137** was prepared in a three step synthesis from precursor **1.135**,[84] commencing with lithium borohydride reduction and Moffatt oxidation to afford aldehyde **1.136** in 63% overall yield. Subsequent stereoselective Tiffaneu-Demyanov-type ring expansion in the presence of boron trifluoride diethyl etherate afforded solely the desired product (+)-**1.137** in excellent yield (85%). The synthetic utility of this intermediate is apparent for two reasons: a) the chiral centres common to indolocarbazole natural products are pre-defined, and b) stereocontrolled chemistry can readily be performed at positions C4' and C5' in accordance with structural requirements of the desired product (ie. through reductive amination, stereoselective reductions, elimination reactions, etc., as shown above), providing convenient routes to a variety of related natural product scaffolds through a convergent synthesis approach.

1.4 Aims of Research

As noted above the flavin dependent monoxygenases RebC and StaC occupy a key branch point in the biosynthesis of indolocarbazoles. This leads to two categories of indolocarbazole aglycons, differing in oxidation state, as exemplified by rebeccamycin (di-oxygenated) and staurosporine (mono-oxygenated). StaC and RebC are also closely related enzymes, having high overall amino acid sequence homology indicative of a common evolutionary origin. However, it is clear that their mechanisms of flavin dependent oxidation are very different, as RebC must perform sequential rounds of oxidation on one equivalent of substrate in order to generate a di-oxygenated aglycon. Thus, the specific features of the RebC and StaC active sites that are necessary to produce the correct oxidation state of the indolocarbazole aglycon remain elusive. To this end a primary goal of my thesis was to elucidate mechanistic differences between RebC and StaC. A simple hypothesis is that the different reactions mediated by RebC and StaC are the result of differences in the amino acid side chains present in the enzyme active sites.

The research aims to test this hypothesis are as follows: i) to reconstitute the indolocarbazole biosynthetic pathway in *E. coli* (because the RebC substrate is too difficult to study *in vitro*), ii) study the effect of active site substitutions on regioselectivity, and iii) propose a

mechanism that can inform further experiments. The work described in the remainder of this chapter is based on the hypothesis that mutation of the six amino acids indicated would convert RebC to a StaC like variant, and therefore impose StaC reactivity to RebC and lead to production of the staurosporine aglycon. This would serve as a starting point for understanding the specific amino acid residues responsible for controlling the oxidative outcome, guide the design of additional RebC variants, and allow the proposal of plausible mechanisms in wild-type RebC and RebC variants.

1.5 Results

1.5.1 Sequence and Structural Analysis of RebC

An alignment of the active site amino acids of RebC, AtmC, StaC and InkE suggests a predictive relationship between enzyme structure and corresponding function among RebC and related indolocarbazole biosynthetic enzymes. Many of the amino acids within and in the vicinity of the actives sites are conserved amongst these monooxygenases. The differences between the enzyme active sites are indicated in Figure 1.14 (page 50). Clear differences are observed between specific active site residues that cleanly divide the enzymes into two groups, mirroring the two classes of indolocarbazoles observed (ie.: di- and monoxygenated). Specifically, while RebC and AtmC have R46, G48, F216, A231, R239, and T241 in their respective active sites (RebC numbering), StaC, InkE and NokD utilize K, S, V, S, N and V at these positions, and are indicated in brackets in Figure 1.15 (page 50).

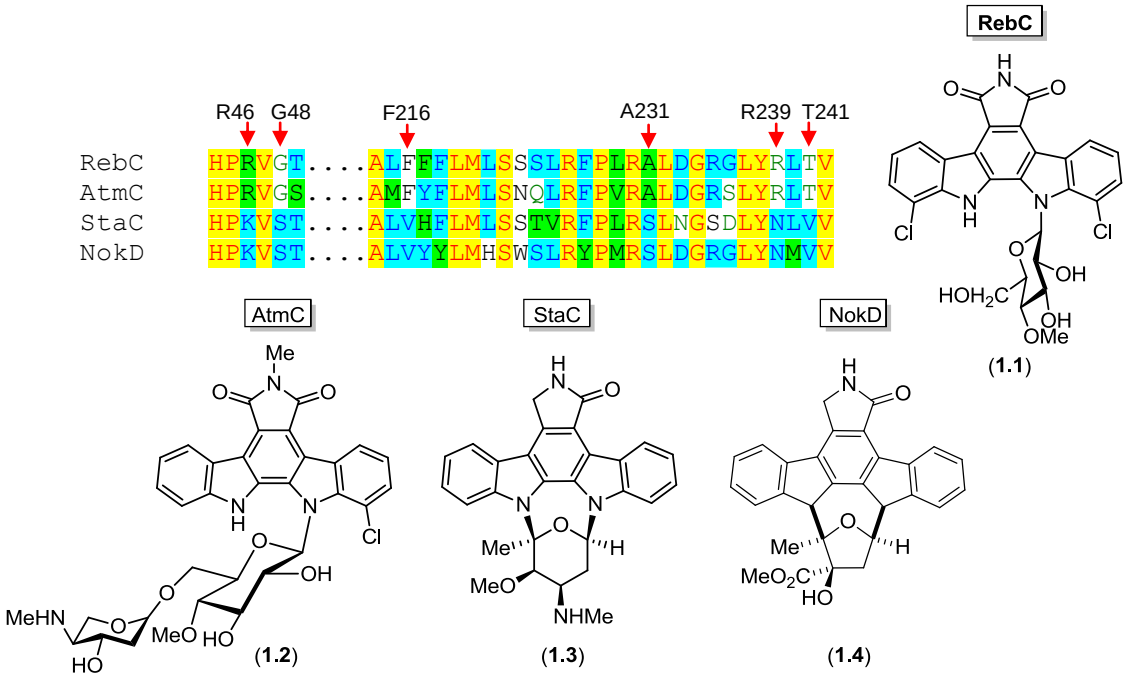

Figure 1.14. Sequence alignment of active site regions in RebC and homologues

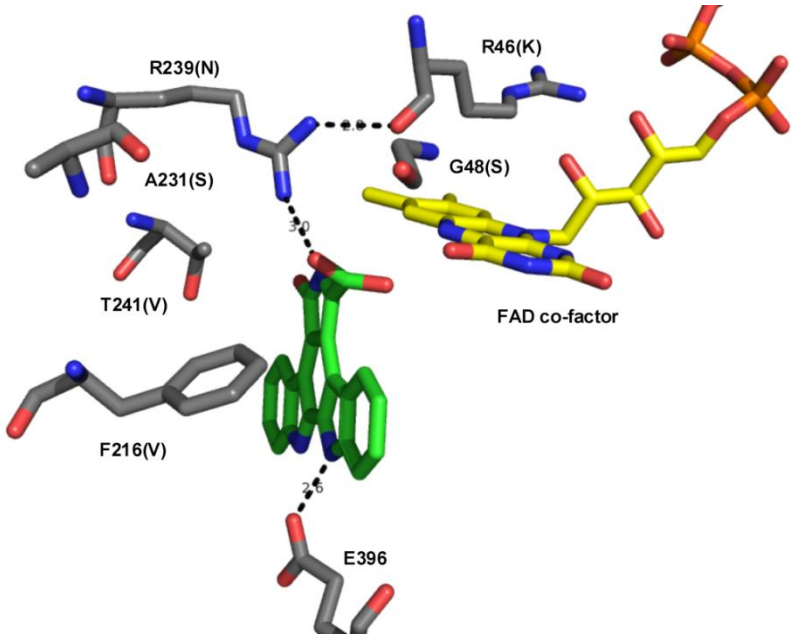

Figure 1.15. RebC active site with StaC residues indicated in brackets. Active site residues are shown in grey, the reactive intermediate in green and the FAD co-factor in yellow. Figure prepared with PyMol (PDB: 2R0G)

1.5.2 PCR amplification of the *rebO*, *rebD*, *rebP* and *rebC* genes

Cloning the rebeccamycin *rebODPC* genes commenced with PCR amplification of the *rebO*, *rebD*, *rebC* and *rebP* genes from the genomic DNA of the producing strain *Lechevalieria aerocolonigenes* ATCC39243. Primers for amplification of *rebO*, *rebP* and *rebD*, *rebC* included NdeI, KpnI and EcoRI, HindIII restriction sites, respectively, for ligation into the corresponding sites of the pET-Duet or pRSF-Duet vectors. The results for the PCR amplification of *rebO*, *rebD*, *rebP* and *rebC* are shown in Figure 1.16. The left lane in each electrophoresis gel image corresponds to a DNA molecular weight ladder, and the right lane shows the result of the individual PCR amplification reactions. The expected sizes of the four genes are as follows: *rebO* (1422 bp), *rebD* (3042 bp), *rebP* (1194 bp) and *rebC* (1607 bp), and the amplified DNA band corresponding to each gene is clearly labeled in Figure 1.16.

Although *rebO*, *rebP* and *rebC* were amplified successfully with negligible amounts of side-products, *rebD* proved to be more challenging due to its large size (3042 bp, Figure 1.16). As indicated by agarose gel electrophoresis, side products were formed in the PCR reaction. Nevertheless, the band corresponding to *rebD* was readily purified from the agarose gel.

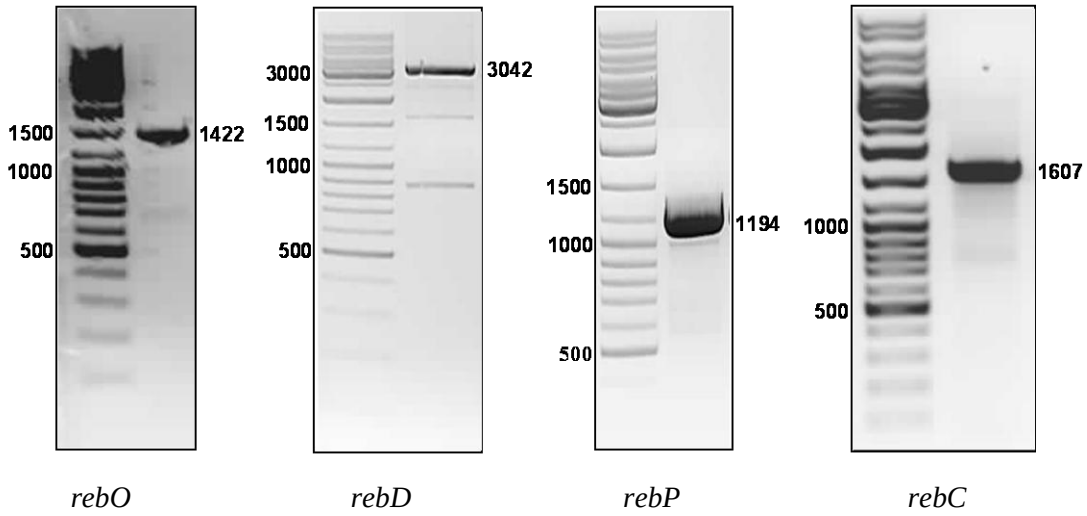

Figure 1.16. PCR amplification of *rebO*, *rebD*, *rebP* and *rebC* as analyzed by agarose gel electrophoresis

1.5.3 Cloning the *rebO, rebD, rebP* and *rebC* genes

The *rebO* and *rebP* PCR products were digested with NdeI and KpnI and ligated into the corresponding sites of pRSF-Duet and pET-Duet, yielding pRSF-Duet-*rebO* and pET-Duet-*rebP*. The *rebD* and *rebC* PCR products were digested with EcoR1 and HindIII and ligated into the corresponding sites of pRSF-Duet and pET-Duet, yielding pRSF-Duet-*rebD* and pET-Duet-*rebC*. After selecting individual clones and isolating plasmid DNA, the presence of the desired insert was confirmed by analytical digests with the same restriction enzymes used for cloning (Figure 1.17). The sequences of the *reb* genes from positive clones were confirmed by DNA sequencing.

Gene inserts were identified in *rebO*, *rebP* and *rebC* clones following analytical digests involving the restriction sites flanking the gene (Figure 1.17a,c,d). DNA sequencing of several clones for each gene resulted in the identification of perfect clones (having no mutations) which were used in future research. The comparable sizes of the cut pRSF-Duet vector (3829 bp) and *rebD* gene (3042 bp) could lead to false conclusions as to whether the insert was present, thus a different set of restriction enzymes was used to analyze the clones for the presence of *rebD*. A fragment of 1898 bp would be observed on the gel if NdeI and RsrII were used for the analytical restriction digest. *RebD* clones analyzed with these enzymes were found to contain this 1898 bp fragment (Figure 1.17b), showing results obtained for 2 clones). DNA sequencing identified a positive clone which was used in future work.

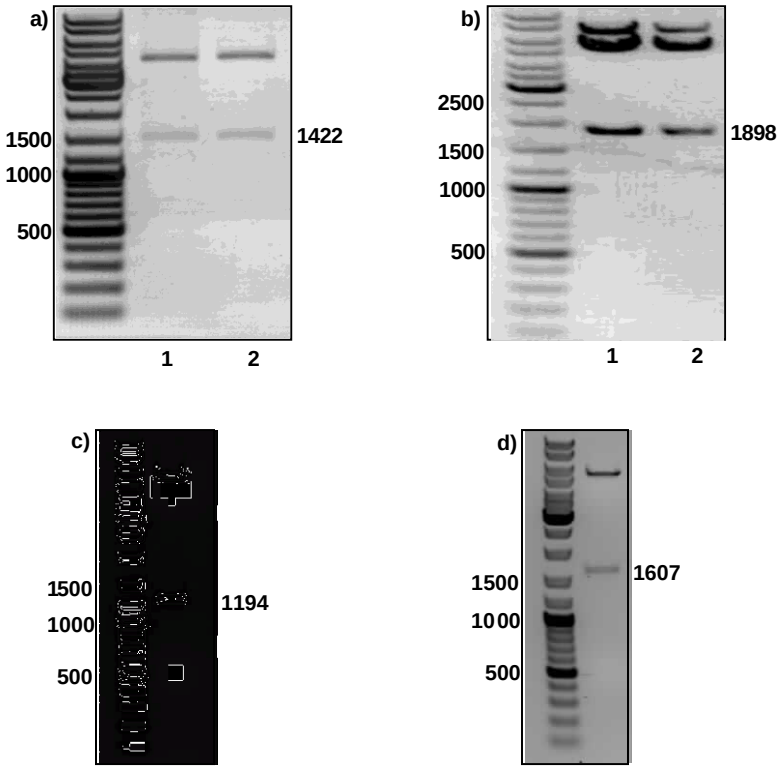

Figure 1.17. Analysis of selected clones by restriction enzyme digests. a) pRSF-Duet-*rebO* clones (digested with NdeI and KpnI (1422 bp fragment expected)); b) pRSF-Duet-*rebD* clones digested with RsrII and NdeI. The *rebD* gene is predicted to afford an 1898 bp fragment when digested with RsrII / NdeI due to an internal RsrII site; c) pET-Duet-*rebP* clones (digested with EcoRI and HindIII (1194 bp fragment expected); d) pET-Duet-*rebC* clones (digested with NdeI and KpnI (1607 bp fragment expected)

Following cloning of the individual *rebO, rebD, rebP and rebC* genes, the *rebO* and *rebP* genes were excised and subcloned into the plasmids containing *rebD* and *rebC*. Analytical digests of resulting pRSF-Duet-*rebOD* and pET-Duet-*rebPC* plasmids showing the presence of the desired *rebO* and *rebP* inserts are shown in Figure 1.18. Schematics of the final pRSF-Duet-*rebOD* and pET-Duet-*rebPC* plasmids are shown in Figure 1.19.

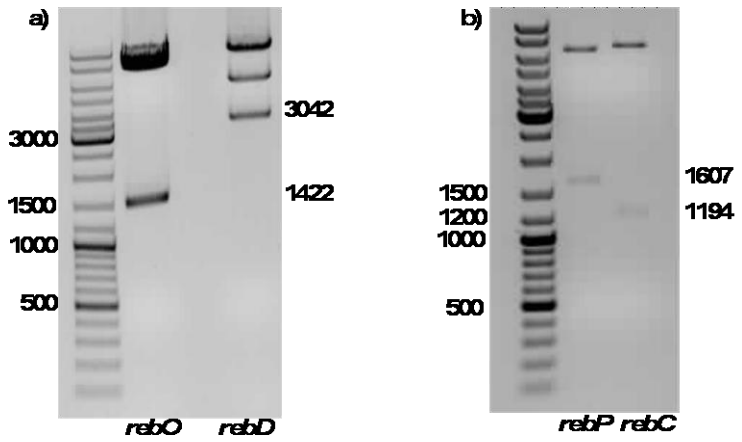

Figure 1.18. Analysis of pRSF-Duet-*rebOD* and pET-Duet-*rebPC* plasmids by restriction enzyme digests; a) pRSF-Duet-*rebOD* (digested with EcoRI / HindIII (1422 bp expected - *rebO*) and NdeI / KpnI (3042 bp expected – *rebD*)); b) pET-Duet-*rebPC* (digested with EcoR1 / HindIII (1607 bp expected – *rebP*) and NdeI / KpnI (1194 bp expected – *rebC*))

.

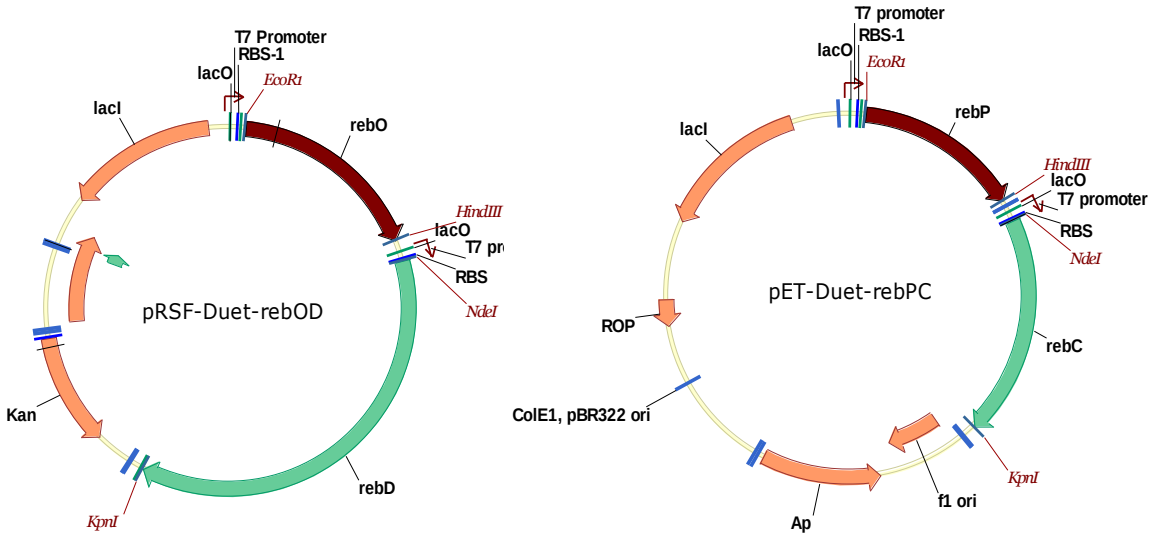

Figure 1.19. Plasmid maps for the final pRSF-Duet-*rebOD* and pET-Duet-*rebPC* constructs. Origins of replication, resistance genes, T7 promoter elements, *reb* genes and restriction enzyme sites used for cloning are indicated.

1.5.4 Generation of *rebC* alleles

As described in the introduction to this chapter, clear differences are observed between specific active site residues of RebC and its protein homologues from other bacterial species, which divide the monooxygenase enzymes into two groups that relate to the types of indolocarbazole products formed. Specifically, the active site of RebC (and AtmC) has R46, G48, F216, A231, R239, and T241, whereas StaC (and NokD, InkE) utilize K46, S48, V216, S231, N239, and V241 at these positions (residues indicated in RebC numbering). We first generated a RebC variant with four of these residues exchanged for the corresponding StaC residues (referred to hereafter as *rebC_4X*). The approach to introducing the mutations in the *rebC* gene by PCR is outlined in Scheme 1.21.

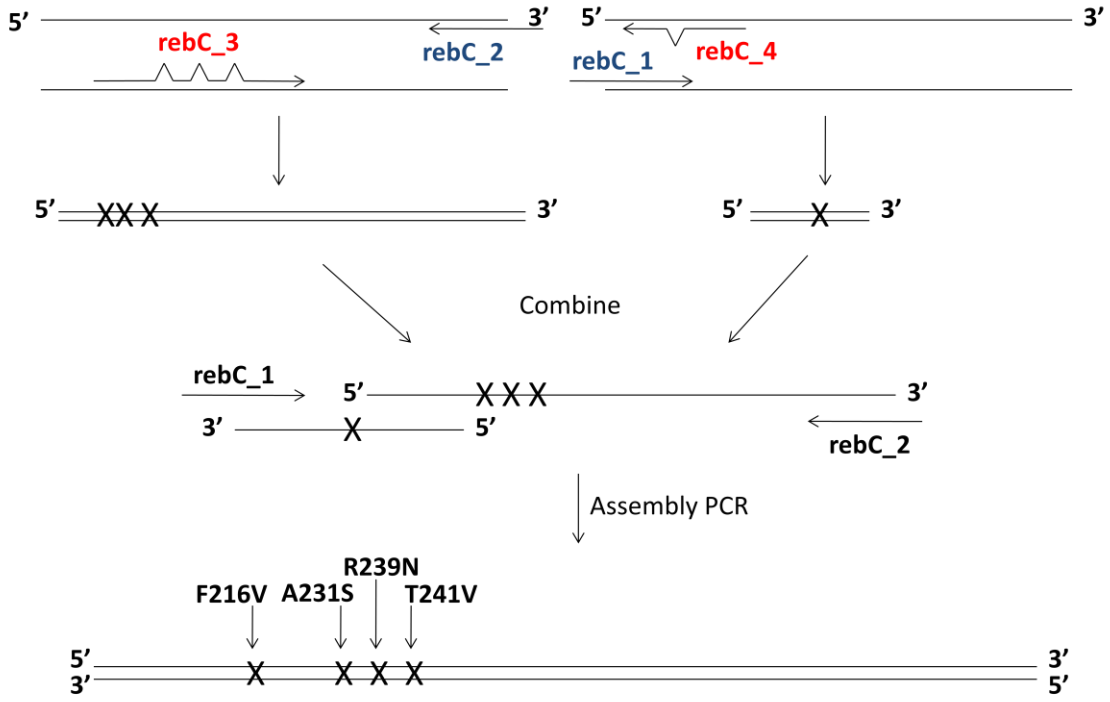

Scheme 1.21. Creation of the *rebC_4X* mutant using a four-primer PCR strategy. The initial mutagenic PCR involves two reactions; the first involves substitution of three base pairs upon amplification of a specific section of the sense strand by the rebC_3 and rebC_2 primer set, and the second involves substitution of a single base pair upon amplification of a specific region of the anti-sense strand by the rebC_1 and rebC_4 primers

Results of the mutagenic PCRs are shown in Figure 1.20. Lanes 1 and 2 correspond to duplicate reactions generating the fragment encoding the A231S, R239N and T241V substitutions (918 bp expected), whereas lanes 3 and 4 correspond to duplicate reactions generating the fragment encoding the F216V substitution (696 bp expected). The PCR products, having complementary sequences, were purified by agarose gel electrophoresis prior to assembly PCR.

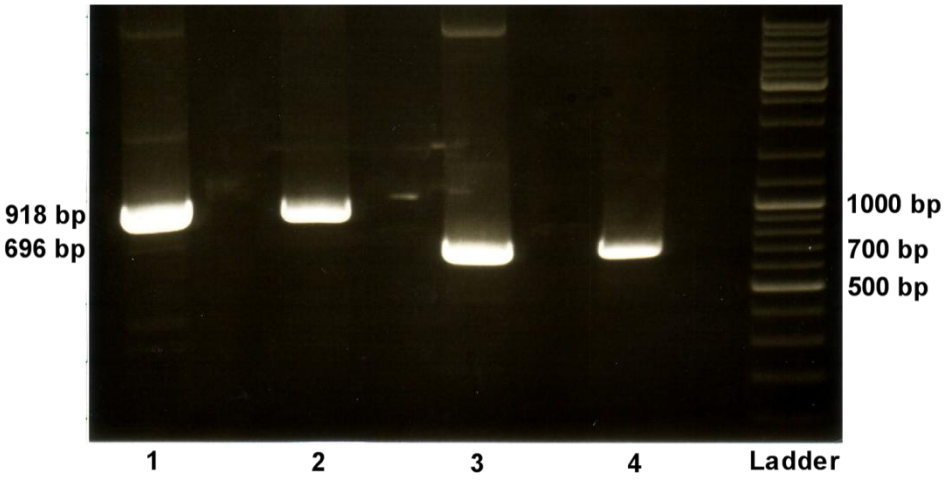

Figure 1.20. Agarose gel electrophoresis (1%) of mutagenic PCRs for construction of the r*ebC_4X* mutant. Lanes 1 and 2: reaction with primers rebC_2 and rebC_3 (918 bp expected). Lanes 3 and 4: reaction with primers rebC_1 and rebC_4 (696 bp expected)

Low molecular weight PCR products were observed when assembly PCR was attempted using standard conditions. Variation of several parameters was tested, and it was found that use of Herc, Vent, or Pfu turbo DNA polymerases did not solve the problem (low molecular weight PCR products were observed, even when longer extension times were used); and increasing the amount of template DNA (mutagenic PCR products) in the reaction mixture (up to 10-fold) also failed to produce any of the desired assembly PCR product using Pfu turbo or Vent polymerase. The assembly PCR was successful when a decreased amount of purified PCR products was used (1/4 as much), using rebC_1 and rebC_2 as the forward and reverse flanking primers and Pfu Ultra II DNA polymerase. In addition to the desired product, low molecular weight PCR products were also observed, but their formation was prevented by an increase in the annealing temperature from 55-58 ˚C (a common tactic to avoid formation of non-specific products), and by

increasing the number of PCR cycles from 25 to 30. Interestingly, use of the same samples and quantity of the mutagenic fragments with Herc polymerase failed to produce the desired *rebC_4X* product. Therefore, it was concluded that the assembly PCR reactions are very sensitive to quantities of DNA template, polymerase, and cycling parameters.

The final pET-Duet-*rebC(4X)P* construct was obtained by ligating the mutant gene into the NdeI and KpnI restriction sites of pET-Duet-*rebP*. Once the *rebC_4X* mutant was verified by DNA sequencing, it was used as the template for creation of the *rebC_6X* mutant encoding the two additional substitutions R46K and G48S (Scheme 1.22). The close proximity of the two mutations allowed the mutagenic primers to encode both substitutions.

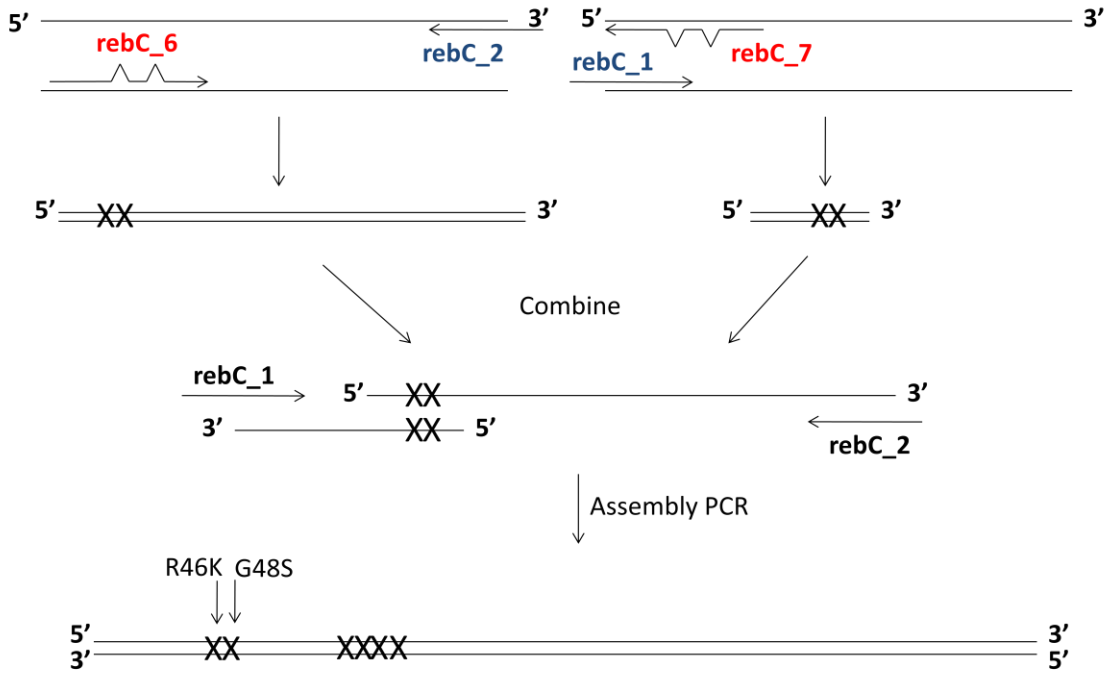

Scheme 1.22. Creation of *rebC_6X* mutant using four-primer PCR strategy. The initial mutagenic PCR involves two reactions; the first involves substitution of two base pairs upon amplification of a specific section of the sense strand by the rebC_6 and rebC_2 primer set, and the second involves substitution of two base pairs upon amplification of a specific region of the anti-sense strand by the rebC_1 and rebC_7 primers

Agarose gel electrophoresis of the mutagenic and assembly PCR reactions that introduced the mutations encoding R46K and G48S are shown in Figure 1.21.

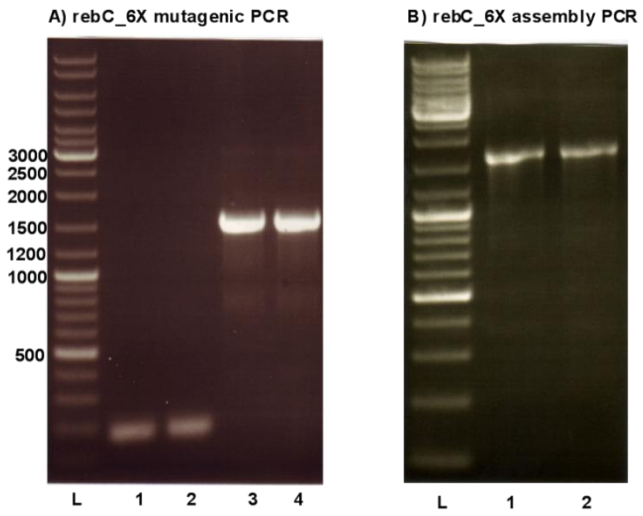

Figure 1.21. Agarose gel electrophoresis (1%) of mutagenic (a) and assembly (b) PCRs used to generate the r*ebC_6X* mutant; a) Lanes 1 and 2: duplicate reactions with primers rebC_1 and rebC_4 (161 bp expected), Lanes 3 and 4: duplicate reactions with primers rebC_8 and rebC_2 (1472 bp expected)

In a similar fashion as the two previous mutants, the *rebC_2X* mutant (F216V, R239N) was likewise created using the 4-primer PCR approach as shown in Scheme 1.23.

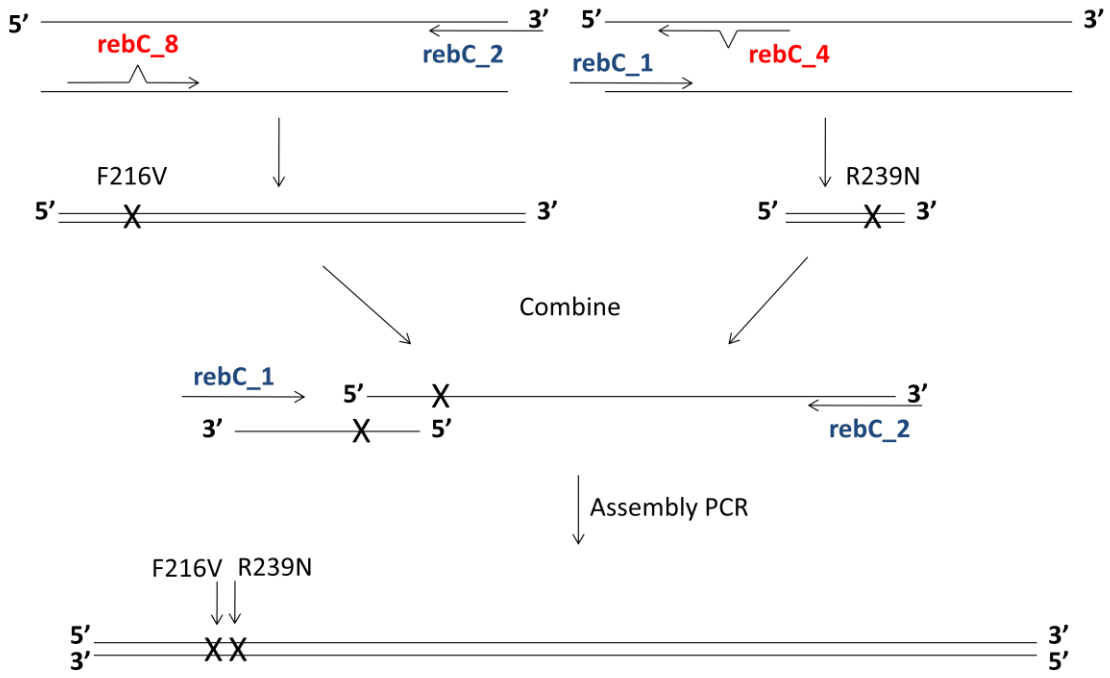

Scheme 1.23. Creation of *rebC_2X* mutant using four-primer PCR strategy. The initial mutagenic PCR involves two reactions; the first involves substitution of one base pair upon amplification of a specific section of the sense strand by the rebC_8 and rebC_2 primer set, and the second involves substitution of a single base pair upon amplification of a specific region of the anti-sense strand by the rebC_1 and rebC_4 primers

1.5.5 Heterologous expression of *rebO, rebD, rebP* and *rebC* in *E. coli* and analysis of indolocarbazole products

Based on the results of previous studies describing indolocarbazole biosynthesis in heterologous hosts,[92] we designed a system in which four genes (*rebO*, *rebD*, *rebC* and *rebP*) would be co-expressed from a pair of compatible Duet plasmids (each having different origins of replication and antibiotic resistance genes) in *E. coli*. Incubation with L-Trp was expected to produce the rebeccamycin aglycon, arycriaflavin A. We expected that this *in vivo* approach to studying indolocarbazole biosynthesis would allow rapid comparison of the regioselectivities of RebC variants.

In preparation for *in vivo* indolocarbazole biosynthesis, it was necessary to introduce both the pET-Duet-*rebPC* and pRSF-Duet-*rebOD* plasmids into *E. coli* BL21(DE3) cells. This strain of *E. coli* has been engineered to lack certain proteases to enhance the stability of the corresponding expressed proteins. The initial idea was to prepare competent BL21 (DE3) cells harbouring the pRSF-Duet-*rebOD* plasmid, and transform these cells with pET-Duet-*rebPC* plasmids containing WT *rebC* or variants of *rebC*, which would be used in the *in vitro* experiments. However, transformation of *E. coli* BL21(DE3) / pRSF-Duet-*rebOD* with the pET-Duet-*rebPC* plasmid proved to be extremely difficult. Plasmid toxicity was considered to account for the low transformation efficiency of pET-Duet-*rebPC*. In order to test this possibility, the plasmids pET-Duet-*rebC*, pET-Duet-*rebPC*, pRSF-Duet-*rebD* and pRSF-Duet-*rebOD* were transformed into *E. coli* BL21(DE3). The results suggested that *E. coli* BL21(DE3) was more readily transformed with the pRSF-Duet than with pET-Duet. For example, using a standard protocol, transformation with pRSF-Duet-*rebD* afforded 129 (365) colonies, pET-Duet-*rebC* afforded 2 (33) colonies, pRSF-Duet-*rebOD* afforded 8 (61) colonies, and pET-Duet-*rebPC* afforded 0 (5) colonies (the number in brackets corresponds to the number of colonies counted when the concentrated cells were plated). To circumvent this problem, BL21(DE3) was first transformed with the low efficiency plasmid pET-Duet-*rebPC*. The presence of the *rebP* gene in five colonies observed on the LB/Amp/Glc plates was verified using colony PCR, along with a control (purified pET-Duet-*rebP* plasmid). Positive colonies were used to prepare competent cells (using kanamycin to maintain the pET-Duet-*rebPC* plasmid). Transformation of BL21(DE3) / pET-Duet-*rebPC* with the high efficiency plasmid pRSF-Duet-*rebOD* proceeded smoothly, with ~200 colonies isolated on the LB/Kan/Amp/Glc plate. The presence of *rebO* and *rebP* in the competent cells was further verified by colony PCR. Glycerol stocks of *E. coli* BL21 DE(3) / pET-Duet-*rebPC* / pRSF-Duet-*rebOD* were prepared and stored at -80˚C for future use.

For expression of indolocarbazole biosynthesis in *E. coli*, cultures were grown in LB medium supplemented with antibiotics (kanamycin, ampicillin), glucose (1%), and L-Trp at 37˚C. Upon reaching an optical density of 0.6 (measured at 600 nm), gene expression was induced by addition of isopropyl-β-D-thiogalactopyranoside (IPTG). After 24 hours of culture growth, the cells were removed by centrifugation and the resulting supernatant was extracted with EtOAc and concentrated to an oily residue that was analyzed for indolocarbazole production using reversed-phase HPLC (Figure 1.22).

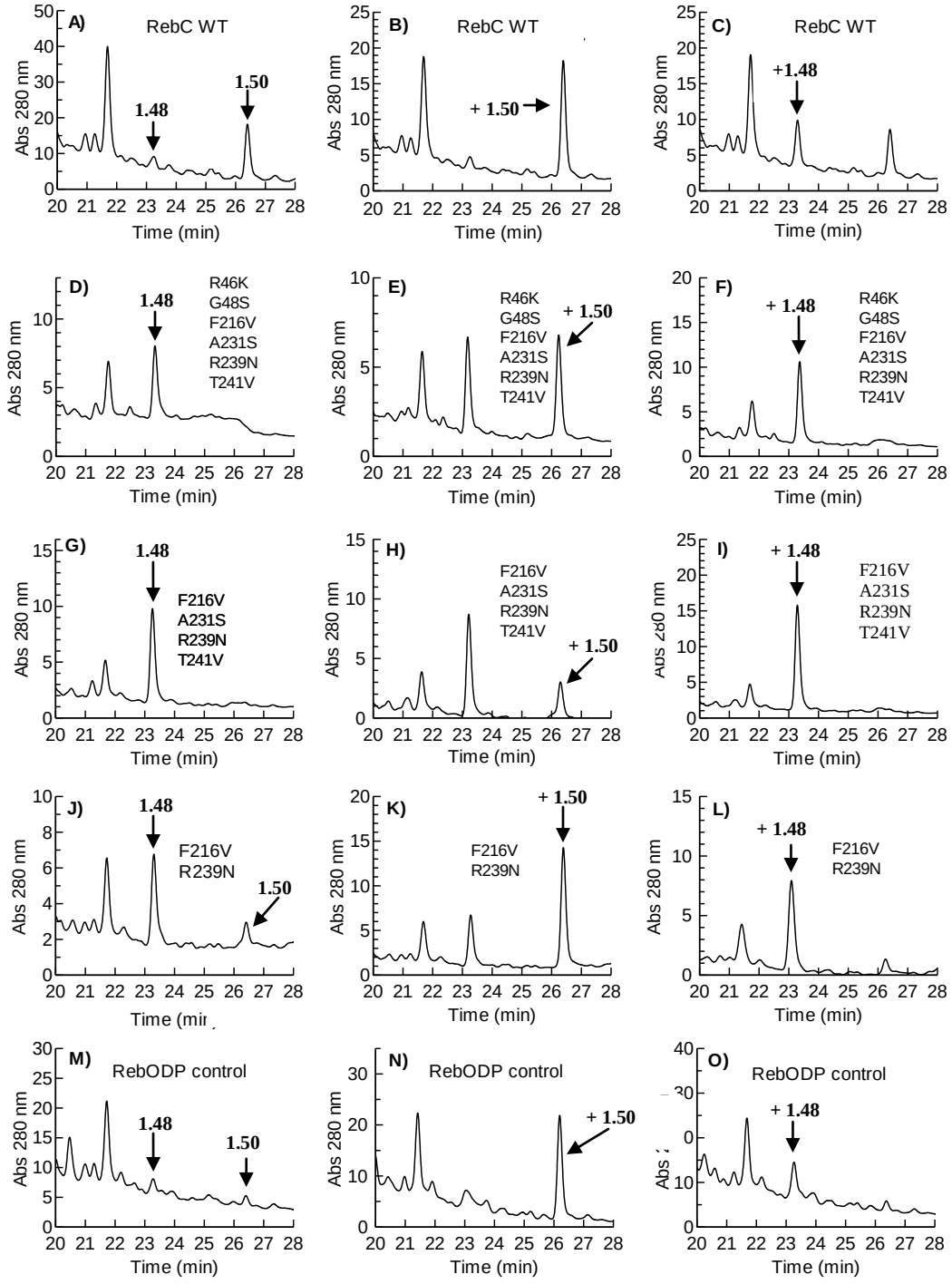

Figure 1.22. HPLC analysis of *E. coli* cultures expressing *rebODPC* genes substituted with various *rebC* alleles. The peaks corresponding to K-252c **1.48** arycriaflavin A **1.50** are indicated, with co-injected standards highlighted with a + sign. Active-site substitutions in RebC are indicated

As shown in Figure 1.22(A), co-expression of wild-type *rebODCP* genes in *E. coli* successfully produced the expected indolocarbazole **1.50** (t_R = 26.5 min), along with a very small amount of **1.48** (t_R = 23.3 min). The identities of **1.50** and **1.48** were verified by co-injection with authentic samples of arcyriaflavin A (**1.50**) and K-252c (**1.48**), as shown in Figure 1.22 (B-C). A complete reversal of oxidative regioselectivity was observed when the *rebC_6X* mutant gene was substituted for wild-type *rebC*. As shown in Figure 1.22(D-F), exclusive formation of **1.48** was observed in this case, with no evidence for formation of the wild-type product **1.50**. In order to determine whether fewer substitutions could confer a switch in the regioselectivity, we designed the *rebC_4X* mutant (F216V, A231S, R239N, and T241V). Once again, the predominant product was **1.48**, with negligible formation of **1.50** (Figure 1.22(G-I)). In order to further probe the active site amino acid residues involved in determining the oxidative outcome, the *rebC_2X* mutant (F216V, R239N) was created. Remarkably, co-expression of the wild-type *rebODP* genes with the *rebC_2X* variant (Figure 1.22(J-L)) showed that **1.48** was the predominant product, according to HPLC analysis. In contrast to the above, co-expression of only the *rebODP* genes produced only trace amounts of **1.48** and **1.50** (Figure 1.22(M-O)). This further supports the necessity of the *rebC* gene or its alleles for producing indolocarbazole aglycons **1.48** or **1.50** in significant quantities.

1.6 Discussion

This research was led by our hypothesis that the difference in the oxidation states between arcyriaflavin A and K-252c arises from differences between the RebC and StaC active sites. In context of the sequence and structural analysis of RebC described in section 1.5.1, our objective to unravel mechanistic differences between RebC and StaC commenced with generation of the *rebC_6X* mutant. Based on our hypothesis, we predicted that this substitution of amino acid residues would impart StaC reactivity to RebC and generate K-252c, which proved to be the case. In order to further investigate the crucial active site residues, we assumed that the interaction of the substrate with the RebC active site residues R46 and G48 was of lesser significance than the interaction of the substrate with the four other residues of interest. Consequently, the *rebC_4X* mutant was generated, and once again, only the K-252c indolocarbazole was identified. In our third iteration, we proposed that the substitutions F216V and R239N would be sufficient to

impart StaC reactivity to RebC. Conceptually, we considered that these two residues were absolutely required in the RebC pathway for maintaining the substrate in the proper orientation to allow multiple rounds of oxidation and generate arcyriaflavin A. Analysis of indolocarbazole products produced by RebC_2X revealed that two substitutions, R239N and F216V, were in fact sufficient to infer StaC reactivity to RebC.

Based on these results, different substrate binding modes can be proposed for wild-type RebC (Figure 1.23) and the RebC F216V / R239N variant (Figure 1.24) to rationalize the observed differences in regioselectivity. Initially we considered the effect of the F216V and R239N substitutions on the interactions of putative substrate **1.47** within the enzyme active site. Significant steric interactions between **1.47** and F216 would be expected, which would push **1.47** towards the flavin ring and allow both C5 and C7 to be within reach of the hydroperoxide of the FAD(C4α)-OOH intermediate. Conversely, the presence of a Val at this position in the StaC active site would create a void that could potentially allow **1.47** to rotate away from the flavin ring, whereby one of the reactive carbons (e.g. C7) is moved beyond the reach of the flavin hydroperoxide. R239 is observed to interact electrostatically with the carboxylate group of the bound substrate, and this interaction is reinforced in the presence of R230 (omitted from Figure 1.15 for clarity), a residue that is conserved amongst RebC homologues, including the more distantly related *p*-hydroxybenzoate hydroxylase (R220)[93] and phenol hydroxylase (R288).[94] Substitution of R239 with the Asn residue observed in the StaC active site would be expected to significantly weaken, or remove entirely, the interaction with the carboxylate of **1.47**. This is because Asn has a neutral amide side chain, whereas the guanidinium side chain of Arg is positively charged at neutral pH. Likewise, the Asn side chain is shorter than that of Arg. The R239N substitution also likely weakens the substrate-R239-R46 hydrogen-bonding network.

Although F216 and R239 were determined to be key residues in determining the regioselectivity of oxidation by RebC, other residues targeted in this study can also be expected to play a role in catalysis. The hydroxyl group of the T241 side chain has the potential to provide a polar interaction with a carboxyl or carbonyl moiety of a reactive intermediate, but is observed slightly beyond hydrogen-bonding range (4.5 Å) of the substrate carbonyl group. The side chain of A231 faces away from the active site, thus its role may be subtler, possibly modulating the adjacent R230. R46 and G48 reside on a loop above the FAD ring, with the R46 side chain interacting with the ribitol chain and pyrophosphate oxygen of the cofactor. Although substitution of these

residues for StaC side chains slightly improves the regioselectivity of oxidation, the fact that they are not critical suggests they may more be important for the overall activity of RebC rather than the selectivity. The *in vivo* approach adopted here is silent on this aspect as measurement of kinetic parameters requires *in vitro* analysis of reaction kinetics with purified RebC variants, as well as access to the RebC substrate.

Using F216 and R239 as the key residues, the following mechanisms are proposed to account for the observed differences in regioselectivity between RebC and the StaC like variant F216V / R239N. As shown in Figure 1.23, the RebP product, putative intermediate **1.47**, is immobilized in the active site of wild type RebC by hydrogen-bonding interactions with T241, R230 and R239, as well as steric interactions with F216.

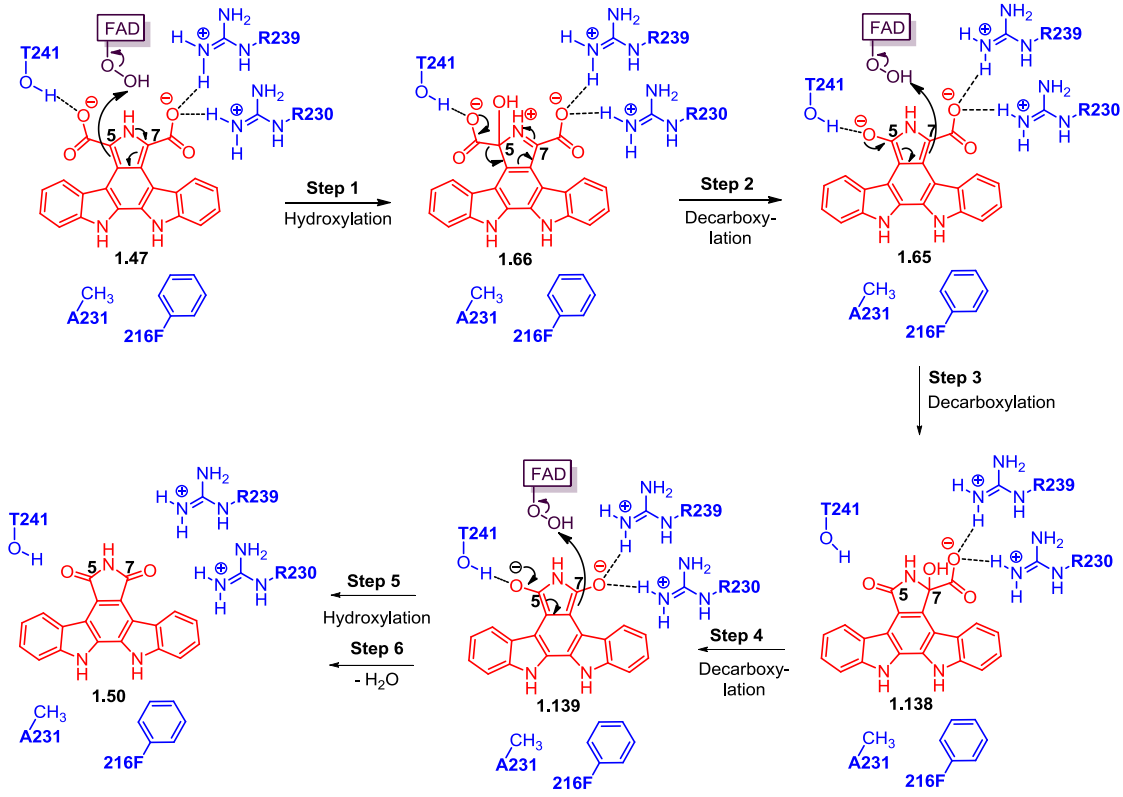

Figure 1.23. Proposed catalytic cycle of wild-type RebC producing **1.50**

We hypothesize that F216 and R239 ensures that the substrate remains close to the FAD co-factor throughout the catalytic cycle, necessary for three successive reactions of the substrate

with the flavin hydroperoxide (FAD(C4α)-OOH). Reaction of **1.47** with FAD(C4α)-OOH is expected to produce hydroxylated **1.66**, which undergoes a subsequent decarboxylation to form **1.65**. Reaction of **1.57** with a second equivalent of FAD(C4α)-OOH produces hydroxylated **1.138**, which decarboxylates to form **1.139**. This product reacts with the third equivalent of FAD(C4α)-OOH, followed by loss of water to form arycriaflavin A, **1.50**. We propose that F216V / R239N RebC deviates from this mechanism in that the substrate reacts only once with FAD(C4α)-OOH. The reaction begins in the same way, with reaction of C5 of **1.47** with the FAD(C4α)-OOH to produce hydroxylated **1.66**, followed by decarboxylation in step 2. The reactive intermediate **1.65** is able to adopt a different conformation in the active site, with one of the indole rings occupying the vacant space created by the F216V mutation. This conformation is also enabled by the decreased interaction resulting from the R239N substitution. Overall, this conformation places the C7 carbon of the intermediate out of reach of the distal oxygen of FAD(C4α)-OOH and a second hydroxylation is prevented. Intermediate **1.65** is subsequently protonated and undergoes decarboxylation to **1.141**, which in turn forms K-252c **1.48** upon tautomerization to the lactam.

F216 and R239 may also facilitate multiple oxidations of the substrate by RebC. The possibility of successive hydroxylation events has been suggested in a previous discussion, with the requirement of tight control over accessibility to the active site provided by the melting helix. Ligand binding in the RebC active site has been observed to trigger a conformational change in the FAD co-factor between a solvent exposed OUT position and the reactive IN conformation within the active site. NAD(P)H reduction of the flavin co-factor to $FADH_2$ (OUT conformation) is accompanied by the conformational change which positions $FADH_2$ within the active site (IN conformation). Subsequent reaction with molecular oxygen forms the flavin hydroperoxide FAD(C4α)-OOH, which is protected from exposure to bulk solvent and positioned for regioselective hydroxylation of the substrate, and the "melting helix" becomes ordered, sealing off the active site. These snapshots of the catalytic cycle obtained from X-ray crystallographic studies are consistent with the "cautious hydroxylase" description of RebC, which requires substrate binding prior to flavin reduction and reaction with molecular oxygen. The resulting rapid substrate oxidation minimizes wasteful NAD(P)H oxidase activity as well as undesired elimination of hydroperoxide from the FAD co-factor.

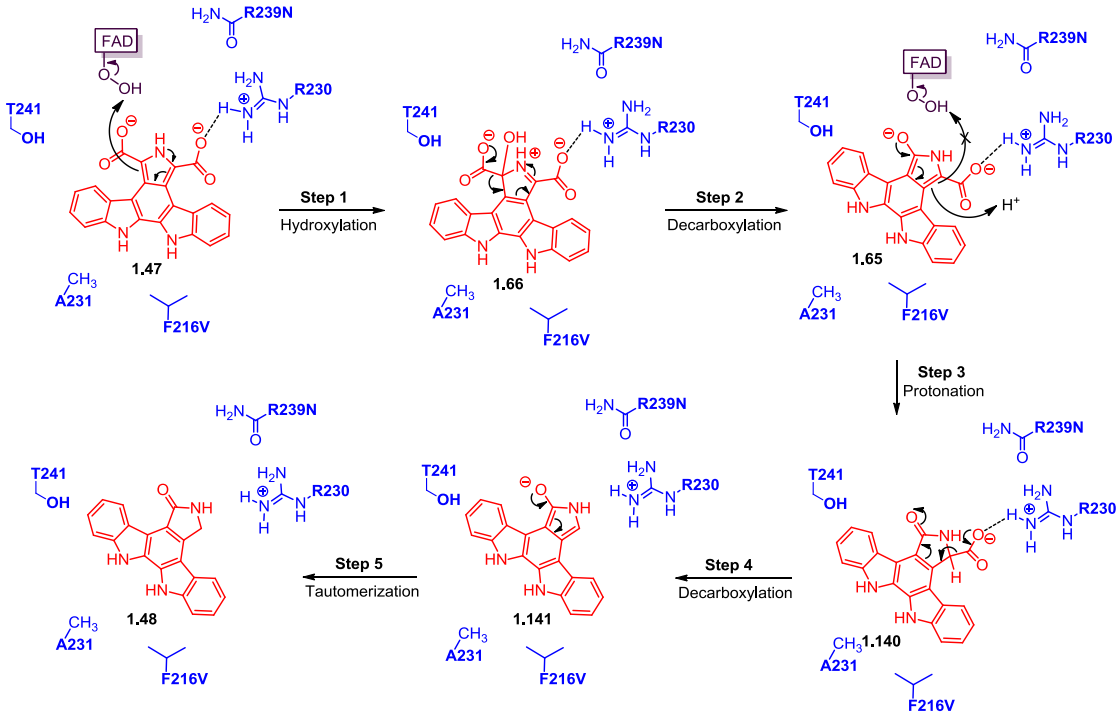

Figure 1.24. Proposed catalytic cycle for RebC F216VR239N variant producing **1.48**

Although multiple rounds of oxidation on a single equivalent of substrate are rarely observed in flavin-dependent monooxygenases, premature release of **1.65** from the active site of RebC could result in rapid protonation by solvent and spontaneous decarboxylation and tautomerization, resulting in non-specific formation of the staurosporine aglycon K252c **1.48** (Figure 1.25).

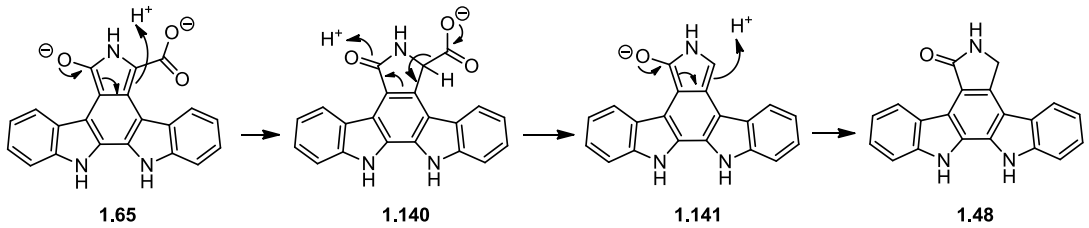

Figure 1.25. Non-specific formation of **1.48** resulting from premature release of **1.65**

In this context, release of **1.65** from the RebC active site followed by binding in a 180˚ flipped orientation for successive oxidation of C-7 is unlikely. Thus we propose that the flavin ring must successively pivot between the IN and OUT conformations for successive reduction and oxidation steps while intermediates remain bound in order to maintain specificity. Additional evidence supporting **1.65** as an intermediate in the catalytic cycle is provided by the X-ray crystal structure of RebC containing **1.65** (or its tautomer) in the active site. The occurrence of multiple oxidations (of one equivalent of substrate) could also be facilitated by the presence of R239, which increases RebC substrate affinity through positive interactions with the carboxylate of intermediates **1.65**, **1.138** and **1.139** (Figure 1.23). This would be analogous to the strong correlation observed between substrate affinity and oxidation efficiency for *p*-hydroxybenzoate hydroxylase.

Subsequent to our demonstration that two RebC active site mutations F216V and R239N were sufficient to impart StaC-like activity to RebC and generate K-252c *in vivo*, Onaka and co-workers demonstrated through *in vivo* studies that the RebC F216VR239N variant increased production of K252c 166-fold as compared to WT RebC.[95] Single RebC substitutions of F216V or R239N completely abolished the catalytic activity of RebC. Correlation between FAD binding affinity and RebC-like reactivity was suggested by selective formation of arycriaflavin A by the StaC A118QN244RV246T variant, specifically engineered to have a higher FAD content than wild type StaC.

Subsequently, Drennan and co-workers quantified the FAD binding ability of indolocarbazole biosynthetic enzymes, and observed that RebC/AtmC strongly bound FAD (nM range), whereas a lower FAD affinity was reported for StaC/InkE (μM range).[96] As a result, correlation between FAD binding ability and conversion of CPA to an indolocarbazole aglycon via a net 4-electron oxidation (StaC reactivity) or net 8-electron oxidation (RebC reactivity) was suggested. However, the knowledge that StaC shares 65% sequence identity with RebC, has an FAD binding domain, and requires flavin for catalytic activity appears contradictory to the fact that recombinantly expressed StaC (and InkE) have been purified without bound FAD. The origin of this phenomenon has been the subject of further mechanistic studies of RebC and StaC.[94] A RebC_10X variant was generated by replacement of six catalytic RebC active site residues (Figure 1.15, Section 1.5.1) and four RebC FAD binding residues for their StaC counterparts, and was found to bind FAD more tightly than StaC and yet possess greater StaC reactivity than StaC

itself (K252c was produced at a rate 3-fold faster than that of the StaC-catalyzed reaction). Co-crystallization of RebC_10X with CPA resulted in accumulation of the indolocarbazole (*S*)-keto-7-carboxy-K252c (**1.140**, Figure 1.24) in the active site, indicative of unique substrate binding modes of RebC and StaC (as RebC was previously shown to co-crystallize with the enol form of 7-carboxy-K252c).[47] Comparison of the RebC and RebC_10X active sites suggest the ability of the latter to preferentially accommodate the (*S*)-keto-7-carboxy-K252c tautomer **1.140** instead of the enol, because of the altered positioning of key catalytic residues. In their analysis, Drennan and co-workers recognized that the R239N substitution prevents salt bridge formation and removes the stabilizing hydrogen bonding interaction normally existing between R239 and the substrate. The position of R230 was also altered as a result of the mutations, occupying a lower position in the active site with a concurrent decrease in the interaction with bound substrate (due in large part to the sterically bulky G48S substitution and additional space created by the F216V substitution). This combination of active site manipulations was suggested to effectively disrupt the interaction between the 7-carboxy group of the enol substrate and the guanidinium group of R230, and favour stabilization of the (*S*)-keto-7-carboxy-K252c tautomer. Additionally, the X-ray structure of RebC_10X did not contain bound FAD, and upon consideration of the crowded active site region, the authors proposed that the mobile FAD co-factor is not involved in direct substrate hydroxylation, but rather plays a role in steric or electrostatic decarboxylation upon adopting the IN conformation (as shown in Figure 1.9b) during catalytic turnover. This description represents a significant departure of StaC from the traditional behavior of flavin-dependent monooxygenases, adopting a role as a chaperone in order to protect the substrate from partaking in undesired reaction pathways while waiting for the presence of a chaperone flavin to drive substrate decarboxylation.

1.7 Conclusions

Cloning of indolocarbazole biosynthetic genes relevant to the formation of the aglycon of rebeccamycin was carried out, and an *in vivo* system for the production of indolocarbazoles was developed. Use of compatible Duet vectors allowed for the simultaneous expression of *rebO*, *rebD*, *rebP* and *rebC*, and in the presence of L-Trp as substrate, the conversion to aglycon (arcyriaflavin A) was readily detected using reversed-phase HPLC analysis. In order to explore

the relationship between the StaC and RebC active sites leading to differently oxidized indolocarbazoles, six key amino acid residues were selected for mutagenesis studies. Although it was demonstrated that changing all six residues in RebC to the StaC counterparts resulted in reversal of regioselectivity, further investigation revealed that the RebC F216VR239N variant was significant to impart StaC reactivity to RebC, and was accompanied by a reversal in regioselectivity producing the staurosporine aglycon 1.37. Based on the implications of these results, specific catalytic cycles were proposed for wild-type RebC (Figure 1.23) and the RebC F216VR239N variant (Figure 1.24), which we used to rationalize the observed differences in regioselectivity. In this context, the possible roles of the F216 and R239 residues in facilitating multiple rounds of oxidation were considered.

1.8 Future Work

A natural progression of the *in vivo* work described here would be *in vitro* studies of the RebC F216V R239N variant, and also investigation of RebC F216V and RebCR239N variants. As noted above, shortly after publishing our own work,[97] Onaka and co-workers reported the *in vitro* characterization of active site variants of RebC that verified our results.[90] Drennan and co-workers also structurally characterized a number of RebC active site variants with StaC reactivity, which also provided a contrasting mechanism for their differing reactivity.[91]

A common problem encountered when studying enzyme-catalyzed reactions is the limited stability of reactive intermediates. When chemical synthesis is not a viable option, computational calculations can provide significant insight into the mechanism of enzymatic reactions (and their predictive power can also guide chemical synthesis, making these two methods complementary in nature). Computational analysis of the RebC reaction could provide specific information about interactions of the proposed reactive intermediates with residues in wild type RebC and the variants identified in this work. Additionally, the well defined conformations adopted by RebC and the flavin co-factor could serve as a starting point for calculations along the reaction cycle. The proposed mechanism could also be tested with the use of stable analogues of the proposed reactive intermediates (see Figure 1.26). For example, the bis-amide inhibitor **1.134** could be hydroxylated by the FAD(C4α)-OOH co-factor **1.25**, but would not be able to undergo decarboxylation. Studying the fate of the hydroxylated bis-amide (if any

further chemistry occurs) would be very interesting and potentially informative. Chemical synthesis of stable analogues of the dimethyl ester of chromopyrrolic acid has generated some interesting heterocyclic structures (as examples, see **1.142-1.144**) that could be used as mechanistic probes. This is the subject of Chapter 2.

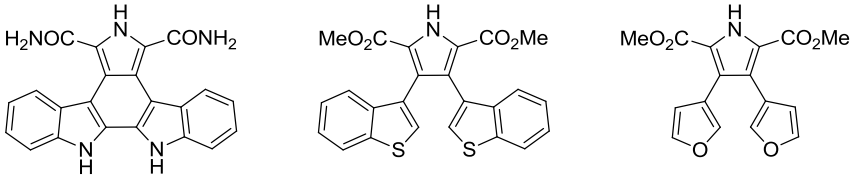

1.142 **1.143** **1.144**

Figure 1.26. Stable analogues of proposed reactive intermediates with potential application as mechanistic probes

1.9 Experimental Section

Materials and General Methods.

Lysogeny broth (LB) and agar were purchased from Fisher Scientific Canada. Super optimal broth (SOB) was prepared by weighing 20.0 g of tryptone, 5.0 g of yeast extract, and 0.5 g of NaCl into a 1 L glass bottle, dilution to 1 L with deionized water and autoclaving. Filter sterilized 1 M $MgCl_2$ (10 mL) and 1 M $MgSO_4$ (10 mL) were added to the autoclaved solution. Restriction enzymes and T4 DNA ligase were obtained from Fermentas and New England Biolabs. Pfu Ultra II was obtained from Stratagene. Vent DNA polymerase was obtained from New England Biolabs, and Pfu Ultra II, Pfu turbo and Herc DNA polymerases were obtained from Stratagene. Agarose gel and plasmid purification kits were obtained from Qiagen and Macherey–Nagel, respectively. DNA ladder SM033 was obtained from Fermentas. Antibiotics and L-tryptophan were obtained from Sigma–Aldrich. Authentic samples of arcyriaflavin A and K252c were obtained from Tocris Bioscience (Ellisville, MO, USA) and Santa Cruz Biotechnology, respectively. The pET-Duet and pRSF-Duet vectors were obtained from Novagen. Routine cloning was performed in *E. coli* XL1-Blue cells (Stratagene), as this genotype has been engineered to lack endonucleases and recombinases and therefore favours stable DNA propagation. Expression of indolocarbazole biosynthetic genes was performed in *E. coli*

BL21(DE3) cells (Novagen), a strain that does not contain certain common proteases and therefore facilitates synthesis of intact and functional enzymes. Plasmid propagation and isolation, PCR, restriction digests, ligation reactions, and agarose gel electrophoresis were performed according to standard protocols[91] or the manufacturer's instructions. DNA sequencing was performed by the Robarts Research Institute (University of Western Ontario, Canada).

General Procedures.

A. **PCR amplification of *reb* genes from genomic DNA**. Unless specified otherwise, each PCR reaction contained the following reagents (with their associated stock solution concentrations and volumes): Pfu Ultra II reaction buffer (10x, 5 µL), dNTP's (25 mM, 0.5 µL), deionized H_2O (38.5 µL), DMSO (2.5 µL), primer 1 (10 µM, 1 µL), primer 2 (10 µM, 1 µL), and DNA template (0.5 µL), in a total reaction volume of 49 µL. The solution was heated to 95 ˚C in a PCR thermocycler (MJ research) for approximately 30 s before adding the DNA polymerase (1 µL, 2.5 U/µL). In general, each reaction was heated at 95 ˚C for an additional 3 min, followed by 25 cycles of 95 ˚C for 30 s, 58 ˚C for 30 s, 72 ˚C for 30 s, then a final step of 72 ˚C for 3 mins. The PCR reactions were analyzed using agarose gel electrophoresis (1 or 1.5% agarose, 120V). The size of the amplified PCR products were determined with a DNA ladder (New England Biolabs, SM033, 5 µL) loaded into one of the remaining lanes. The PCR products were purified using the Qiagen PCR reaction clean-up or gel extraction kits, depending upon the application, according to the manufacturers instructions.

B. **Double digest of PCR products and vectors for ligation reactions.** The components indicated in Table 1.2 were combined in sterile Eppendorf tubes, then incubated at 37 ˚C for 90 mins. The volumes of components used are reported in µL.The digested vector and PCR products were purified using the standard enzymatic reaction clean-up protocol specified in the Qiagen gel extraction manual prior to ligation.

Table 1.2 Restriction digests of vectors and PCR products prior to ligation.

	Vector	PCR product
reaction buffer	3	3
dH_2O	2	3
DNA	20	20
BSA (100X)	1	1
RE 1 (units/µL)	1.5	1.5
RE 2 (units/µL)	1.5	1.5
alkaline phosphatase (units/µL)	1	0
	30	**30**

C.Ligations.

For each ligation three separate reactions were carried out with variable amounts of the PCR insert, as well as a control reaction omitting the PCR insert (Table 1.3). The volumes of components used are reported in µL.After mixing the specified components in sterile Eppendorf tubes, they were maintained at 16 ˚C overnight (~15 h). The T4 DNA ligase was denatured upon heating at 65 ˚C for 10 min, and the ligation products were purified using the Qiagen PCR reaction clean-up kit.

Table 1.3 Ligation of PCR insert into digested vector.

Ligation	1	2	3	C
Vector	5	5	5	5
PCR insert	2	5	10	0
T4 ligase buffer (10X)	2	2	2	2
dH_2O	10	7	2	12
T4 DNA ligase	1	1	1	1
	20	**20**	**20**	**20**

D. Preparation of heat-shock competent *E. coli* cells.

Transformation buffer was prepared according to the INOUE method described in Sambrook and Russell,[91] and is described in the Appendix. In preparing competent cells (not harbouring a plasmid), the protocol described in Sambrook and Russell was followed exactly. Competent cells containing a plasmid were prepared by a similar protocol, as follows. *E. Coli* BL21(DE3) were transformed with the desired plasmid according to the General Procedure E and transformants were selected on LB-agar plates supplemented with the appropriate antibiotic. A single colony was used to inoculate 2.5 mL of LB broth in a 10 mL culture tube which was incubated overnight in an air shaker (37 ˚C, 240 rpm, 15 h). Subsequently, a 25 mL LB solution supplemented with antibiotic was inoculated with 0.25 mL of the overnight culture, and incubated at 37 ˚C, 240 rpm until reaching OD_{600} of 0.6. The cells were chilled on ice for 10 min., centrifuged for 10 min at 3000 rpm, and the supernatant discarded. Residual supernatant was removed by pipette, and the cell pellet resuspended in 8 mL of transformation buffer. After centrifugation and decanting of the supernatant, the cells were resuspended in 2 mL of transformation buffer and molecular biology grade DMSO (150 µL). Aliquots of 100 µL were transferred into ice-cold, sterile Eppendorf tubes, flash-frozen in liquid N_2, and then stored at -80 ˚C.

E. Transformation of *E. coli*.

In the case of ligation reactions, four aliquots of heat-shock competent *E. coli* XL1-Blue cells (100 µL aliquots) were thawed on ice. Thawed cells were gently mixed with 1.7 µL of β-mercaptoethanol and kept on ice for 10 mins. Into each aliquot was added 5 µL of a ligation reaction, which was further incubated on ice for 30 mins, with periodic gentle swirling of the Eppendorf tube. In the meantime, SOC medium was prepared by mixing 50 mL of autoclaved SOB medium with 1.6 mL of an autoclaved solution of 25% (w/v) glucose using sterile technique. Culture tubes (10 mL) were filled with 900 µL of SOC media, and pre-heated to 37 ˚C in a shaker until required. After the 30 minute incubation of the *E. coli* cells with the respective ligation mixtures, the cells were subjected to heat-shock treatment by placing the Eppendorf tubes in a 42 ˚C heating block for 45 seconds, and then placed on ice for 2 mins. The cells were then quickly added to a culture tube containing pre-warmed SOC media and shaken at 37 ˚C / 250 rpm for 1 h. Following incubation, 100 µL of the heat-shocked cells was spread on pre-warmed (37 ˚C) LB-agar plates supplemented with the appropriate antibiotics. The cells of the remaining

culture (800 µL) were collected by centrifugation, resuspended in 200 µL SOC media, and 100 µL used to spread on a second plate. Dilute and concentrated cells were incubated at 37 ˚C overnight (15 h). Each plate was analyzed for the number of colonies present, and compared with the number of colonies derived from the control ligation reaction (no PCR insert). Transformation of heat-shock compentent *E. coli* cells with purified plasmids was performed essentially as above, with the following exceptions. Only one aliquot of cells was used per transformation, and in general 0.5 µL plasmid was used to transform XL1-Blue cells and 1-5 µL plasmid with BL21(DE3) cells.

PCR amplification of *rebO, rebD, rebP,* and *rebC* genes.

The *rebO*, *rebD*, *rebP*, and *rebC* genes were amplified by PCR from *Lechevalieria aerocolonigenes* genomic DNA (ATCC 39243), using the primer pairs indicated in Table 1.4.

Table 1.4 PCR primers used to amplify *reb* genes. Restriction enzyme recognition sites are underlined.

Primer	Sequence (5'-3')	Restriction Site
rebO_for	atccgaattcgtcacgcggacacaagaaga	EcoR1
rebO_rev	ccgcaagctttcgtccgtcgcccgcctc	HindIII
rebD_for	tatacatatgagcgtcttcgacctgcc	NdeI
rebD_rev	cgagggtacctcgcggtccttccgttg	KpnI
rebP_for	atccgaattcgtgaagccgttcgacctc	EcoR1
rebP_rev	ccgcaagctttcaacgtgtcagcatcggc	HindIII
rebC_for	tatacatatgaacgcgcccatcgaaacag	NdeI
rebC_rev	cgagggtacctcacgcggcacccctcac	KpnI

Cloning the *rebO, rebD, rebP,* and *rebC* genes.

The *rebO* and *rebP* PCR products were ligated into the NdeI and KpnI restriction sites of pRSF-Duet and pET-Duet vectors, respectively, by performing double restriction digests of the PCR products and vectors prior to ligation (General Procedures B and C). Similarly, *rebD* and *rebC* PCR products were ligated into the EcoR1 and HindIII restriction sites of pRSF-Duet and pET-

Duet vectors, respectively. The purified ligation products were used to transform into heat shock competent *E. coli* XL-1 Blue cells (General Procedure E). Transformants were selected on LB-agar plates supplemented with 100 µg / mL ampicillin (for pET-Duet clones) or 50 µg / mL kanamycin (for pRSF-Duet clones). In order to obtain pure plasmids of clones for sequencing, single colonies were picked with a toothpick from LB-agar selection plates and transferred into individual 10 mL culture tubes containing 5 mL of LB supplemented with 1% glucose and ampicillin or kanamycin (depending on the plasmid). The culture tubes were shaken at 37 ˚C, 250 rpm, for 15 h, then centrifuged for 0.5 h at 3500 rpm, 4 ˚C, to collect the cells. The plasmid DNA was isolated from the cells using the Qiagen plasmid mini-prep kit, and subjected to analytical double restriction digests in order to verify the presence of the desired insert. The sequence of each clone was confirmed by sequencing both DNA strands of the insert using the primers listed in Table 1.5. DNA sequencing was performed by the Robarts Research Institute (University of Western Ontario).

Table 1.5 Sequences of oligonucleotide primers used for DNA sequencing.

Primer	Sequence (5'-3')
rebO_for	tcgtcgaggccgtgagcag
rebO_rev	ccagctcgacgaacggcac
rebD_1	agggtcctgcaccagttcac
rebD_2	cgagcggatcgtggtgtc
rebD_3	cttcgcgttctacgaactg
rebD_4	gtcaacaacgttctcatg
rebD_5	gttgatgaaggaacgcctc
DuetUP2	ttgtacacggccgcataatc
T7 Term	gctagttattgctcagcgg

Construction of pRSF-Duet-*rebOD* and pET-Duet-*rebPC* plasmids.

Upon cloning the individual *rebODPC* genes into their respective pET-Duet or pRSF-Duet vectors (as indicated in Table 1.6), the four genes were combined into two Duet plasmids.

Table 1.6 Organization of genes in pET-Duet or pRSF-Duet vectors.

Cloning Site	pET-Duet (A)	pET-Duet (B)	pRSF-Duet (A)	pRSF-Duet (B)
NdeI/KpnI	*rebP*	empty	*rebO*	empty
EcoR1/HindIII	empty	*rebC*	empty	*rebD*

Subcloning was achieved by transfer of the *rebP* gene from pET-Duet-*rebP* into the NdeI / KpnI site of pET-Duet-*rebC*, affording pET-Duet-*rebPC*. Similarly, the *rebO* gene from pRSF-Duet-*rebO* was transferred into the NdeI / KpnI site of pRSF-Duet-*rebD*, affording pRSF-Duet-*rebOD*. The *rebO* or *rebP* genes were excised from their respective plasmids by digestion with NdeI and KpnI and purified by agarose gel electrophoresis. Concurrently, the pET-Duet or pRSF-Duet plasmids containing *rebD* or *rebC* were digested with the same pair of enzymes, along with calf intestine alkaline phosphatase (CIAP). Digests and ligations were performed according to General Procedures B and C. The resulting ligation mixtures were transformed into *E. coli* XL-1 Blue cells and grown on LB-agar plates supplemented with ampicillin or kanamycin for selection of pET-Duet and pRSF-Duet, respectively. Single colonies were picked and cultured overnight with appropriate antibiotic selection. The plasmid DNA was isolated and purified using the Qiagen mini-prep kit. Finally, the presence of the desired *reb* genes was determined by analytical restriction digests.

Generation of *rebC* alleles.

Mutations were introduced by the overlap-extension PCR technique by using the primers listed in Table 1.7 and Pfu Ultra II as the DNA polymerase.

Table 1.7 Sequences of oligonucleotide PCR primers used to generate *rebC* mutants. Restriction enzyme recognition sites are underlined and mutagenic codons are in bold.

Primer	Sequence (5'-3')	Comments
rebC_1	tatacatatgaacgcgcccatcgaaacag	NdeI site
rebC_2	cgagggtacctcacgcggcacccctcac	KpnI site
rebC_3	ctgcgcttccccttgcgc**agc**ctggacggccg cggcctgtac**aac**ctc**gtg**gtcggggtcgacgac	A231S, R239N, T241V
rebC_4	cagcgcgcgcaaggggaagcgcagcgacgagga cagcatcaggaagaa**cac**caacgcggcgcgctc	F216V
rebC_6	gtacgatcacccacccg**aaa**gtc**agc**accatcggc ccgcggtccatggaactc	R46K, G48S
rebC_7	gagttccatggaccgcgggccgatggt**gct**gac**ttt**cggg tgggtgatcgtac	R46K, G48S complement
rebC_8	ctgcgcttccccttgcgcgcgctggacggccgcggcctgtac**aac**ct cacggtcggggtcgacgac	R239N

The *rebC_4X* mutant (A231S, R239N, T241V, F216V) was created by two sets of mutagenic PCR reactions using wild-type pET-Duet-*rebPC* as the template. Unless otherwise noted, each mutagenic PCR reaction was performed according to General Procedure A. The mutagenic PCR reaction which introduced the A231S, R239N, and T241V mutations used rebC_3 and rebC_2 as forward and reverse primers respectively, and formed a 918 bp fragment. The F216V mutation was introduced in the second mutagenic PCR reaction using rebC_1 and rebC_4 as forward and reverse primers respectively, and formed a 696 bp fragment. The resulting PCR products were gel purified and assembled using rebC_1 and rebC_2 flanking primers, and Pfu turbo as DNA polymerase. Three exceptions were made to the PCR reaction mixture described in General Procedure A: 0.25 µL of the *rebC_3X* mutagenic fragment (A231S, R239N, T241V) and 0.25 µL of the *rebC_1X* mutagenic fragment (F216V) were used and the extension time was increased to 60 s.

The *rebC_6X* mutant (R46K, G48S, F216V, A231S, R239N, T241V) was created by using the *rebC_4X* mutant as the DNA template. Two mutagenic PCR reactions were carried out, the first with rebC_6 as the mutagenic forward primer and rebC_2 as the reverse primer, and the second with rebC_1 and rebC_7 as forward and mutagenic reverse primers, respectively. The only variation to the general PCR conditions was the annealing step of each cycle (55 ˚C for 30 s). Assembly PCR with the gel purified products was carried out using rebC_1 and rebC_2 as flanking primers. The general PCR conditions were followed, with the exception of the annealing (55 ˚C for 30 s) and extension (72 ˚C for 1 min) steps in each cycle.

The *rebC_2X* mutant (R239N, F216V) was generated from pET-Duet-*rebPC* DNA template by using rebC_8 as the mutagenic forward primer and rebC_2 as the reverse primer in one PCR reaction, and rebC_4 as the mutagenic reverse primer and rebC_1 as the forward primer in a second reaction. In the former reaction, the annealing (55 ˚C for 30 s) and extension (72 ˚C for 1 min) steps were the only deviations from the general protocol. For the second reaction, an annealing step of 55˚C for 30 s was used in each cycle. Assembly PCR of the purified products was performed with rebC_1 and rebC_2 flanking primers by using the same cycling parameters as described for the assembly of the rebC_6X mutant.

The final mutant PCR products were ligated into the NdeI and KpnI sites of pET-Duet-*rebP*, and the resulting products were used to transform heat-shock-competent *E. coli* XL1-Blue cells. The mutant genes of plasmids isolated from single clones were verified by sequencing both DNA strands.

Expression of indolocarbazole biosynthesis in *E. coli.*

A single colony of *E. coli* BL21(DE3) co-transformed with pRSF-Duet-*rebOD* and pET-Duet-*rebPC* was used to inoculate LB broth (100 mL) supplemented with ampicillin (100 µg/mL), kanamycin (50 µg/mL) and glucose (1%). The pre-culture was incubated overnight in an air shaker at 37 ˚C and 240 rpm. An aliquot of the pre-culture (10 mL) was used to inoculate 1 L of LB broth supplemented as above along with L-tryptophan (1 mM). Upon reaching an absorbance value of approximately 0.6 at 600 nm (at 37 ˚C), expression of the *reb* genes was induced by adding 500 µL of isopropyl-β-D-thiogalactopyranoside to the culture (0.5 mM final). The culture was then incubated at 25 ˚C (240 rpm) for 24 h. The cells were removed by centrifugation and the resulting supernatant (1 L) extracted with EtOAc (3 x 350 mL). After evaporating the solvent the

resulting concentrate was analyzed by HPLC on a reversed phase C18 column. The optimized method used to analyze all reactions (wild-type and mutant pathways) was as follows: 1) time = 0 min; solvent = 80% H_2O:20% CH_3CN, 2) time = 20 min; solvent = 25% H_2O:75% CH_3CN and 3) time = 60 min; solvent = 25% H_2O:75% CH_3CN. A flow rate of 0.3 mL/min was used, with detection at λ = 280 nm. HPLC traces were obtained using an Agilent HPLC 1100 series with VWD, and a Zorbax SB-C18 column with dimensions of 4.6x250 mm.

1.10 Appendix

A. **Preparation of chemically competent, heat shock sensitive *E.coli* cells.**

Transformation buffer was prepared according to the Inoue method described in Sambrook and Russell.[98] First, 5 mL of 0.5 M PIPES (pH 6.7, KOH) was prepared with Milli-Q purified water. Subsequently, the following reagents were combined in a sterile container: $MnCl_2 \cdot 4H_2O$ (4.4 mmol, 0.87 g, 55 mM final), $CaCl_2 \cdot 2H_2O$ (1.2 mmol, 0.18 g, 15 mM final) and KCl (20 mM, 1.5 g, 250 mM final). This was followed by 1.6 mL of the 0.5 M PIPES solution and Milli-Q water to a final volume of 80 mL. The transformation buffer was sterilized by filtration through a 0.22 µm Nalgene filter. In preparing competent cells (not harbouring a plasmid), the protocol described in Sambrook and Russell was followed exactly. Competent cells containing a plasmid were prepared by a similar protocol, as described. *E. coli* BL21(DE3) or XL1-Blue cells were transformed with the desired plasmid according to the general procedure described below and transformants selected on LB-agar plates supplemented with the appropriate antibiotic. A solution of LB broth (2.5 mL) was inoculated with a single colony and incubated overnight (37˚C, 240 rpm, 12 h). Subsequently, a 25 mL culture was inoculated with 0.25 mL of the overnight starter culture, and incubated at 37˚C / 240 rpm until reaching OD_{600} of 0.55. The cells were kept on ice for 10 mins, centrifuged for 10 mins at 3000 rpm, and the supernatant discarded. Residual supernatant was removed by pipette, and the cell pellet resuspended in 8 mL of transformation buffer. After centrifugation and decanting of the supernatant, the cells were resuspended in transformation buffer (2 mL) and molecular biology grade DMSO (150 µL). Aliquots of 100 µL were transferred into ice-cold, autoclaved Eppendorf tubes, flash-frozen in liquid nitrogen, then stored at -80 ˚C.

B. Preparation of solid media plates.

A solution of LB-agar (40 g suspended in 500 mL milli-Q water) was autoclaved and once sufficiently cool (~50 ˚C), was supplemented with 100 µg/mL ampicillin or 50 µg/mL kanamycin (using aliquots from 100 mg/mL stock or 50 mg/mL stock solutions, respectively) and 1% glucose (from 25% stock solution). Using sterile technique, the solution of media, antibiotic and glucose was poured into plates and allowed to solidify. Plates were stored at 4˚C.

Chapter 2

Synthesis of Analogues of Chromopyrrolic Acid using the Suzuki-Miyaura Cross-Coupling Reaction

2.1 Introduction

2.1.1 Chemical Synthesis of Chromopyrrolic acid (CPA, 2.1) and Lycogarubin C (2.5)

Intense studies on the biosynthesis of indolocarbazole natural products have attracted considerable attention to a specific reaction, the unusual oxidative aryl-aryl coupling of CPA (**2.1**) to putative intermediate **2.2** (Scheme 2.1), which is performed by the cytochrome P450 enzymes StaP and RebP.[99a-c] Although enzymatic aryl-aryl coupling reactions have been previously reported,[100a-d] only limited examples have been described and the biochemical characterization of the enzymes involved is incomplete.

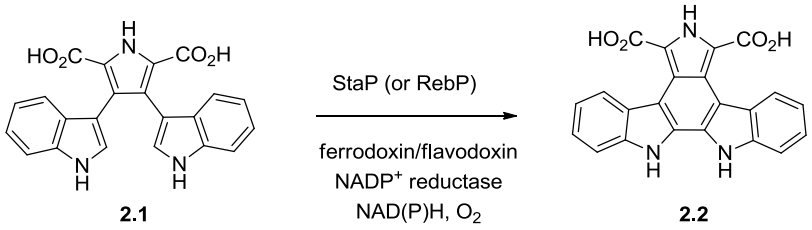

Scheme 2.1. Enzymatic conversion of CPA **2.1** to putative intermediate **2.2**

Three synthetic routes to RebP / StaP substrate **2.1** have been described, two of which rely on a biomimetic approach (Scheme 2.2), which mimics the biosynthesis of rebeccamycin from tryptophan. Sherman's synthesis of **2.1**,[101] shown in Scheme 2.2a, commences with esterification of indole-3-pyruvic acid **2.3** to form β-keto ester **2.4**. The enolate resulting from NaOMe deprotonation of **2.4** undergoes smooth oxidative dimerization in the presence of iodine, with subsequent formation of the pyrrole ring achieved in refluxing ammonium hydroxide to give lycogarubin C (**2.5**). Hydrolysis of **2.5** affords analytically pure CPA (**2.1**) in a low isolated yield

of 1%, which could be attributed to the multiple purification steps (flash chromatography and preparative HPLC), as well as the known ease of decarboxylation of pyrrole-2-carboxylic acids in acidic environments.[102] Steglich and co-workers discovered that lycogarubin C (**2.5**) could be prepared in 42% yield upon treatment of methyl 3-(indol-3-yl)pyruvate (**2.4**) with iodine in methanolic ammonia,[103] and applied this methodology to the biomimetic synthesis of CPA (**2.1**) from free indole-3-pyruvic acid (**2.3**).[104] Use of anhydrous, basic reaction conditions eliminated the need for initial esterification of **2.3** (the first step in Sherman's synthesis), and provided a solution for methyl arylpyruvates being prone to ester hydrolysis in the original *aqueous*, basic reaction conditions. The resulting enhanced synthetic utility allowed efficient access to simple 3,4-diarylpyrrole-2,5-dicarboxylic acid analogues of **2.1** (which are also produced by the marine *Halomonas* bacterium), as well as **2.1** in 36% overall yield (Scheme 2.2b). This methodology was extended to the preparation of unsymmetrical pyrrole-2,5-diesters (bearing different aryl groups at the pyrrole 3-, and 4-positions), and to a related 3,4-diaryl pyrrole half-ester used in the total synthesis of lukianol A (**2.48**, Figure 2.1).[104]

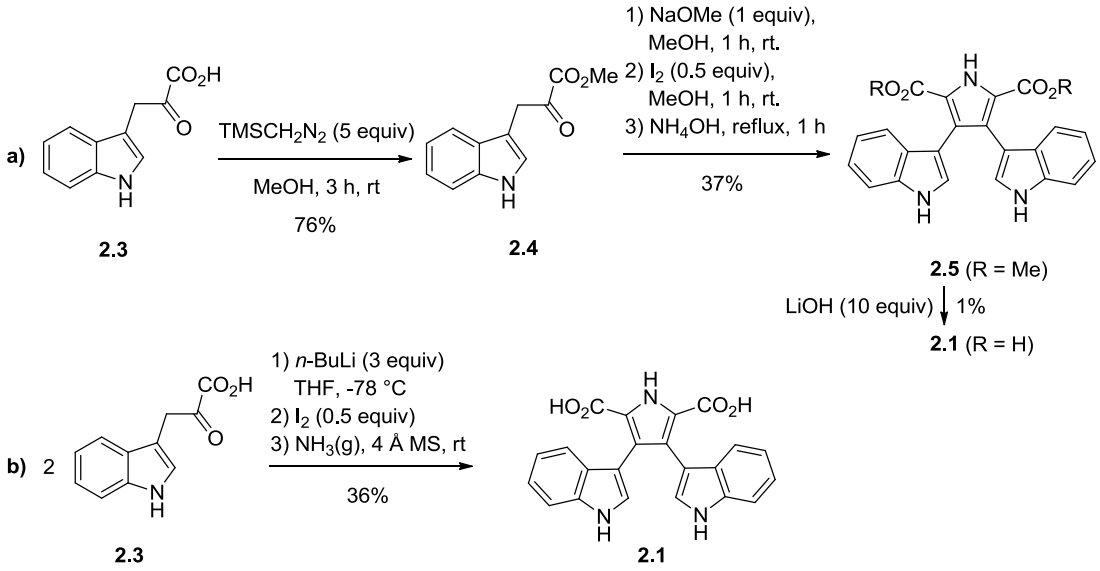

Scheme 2.2. Carbanionic routes to chromopyrrolic acid **2.1** (a) Sherman's synthesis[101] from β-keto ester **2.4**; (b) Steglich's synthesis[103] of **2.1** from indole-3-pyruvic acid **2.3**

Alternative methods for the total synthesis of CPA (**2.1**) and the dimethyl ester of CPA (lycogarubin C, **2.5**) involving the combination of cross-coupling chemistry and heterocycle synthesis have been recently reported. Fu and Gribble attempted a synthesis of **2.5** (Scheme 2.3)

based upon the hypothesis that an inverse electron demand Diels-Alder (IEDDA) reaction between either dienophile 1,2-di(1*H*-indol-3-yl)ethyne **2.6** or 1,2-di(1-(phenylsulfonyl)-indol-3-yl)ethyne **2.7** with the well known diene 1,2,4,5-tetrazine dimethyl ester **2.8** would generate **2.9** or **2.10**. Subsequent Kornfeld-Boger ring contraction would afford lycogarubin C (**2.5**) or the *N*-phenylsulfonyl protected variant **2.11**.[105]

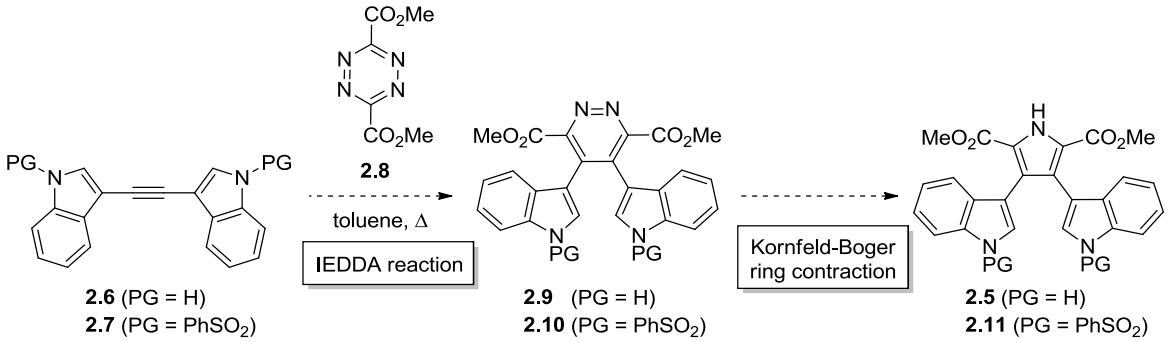

Scheme 2.3. Fu and Gribble's proposed synthetic route to lycogarubin (**2.5**)[105]

In contrast to diarylacetylenes which have found extensive application in heterocycle synthesis,[106] preparative routes to the related bis(3-indolyl)acetylenes have been underexplored. Kamenskii and co-workers[107] described a multi-step synthesis of **2.6** involving reaction of the unstable precursor indolyl-3-acetyl chloride **2.12** with indole Grignard reagent **2.13**, producing 1,2-di-1*H*-indol-3-yl-ethanone **2.14** in 44% yield. Subsequent reaction with PCl_5 affords the desired bis(3-indolyl)acetylene **2.6** in a low yield of 8% (Scheme 2.4).

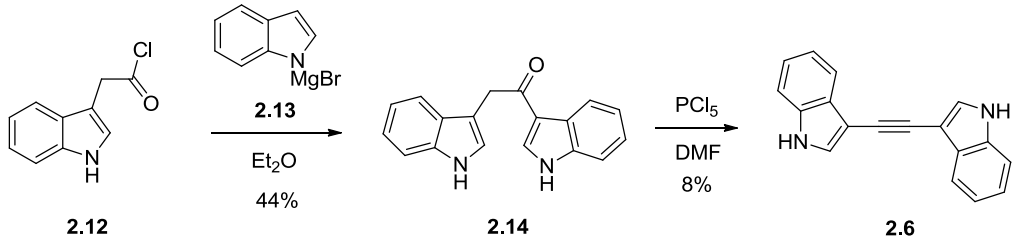

Scheme 2.4. Kamenskii's synthesis of 1,2-di(1*H*-indol-3-yl)ethyne **2.6**[107]

Fu and Gribble developed an improved synthesis of **2.6** and **2.7** (Scheme 2.5),[108] which allowed for investigation of either **2.6** or **2.7** as a Diels-Alder reaction partner in the synthesis of **2.5**. As shown in Scheme 2.5c, the key reaction was a Sonogashira coupling of 3-iodo-(1-phenylsulfonyl)indole **2.17** with 3-ethynyl-1-(phenylsulfonyl)indole **2.22**. The dienophile **2.6** was simply prepared by treatment of **2.7** with aqueous NaOH. Compound **2.17** was prepared from indole **2.15** via a straightforward iodination and *N*-protection sequence (Scheme 2.5a). Preparation of compound **2.22** (Scheme 2.5b) was achieved in several steps, commencing with *N*-phenylsulfonyl protection of 3-formylindole **2.18**, affording **2.19** in 96% yield. The geminal dibromo intermediate **2.20** was prepared using the Corey-Fuchs reaction,[109] and converted into the ethynyl indole via the bromoalkyne **2.21** affording **2.22** in 60% overall yield over 2 steps. Although treatment of **2.20** with excess *n*-BuLi (2 equiv) provided a more direct synthesis, the yield of the final product suffered (37% from **2.20**).

Unfortunately dienophile **2.7** did not perform well in the IEDDA reaction with tetrazine **2.8**, potentially due to unfavourable electronic properties (likely due to deactivation of the dienophile in the presence of the strongly electron-withdrawing benzenesulfonyl groups), along with decomposition of the tetrazine reagent. Sensitivity of the IEDDA reaction to steric hindrance in the dienophile was also concluded in the unsuccessful reaction of unprotected **2.6** with **2.8**, consistent with recovery of unreacted starting material. A modified synthetic approach involved the use of (*Z*)-1,2-di(1*H*-indol-3-yl)ethene **2.23** as the dienophile[105] (Scheme 2.6), based on the hypothesis that the reaction would proceed more effectively with less steric hindrance in the dienophile. Reagent **2.23** was easily prepared from *N*-phenylsulfonylindole-3-carbaldehyde as reported,[110] and underwent a smooth Diels-Alder reaction with tetrazine **2.8** affording product **2.11** in 54% yield upon reductive Kornfeld-Boger ring contraction. Mild benzenesulfonyl group deprotection using Mg and ammonium chloride afforded the desired lycogarubin C (**2.5**) in excellent yield.

Shortly after the publication of Fu and Gribble appeared, Oakdale and Boger reported a related synthesis of **2.5**,[111] prepared via Boger pyridazine-pyrrole ring contraction of intermediate **2.29** (Scheme 2.7). Two methods were described for preparation of **2.29**, involving either a Sonogashira coupling / Diels-Alder reaction sequence (Scheme 2.7a) or Diels-Alder / Stille coupling sequence (Scheme 2.7b). In the first approach, Sonogashira coupling of 3-alkynyl indole **2.24** with 3-iodoindole **2.25** generated the 1,2-bis(indol-3-yl)acetylene **2.26** in 85% yield.

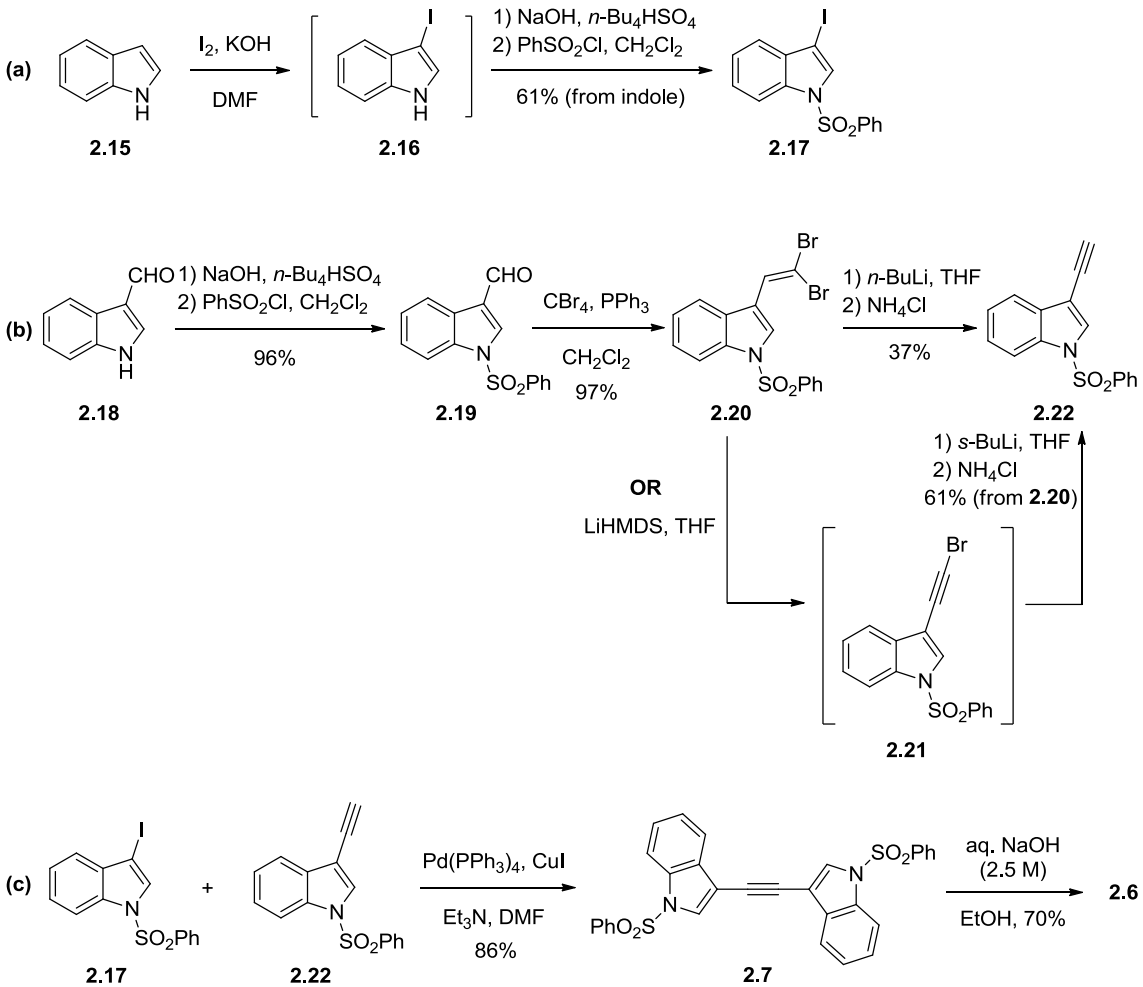

Scheme 2.5. Fu and Gribble's synthesis of **2.6** and **2.7**[108]

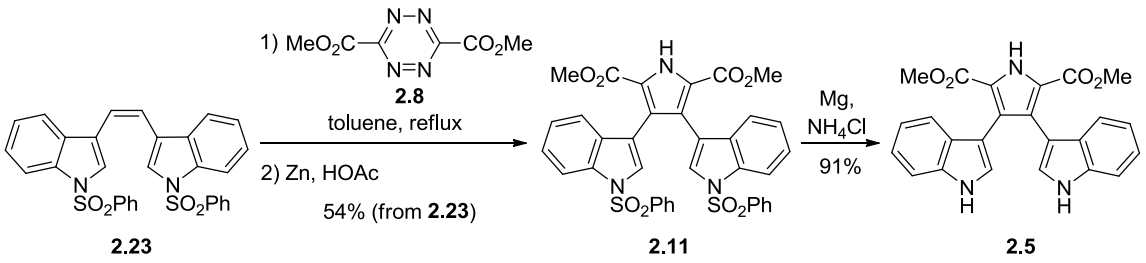

Scheme 2.6. Fu and Gribble's synthesis of lycogarubin C **2.5**[105]

yield (85%). Subsequent IEDDA reaction between **2.26** and tetrazine **2.8** proceeded very sluggishly, generating Diels-Alder adduct **2.29** in 65% yield after 15 d in refluxing toluene, along with addition of fresh tetrazine **2.8** every 3 d in order to compensate for decomposition. These results are consistent with those obtained by Fu and Gribble, who also encountered problems associated with the low reactivity of related dienophiles **2.6** and **2.7** in the IEDDA. Unlike Fu and Gribble who resorted to the use of the less sterically hindered dienophile **2.23**, Oakdale and Boger overcame this synthetic problem through the use of dienophile **2.27**, which has been shown to undergo IEDDA reactions with 3,6-disubstituted tetrazines.[112,113,114] This reaction proceeded very well, giving the desired Diels-Alder product **2.28** in 97% yield after 24 h in dioxane at 45 ˚C. Effective Stille cross-coupling of **2.25** with **2.28** was achieved by modification of the Stille reaction conditions developed by Corey and co-workers ($Pd(PPh_3)_4$/CuCl/LiCl in 1/1 DMSO/THF),[115] and eliminated formation of the proto-deiodination side product. Reductive Kornfield-Boger ring contraction of **2.29** affords *N*-protected lycogarubin C **2.30**, which undergoes subsequent indole deprotection and ester hydrolysis, using LiOH and KOH, respectively, and affords lycogarubin C (**2.5**) and CPA (**2.1**).

Suzuki cross-coupling has also been applied to the synthesis of **2.5** by Fürstner and co-workers,[116] who established effective conditions for the cross-coupling of dimethyl 3,4-dibromopyrrole-2,5-dicarboxylate **2.31** (prepared in 3 steps from *N*-Boc pyrrole) with *N*-TBS indol-3-yl boronic acid **2.32** followed by desilylation (Scheme 2.8). Compound **2.32** was prepared by metal-halogen exchange of *N*-TBS-3-bromoindole followed by electrophilic quench with trimethylborate.[117] Limited stability of this boronic acid required immediate use after preparation.

2.1.2 Biochemical and Combinatorial Synthesis of CPA (2.1) and Related Derivatives

Several enzymatic syntheses of CPA (**2.1**) have been reported as a result of studies designed to elucidate and characterize indolocarbazole biosynthetic intermediates, as well as the associated enzymes. Indeed, **2.1** has been identified as a prevalent intermediate in the biosynthesis of indolocarbazole natural products (Scheme 2.9), including rebeccamycin (**2.34**), staurosporine (**2.35**) and K-252a (**2.36**). *In vitro* studies by Sherman[101] and Walsh[118] have demonstrated the production of CPA (**2.1**) upon RebO and RebD-mediated catalytic turnover of

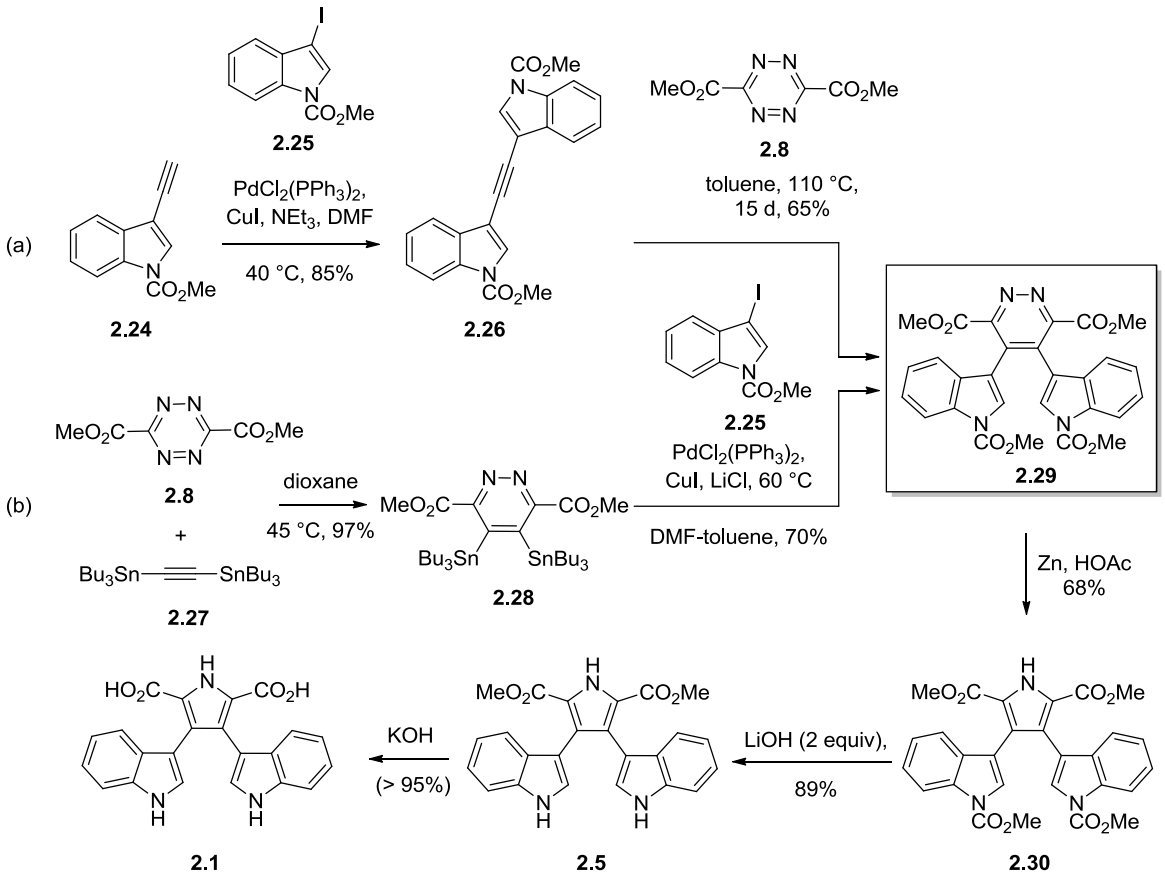

Scheme 2.7. Synthesis of lycogarubin C **2.5** or CPA **2.1** via (a) Sonogashira coupling / Diels-Alder reaction sequence, or (b) Diels-Alder / Stille coupling sequence[111]

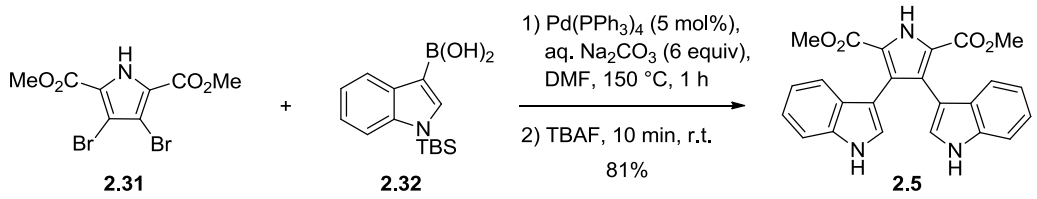

Scheme 2.8. Synthesis of lycogarubin C (**2.5**) using Suzuki-Miyaura cross-coupling[116]

L-Trp (**2.33**), as shown in Scheme 2.9, conditions(a). The results of mechanistic studies are described in Chapter 1, section 1.2.2. Other indolocarbazole biosynthetic enzymes have also been shown to generate CPA (**2.1**). The ability of StaD to turnover indole-3-pyruvic acid (in the

presence of exogeneous ammonium chloride) to CPA **2.1** has been demonstrated *in vitro* (Scheme 2.9, conditions (b)) by Onaka and co-workers in 2006,[119] and *in vivo* studies involving co-expression of the K252a indolocarbazole biosynthesis genes *inkO* and *inkD* in *S. albus* also showed the accumulation of **2.1** (Scheme 2.9, conditions (c)).[120] Isolation and full characterization of CPA (**2.1**) has been achieved through HPLC, HRMS, and NMR spectroscopy investigations.

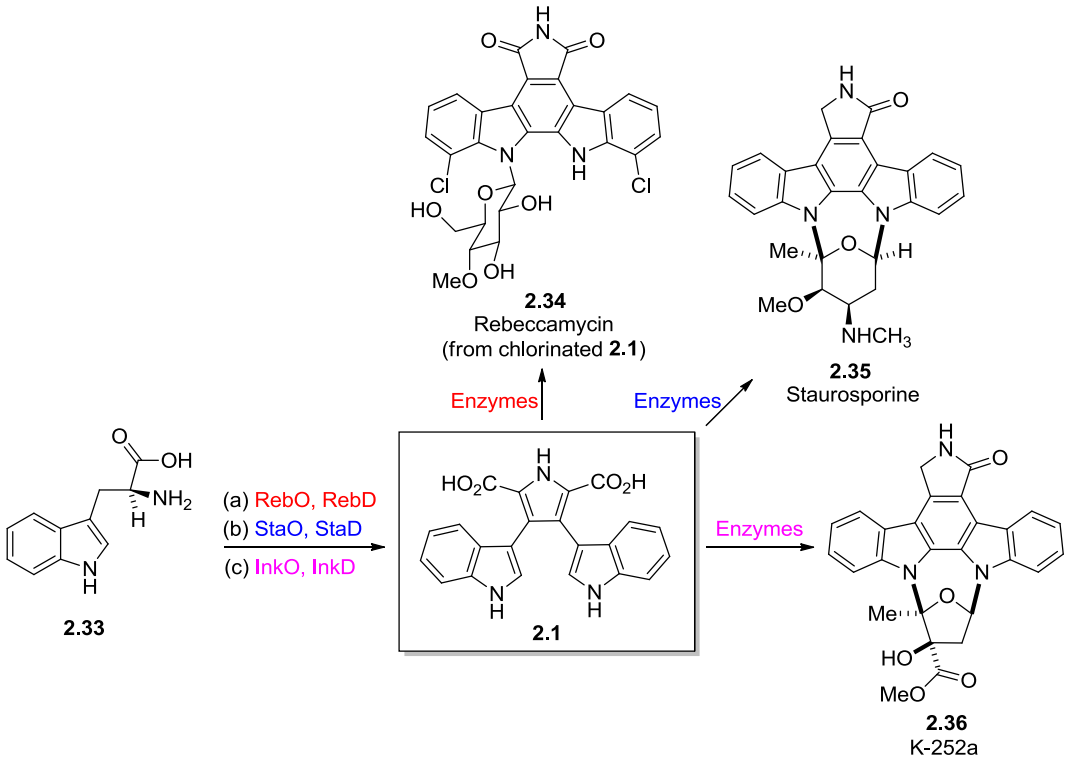

Scheme 2.9. Enzymatic synthesis of prevalent indolocarbazole biosynthetic precursor **2.1** via a-b) *in vitro* studies with RebO/RebD,[101,118] StaD,[119] c) *in vivo* heterologous co-expression of *inkO* and *inkD* in *S. albus*[120]

Modified CPA derivatives, arising from regioselective functionalization of the indole moieties, have resulted from recent combinatorial biosynthesis strategies based on a "plug and play" concept in unnatural gene combination. In an effort to explore the potential for combinatorial biosynthesis using the NokA and NokB enzymes involved in K-252c biosynthesis, Chiu and co-workers described an *in vitro* precursor feeding experiment involving 5-F-L-Trp **2.37**, which resulted in the production of the fluorinated derivative **2.38**[121] (Scheme 2.10a). Sanchez and co-workers reconstituted the rebeccamycin biosynthetic pathway in *S. albus*, and

utilized combinatorial biosynthesis in order to generate unnatural chlorinated CPA analogues (Scheme 2.10b).[122] Co-expression of *rebOD* with *pyrH* (encoding a tryptophan 5-halogenase involved in pyrroindomycin biosynthesis in *S. Rugosporus*)[68] or *thaI* (encoding a tryptophan 6-halogenase participating in thienodolin biosynthesis in *S. Albogriseolus*)[69] afforded C-5 mono-, or di-chlorinated products **2.39** or **2.40**, or C-6 mono-chlorinated product **2.41**, respectively. Unfortunately, the majority of the bis-indole products resulting from strains expressing *pyrH* or *thaI* were non-chlorinated, and the low production levels of **2.39**-**2.41** were attributed either to low production of 5-, or 6-chlorotryptophan, or inefficient conversion of these substrates to chlorinated bis-indole products **2.39**-**2.41** by the rebeccamycin biosynthetic enzymes.

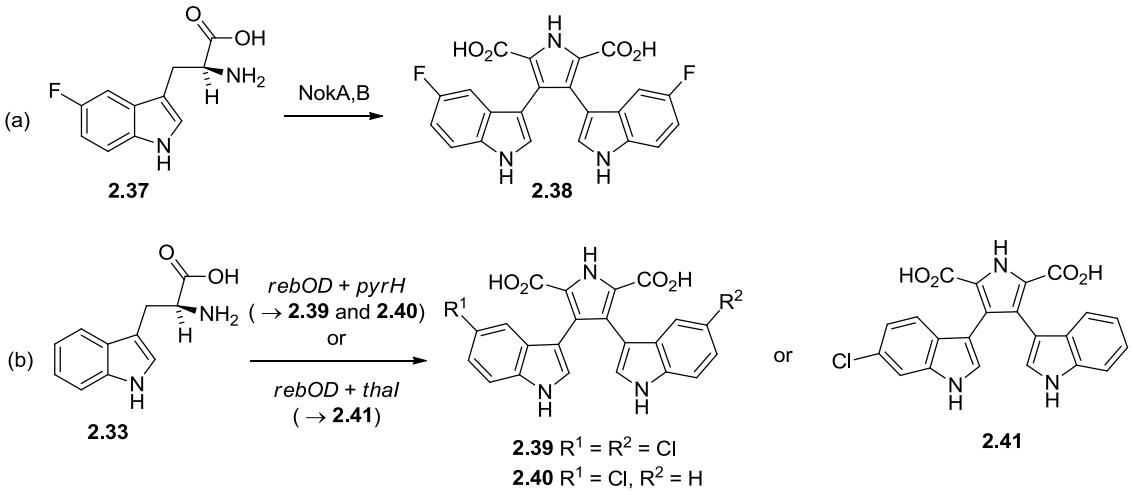

Scheme 2.10. Generation of CPA analogues via (a) precursor feeding[121] or (b) combinatorial biosynthesis[122]

2.1.3 Synthesis and biological relevance of 3,4-diaryl pyrrole natural products

The 3,4-diaryl pyrrole marine alkaloids comprise a very large family of natural products, including (but not limited to) the lamellarins **2.42**-**2.44** (classified as lamellarins A-D, E-H, I-N, O-R, S, N, T-X, Y, Z, and lamellarins α, β, γ, ζ, ε, η, φ, χ), ningalins **2.45**-**2.46**, halitulin **2.47**, Lukianol A (**2.48**), storniamides **2.49**-**2.50**, polycitrins and polycitones **2.51**-**2.54**, and lycogarubins A-C **2.55**-**2.56, 2.5**. The lamellarins are further categorized as Type I (saturated C5-C6, as in lamellarin K (**2.42**)), Type II (unsaturated C5-C6 as in lamellarin D (**2.43**) and lamellarin G trimethyl ether (**2.44**)), or the least bioactive type III (a non-fused ring system).

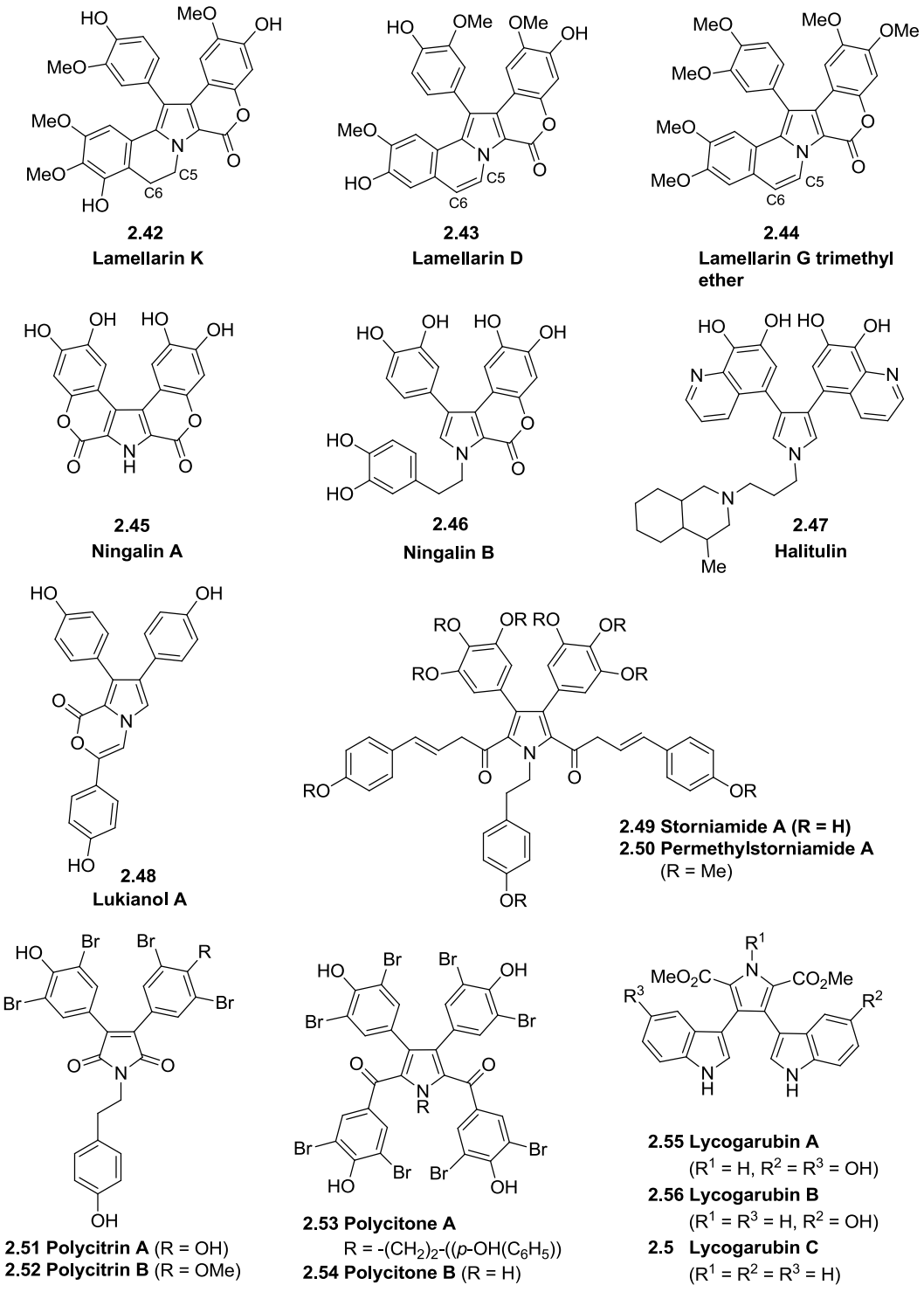

Figure 2.1. Representative examples of biologically active diarylpyrrole alkaloids

Representative members corresponding to each family of the 3,4-diaryl pyrrole marine alkaloids are shown in Figure 2.1. As of 2008, greater than 70 lamellarins and related pyrrole-derived alkaloids had been described.

Since the first reported isolation of lamellarins from the prosobranch mollusc *Lamellaria sp*. by Faulkner and co-workers[123] in 1985, the isolation, structural determination, synthesis, SAR studies, and identification of bioactivity of the lamellarins have been important research areas, and the subject of recent, comprehensive reviews.[124] The lamellarin family of natural products is well known for its significant range of biological activities including cytotoxicity and anti-tumor activity,[125] HIV-1 integrase inhibition,[126] and efficacy in the treatment of multi-drug resistant (MDR) tumor cells,[127] among others. Consequently, numerous synthetic approaches are now available in order to develop and exploit this important class of compounds, as well as related pyrrole-derived natural products.[128] The major synthetic strategies are presented through the following discussion which combines historical aspects with examples from the recent literature. For a fully comprehensive coverage of this topic, the reader is encouraged to access the aforementioned reviews.[124]

Biomimetic syntheses of the lamellarins were pioneered by Steglich and co-workers,[128a] and the first total synthesis of lamellarin G trimethyl ether (**2.44**), involving early stage pyrrole ring formation, is presented in Scheme 2.11. The methodology involved anionic coupling of arylpyruvic acid **2.57** to form the diketo-acid **2.58**, which, upon reaction with amine **2.59** generates pyrrole-2,5-dicarboxylic acid **2.60**. Oxidative cyclization of **2.60** with $Pb(OAc)_4$ followed by a decarboxylative Heck reaction completes the synthesis of **2.44** in 33% overall yield. Subsequent generalization of the procedure resulted in the biomimetic synthesis of lamellarin L, also achieved by Steglich in 2000.[128b] This strategy has since been successfully applied to the biomimetic total synthesis of numerous related diarylpyrrole natural products, including lamellarin K (**2.42**),[128c] ningalin B (**2.46**),[128c] polycitones **2.53** - **2.54**,[128d,e] polycitrins **2.51**-**2.52**,[128e,f] and lukianol A (**2.48**).[128c,e]

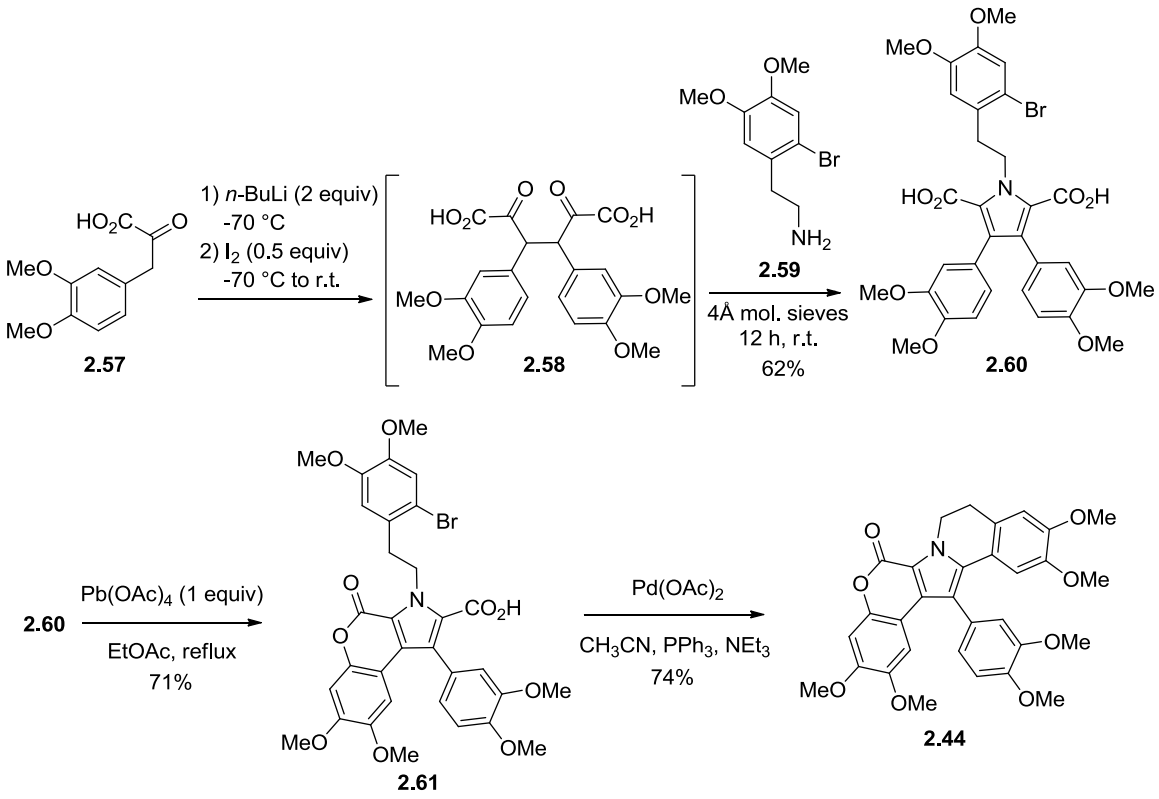

Scheme 2.11. Steglich's biomimetic total synthesis of lamellarin G trimethyl ether (**2.44**)[128a]

Recently, Li and co-workers described an alternative, biomimetic approach for the total synthesis of lamellarins D, H, R, and ningalin B, [128g] and this is demonstrated in the synthesis of lamellarins D and H presented in Scheme 2.12. Key features include pyrrole ring synthesis resulting from AgOAc mediated oxidative coupling of aldehyde **2.62** with amine **2.63** to form **2.64**, oxidative cyclization of **2.64** in the presence of $Pb(OAc)_4$ to form lactone **2.66**, and oxidative coupling using Kita's oxidation conditions to form **2.67**. Subsequent deprotection afforded lamellarin D (**2.43**) or lamellarin H (**2.68**), depending on the choice of reaction conditions. Ningalin B (**2.46**) was prepared by global deprotection of lactone **2.66**, and lamellarin R was prepared using a similar sequence of reactions (not shown).

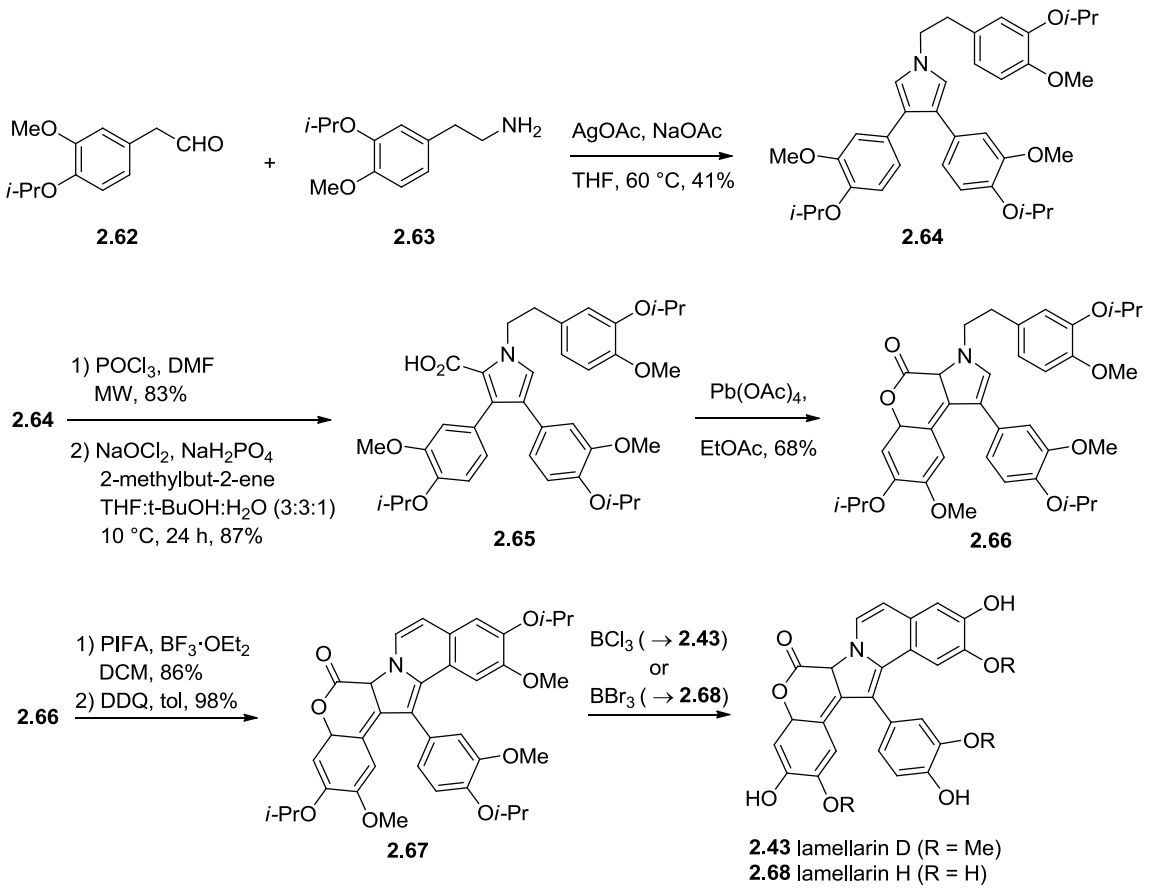

Scheme 2.12. Li's biomimetic total synthesis of lamellarin D (**2.43**) and lamellarin H (**2.68**)[128g]

Iwao and co-workers developed an alternative convergent synthetic route to the lamellarin class of natural products, which was first applied in the total synthesis of lamellarin D (**2.43**) and H (**2.68**) in 1997.[129a] The synthesis is summarized in Scheme 2.13, and commenced with the condensation of benzylisoquinoline **2.69** with benzoate **2.70**. Construction of the lamellarin core was achieved in a one-pot, three-step sequence from **2.71**, via quaternization of the isoquinoline with a haloacetate to generate **2.72**, followed by cleavage of the MOM protecting group, and base-mediated ylide formation/reductive cyclization (with simultaneous aromatization and lactonization) to form **2.74**. Lamellarin D (**2.43**) was obtained by debenzylation, whereas lamellarin H (**2.68**) was obtained by global deprotection using BBr_3. In contrast to the biomimetic approach described in Scheme 2.12, the Iwao synthesis involved late-stage construction of the pyrrole ring.

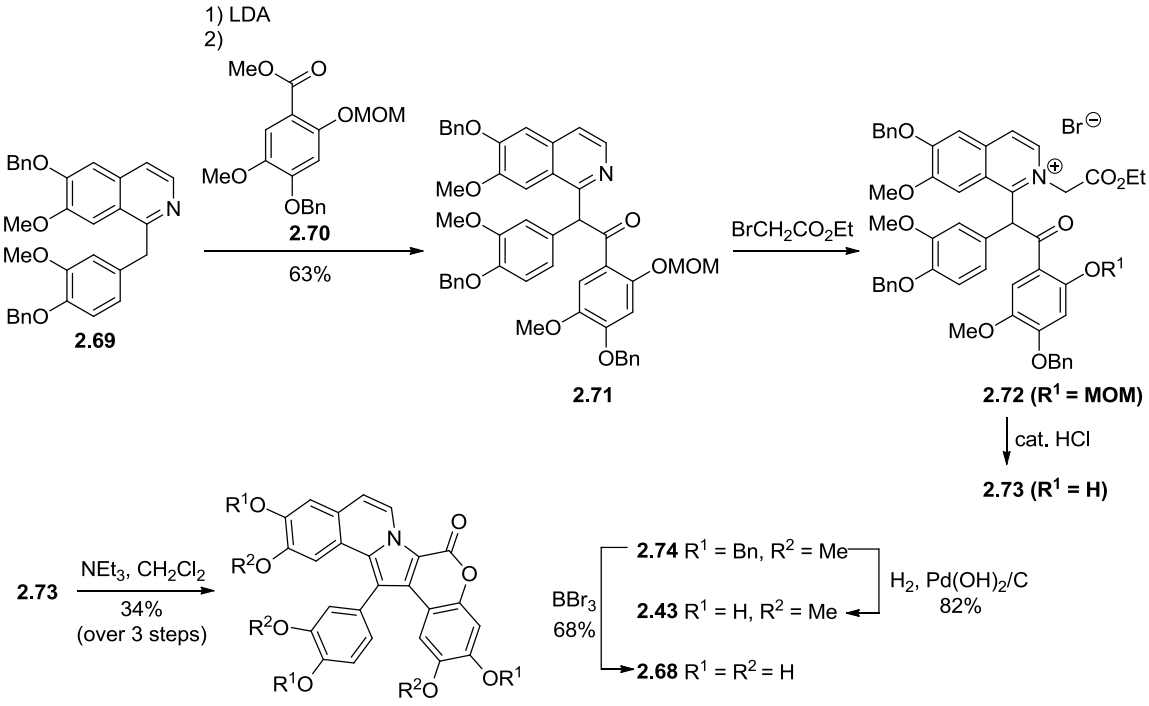

Scheme 2.13. First total synthesis of lamellarin D (**2.43**) and H (**2.68**) developed by Iwao[129a]

Shortly thereafter, Banwell disclosed a related total synthesis of lamellarin K (**2.42**) via an intramolecular [3+2] cycloaddition reaction between an isoquinoline-based azomethine ylide and a tethered tolan,[129b] as shown in Scheme 2.14. The common feature of the Iwao and Banwell synthetic routes to lamellarins is the generation of the intermediate quaternized isoquinoline (obtained by the reaction with a haloacetate in both cases), however, the reactivity of the corresponding ylide was exploited in different ways. In the Banwell synthesis, the azomethine ylide of intermediate **2.80**, generated using Hunig's base, undergoes intramolecular 1,3-dipolar cycloaddition with the proximal acetylene to afford the lamellarin framework **2.81**, which, upon $AlCl_3$-mediated deisopropylation leads to lamellarin K (**2.42**).

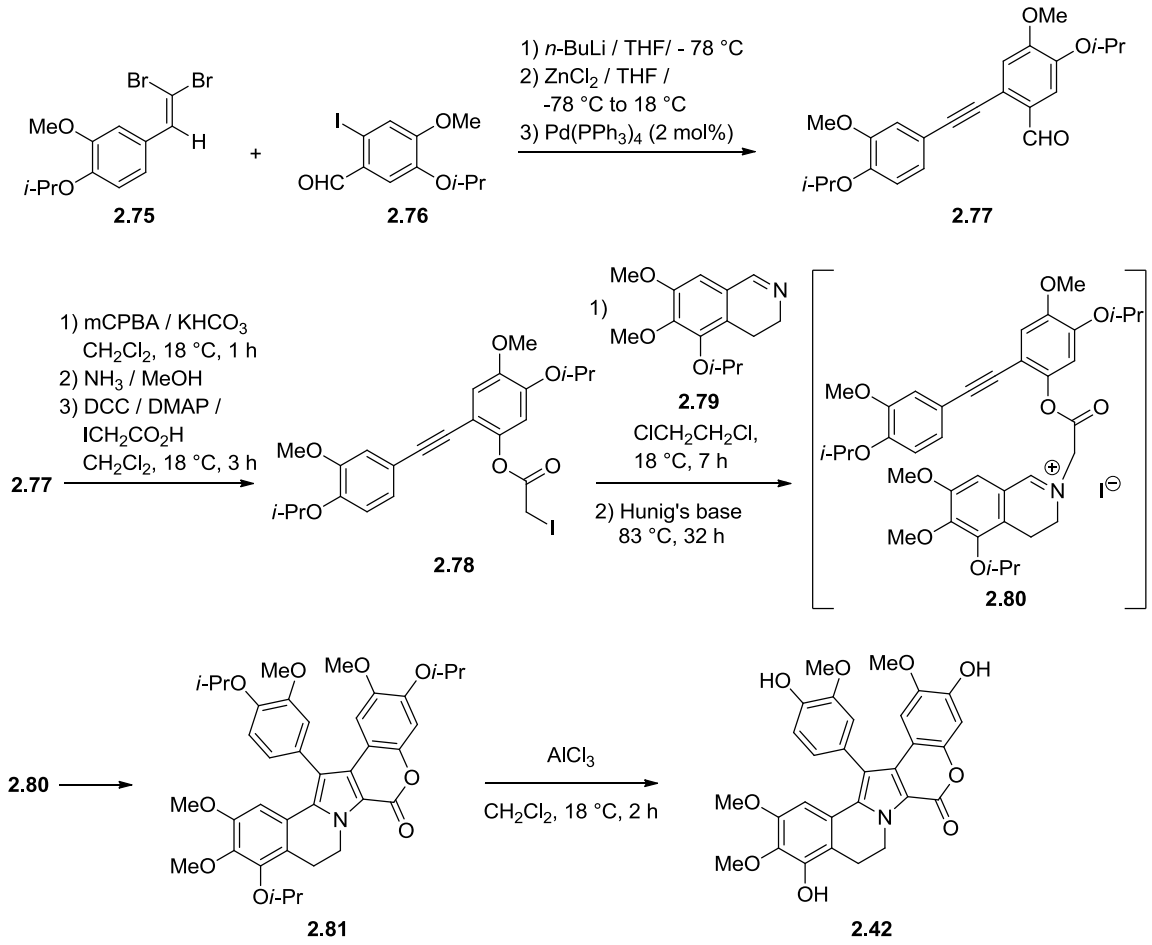

Scheme 2.14. Banwell's total synthesis of lamellarin K (**2.42**)[129b]

In comparison to the Iwao synthesis, the Banwell route involved longer synthetic sequences, due to the required preparation of Sonogashira coupling partners **2.75** and **2.76**, and the three step synthesis of functionalized diarylalkyne **2.78** from **2.77**. This synthetic methodology was recently extended to the successful total synthesis of lamellarins T, U and W,[129c] and Alvarez and co-workers applied Banwell's synthetic method to the first solid-phase synthesis of lamellarins U and L,[129d] providing the potential opportunity for high-throughput screening applications. Liermann and Opatz reported a short synthesis to lamellarin G trimethyl ether[129e] by a modification of the Banwell route starting with 1-benzyl-3,4-dihydroisoquinoline.

Regioselective functionalization of a pre-existing pyrrole via cross-coupling chemistry has also found application in the synthesis of diarylpyrrole-derived natural products.[130] Iwao demonstrated the application of pyrrole-3,4-bistriflate **2.82** as a Suzuki-Miyaura cross-coupling partner for the synthesis of lamellarin G trimethyl ether (**2.44**),[130a] as shown in Scheme 2.15. Key synthetic steps involve successive cross-couplings of **2.82** with boronic acids **2.83** and **2.86** followed by acid-catalyzed lactonization to generate intermediate **2.88**. Ester hydrolysis and decarboxylative cyclization complete the synthesis of **2.44**. Convenient access to ningalin B (**2.46**) from intermediate **2.88**, as well as the key building block required for the total synthesis of storniamide A (not shown) demonstrates the advantage of such a modular and divergent methodology, which has since been applied to the synthesis of related lamellarins D (**2.43**), N (**2.91**), and L (**2.92**),[130b] also shown in Scheme 2.15, as well as lamellarin D analogues.[130c] Successive couplings of **2.82** with boronic acids **2.84** or **2.85**, followed by **2.87**, allowed for regioselective incorporation of appropriately functionalized aryl groups necessary to construct the lamellarin D and N precursors. Also of note, *ortho*-OMOM aryl boronic acids, prepared from the corresponding aryl bromides or iodides by metal-halogen exchange with *t*-BuLi and subsequent $B(OMe)_3$ quench, were required for regioselective lactonization in all cases. Intramolecular cyclizations and protective group cleavage steps completed the syntheses, affording lamellarins D **2.43**, N **2.91** and L **2.92**. This methodology was subsequently used in the first total synthesis of the HIV-1 integrase inhibitor, lamellarin α 20-sulfate,[130d] as well as in improved divergent syntheses of lamellarin α 13-sulfate, 20-sulfate, and 13,20-disulfate.[130e] Recent reports on the synthesis, SAR studies, and mechanism of action of the lamellarin sulfates have also appeared.[130f] Simpler lamellarins O, P, Q, and R were subsequently prepared by Suzuki-Miyaura cross-coupling of *N*-benzenesulfonyl-3,4-dibromopyrrole with appropriately functionalized boronic acids.[130g]

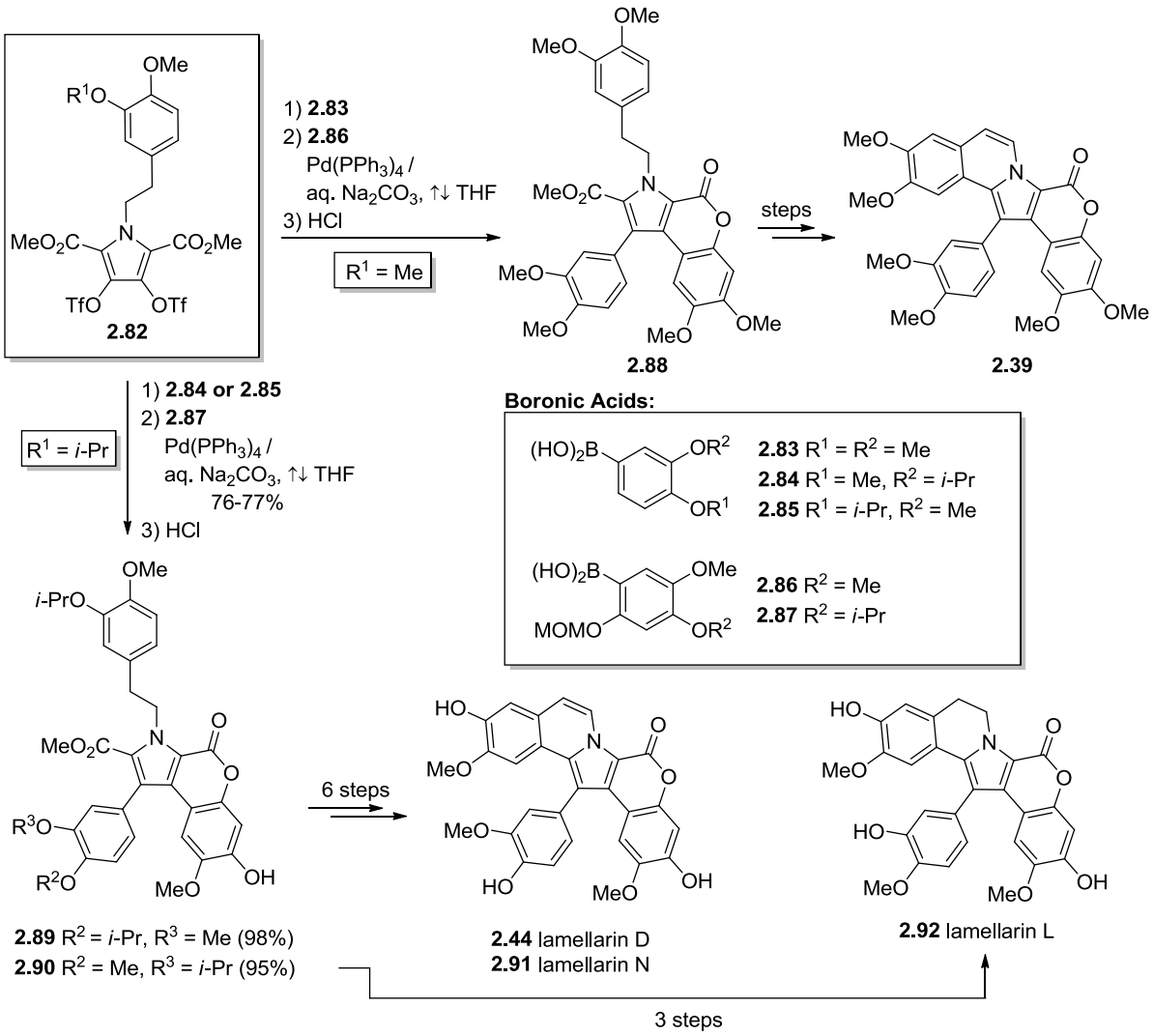

Scheme 2.15. Application of the Suzuki-Miyaura cross-coupling reaction in the synthesis of lamellarin G trimethyl ether (**2.44**), lamellarin D (**2.43**), N (**2.91**) and L (**2.92**)[130a]

A related synthetic theme involves iterative halogenation/Suzuki-Miyaura cross-coupling reaction sequences. Handy was the first to demonstrate this concept in the total synthesis of lamellarin G trimethyl ether (**2.44**),[130h] presented in Scheme 2.16. Commencing from the readily available **2.93**, prepared in four steps from pyrrole,[130h, 131] this modular and very efficient synthesis was carried out in only five reactions (three cross-couplings and two intermediate brominations). Of particular significance was the demonstrated ability to perform regioselective bromination of substituted pyrrole in the presence of electron-rich aryl rings.

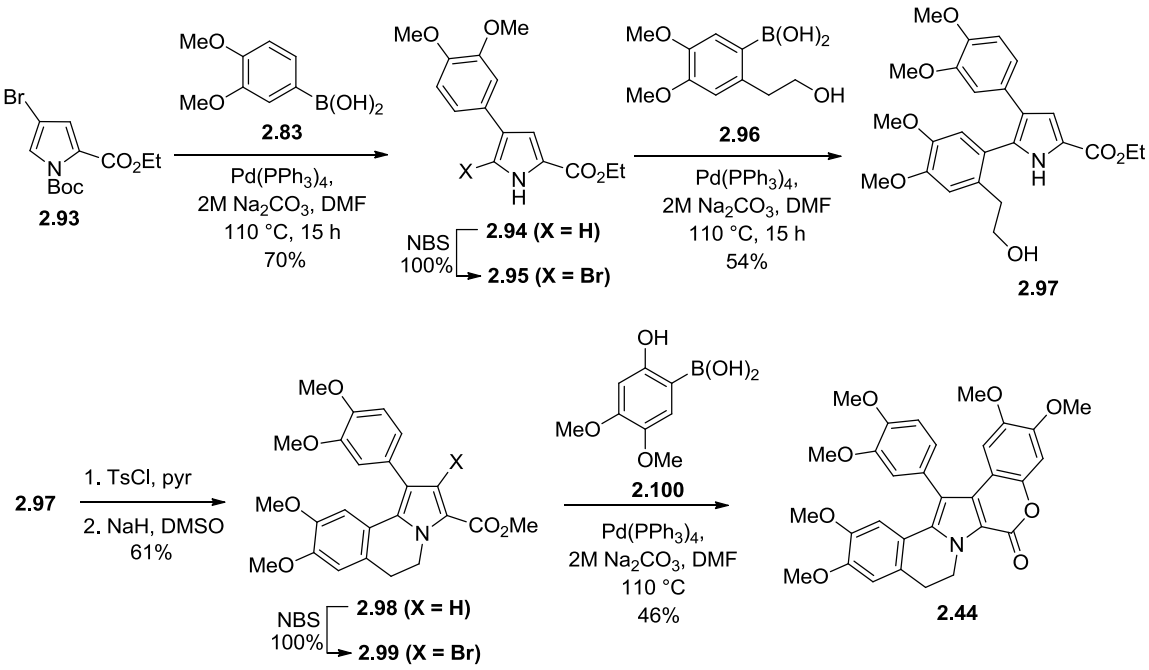

Scheme 2.16. Handy's synthesis of lamellarin G trimethyl ether (**2.44**) using an iterative halogenation / Suzuki-Miyaura cross-coupling reaction sequence[130h]

Alvarez and co-workers used a similar strategy to achieve the total synthesis of lamellarin D (Scheme 2.17).[130i] The synthesis commences with *N*-alkylation of methyl pyrrole-2-carboxylate **2.101** with tosylate **2.102**, and subsequent intramolecular Heck cyclization to form dehydro-isoquinoline **2.103** in high yield. Regioselective bromination and Suzuki coupling with arylpinacolatoboronate **2.105** affords mono-coupled product **2.106**. Etherification and a second regioselective bromination affords **2.108**, which, upon Suzuki-Miyaura cross-coupling with **2.109** generates lamellarin D precursor **2.110**. Oxidative dehydrogenation, ester hydrolysis, selective cleavage of the isopropyl ethers, and lactonization complete the synthesis of **2.43**. The most recent applications of this synthetic strategy have been performed by Banwell and co-workers, in their successful total syntheses of lamellarin G trimethyl ether and lamellarin S.[130j]

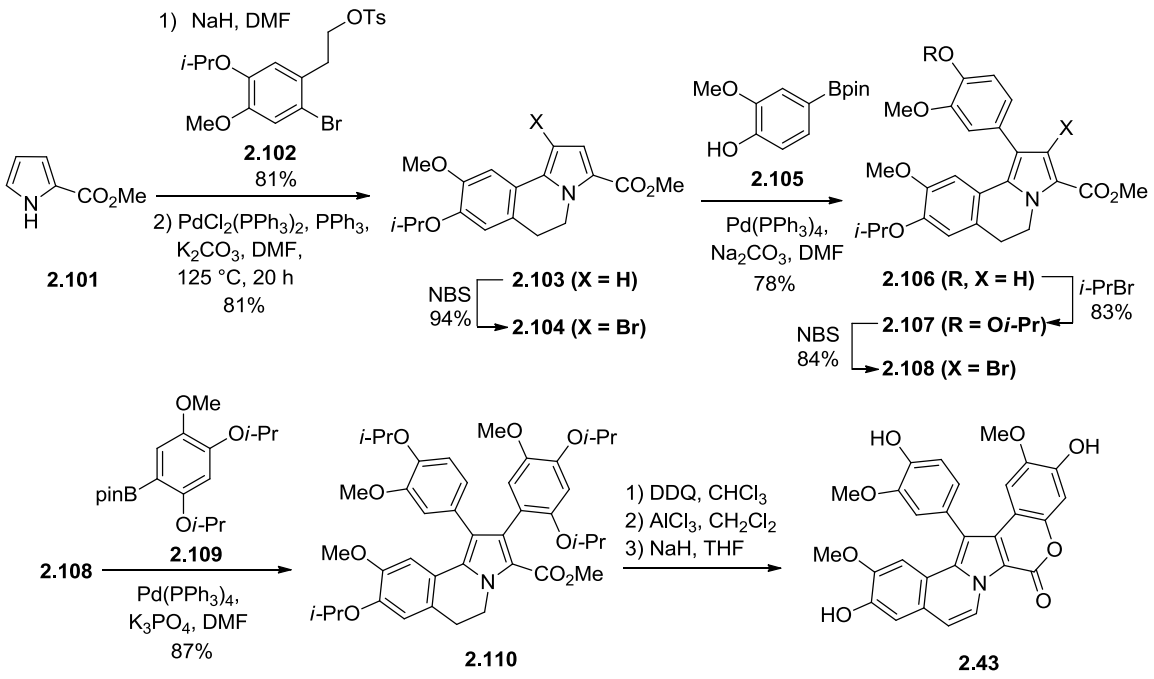

Scheme 2.17. Alvarez' synthetic route to lamellarin D (**2.43**)[130i]

Boger and co-workers have developed a synthetic route to 3,4-diarylpyrrole natural products incorporating a heterocyclic azadiene Diels-Alder reaction and pyrrole synthesis via Boger ring contraction (concepts previously introduced in the total synthesis of lycogarubin C (Section 2.1, Schemes 2.3 and 2.7)).[111] Subsequent application of this methodology to the synthesis of ningalin B (**2.46**) is presented in Scheme 2.18.[132] The product of the Diels-Alder reaction, **2.111**, was subjected to the pyridazine-pyrrole ring interconversion reaction conditions (Zn/HOAc), affording intermediate pyrrole **2.112**. *N*-alkylation with phenethyl bromide **2.113**, followed by acid-catalyzed MOM deprotection / lactonization and ester group cleavage afforded mono-lactone **2.114**. Selective hydrolysis of the methyl ester by treatment with LiI proceeded in 80% yield, and subsequent decarboxylation (Cu_2O / quinoline) afforded hexamethyl ningalin B **2.115** in 70% yield. Global methyl ether deprotection using BBr_3 completed the synthesis of **2.46**.

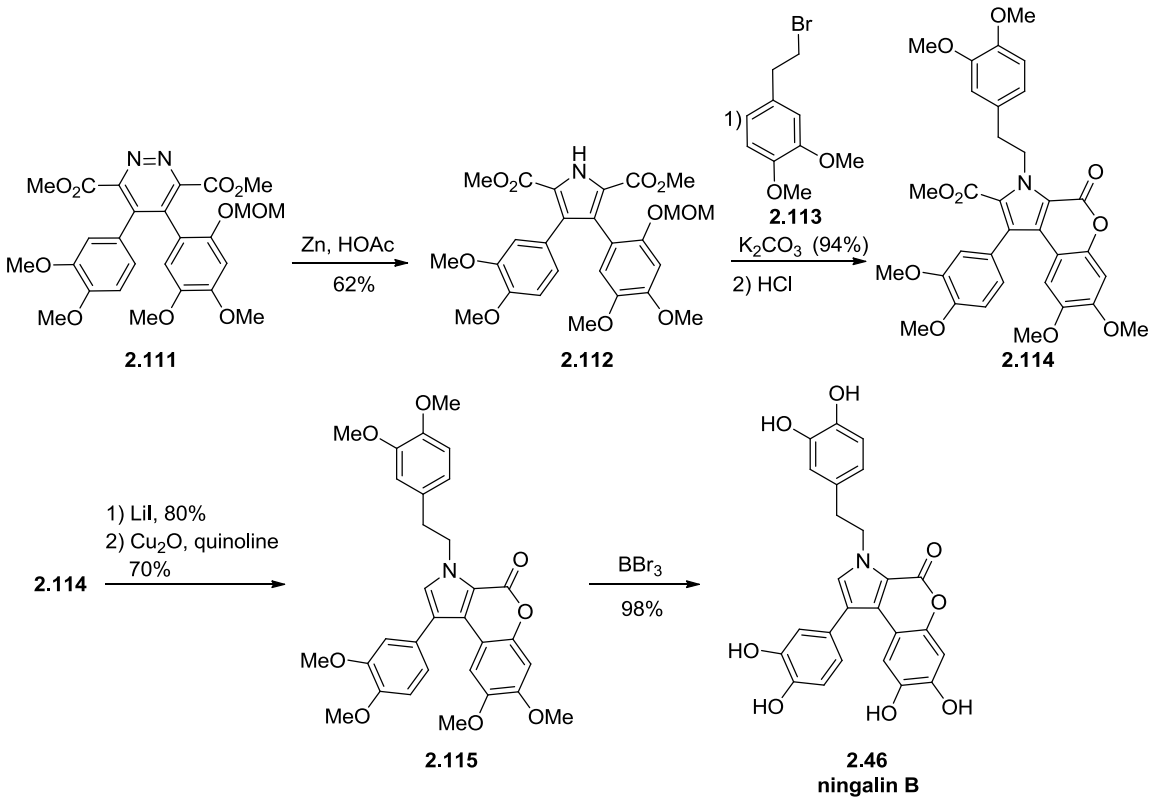

Scheme 2.18. Boger's synthesis of ningalin B (**2.46**) incorporating an inverse electron demand azadiene Diels-Alder reaction / ring contraction strategy[132]

Gupton has developed the use and application of vinylogous iminium salts in the synthesis of diarylpyrrole marine alkaloids,[133] including lamellarin G and lamellarin O (dimethyl ether),[133a,b] lukianol A,[133a] ningalin B (hexamethyl ether),[133c] rigidins,[133d] polycitrones A and B,[133e,f] and storniamides.[133f] In a recent example of total syntheses of polycitone B (**2.54**) and permethylstorniamide A (**2.50**),[134] shown in Scheme 2.19, Gupton and co-workers combined the use of vinylogous iminium salts with a regioselective, microwave accelerated Vilsmeier-Haack formylation to intercept Steglich's polycitone B intermediate **2.120**[128d] (Scheme 2.19a) and Boger's permethylstorniamide intermediate **2.126**[127b] (Scheme 2.19b).

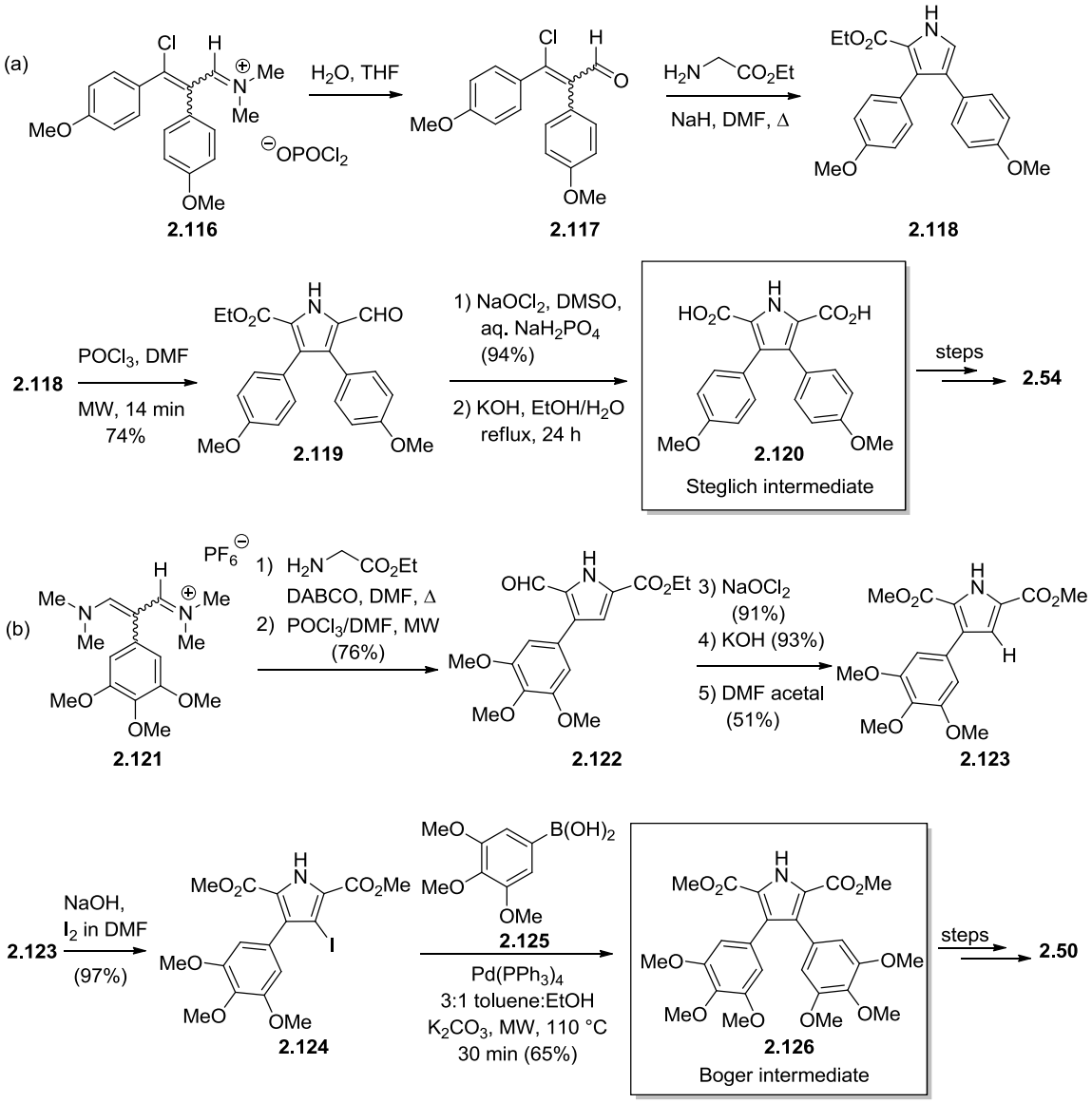

Scheme 2.19. Gupton's synthesis of polycitone B **2.54** and permethylstorniamide A **2.50** through (a) interception of Steglich's intermediate **2.120**; (b) interception of Boger's intermediate **2.126**[134]

Iminium salts **2.116** or **2.121** were prepared in short sequence from readily available phenylacetic acid or 2- phenyl-acetophenone, as reported.[134] The described routes correspond to a second generation synthesis in which optimized conditions for a previously inefficient Vilsmeier-Haack formylation have been incorporated. As shown in Scheme 2.19a, synthesis of polycitone B

(**2.54**) commences with initial hydrolysis of the appropriately substituted vinylogous iminium salt **2.116** to generate chloroenal **2.117**. Reaction of **2.117** with ethyl aminoacetate generates 3,4-diarylpyrrole mono-ester **2.118**, followed by an efficient microwave accelerated Vilsmeier-Haack formylation to afford **2.119** in good yield (74%). Synthesis of Steglich intermediate **2.120** is achieved by Pinnick oxidation and ester hydrolysis, and **2.120** may be readily converted in a few subsequent steps to the desired **2.54**. Synthesis of permethylstorniamide A **2.50** is shown in Scheme 2.19b, and commences with reaction of the vinylogous iminium salt **2.121** with ethyl aminoacetate, affording an intermediate pyrrole. Microwave accelerated Vilsmeier-Haack formylation generates mono-arylated pyrrole aldehyde **2.122**, which is converted over three steps to the pyrrole dimethyl ester **2.123**. Regioselective iodination and subsequent Suzuki-Miyaura cross coupling of **2.124** with arylboronic acid **2.125** affords the Boger intermediate **2.126**, which is readily converted to permethylstorniamide A (**2.50**).

Numerous other creative strategies for the construction of the pentacyclic lamellarin core and related natural products have been developed. As the intention of this introduction is to present an overview of the major synthetic efforts, the reader is encouraged to refer to the cited reviews[124] for additional synthetic approaches.

2.2 Structure-Activity Relationships (SARs): Strategies for the synthesis of biologically active indolocarbazoles.

Total syntheses of naturally occurring indolocarbazoles related alkaloids have been the focus of many research efforts, with the intention of exploiting their known or potential biological activities. Comprehensive reviews on the synthesis of indolocarbazoles,[135] and on the occurrence, biosynthesis, and biological activities of these natural products[136] are available. Analysis of the indolocarbazole scaffold (Figure 2.2) shows the most common strategies used in SAR studies. In this analysis, the indolocarbazole scaffold is divided into three functional domains:[137] the maleimide region of the molecule is the enzyme-interacting domain, the pentacyclic indolocarbazole core is the DNA-intercalative binding domain, and the sugar moiety is the DNA-groove binding domain. Systematic modification of these functional domains is carried out by four common strategies used to enhance pharmacokinetic and bioactive properties (including water solubility, DNA binding, topo I/II inhibition and cytotoxicity): i) substitution of the imide nitrogen with hydrophilic groups,[138] ii) carbohydrate modification,[139] iii) functionalization of the

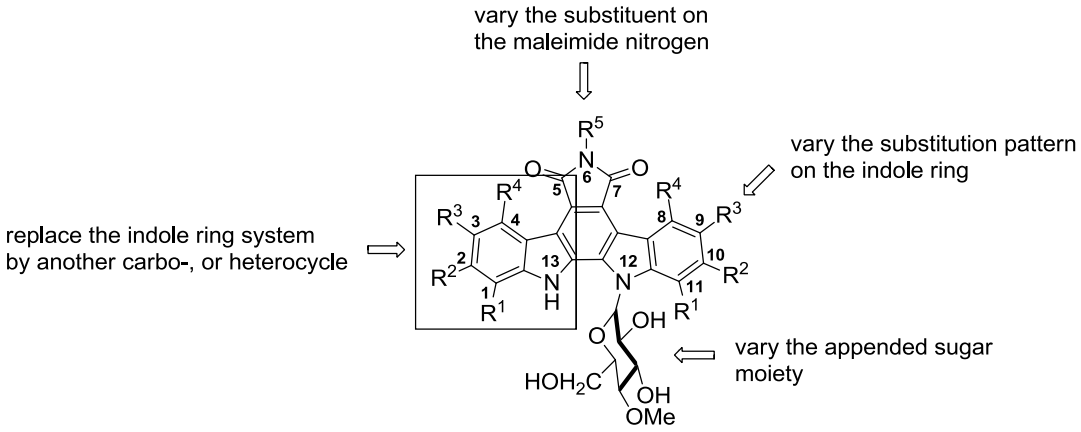

Figure 2.2. SAR Strategies for development of new series of indolo[3,4-*c*]pyrrolo[2,3-*a*]carbazoles

indole heterocycle and iv) replacement of indole by other heterocycles and by carbocycles. Arcyriaflavin analogues obtained by homologation of the indole C2-C2' bond, containing a central 7-membered ring or tropone core have also been described.[140] Sections 2.2.1 – 2.2.3 are limited to discussion of indolocarbazole SAR studies involving the latter two strategies (indole functionalization or indole replacement by a carbo-, or heterocycle), in that they are most relevant to the thesis work described in Chapter 2.

2.2.1 Regioselective functionalization of the indolocarbazole heteroaromatic scaffold.

Identification of indolocarbazole inhibitors with improved cytotoxicity profiles and/or specific molecular targets is the objective of SAR studies, and analogues have typically been prepared in a semi-synthetic approach from rebeccamycin, or through total synthesis efforts. A powerful driving force behind SAR studies is the knowledge that staurosporine[141] and UCN-01,[142] two of the most potent inhibitors of cyclin-dependent kinases (CDK's),[143] suffer from poor selectivity (as they inhibit other kinases such as PKC and CAMKII).

Regioselectively functionalized rebeccamycin derivatives, for which SAR studies have revealed significant biological activities (as discussed below), are shown in Figure 2.3.

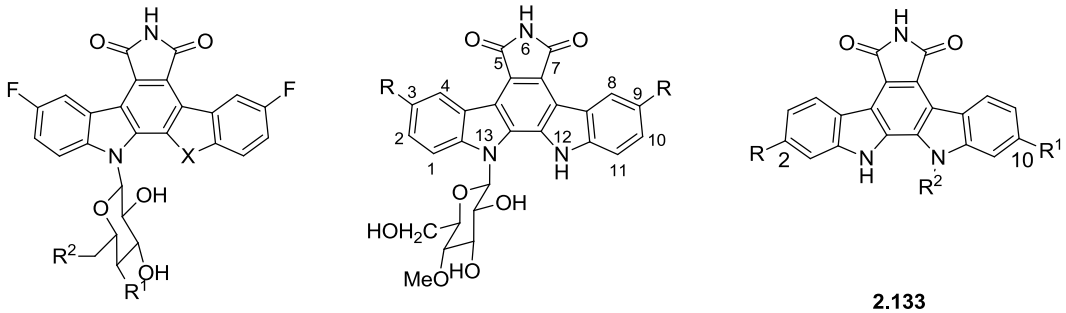

2.127 X = NH, R^1 = OMe, R^2 = OH
2.128 BMS-251873
X = S, R^1 = OH, R^2 = NH_2
2.129 BMS-250749
X = NH, R^1 = F, R^2 = OH

2.130 R = OH
2.131 R = CHO
2.132 R = NH_2

2.133
R = Br, F,Cl, CF_3, Me, OMe
R^1 = 2'-OMe
R^2 = H or Me

Figure 2.3. Biologically active rebeccamycin analogues identified from SAR studies[145-148]

SAR studies carried out on 3,9-difluorinated rebeccamycin **2.127**, previously isolated from fluorotryptophan precursor feeding experiments and possessing superior topo I potency and selectivity,[144] culminated in the identification of two potential clinical candidates BMS-251873[145] **2.128** and BMS-250749[146] **2.129** (Figure 2.3). **2.128** and **2.129** (and related analogues thereof) have been prepared by sequential reaction of heteroaromatic Grignard reagents with 3,4-dibromomaleimide (Scheme 2.20a), or by the synthetic route shown Scheme 2.20b (if appropriately substituted benzothiophenes, benzofurans or indoles were unavailable).

Achievement of a desirable pharmacokinetic profile required significant chemical modifications of the core structure of **2.127**: incorporation of a 6'-aminosugar moiety into **2.127** resulted in increased water solubility, cytotoxicity and distal site activity, although an associated decrease in topo I inhibition was observed (attributed to the likely inability of the 6'-aminosugar indolocarbazole to achieve the "closed conformation" essential for topo I inhibition, consistent with biological studies of indolocarbazole analogues bearing uncommon or unnatural sugars).[139c,d,h] Remarkably, 6'-aminobenzothiophene analogue **2.128** displayed robust, *in vitro* topo I mediated DNA cleavage activity (2-fold higher than that of camptothecin), topo I selectivity, broad spectrum cytotoxicity and improved solubility and pharmacokinetic parameters, resulting in the selection of **2.128** as a candidate for clinical trials. The fluoroindolocarbazole BMS-250749 (**2.129**) having a fluoroglycosyl moiety and bis-indole heteroaromatic framework,

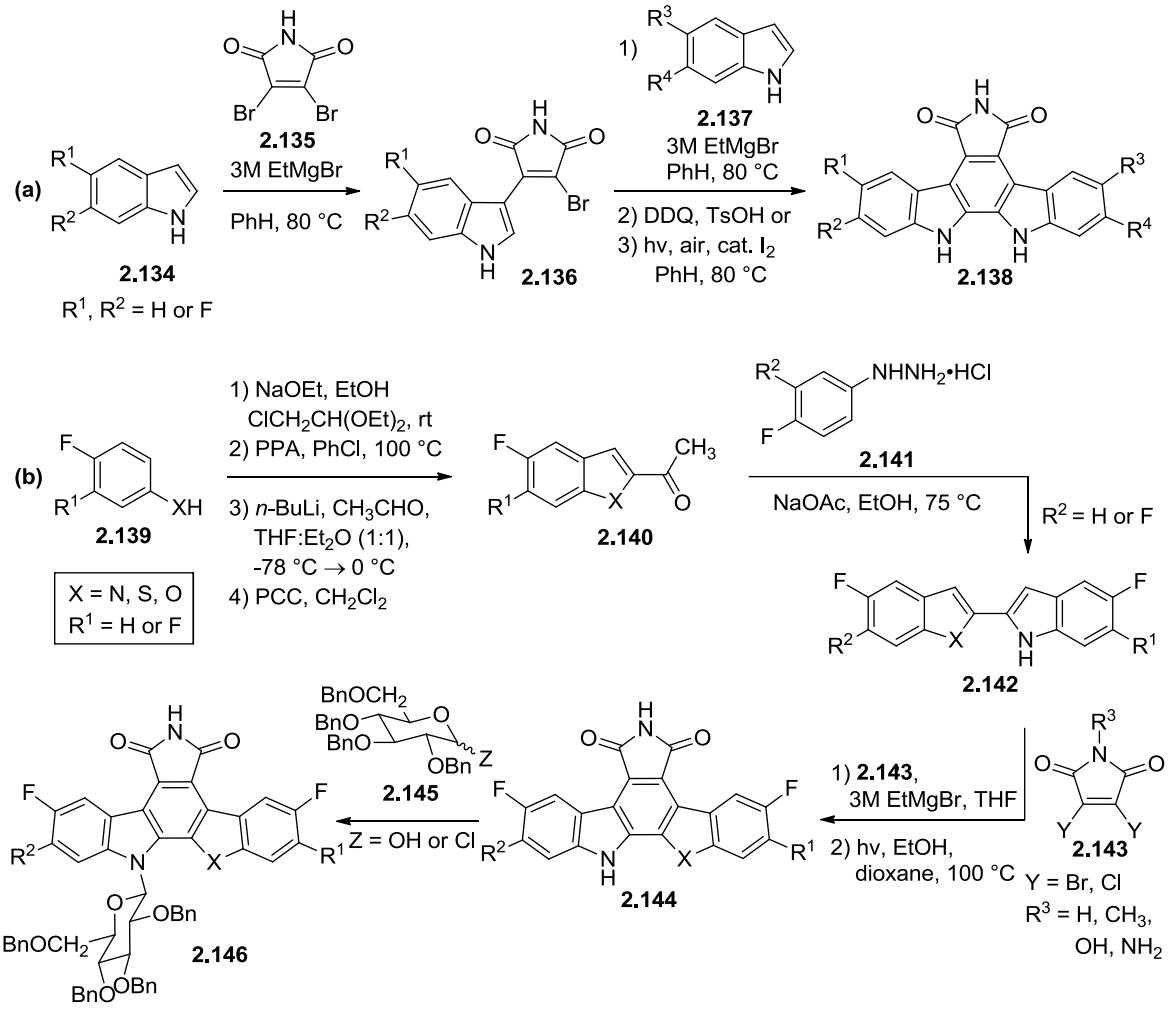

Scheme 2.20. Synthesis of fluoroindolocarbazole analogues[146,147] via (a) Grignard addition to maleimides, or (b) Fischer indole synthesis / maleimide addition

was subsequently identified as a superior drug to **2.128** on the basis of decreased metabolic liability, favourable lipophilicity, improved distal site activity and cytotoxic potency. Although **2.129** was entered into Phase I human clinical trials, no subsequent developments have been reported (as of 2010).[147]

Subsequently, SAR studies involving rebeccamycin derivatives regioselectively functionalized at the 3- and 9- positions (obtained by electrophilic aromatic substitution of rebeccamycin)[148] revealed that three of the analogues **2.130**-**2.132** displayed selective cytotoxicity, and their influence on the cell cycle suggested that these analogues were potent

inhibitors of cyclin-dependent kinases (CDK's), and CDK1/cyclin B in particular. Compound **2.130** had the broadest spectrum of molecular activity (DNA binding, DNA topoisomerase I inhibition, CDK1, CDK5 inhibition) and was a candidate for *in vivo* studies. SAR studies of unsymmetrically substituted arcyriaflavin A analogues functionalized at the C-1, C-2, C-3 or C-4 positions revealed that the C-2 position was most significant in terms of D1/CDK4 inhibition. Further SAR studies of a series of C-2 substituted analogues **2.133** (synthesized by reaction of an indole-3-acetamide with indole-3-glyoxylate and subsequent oxidative cyclization, as shown in Scheme 2.21),[149] resulted in the identification of potential cyclin D1/CDK4 inhibitors.[150] Particularly noteworthy among analogues **2.133** was the consistently high D1/CDK4 potency and selectivity profile, that was generally independent of the nature of the C-2 functional group (Br, F, Cl, CF_3, Me, or OMe).

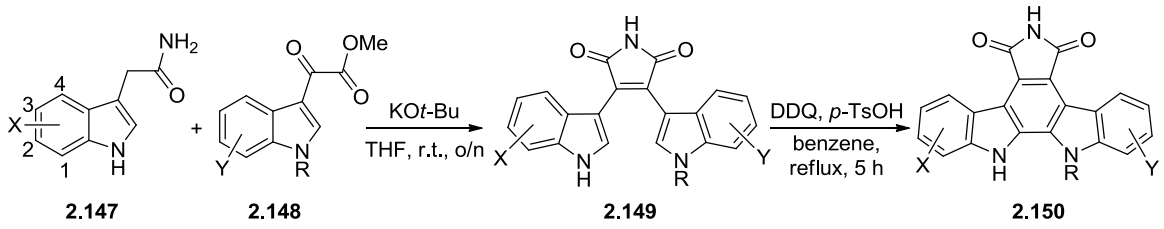

Scheme 2.21. Synthesis of unsymmetrical indolocarbazoles using Faul's procedure[149]

2.2.2 Indole replacement with a carbocyclic ring system.

2.2.2.1 Naphthylpyrrolocarbazoles

SAR studies of indolocarbazole analogues obtained by replacement of one indole ring by a carbocycle (naphthyl, phenyl, tetrahydronaphthyl) or heterocycle (imidazolyl, benzothienyl, 7-azaindolyl, pyridyl, thienyl) culminated in the identification of naphthyl[2,1-*a*]pyrrolo[3,4-*c*]carbazole analogue **2.151** (Figure 2.4) as a potent, highly selective, and ATP-competitive inhibitor of D1/CDK4,[151] prepared according to Faul's methodology (see Scheme 2.21).

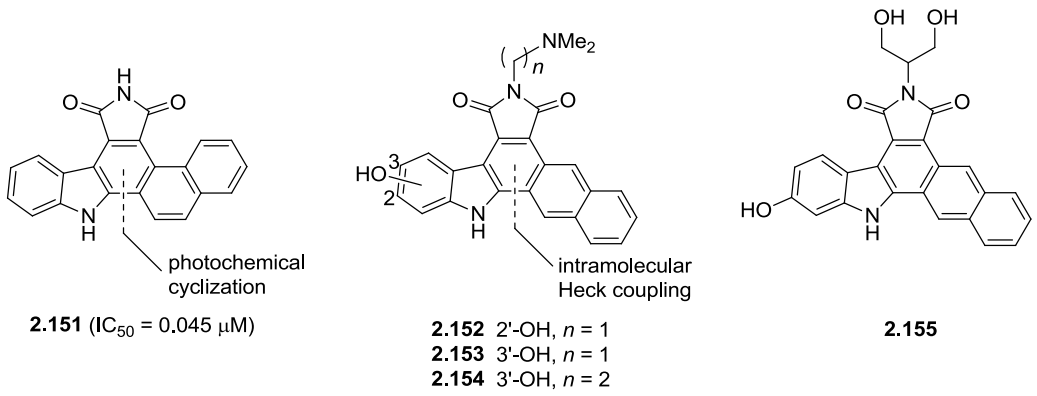

2.151 (IC_{50} = 0.045 μM)

2.152 2'-OH, *n* = 1
2.153 3'-OH, *n* = 1
2.154 3'-OH, *n* = 2

2.155

Figure 2.4. Inhibition of cyclin D1/CDK4 by regioisomeric naphthylpyrrolocarbazoles[151]

In comparison to staurosporine (IC_{50} = 0.059 μM: D1/CDK4a), **2.151** has an IC_{50} = 0.045 μM against D1/CDK4, however low anti-proliferative activity in cell-based assays likely arises from the limited water solubility of **2.151**. Requirement of further SAR studies to increase activity in cell-based assays precluded further *in vitro* and *in vivo* studies. Biological evaluation of the linear naphthylpyrrolocarbazoles **2.152**-**2.154** (Figure 2.4) was facilitated by an improved synthetic method which involves an intramolecular Heck cyclization of mixed aryl/heteroaryl substituted maleimides (Scheme 2.22),[152] in place of an ineffective photochemical cyclization (which suffered from lack of regiocontrol).[151]

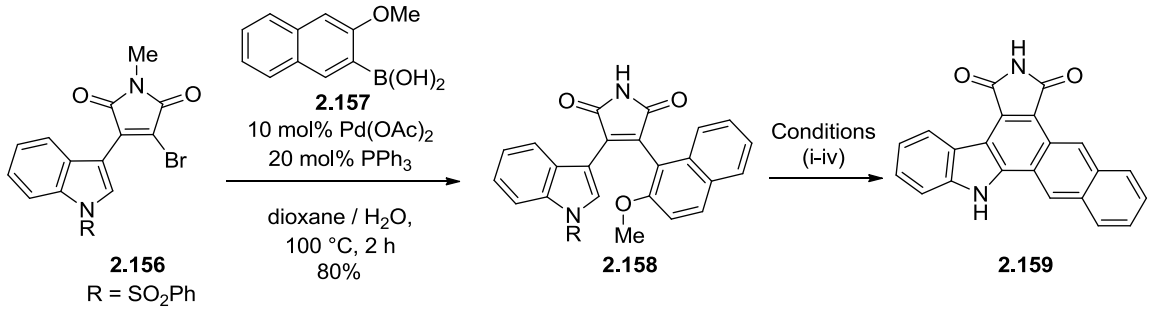

2.156
R = SO_2Ph

2.158

2.159

Conditions: i) BBr_3 (6 eq.), 96%; ii) Tf_2O (3 eq.), 98%; iii) $Pd(OAc)_2$ (1 eq), PPh_3 (0.2 eq), NaOAc (2 eq), Bu_4NCl (1 eq.), dioxane, 3 h, 100 °C; iv) TBAF, THF, reflux, 2 h, 91%

Scheme 2.22. Chemical synthesis of naphthylpyrrolocarbazole analogue **2.159** via a combined Suzuki-Miyaura cross-coupling / Heck cyclization strategy[152]

Naphthylpyrrolocarbazoles **2.152-2.154** (Figure 2.4) were identified as potent, cytotoxic analogues of rebeccamycin, owing to the polar functional groups on the indole framework (OH or OBn in the 2 or 3-position) and the maleimide nitrogen.[153] Of the four drug candidates, the 3-hydroxylated compound **2.153** having a basic (*N*-(2-dimethylamino)) substituent on the maleimide nitrogen was most significant, displaying four-fold greater cytotoxicity against the L1210 cell line than rebeccamycin (**2.34**), likely due to enhanced lipophilicity. Interestingly, analogue **2.155** was highly selective for the DU145 cell line.

During the course of research into the design of potent and selective inhibitors of mixed-lineage kinases (MLKs) superior to K-252c (**2.160**), Hudkins and co-workers identified dihydronaphthyl[3,4-*a*]pyrrolo[3,4-*c*]carbazole-7-one **2.161** and the methylene analogue of the regioisomeric lactam **2.162** (Figure 2.5) as more potent inhibitors of mixed-lineage kinases (MLK1/3) than **2.160**.[154] Replacement of the indole nitrogen in the D-ring of **2.160** by sulfur also results in an effective inhibitor, which, in comparison to **2.160**, is an ~ 1.5 fold less potent inhibitor of MLK1 and ~ 1.5 fold more potent MLK3 inhibitor. Replacement of both indole nitrogens in the B-, and D-rings of **2.160** was generally not favourable. Dihydronaphthyl imide derivative **2.163** displays the most potent inhibitory profile towards MLK1/3 of the series of bis-imide and regioisomeric lactam analogues studied, and is approximately 15-fold more potent than the parent bis-indole compound. Replacement of the D ring carbocycle in **2.163** by a thiophene heterocycle was also tolerated, affording an analogue with 3-fold and 5-fold lower potency towards MLK1 and MLK3, respectively. The SAR studies thus revealed that lactam regiochemistry and shape of the carbo-, or heterocycle are significant factors governing potent MLK1/MLK3 activity, and comparable *in vitro* activity of **2.161** and **2.163** to (+)K-252a suggest that these are novel scaffolds appropriate for continued optimization.

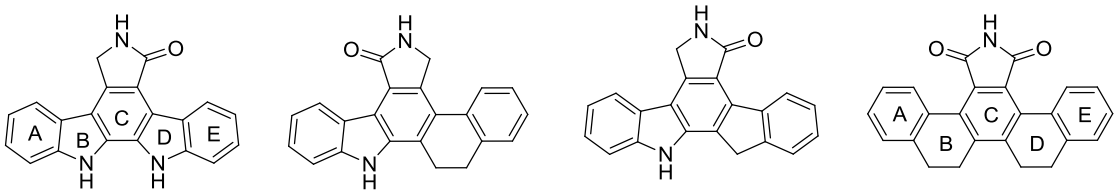

2.160
MLK1: IC_{50} = 138 nM
MLK3: IC_{50} = 49 nM

2.161
MLK1: IC_{50} = 46 nM
MLK3: IC_{50} = 22 nM

2.162
MLK1: IC_{50} = 69 nM
MLK3: IC_{50} = 40 nM

2.163
MLK1: IC_{50} = 22 nM
MLK3: IC_{50} = 12 nM

Figure 2.5. Analogues of K-252c with enhanced MLK activity[154]

2.2.2.2 Phenylpyrrolocarbazoles

Concurrently with the development of the naphthylpyrrolocarbazole series, Routier and co-workers prepared a related phenylpyrrolocarbazole series in order to explore SARs (Scheme 2.23),[155] and the effect on CDK4 inhibition and anti-proliferative activity. The synthesis was a variation of that used to prepare the naphthylpyrrolocarbazole series (Scheme 2.22), and also involved efficient Suzuki-Miyaura cross-coupling of substituted maleimides **2.156** with aryl boronic acid **2.164** early in the synthesis. The intramolecular Heck reaction using the triflate version of **2.165** failed to affect the benzannulation in the benzopyrrolocarbazole series, due to cleavage of the triflate group under all reaction conditions tested. However, the corresponding bromo derivatives **2.165**, when desulfonylated and subjected to Heck conditions, afforded products **2.166** in high yields.

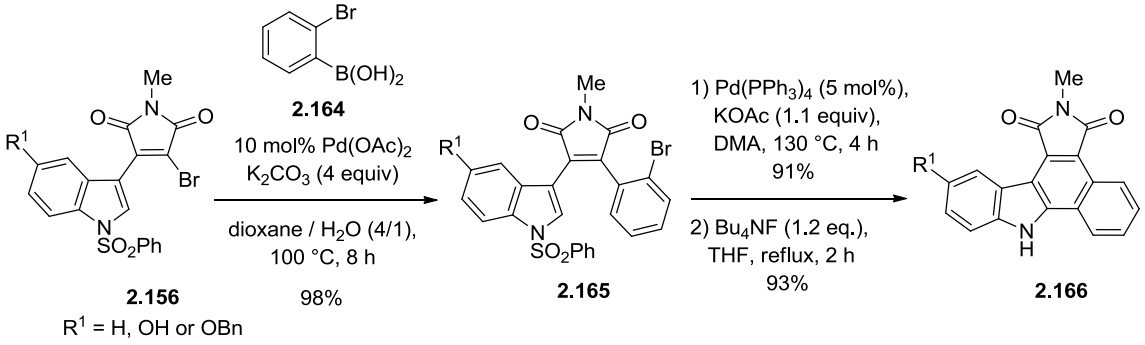

Scheme 2.23. Chemical synthesis of phenylpyrrolocarbazole analogues[155]

In analogy to previous work on the naphthopyrrolocarbazole series, the effect of maleimide substitution and indole ring oxygenation on cytotoxicity and kinase inhibition was also explored in the phenylpyrrolocarbazole series of compounds (Figure 2.7). Once again, the combination of polar hydroxyl group on the 3-position of the indolocarbazole core and *N*-diethylaminoethyl group on the 3-position of the indolocarbazole core and *N*-diethylamino group on the maleimide nitrogen produced the most cytotoxic compound **2.167** against CEM human leukemia cells (IC_{50} = 12 nM). The significance of the hydroxyl group (in terms of efficacy) was evident upon comparison with the non-hydroxylated analogue (IC_{50}=100 nM), and was a general trend in the naphthopyrrolocarbazole series. Analogues bearing basic, hydrophilic side chains on

the maleimide nitrogen had significantly greater efficacy than the corresponding unsubstituted variants. A plausible explanation is the establishment of an electrostatic interaction between DNA and the drug-like molecule at physiological pH (arising from interaction with the protonated terminal amine (appended to the maleimide) with the negatively charged DNA backbone), along with enhanced hydrophilicity. Analogues bearing bis-hydroxy or histamine side chains on the maleimide nitrogen were found to be less active than dimethylamino substituted **2.167**, although measurement of T_m values (an experimental parameter correlating to DNA stability) of duplex DNA did indicate an interaction with DNA for **2.168**-**2.169**, and DNase I footprinting experiments indicated a distinctive sequence selectivity. With the exception of **2.167** (and the non-hydroxylated relative), the analogues performed very poorly in kinase activity assays with IC_{50} values exceeding 10 μM against CDK1 and CDK5 in all cases, and the molecular targets of this class of compounds remains unknown.

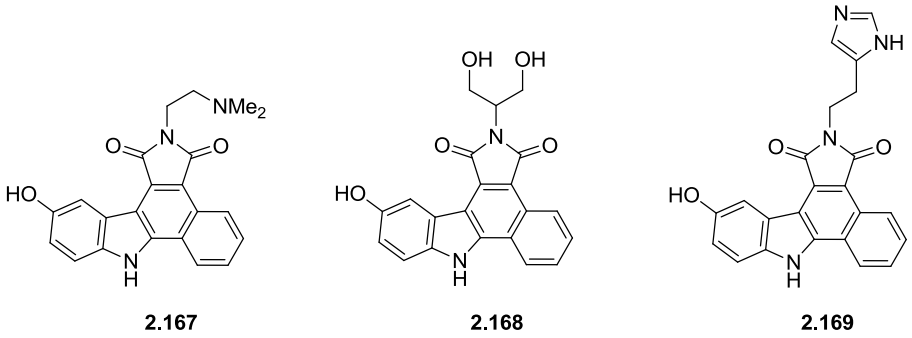

2.167 **2.168** **2.169**

Figure 2.6. Analogues of phenylpyrrolocarbazoles obtained by maleimide and indole substitution

2.2.3 Indole replacement with a heterocyclic ring system

2.2.3.1 Azaindolopyrrolo[3,4-c]carbazoles

Routier and co-workers pioneered the synthesis and investigation of azaindolocarbazole analogues of rebeccamycin, following their initial report of a synthetic methodology applicable to the preparation of symmetrical and non-symmetrical 7-azaindolocarbazoles in 2002 (Scheme 2.24).[156]

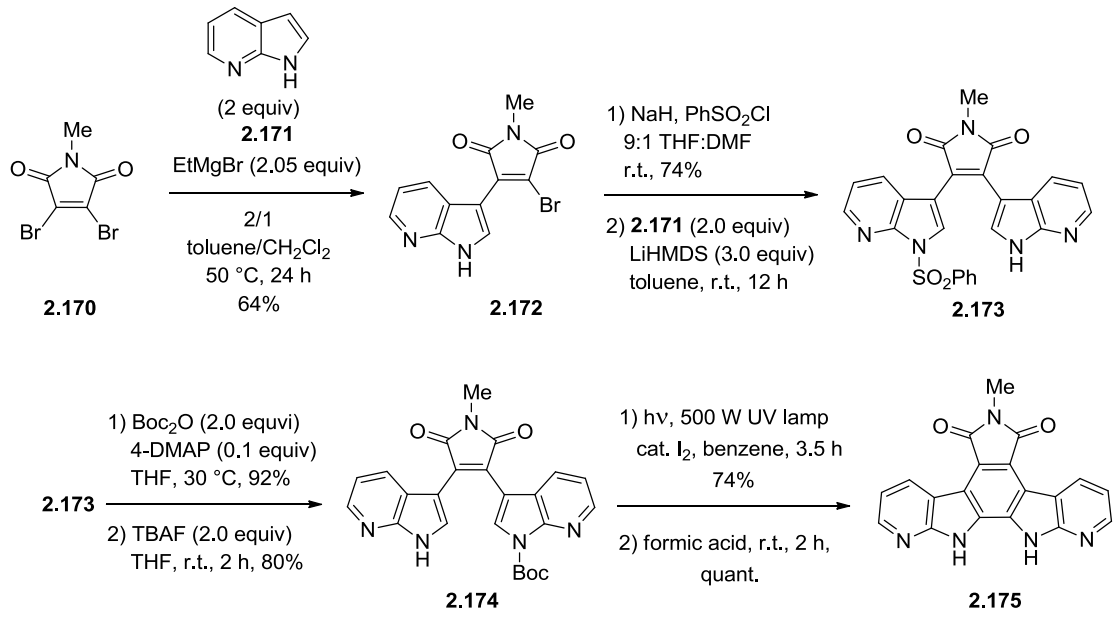

Scheme 2.24. Routier's synthesis of 7-azaindolocarbazole variants of the rebeccamycin aglycon[156]

Interest in azaindolocarbazole derivatives **2.175** and related compounds was driven by the demonstrated enhancement of DNA binding capability in antitumor compounds containing a pyridine nitrogen,[157] and numerous researchers have pursued SAR studies of 7-azaindolocarbazoles, 5-azaindolocarbazoles, and diazaindolocarbazoles (Figure 2.7).

Preliminary investigation of DNA interaction and topoisomerase I inhibition of a series of *N*-methylated 7-azaindolocarbazoles **2.176** bearing indole C-2 or C-3 hydroxyl or benzyl groups was performed by Routier and co-workers.[158] Results revealed that the C-3 hydroxylated analogue was superior in its ability to bind DNA and alter DNA topoisomerase I reactivity to other analogues (and diazaindolocarbazole **2.175**), suggesting that C-3 hydroxylation is a significant element for DNA recognition.

Prudhomme and co-workers demonstrated that the DNA binding ability of glycosylated 7-azaindolocarbazoles **2.177** or **2.178** was dependent on the position of the newly incorporated nitrogen atom in the indolocarbazole framework.[159] Compounds **2.177** bearing the sugar on the azaindole moiety lost DNA binding abilities, however, these analogues had intrinsically consistent cytotoxicity profiles and were also more selective with regards to specific cell lines.

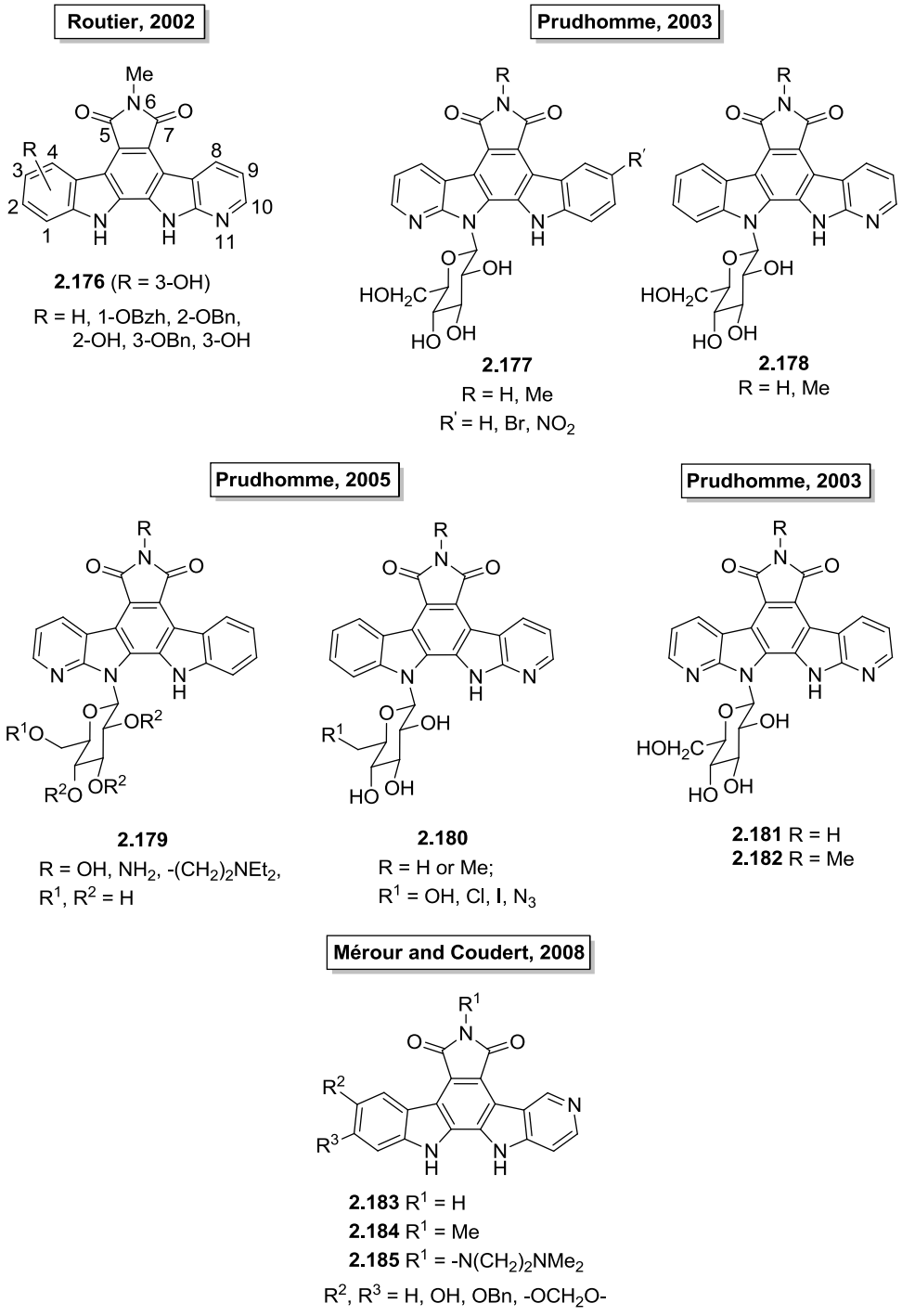

Figure 2.7. 5-azaindolocarbazole and 7-azaindolocarbazole analogues of rebeccamycin

This is suggestive of a common mechanism of action and specific biological target for compounds **2.177** which is different than that of rebeccamycin. In contrast, compounds **2.178** having the sugar on the indole moiety had superior DNA binding capability as compared to non-chlorinated rebeccamycin. Similar cell cycle effects were observed for all azaindolocarbazoles (**2.177** and **2.178**), and did not offer further insight into the specific biological targets of this series of compounds (although a few of the analogues were identified as potent DNA topo I inhibitors).

In a subsequent investigation, Prudhomme and co-workers synthesised and investigated the antiproliferative activity of unsymmetrical glycosylated 7-azaindolocarbazole derivatives (**2.179** and **2.180**) against a panel of four tumor cell lines.[160] Typically, the core structure has been derivatized by attachment of basic, hydrophilic groups (NH_2, OH or $–(CH_2)_2NEt_2$) to the maleimide nitrogen (**2.179**), or by modification of the appended sugar moiety (**2.180**). Based on the results of the study it is difficult to reach a general conclusion that relates structural variation with cytotoxicity. It is apparent, however, that specific cell lines are more sensitive to structural modification (as in the case of maleimide *N*-hydroxylation or aminoalkylation (**2.179**)), although the precise cellular targets have yet to be established. Meaningful correlation between sugar modification and cytotoxicity was not readily apparent, and it was generally observed that functional modifications were not detrimental to *in vitro* cytotoxicity. Synthetic methods for bridged aza-rebeccamycin analogues[161] and 7-azaindolocarbazole analogues of staurosporine[162] have also been described, although detailed biological studies await.

Further studies of di-azaindolocarbazoles **2.181** and **2.182** have been performed with the expectation that the additional nitrogen would contribute to hydrogen bonding interactions with target enzyme(s) in tumor cell lines, enhancing cytotoxicity.[163] Synthesis of **2.181** and **2.182** was achieved using Routier's protocol (Scheme 2.24), followed by late stage glycosylation and oxidative cyclization. Cytotoxicity profiles of analogues **2.181** and **2.182** suggest that *N*-H or *N*-Me substitution plays a significant role in determining selectivity (and potency) towards specific cell lines, with the possible implication that the azaindolocarbazoles involve different mechanisms of action and biological targets than non-azaindolocarbazoles (e.g. rebeccamycin and non-chlorinated rebeccamycin).

Coudert and Mérour investigated the potential of 5-azaindolocarbazole analogues of rebeccamycin (**2.183** – **2.185**) as cytotoxic agents and checkpoint kinase 1 (Chk1) inhibitors,[164]

obtained by substitution of the indole ring with hydroxyl, benzyloxy or methylenedioxy groups and/or *N*-maleimide substitution (*N*-H, *N*-Me, *N*-$(CH_2)_2NMe_2$) and prepared according to the general procedure in Scheme 2.25. Although significant variation in analogue cytotoxicity was observed as a function of substituent properties and positions, several trends could be identified. Cytotoxicity studies indicated that all analogues **2.183**-**2.185** were highly selective for the L1210 cell line, and cytotoxicity values of malemide *N*-H and *N*-Me analogues suggested that micromolar potency was due to the basicity of the 5-azaindolocarbazole heterocycle (independent of *N*-substitution). Curiously, the most L1210 cytotoxic compounds were found in the *N*-$(CH_2)_2NMe_2$ substituted series of azaindolocarbazoles and contained a 2,3-methylenedioxy unit or 2-OH group, whereas nanomolar Chk1 inhibitors were only identified in the malemide *N*-H series **2.183** (and were superior to potent Chk1 inhibitor isogranulatimide (**2.189**, Figure 2.8) having IC_{50} = 0.438 μM).[165]

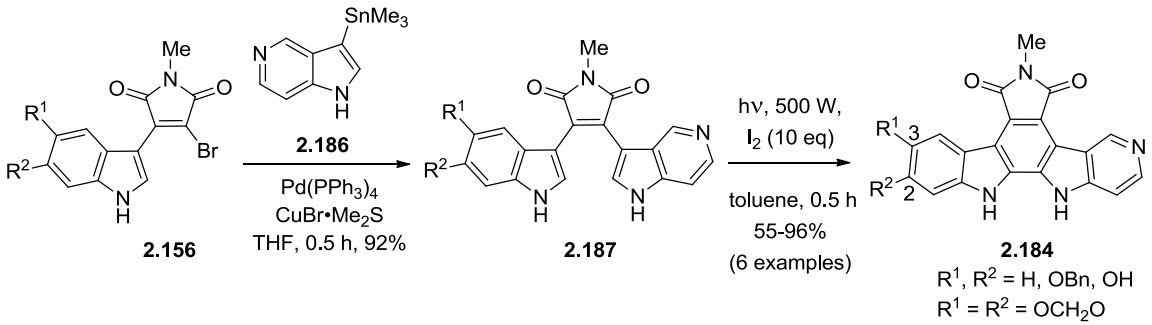

Scheme 2.25. Coudert and Mérour's synthesis of 5-azaindolocarbazole analogues[164]

2.2.3.2. Pyrido-, pyrrolo-, and pyrazolylpyrrolo[3,4-c]carbazoles

Establishment of granulatimide **2.188** and isogranulatimide **2.189** (Figure 2.8) as potent Chk1 inhibitors[166] demonstrates the potential of the imidazolylpyrrolocarbazole framework as a lead structure for the development of biologically active compounds. Indeed, discovery of biologically active granulatimide and isogranulatimide derivatives have been comprehensively reviewed,[166] and determination of structural features necessary for bioactivity remains an active area of research.

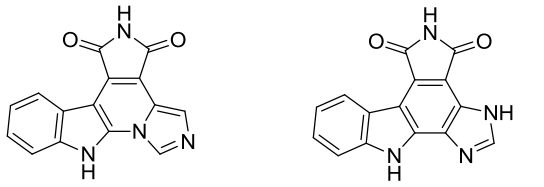

2.188 granulatimide **2.189** isogranulatimide

Figure 2.8. Imidazolylpyrrolocarbazole derivatives **2.188** and **2.189**[165]

As part of a research program focused on the development of Ru complexes that target the ATP binding site of protein kinases, Meggers and co-workers were interested in granulatimide analogues in which the imidazole ring has been replaced by pyridine (Figure 2.9).[167]

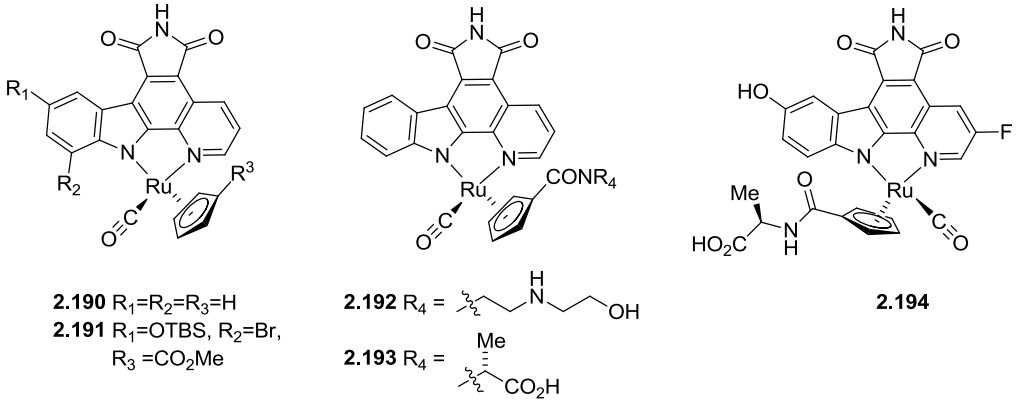

2.190 R_1=R_2=R_3=H
2.191 R_1=OTBS, R_2=Br, R_3 =CO_2Me
2.192 R_4 =
2.193 R_4 =
2.194

Figure 2.9. Pyrido-pyrrolocarbazole half-sandwich ruthenium complexes identified as potent GSK-3 inhibitors through SAR studies[167]

Racemic **2.190** has been identified as a potent and selective inhibitor of glycogen synthase kinase-3 isoforms (GSK-3α: IC_{50} = 3 nM, GSK-3β: IC_{50} = 10 nM), and has comparable or superior potency and selectivity to known, effective GSK-3 inhibitors.[168] Subsequent modification of the indole scaffold and cyclopentadienyl ligand afforded (*R*)-**2.191**, a more potent and selective GSK-3 inhibitor (GSK-3α: IC_{50} = 0.35 nM, GSK-3β: IC_{50} = 0.55 nM) against a panel of 57 kinases.[169] Another series of analogues was prepared from an organoruthenium complex having an *N*-succinimidyl ester appended to the cyclopentadienyl ligand, which was used to generate a diverse library of compounds having an amide appendage.[170] Two of the library compounds (**2.192** and **2.193**) possessed even greater selectivity and potency than (*R*)-

2.191. Further SAR studies culminated in the identification of inhibitor **2.194**, having an exceptionally high binding affinity for GSK-3 (GSK-3β: IC_{50} = 0.04 nM).[171] Co-crystallization of **2.206** with GSK-3β revealed that the structural features of **2.206** were a perfect complement to the ATP binding site.

More recent SAR studies of granulatimide and isogranulatimide analogues have been focused on series of compounds obtained by replacement of the imidazole heterocycle with pyrrole or pyrazole (Figure 2.10), and have culminated in the identification of superior Chk1 kinase inhibitors. Prudho mme and co-workers established that compounds **2.195** (Chk1 IC_{50} = 0.024 μM) and **2.196** (Chk1 IC_{50} = 0.016 μM) are more potent Chk1 inhibitors than granulatimide,[172] although maleimide *N*-methylation, substitution with other R groups (Cl, Br, OBn), or isomeric ring systems (obtained by moving the nitrogen atom in the pyrrole ring) was detrimental to Chk1 inhibition. Furthermore, lack of a correlation between Chk1 inhibition and cytotoxicity or the ability to affect DNA topoisomerase I reactivity was apparent. Significant Chk1 inhibition has also been reported for analogues containing a lactam or bis-imide heterocycle in place of imidazole.[173] Recently, synthetic routes to pyrazole analogues **2.196** and **2.197** have been described,[174] and of these, **2.197** has demonstrated growth inhibitory activity against a panel of cancer cell lines comparable to granulatimide **2.188**.[175]

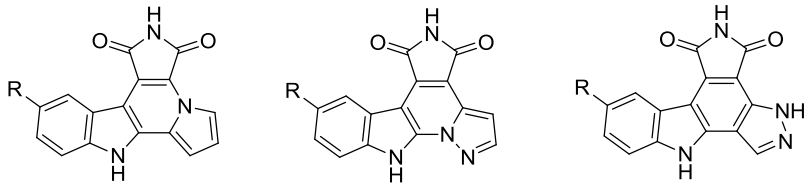

2.195 (R = OH)
2.196 (R = H)

2.197

2.198

Figure 2.10. Granulatimide and isogranulatimide heterocyclic analogues **2.195-2.198**[174-175]

2.2.3.3. Quinolinyl-, and isoquinolinylpyrrolo[3,4-c]carbazoles

Zhu and co-workers prepared a series of quinolinyl-, and isoquinolinylpyrrolo[3,4-c]carbazole analogues **2.199**– **2.202** (Figure 2.11),[176] and identified **2.199** as the most potent cyclin D1/CDK4 inhibitor (IC_{50} = 69 nM). In context of naphthopyrrolocarbazole **2.151** (Section 2.2.2.1, Figure 2.4), **2.199** bears resemblance in terms of the preferential "up-angular"

conformation for interaction in the kinase ATP binding site. Fusion of the quinolinyl groups to the carbazoles as in analogues **2.200** and **2.201** results in ineffective D1/CDK4 inhibition. The position of the nitrogen in the quinolinyl / isoquinolinyl ring is also significant, as moderate or low D1/CDK4 inhibitory activites were observed for **2.202** when the nitrogen occupied position 1 or 2 as indicated. The synthesis was straightforward, typically involving condensation of indolylacetamides with quinolinyl-, or isoquinolinylglyoxalates (according to Faul's methodology, Scheme 2.21). The reverse chemistry was also possible, namely, reaction of indolylglyoxalates with (iso)quinolylacetamides.

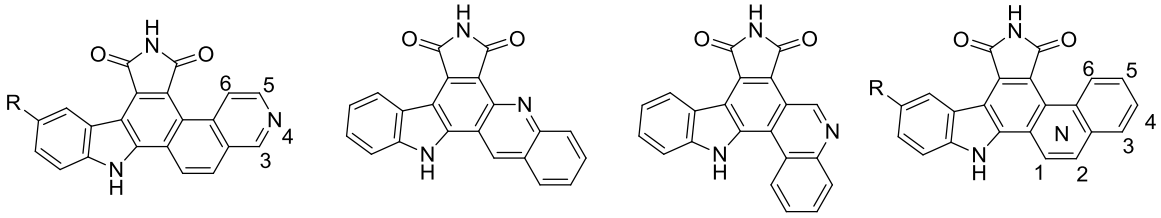

Figure 2.11. Quinolinyl-, and isoquinolinylpyrrolocarbazoles **2.199**-**2.202**[176]

2.2.3.4. Miscellaneous heteroaryl pyrrolo[3,4-c]carbazoles

A highly convergent synthesis of rebeccamycin analogue **2.210**, having structural resemblance to BMS-251873 **2.128** (Figure 2.3, Scheme 2.2.1) has been described (Scheme 2.26).[177] In this synthesis, the use of Fischer indolization is avoided, and key synthetic steps involve consecutive reaction of the Grignard reagent of difluorinated indole **2.203** with dibromomalemide **2.204**, and Suzuki-Miyaura cross-coupling of the resulting mono-heteroarylated maleimide **2.205** with fluorinated benzothiophene-3-boronic acid **2.206**. The results of biological studies of **2.210** have not been described.

More recently, Routier and co-workers disclosed a new series of analogues **2.111** based on a benzodioxinopyrrolocarbazole scaffold (Figure 2.12).[178] **2.112** displays nM cytotoxicity towards the L1210 cell line, and strongly influences the cell cycle in a different fashion than the other analogues (resulting in an accumulation of cells in the G1 phase, whereas the other anal-

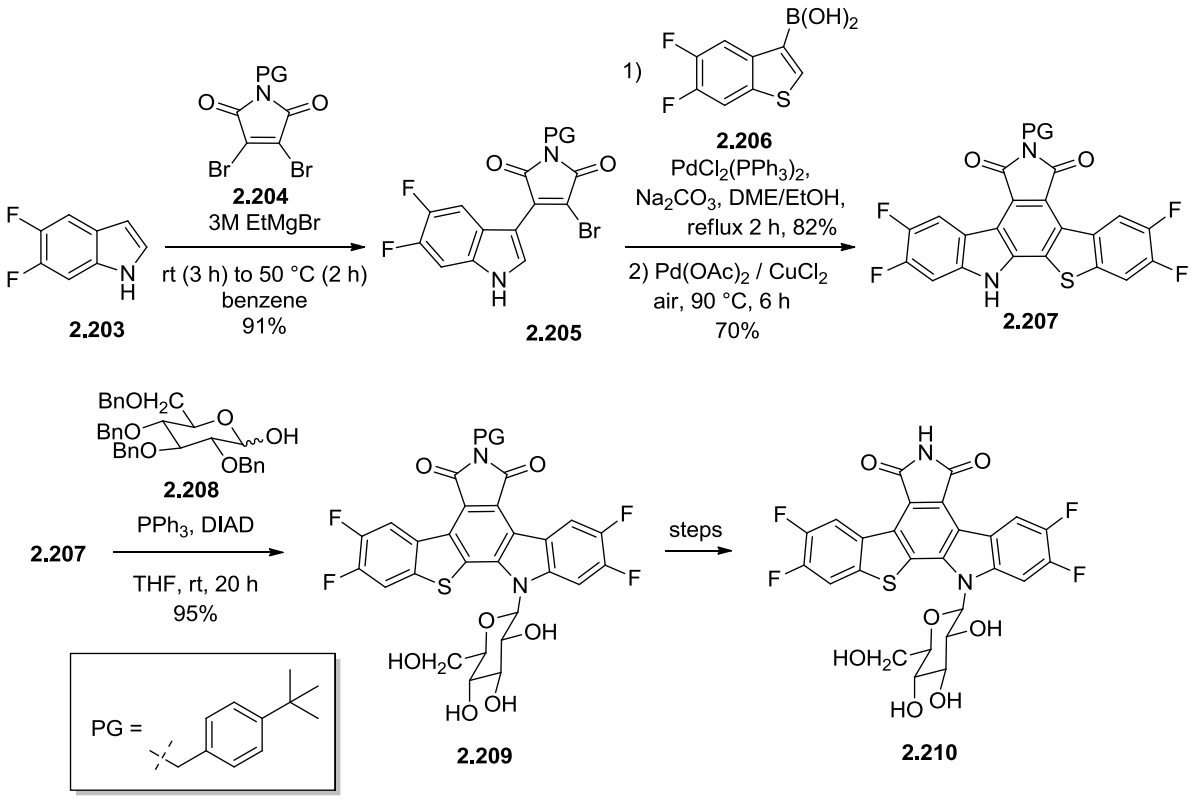

Scheme 2.26. Wang's synthesis of tetrafluorobenzothienylcarbazole analogue **2.210**[177]

ogues resulted in G2+M phase accumulation). Investigation of the molecular target and further structural optimization of **2.112** is reportedly in progress.

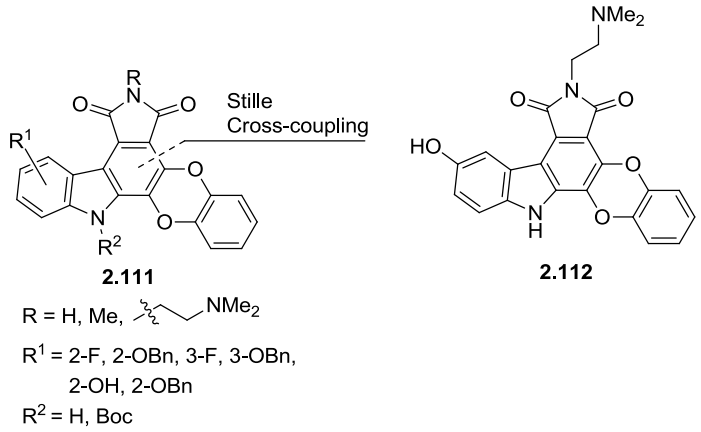

Figure 2.12. Indolocarbazole derivatives containing benzoxazine or benzodioxine heterocycles[178]

2.3 Aims of Research

As described in Chapter 1, the cloning, sequencing and characterization of the biosynthetic gene pathway encoding the enzymes necessary for rebeccamycin biosynthesis in *L. aerocolonigenes* was first reported in 2002.[179] In context of the potential therapeutic applications of indolocarbazole alkaloids, this discovery captured the attention of prominent researchers and resulted in a significant body of research directed towards mechanistic understanding of the indolocarbazole biosynthesis pathways. At the time our research in this area began in 2005, other researchers had been primarily focused on characterization and mechanistic studies of enzymes involved in early stages of rebeccamycin biosynthesis (specifically, RebF, RebH, RebO, RebD and StaP).[95, 180]

In connection with cross-coupling chemistry performed in the Snieckus group,[181] we were initially interested in studying the mechanism of RebP, which was believed to catalyze the uncommon enzymatic aryl-aryl bond forming reaction between C2 and C2' of the indole rings in **2.1** (Scheme 2.1). In order to perform this study, access to the substrate CPA (**2.1**) was required, for which several preparative chemical and biochemical methods had been described (Sections 2.1.1 and 2.1.2). Pertaining to the chemical synthesis routes to **2.1**, it has remained relevant knowledge that isolation of the di-carboxylic acid in various degrees of purity has been described. High isolated yields (> 95%) were reported when **2.1** was isolated by acidic work-up of the reaction mixture and extraction without purification (Scheme 2.7),[106] whereas other preparative methods reported significantly lower yields of **2.1** isolated after flash chromatography (37%) or flash chromatography followed by preparative HPLC (1% isolated yield), as in Scheme 2.2. Consequently, the reported yields are not necessarily reproducible as they are dependent on the method of isolation and purification.

We also sought to develop a modular synthetic strategy for the preparation of a small library of stable, heterocyclic analogues of lycogarubin C (**2.5**), which should, theoretically, be readily deprotected to afford derivatives of CPA (**2.1**). For the convenience of the reader, the structures of these compounds are presented again in Figure 2.13. Although 3,4-diarylpyrrole-2,5-dicarboxylates and related compounds belong to a large class of natural products for which total synthesis strategies have been well established (Section 2.2.3), limited syntheses of 3,4-diheteroarylpyrrole-2,5-dicarboxylic acids or diesters have been described. Reported variants are

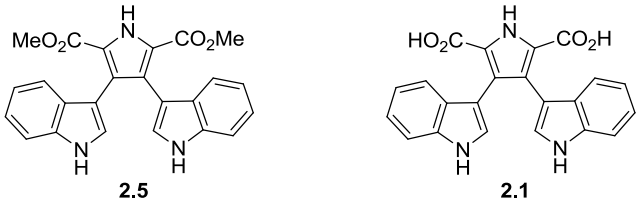

Figure 2.13. Chemical structures of lycogarubin C (**2.5**) and CPA (**2.1**)

typically isolated from natural sources,[99,182] particularly marine actinomycetes thriving in harsh environments whose unique metabolic pathways offer potential for new antibiotics and antimicrobial agents. A single recent patent described scientific contributions to the diversification of this series of compounds, through detailed fermentation / semi-synthetic approaches with the intent of generating potential bis(3,4-(indol-3-yl))pyrrole-2,5-dicarboxylates as antimicrobial agents.[183] Consequently, establishment of an efficient synthetic methodology was required if our library preparation was to be achieved.

Encouraged by the successful application of Suzuki-Miyaura cross-coupling in the synthesis of 3,4-diarylpyrrole natural products (Section 2.1.3), we anticipated that a divergent synthetic strategy from a common building block would allow efficient generation of a library of structurally diverse 3,4-diaryl and heterodiaryl pyrroles as analogues of lycogarubin C (**2.5**). The design of these analogues is based, in part, on our understanding of the interactions between catalytically relevant amino acid residues and the putative substrate in the RebC active site, as well as our mechanistic proposal for RebC catalysis based on the *in vitro* experiments described in Chapter 1. The structural analysis of lycogarubin C (**2.5**) shown in Figure 2.14 summarizes chemical manipulations of **2.5** considered for preparation of the library of analogues.

The rationale for this library development is based on several considerations. The new compounds are considered to have potential application as probes of RebP catalytic activity, in accordance with our initial objective. We also envisage that intramolecular oxidative cyclization would provide access to molecules reminiscent of RebC substrates, and if stable under aerobic oxidative conditions, these could find further application as tools for studying our proposed mechanisms of RebC and RebCF216VR239N catalysis deduced from the *in vitro* studies. Additionally, *in vivo* enzymatic reactions using these substrate analogues represent an alternative approach for studying enzymatic catalysis, by altering the enzyme/substrate interaction through

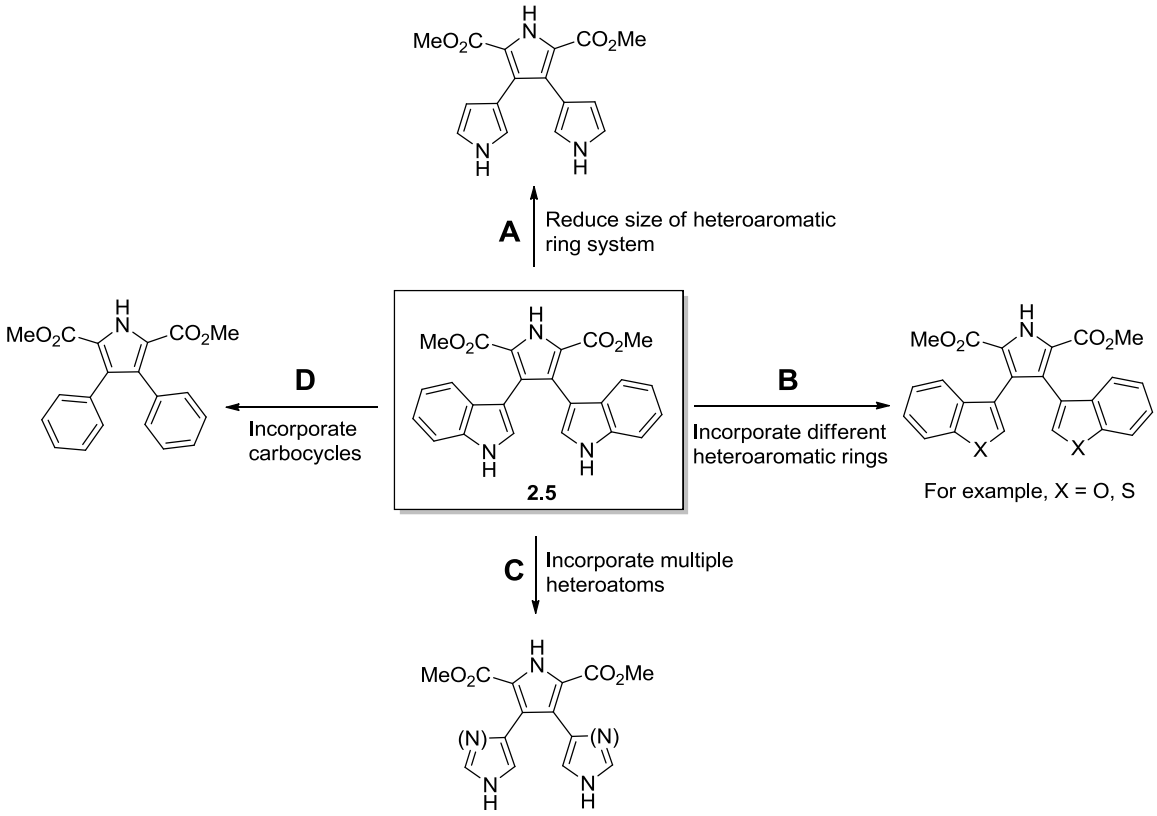

Figure 2.14. Pertinent structural manipulations of lycogarubin C (**2.5**)

variation in substrate structure, as opposed to direct manipulation of the active site through site-directed mutagenesis. The relationship of these analogues to the 3,4-diarylpyrrole family of natural products implies that they could possess important biological properties, and they are also biosynthetic precursors to new indolocarbazole derivatives that could possess important biological activity (indolocarbazoles derived from replacement of either one or both indole rings with another heteroaromatic were discussed in Section 2.2.3). Finally, we anticipated that oxidative cyclization to corresponding tetra-, or hexacyclic compounds would be facile chemistry and allow establishment of robust synthetic chemistry for the preparation of structurally complex indolocarbazole derivatives.

2.4 Results and Discussion

2.4.1 Attempted synthesis of chromopyrrolic acid CPA (2.1) via a biomimetic approach

As mentioned in Section 2.3, the initial goal of this project was to achieve the synthesis of chromopyrrolic acid (**2.1**) as a substrate for RebP. The synthetic route described by Sherman and co-workers commencing from indole-3-pyruvic acid was initially attempted (see Scheme 2.27), and found to be unsuccessful. Although the esterification **2.3** → **2.4** proceeded as described, the published experimental procedure for oxidative coupling and cyclization to **2.5** contained many discrepancies. The quantities of reactants used for the preparation of **2.5** were incorrectly described, as the quantities of **2.4** and NaOMe used in the reaction did not correspond to the mmol values reported. Consequently, equimolar amounts of **2.4** and NaOMe were not used in the reaction, as described. The reported characterization data was inadequate to support formation of lycogarubin C (**2.5**) using the described methodology. Although the ^{1}H-NMR data contained two sets of doublets corresponding to the indole H-4/(H-4)' and H-7/(H-7)' protons, the reported coupling constants (J = 6.0 Hz and 3.0 Hz) did not match each other, and the J value of 3.0 Hz is too low for coupling of an aromatic proton with an ortho neighbor. A similar situation was observed for coupling of the indole H-5/(H-5)' and H-6/(H-6)' protons, with the value of the coupling constants for the triplets reported as J = 4.2 Hz and 5.4 Hz. Additionally, the NMR spectra was obtained in CD_3OD and observation of the indole and pyrrole NH groups would not be expected, and only one ester methyl group at δ 3.33 was given. ^{13}C NMR data was not provided. Attempted preparation of **2.5** according to the published procedure involved isolation of reaction products by preparative TLC. Subsequent MS analysis failed to give evidence for the formation of **2.5**. After multiple failed attempts, attention was turned to other methods for the preparation of CPA, specifically by Suzuki cross-coupling of dimethyl 3,4-dibromo-2,5-pyrrole dicarboxylate **2.31** with an indole-3-boronic acid according to Fürstner's synthesis of lycogarubin C[111] (**2.5**), shown in Scheme 2.8. Preparation of the required coupling partners is described in Sections 2.4.2.1-2.4.2.2 and the results of cross-coupling are found in Section 2.4.2.3.

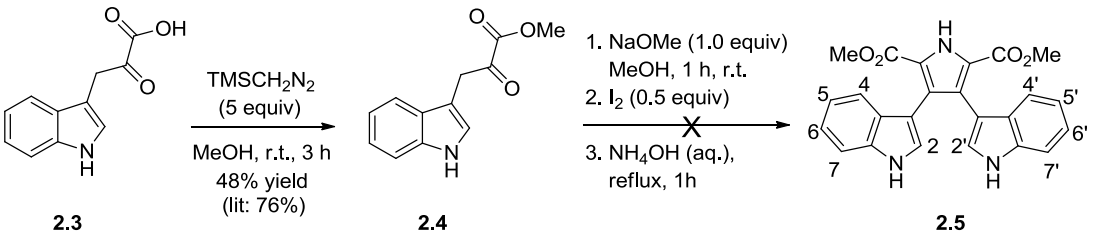

Scheme 2.27. Attempted reproduction of Sherman's synthesis of chromopyrrolic acid (**2.1**)

2.4.2 Synthesis of CPA (2.1) using the Suzuki-Miyaura cross-coupling reaction

2.4.2.1 Preparation of dimethyl 3,4-dibromo-2,5-pyrrole dicarboxylate (2.31)

Pursuance of Fürstner's synthetic route to lycogarubin C[116] (**2.5**), Scheme 2.28a, required the preparation of pyrrole cross-coupling partner **2.31**. Initially the most direct synthetic route developed by Fürstner[116] (Scheme 2.28a) was attempted. Five years after the Fürstner synthesis of **2.31**, Donohoe and Thomas reported an alternative synthetic route to **2.215**,[184] which relied on D*o*M (Directed *ortho* Metalation) chemistry instead of metal-halogen exchange of **2.214** to generate the di-lithiated intermediate **2.216** (Scheme 2.28b).

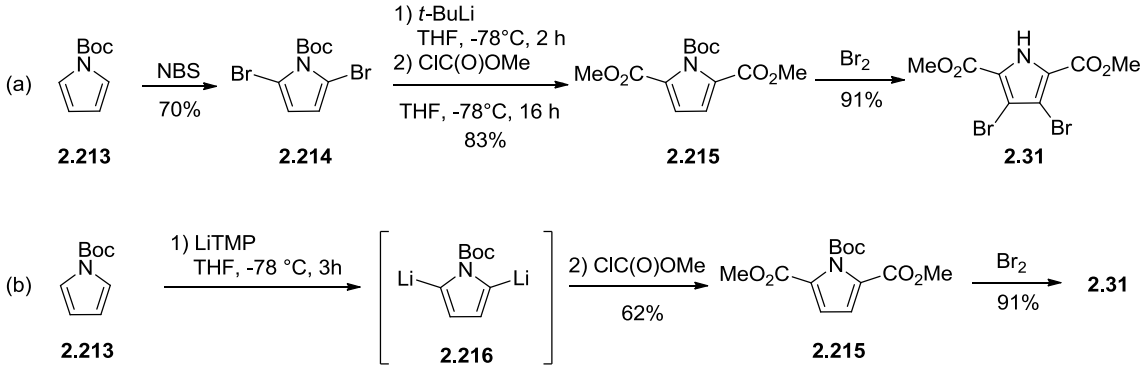

Scheme 2.28. Synthetic routes to **2.31** reported by (a) Fürstner[116] and (b) Donohoe[184]

Although formation of diester **2.31** was reported to occur in high yield using the Fürstner methodology, specific requirements of the experimental procedure did not allow for successful reproduction of this reaction. A significant practical limitation of the procedure arose from the requirement to cannulate the di-lithiated pyrrole **2.216** into methyl chloroformate,

while maintaining cryogenic conditions. The necessity for performing the reaction according to this "inverse addition" procedure was attributed to the importance of having a high concentration of electrophile (methyl chloroformate) present during the quench step. In an effort to perform the reaction and obtain a synthetically useful amount of **2.31**, cannulation of the di-lithiated species resulting from metal-halogen exchange of **2.214** into a solution of methyl chloroformate (at -78 °C) was achieved over 1 h, as described. However, it was difficult to maintain cryogenic conditions during the transfer (due to inherent warming while the di-lithiated pyrrole was in the cannula). Additionally, it was not possible to maintain the reaction at -78 °C for a subsequent 16 h as described using the equipment available. The result was a chromatographically inseparable mixture of mono-, and bis-esterified products, identified upon analysis of the NMR spectrum corresponding to the isolated material.

The preparation of aldehyde ester **2.220** (Scheme 2.29) from pyrrole is well documented, being a key intermediate in the synthesis of guanidinocarbonylpyrrolecarboxylic acids,[185] Boc-protected 4-,5-aminopyrrole-2-carboxylic acid methyl esters,[186] a rationally designed HCV helicase inhibitor,[187] and 5-substituted pyrrole-2-carboxaldehydes obtained by lithiation of a 6-dimethylamino-1-azafulvene dimer.[188] The procedure reported by Schmuck was followed for the preparation of **2.220**,[91] and proceeded effectively. The overall six-step preparation of **2.31**, *via* **2.220** as a key intermediate, is presented in Scheme 2.29.

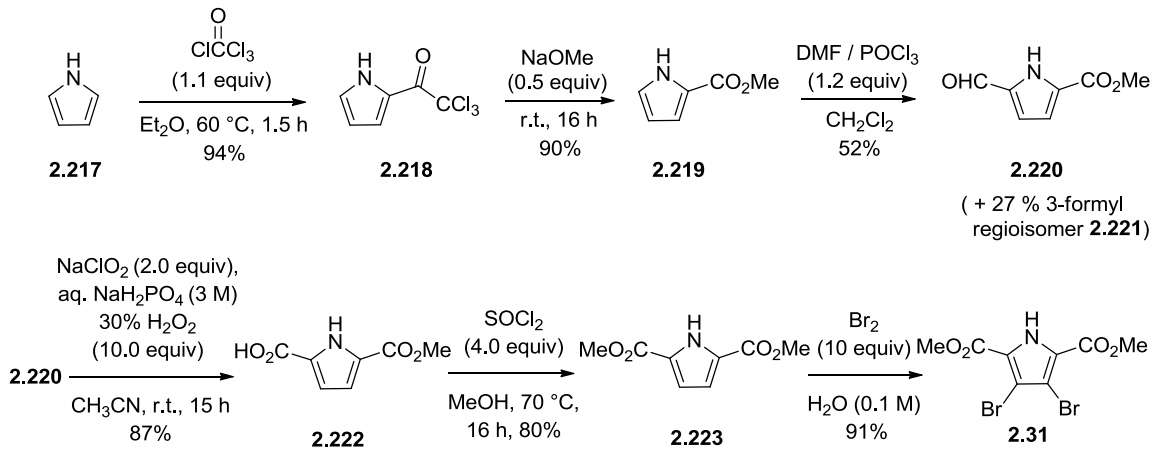

Scheme 2.29. Synthesis of 3,4-dibromopyrrole-2,5-dicarboxylate dimethyl ester **2.31**

The synthesis commences with the acylation reaction of pyrrole, affording trichloroacetyl pyrrole **2.218** in 90% yield. Simple esterification of **2.218** with sodium methoxide furnishes ester **2.219**. The Vilsmeier-Haack formylation of **2.219** affords the two regioisomeric aldehydes **2.220** and **2.221**, consistent with the product ratio reported by Schmuck (~2:1 **2.220** : **2.221**). From **2.220**, the synthesis of the desired dibromopyrrole **2.31** is readily achieved in three steps by oxidation to the carboxylic acid **2.222**, esterification to afford **2.223**, and bromination to give pyrrole dibromo diester **2.31**. For other conditions which led to the optimized esterification of **2.222** → **2.223**, see the Experimental Section. Subsequent to the completed synthesis of **2.31** using this approach, an $Fe(acac)_3$-catalyzed method for the direct, quantitative preparation of **2.223** from pyrrole was reported by Khusnutdinov and co-workers (2010),[189] and is of significant merit to be used in future preparation of **2.31**.

Large quantities (9 gram scale) of **2.31** were prepared using this methodology as every reaction performed well upon scale-up. Use of inexpensive reagents, and the requirement of only two flash chromatography purifications (after formylation and final bromination) makes this an efficient and economical procedure.

2.4.2.2 Preparation of indole-3-boronic acids 2.32 and 2.228

Having established a scaleable and efficient route to 3,4-dibromopyrrole **2.31**, preparation of *N*-(*tert*-butyldimethylsilyl)indole-3-boronic acid **2.32** was necessary in order to achieve the synthesis of **2.1**, based on the Fürstner precedent for the preparation of lycogarubin C (**2.5**). The synthetic approach to **2.32** from indole is presented in Scheme 2.30a. Preparation of *N*-(*tert*-butyldimethylsilyl)-3-bromoindole **2.225** was carried out according to a patented procedure,[190] and required immediate purification in order to minimize product decomposition by the contaminant 3-bromoindole formed during the reaction. The material turned slightly purple upon storage in the freezer, and NMR analysis indicated slow decomposition to *N*-(*tert*-butyldimethylsilyl)indole. Therefore, the material was promptly purified by flash column chromatography prior to preparation of boronic acid **2.32** according to a published procedure.[191] Immediate use of **2.32** in subsequent cross-coupling reactions is standard procedure due to limited stability (protodeboronation), and for this reason, characterization of the boronic acid is not reported in procedures describing preparation of **2.32**.[116, 191, 192]

The more stable *N*-(*p*-toluenesulfonyl) indole-3-boronic acid **2.228** was also prepared, according to Scheme 2.30b. The three step synthetic sequence involved initial *N*-toluenesulfonylation of indole **2.224**, by treatment of **2.224** with toluenesulfonyl chloride in the presence of NaOH and the phase-transfer catalyst TBAHS (tetrabutylammonium hydrogen sulfate)[193a-e] to give known compound **2.226**. Numerous other methods have been described.[194] Electrophilic bromination with Br_2 afforded the desired **2.227**, however, a synthetically useful quantity of material was not obtained despite flash column chromatography and recrystallization efforts. Bromination with NBS proceeded slowly but led to pure **2.227**. Gribble described the preparation of an analogous boronic acid by metal-halogen exchange of 3-bromo-*N*-benzenesulfonyl indole at -100 ˚C, followed by electrophilic quench with trimethyl borate,[195] to give the desired boronic acid in 46% yield. A more convenient *in situ* quench approach was followed, in which a solution of **2.227** in anhydrous THF containing triisopropyl borate at -78 ˚C was treated with *n*-BuLi. Consequently the reaction could be performed at a more convenient temperature (-78 ˚C instead of -100 ˚C). Comparable yields were obtained (38% versus Gribble's yield of 46%), and the boronic acid **2.228** was easily isolated by hexane trituration.

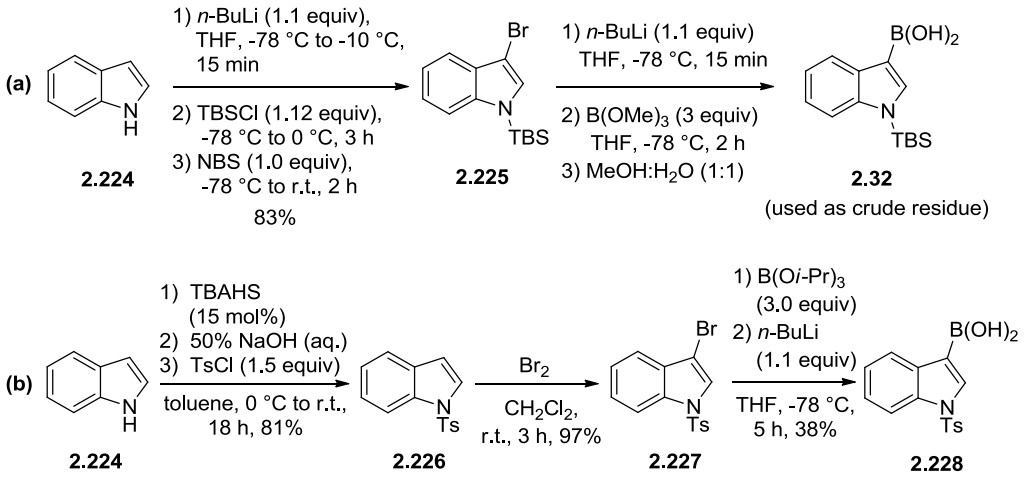

Scheme 2.30. Synthetic routes to indole-3-boronic acids **2.32** and **2.228**

2.4.2.3 Attempted synthesis of Lycogarubin C (2.5) using Fürstner's methodology

Having required coupling partners **2.31** and **2.32** available, Suzuki-Miyaura cross-coupling using the procedure described by Fürstner was tested (Scheme 2.31). Preparation of boronic acid **2.32** was carried out immediately prior to use in cross-coupling and all materials required for the reaction were added to the flask containing the crude boronic acid. Analysis of the reaction mixture by thin layer chromatography indicated the presence of both unreacted starting material **2.31** and *N*-TBS indole, indicative of extensive proto-deboronation. The quantity of water used in Fürstner's synthesis was not specified (only that a minimum amount of water was used), and given the potential for ester hydrolysis under the hot aqueous basic reaction conditions, minimal exposure of cross-coupled to the hot basic reaction media is likely relevant. Further chemistry attempted for the synthesis of **2.5** is discussed in section 2.4.3.

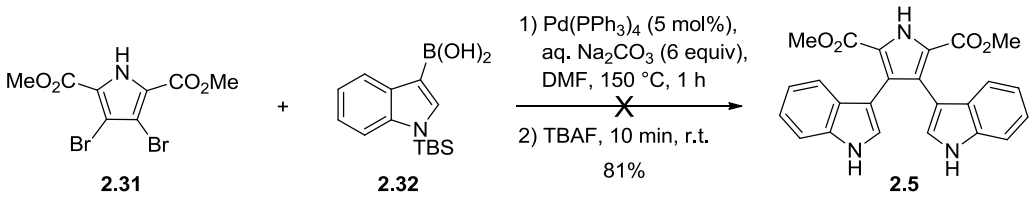

Scheme 2.31. Attempted synthesis of CPA (**2.1**) using Fürstner's methodology

2.4.3 Synthesis of heterocyclic analogues of CPA dimethyl ester (2.5)

Having developed a scaleable synthesis of the desired dibromopyrrole **2.31**, Suzuki cross-coupling conditions which would successfully couple **2.31** with thiophene-3-boronic acid **2.229** and generate **2.230**, a heterocyclic analogue of **2.5**, were established (Table 2.1).

Table 2.1. Optimization of the Suzuki-Miyaura cross coupling of **2.31** with thiophene-3-boronic acid to give compound **2.230**

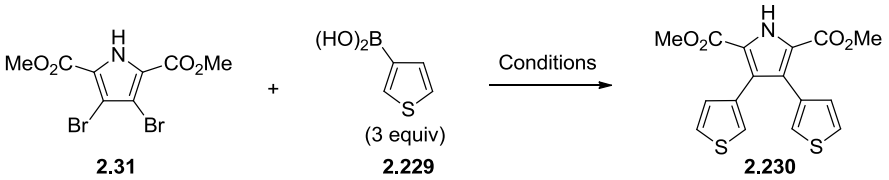

2.31 **2.229** **2.230**

Entry	Catalyst (5 mol%)	Ligand (20 mol%)	Base (4.0 equiv)	Solvent	Time (h)	Product(s)	Yield
1	$Pd(dppf)Cl_2$ $\bullet CH_2Cl_2$	-----	2M K_2CO_3	DME/H_2O	15	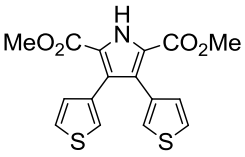 **2.230**	24%
2	$Pd(dppf)Cl_2$ $\bullet CH_2Cl_2$	-----	2M Cs_2CO_3	DME/H_2O	15	**2.230** **2.231** **2.232**	18% 31%[a] 25%[a]
3	Pd_2dba_3	S-Phos	K_3PO_4	*n*-BuOH	2	**2.230** **2.233** **2.234**	22% 19%[b] 13%[b]
4	Pd_2dba_3	S-Phos	K_3PO_4	toluene	5	**2.230**	21%[c]
5	Pd_2dba_3	S-Phos	K_3PO_4	toluene	20	**2.230**	66%
6	Pd_2dba_3	S-Phos	K_3PO_4	*t*-BuOH	4	**2.230**	83%

[a] **2.231** and **2.232** correspond to the reduction products shown in Figure 2.15. [b] **2.233** and **2.234** correspond to the trans-esterification products shown in Figure 2.15. [c] 27% unreacted starting material was recovered.

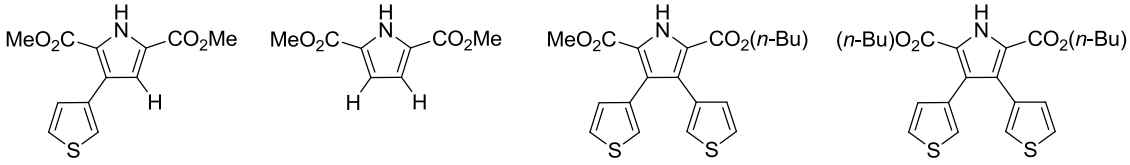

2.231 **2.232** **2.233** **2.234**

Figure 2.15. Side products obtained during optimization of Suzuki coupling of **2.31** with **2.229** arising from reduction (**2.231** and **2.232**), or trans-esterification (**2.233** and **2.234**).

The initial conditions tested (entry 1) were a promising lead, as they resulted in the formation of **2.230** in 24% yield. Replacement of K_2CO_3 by Cs_2CO_3 (entry 2) led to a decreased yield of **2.230** at the expense of formation of the two reduction products **2.231** and **2.232** (Figure 2.14). Given the tendency of thiophene-3-boronic acids to undergo protodeboronation in polar protic solvents,[196] reconsideration of the reaction conditions was necessary. The contradiction that polar protic solvents also accelerate the rate of Suzuki-Miyaura coupling of thiophene boronic acids was addressed by use of Buchwald's monophosphine-palladium catalyst system (comprised of $Pd(OAc)_2$ or Pd_2dba_3 / S-Phos), [197] which accelerates the rate of cross-coupling such that it is competitive with the rate of protodeboronation. Such rate enhancement has been demonstrated effectively for Suzuki-Miyaura couplings involving a wide variety of challenging heteroaromatic boronic acids (thiophene, pyridine, pyrrole, indole and furan).[197] Application of the Buchwald conditions to the coupling of thiophene-3-boronic acid **2.229** with **2.31** (Table 2.2, entry 3) led to the formation of the desired product **2.230** in 22% yield. However, trans-esterification products **2.233** and **2.234** were also identified (Figure 2.14). Use of toluene as a solvent was tested (entries 4 and 5), and resulted in the formation **2.230** in 21% and 66%, respectively, indicating the necessity of longer reaction times in non-polar reaction media. As a final optimization reaction, the Buchwald conditions were applied in *t*-BuOH as solvent (entry 6), and afforded **2.230** in good yield (83%) in a short reaction time without the occurrence of trans-esterification. These optimized conditions were subsequently applied to the cross-coupling of other heteroaromatic boronic acids with **2.31** (Scheme 2.36 and Table 2.3).

Table 2.2. Suzuki-Miyaura cross-coupling reactions of **2.31** with heteroaryl boronic acids

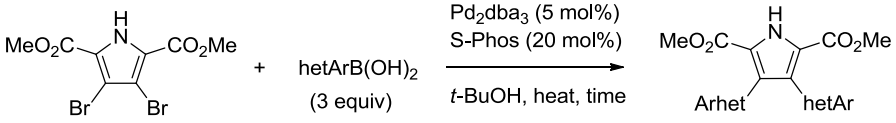

2.31

Entry	hetArB(OH)$_2$	Solvent	Temp (°C)	Time (h)	Product(s)	Yield
1	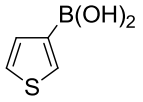 **2.229**	*t*-BuOH	100	4	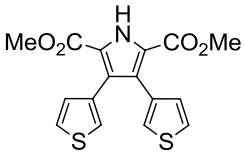 **2.230**	83%
2	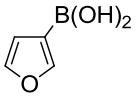 **2.235**	*t*-BuOH	100	38	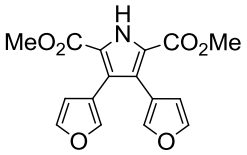 **2.236**	77%
3	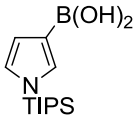 **2.237**	*t*-BuOH	100	38	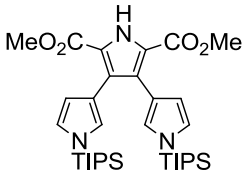 **2.238**	23%[a]
4		*t*-BuOH	120	5 (MW)		30%[a]
5	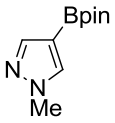 **2.239**	*t*-BuOH	100	38	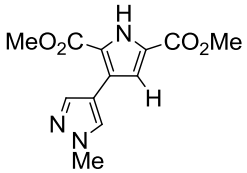 **2.240**	12%[b]
6	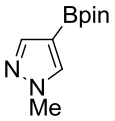 **2.239**	*t*-BuOH/H$_2$O 2.5/1	100	17	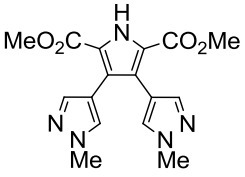 **2.241**	23%

[a] 30% recovery of unreacted **2.31** in both reactions. [b] 51% recovery of unreacted **2.31**.

Table 2.2. (cont'd)

Entry	hetArB(OH)$_2$	Solvent	Temp (°C)	Time (h)	Product(s)	Yield
7	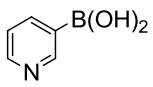	*t*-BuOH	100	38	------[c]	------
8		dioxane	100	38	------[c]	------
	2.242					
9	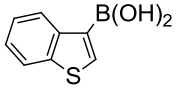	*t*-BuOH	100	42	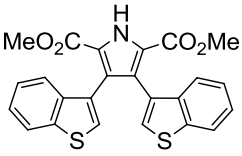	89%[d]
	2.243				**2.244**	
10	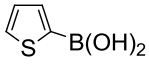	*t*-BuOH	120	5 (MW)	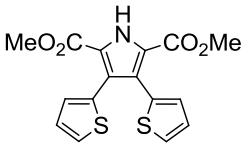	38%
11		toluene	100	38		21%
	2.245				**2.246**	
12	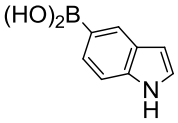	*t*-BuOH	100	16	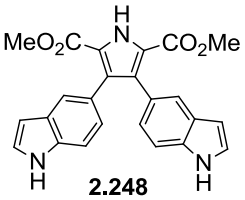	80%
	2.247				**2.248**	
13	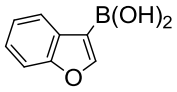	*t*-BuOH	100	17	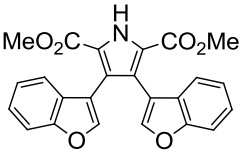	21%
	2.249				**2.250**	
14	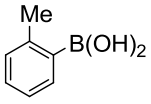	*t*-BuOH	100	22	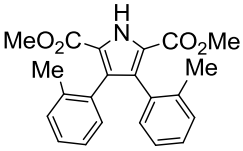	53%
	2.251				**2.252**	

[c] 60% and 72% recovery of unreacted **2.31** from entries 7 and 8, respectively. [d] Reaction was performed using 8 equiv benzothiophene-3-boronic acid and 8 equiv K_3PO_4.

Table 2.2. (cont'd)

Entry	hetArB(OH)$_2$	Solvent	Temp (°C)	Time (h)	Product(s)	Yield
15	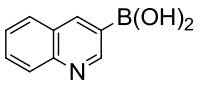 **2.253**	*t*-BuOH	100	32	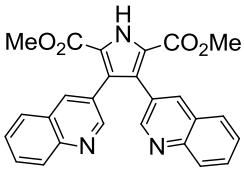 **2.254**	14%[(e)]
16	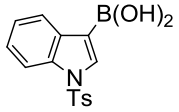 **2.228**	*t*-BuOH	100	42	-----[(f)]	------

[(e)] isolated 24% of unreacted **2.31** [(f)] 35% of **2.226** was isolated, along with 31% recovery of unreacted **2.31**

The results of Suzuki-Miyaura cross couplings involving a variety of heteroaromatic boronic acids show that the conditions optimized for the coupling of **2.229** with **2.31** are not generally applicable across a spectrum of heteroaromatic boronic acids. Good yields of products **2.230**, **2.236** and **2.244** (entries 1, 2, and 9) were obtained upon coupling of **2.31** with π-excessive heteroaromatic boronic acids **2.229**, **2.235**, and **2.243** having the boronic acid functionality at the 3-position. Initial coupling of **2.31** with three equivalents of benzothiophene-3-boronic acid **2.243** did not proceed to completion after a long reaction time (40 h), and although the bis-coupled product **2.244** was formed, it was very difficult to obtain pure material by flash chromatography. However, using a large excess of benzothiophene-3-boronic acid (8 equiv), afforded the desired product **2.244** in 89% yield. Additionally, the arylboronic acids **2.247** and **2.251** also underwent effective Suzuki-Miyaura coupling affording products **2.248** and **2.252** (entries 12, 14), with the latter result indicating that the reaction conditions were quite tolerant of steric congestion in the boronic acid.

In comparison to **2.229**, thiophene-2-boronic acid **2.245** was observed to undergo Suzuki coupling less effectively, even under microwave conditions (entry 10), and this result is attributed to lower stability of the boronic acid. A similar effect was also reported by Buchwald and co-workers, who demonstrated that coupling of **2.245** with unactivated aryl or heteroaryl chlorides did not proceed to completion (due to more rapid decomposition of **2.245** than cross-coupling).[197] They did observe, however, that this problem could be partially alleviated by use of less polar

solvents (such as toluene or dioxane), which decreased the rate of competitive boronic acid decomposition. In accordance with this knowledge, the reaction was repeated using toluene as solvent, but resulted in a lower yield of coupled product under prolonged reaction times (entry 11).

The optimized reaction conditions were found to be less effective for the coupling of **2.31** with π-deficient heteroaromatic boronic acids. Thus, a poor yield of product **2.238** was obtained upon coupling of *N*-protected pyrrole-3-boronic acid **2.237** (entry 3), and the recovery of unreacted starting material after a reaction time of 38 h suggested that boronic acid decomposition played a significant role in preventing the reaction from proceeding to completion. This result is consistent with the known propensity of (*N*-triisopropylsilyl)pyrrole-3-boronic acid (and pyrrole borane species in general) to undergo facile, competitive proto-deboronation.[198] Following the precedence of the first microwave accelerated Suzuki cross-coupling reaction reported in 1996,[199] microwave-assisted cross-coupling of compound **2.31** with **2.237** was carried out. The results show that use of microwave conditions has little impact on the yields of isolated product **2.238** (compare entries 3 and 4), although considerable effect on the reaction times was observed (an approximate 8-fold decrease).

Suzuki-Miyaura cross-coupling of pyridine-3-boronic acid **2.242** with **2.31** was also found to be a challenging reaction, and failed to provide any cross-coupling product (only unreacted **2.31** was recovered in isolated quantities of 60% or greater) in *t*-BuOH or dioxane as reaction solvents (entries 7, 8). Recovery of such significant quantities of unreacted **2.31** suggested that oxidative addition did not occur under these reaction conditions. The failure of these reactions may be attributed to the low nucleophilicity of pyridine boronic acids (a consequence of the π-deficient nature of the heteroaromatic ring), and the correspondingly slow rate of transmetalation.[200]

In a few cases (Table 2.3, entries 5, 6, and 13), cross-coupling of **2.31** with heteroaromatic boropinacolate esters was attempted. The outcome of Suzuki coupling of *N*-methyl pyrazole-3-boropinacolate ester **2.239** with **2.31** was found to be dependent on the specific reaction conditions. Attempted cross-coupling of *N*-Me pyrazine-3-pinacolboronate **2.239** using anhydrous conditions (entry 5) afforded mono-coupled product **2.240** (which has also undergone reductive debromination) in low yield of 12%, along with 50% recovery of unreacted **2.31** after an extended reaction time of 38 h. Based on the results of Buchwald's investigation into solvent

requirements for optimal cross-coupling of (*N*-triisopropylsilyl)pyrrole-3-pinacolboronate with 2-chlorothiophene,[197] modification of the reaction solvent (using a 2.5:1 ratio of *t*-BuOH:H_2O) was anticipated to minimize reduction of the aryl halide and increase the yield of the reaction. As a result, bis-coupled product **2.241** was isolated in 23% yield, and only 9% of unreacted **2.31** was isolated (entry 6).

The synthesized chromopyrrolic acid analogue **2.244** was an interesting candidate for detailed NMR study, as the proton signals appeared very broad at room temperature. Variable-temperature NMR (VT-NMR) studies indicated that this was due to a dynamic process which involved slow interconversion of two rotational isomers of **2.244** (Scheme 2.32). Rapid interconversion of the two rotational isomers at elevated temperatures resulted in equivalence (coalescence) of the chemical shifts corresponding to the H-1, H-4 and H-7, H-10 proton pairs (Figure 2.16). The VT-NMR study indicated that the signals corresponding to proton pairs H-1, H-4 and H-7, H-10 reached coalescence at T_c = 327 K. The location of these protons on different benzothiophene rings was confirmed using Nuclear Overhauser Effect (NOE) and Exchange

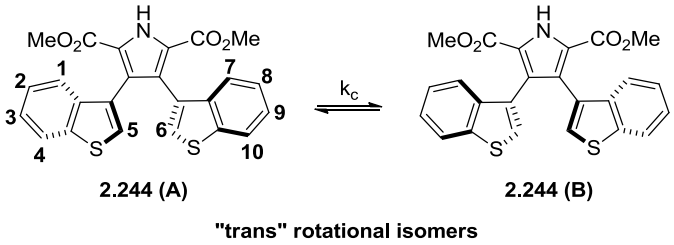

Scheme 2.32. Rotational isomers of dimethyl 3,4-(bis-benzothiophen-3-yl) pyrrole-2,5-dicarboxylate **2.244**

Spectroscopy (EXSY). The rate constant at coalescence (k_c) was calculated to be k_c = 124 s^{-1} (using the approximation $k_c = (\pi\Delta\upsilon)/\sqrt{2}$, applicable to calculations involving uncoupled signals),[201] and use of the Eyring equation ($\Delta G_c^{\ddagger} = RT[23.76 - \ln(k_c/T)]$) allowed determination of the activation barrier at coalescence ($\Delta G_c^{\ddagger}$) to be 68.7 kJ mol^{-1}. Computational studies determined a comparably high energetic barrier ($\Delta G_c^{\ddagger}$ = 60 kJ mol^{-1}) to achieve co-planarity between the aryl and pyrrole ring in C-2 arylated **2.255** (Figure 2.16),[202] consistent with the X-ray crystallographic data showing an essentially orthogonal inter-planar angle of 82.87˚. Specific

structural features of 3,4-bis(hetero)arylated pyrroles **2.244** and **2.246**, and O'Shea's mono-arylated pyrrole **2.255** are shown in Figure 2.17.

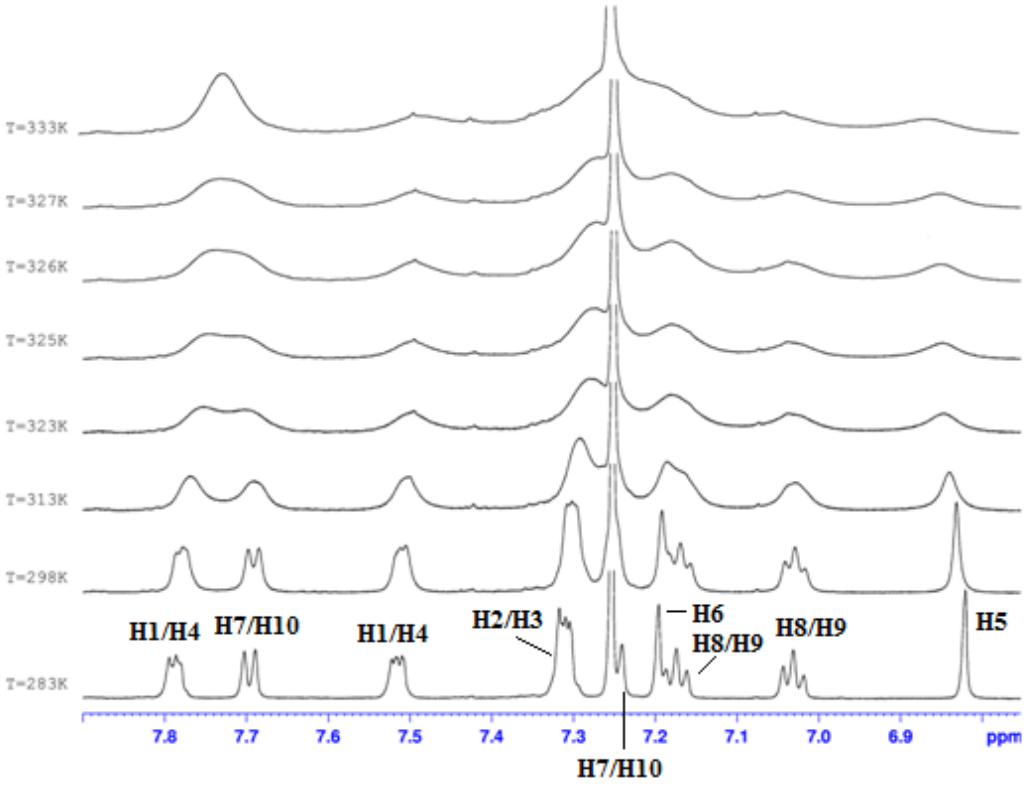

Figure 2.16. Variable-temperature NMR study of **2.244**

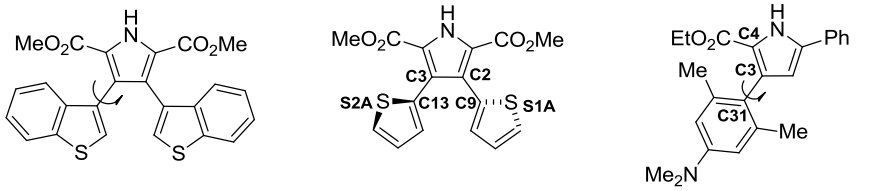

2.244
$\Delta G_c^{\ddagger}$ = 69 kJ mol^{-1}

2.246
∠ **C3-C2-C9: 123.7 °**
∠ **C2-C3-C13: 123.36 °**

2.255
$\Delta G_c^{\ddagger}$ = 60 kJ mol^{-1}
∠ **C3-C13-S2A: 129.06 °**

Figure 2.17. Structural comparison of **2.244** and **2.246** with **2.255**

The X-ray crystal structure of **2.246** was also obtained, and indicated that two conformations of the *trans* isomer were selectively crystallized in the solid state (Figure 2.18).

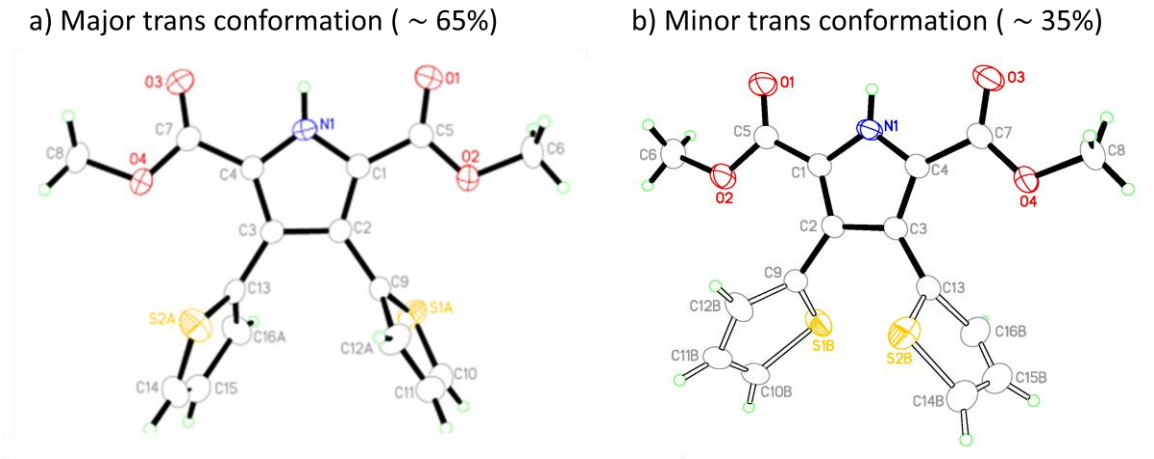

Figure 2.18. X-ray crystal structure of **2.246** a) major portion (65%) and b) minor portion (35%)

The deviation from the expected 50:50 ratio of the two conformations (with the assumption that they are of equal energy and therefore probability) can be rationalized by either an error from the X-ray crystallography refinement or that the two orientations are of slightly different energy levels. If the latter were true, then the first orientation is of lower energy or slightly more stable than the second one and this could be further verified through theoretical calculations based on the X-ray data.

The aryl or heteroaryl ring substituents at the pyrrole 3-position in both **2.246** and **2.255** adopt a similar orientation relative to the C2-C3 pyrrole bond, according to analysis of the bond angles. The inter-planar angle between the thiophene and pyrrole ring in **2.246** was determined to be in the range of 73-77˚ and is between 6-10˚ smaller than the corresponding angle in **2.255**. The influence of bulky substituents on the twist of the C-3 aryl group in **2.255** provides a rational explanation of this difference between the inter-planar angles. These structural features may be important to consider in the design of stable CPA analogues. Perhaps of greatest significance is that these molecules may be considered as ground state analogues of CPA, and have the potential to adopt the "twisted-butterfly" conformation as observed in the X-ray structure of StaP containing CPA in the active site (Chapter 1, Figure 1.6) necessary for catalytic turnover.

2.4.4 Synthesis of heterocyclic analogues of CPA dimethyl ester (2.5) 2.261 and 2.262

Inspired by the Suzuki-Miyaura coupling of *N*-substituted dimethyl (3,4-bistrifluoromethanesulfonyl)pyrrole-2,5-dicarboxylate **2.82** established by Iwao and co-workers (Scheme 2.15), and the efficient published syntheses of **2.259**[203] and **2.260**[204] (Scheme 2.33), we sought to perform a comparison study between the reactivity of **2.31** and pyrrole bis-triflates **2.259** and **2.260** in cross-coupling with a few heteroaromatic boronic acids. The synthesis of **2.259** involved preparation of dimethyl ester **2.257** from iminodiacetic acid **2.256** with subsequent Hinsberg pyrrole synthesis and triflation to form coupling partner **2.259**. The other coupling partner **2.260** was readily accessed upon benzylation of **2.259**.

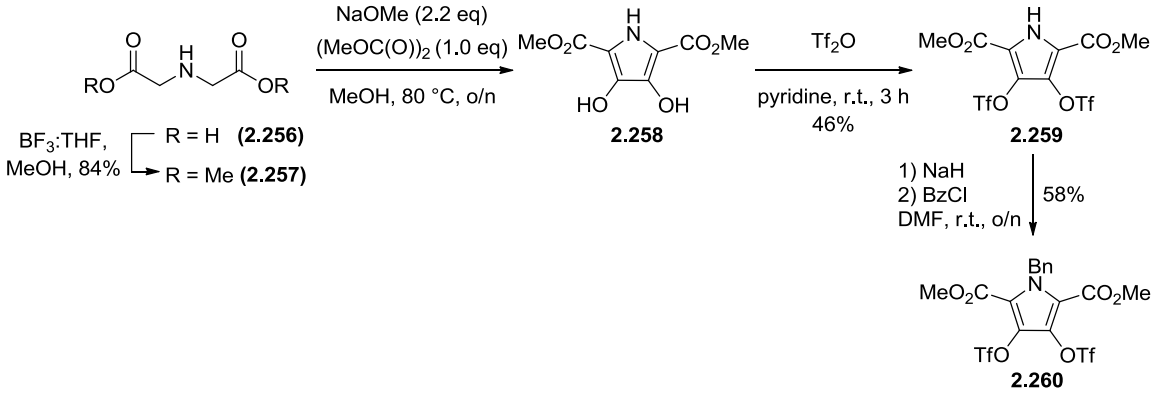

Scheme 2.33. Synthesis of pyrrole bis-triflate coupling partners **2.259** and **2.260**

The results of the cross coupling study are presented in Table 2.3. As a starting point for comparison, thiophene 3-boronic acid **2.229** and indole-5-boronic acid **2.247** were selected as the initial candidates for testing the cross-coupling with **2.259** under the previously optimized conditions (entries 1, 2). In both cases, the reactions failed to produce any bis-coupled product (according to GC/MS and TLC analysis). There was no unreacted starting material in either reaction, and 26% of 3,3'-bithiophene (arising from homocoupling of boronic acid **2.229**) and 21% indole (arising from protodeboronation of **2.247**) were isolated (entries 1, 2). Failure of *N*-unsubstituted pyrrole **2.259** to undergo cross-coupling was consistent with the results obtained by Iwao and co-workers, who demonstrated trace formation of bis-coupled products when **2.259** was coupled with electron-rich (activated) arylboronic acids (using $Pd(PPh_3)_4$ / aq. Na_2CO_3 / refluxing

THF conditions),[204] and that efficient coupling required use of benzylated pyrrole **2.260** as the coupling partner.[204] This analogy was not observed when coupling of **2.260** with thiophene-3-boronic acid **2.229** was attempted using Pd_2dba_3/S-Phos/*t*-BuOH/K_3PO_4 as reaction conditions, as only trace amounts of bis-coupled product **2.261** were isolated (~5%).

Table 2.3. Results of cross-couplings of **2.259** and **2.260** with heteroarylboronic acids

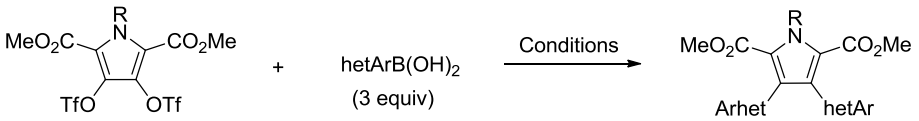

R = H (2.259)
R = Bn (2.260)

Entry	hetArB(OH)$_2$	bistriflate 2.259 or 2.260	Catalyst / Ligand	Solvent, Base	Time (h)	Product	Yield
1	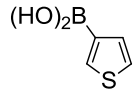 **2.229**	**2.259**	Pd_2dba_3 / S-Phos	*t*-BuOH, K_3PO_4	20	------[a]	-----
2	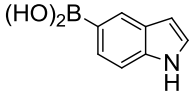 **2.247**	**2.259**	Pd_2dba_3 / S-Phos	*t*-BuOH, K_3PO_4	6.5	------[b]	-----
3	**2.229**	**2.260**	Pd_2dba_3 / S-Phos	*t*-BuOH, K_3PO_4	12	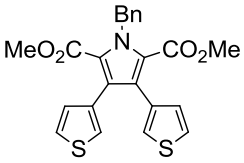 **2.261**	5%
4	**2.229**	**2.260**	$Pd(PPh_3)_4$	THF, 2 M Na_2CO_3	20	**2.261**	89%
5	**2.245**	**2.260**	$Pd(PPh_3)_4$	THF, 2 M Na_2CO_3	15	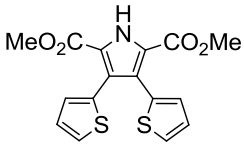 **2.262**	80%

[a] 3,3'-bithiophene (26%) was isolated, [b] indole (21% yield) was isolated

However, and gratifyingly, successful cross-coupling of **2.260** was achieved in excellent yields with both thiophene-3-boronic acid **2.229** and thiophene-2-boronic acid **2.245**, to give products **2.261** and **2.262**, through use of the reaction conditions employed by Iwao ($Pd(PPh_3)_4$ / aq. Na_2CO_3 / refluxing THF). The results in Table 2.3 (entries 4, 5) indicate that cross-coupling of *N*-benzyl protected pyrrole **2.260** with thiophene boronic acids **2.229** or **2.245** resulted in either comparable yields of bis-coupled products **2.230** and **2.261** (see Table 2.2 (entry1), and Table 2.3 (entry 4)), or a significantly improved yield (compare Table 2.2 (entries 10-11) and Table 2.3 (entry 5)). In comparison with cross-couplings involving **2.31**, these results are useful because of the simple and efficient preparation of **2.260**, although two additional benzyl group protection / deprotection steps are required.

The specific connection of the 3,4-bis(aryl/heteroaryl)analogues described in Table 2.3 and Table 2.4 with RebC and StaC indolocarbazole biosynthesis pathways is demonstrated in Scheme 2.34. The heterocyclic analogue **2.263**, obtained by hydrolysis, would be introduced into the biosynthetic pathway at the RebP catalytic step, at which point, by analogy, an enzymatic aryl-aryl bond forming reaction would be expected to occur, generating the reactive RebC substrate **2.264** which would undergo rapid conversion to **2.265** via double oxidative decarboxylation.

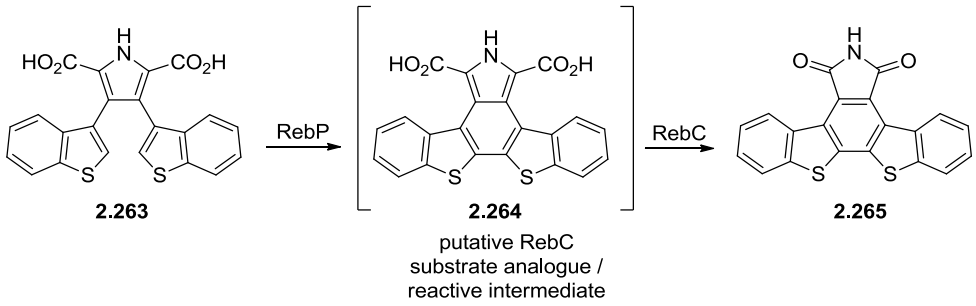

Scheme 2.34. Enzymatic conversion of CPA analogue **2.263** to indolocarbazole **2.265**

As discussed in Section 2.3, the rationale for synthesis of these substrates was based on their ability to disrupt particular interactions in the active site of wild-type RebC or RebC F216VR239N variant. Replacement of the indole NH in the natural substrate by another heteroatom (e.g. S or O, as in analogues **2.244** and **2.250**) is anticipated to disrupt the interaction between Glu396 (conserved among both classes of monooxygenases) and the substrate, and

increase the reliance on the F216 / R239 interactions with the substrate. Analogues **2.230**, **2.236**, and **2.238**, lacking the fused benzene ring, are smaller than the natural substrate and are expected to be more flexible in adopting different conformations in the enzyme active sites. Synthetic substrate **2.241** is expected to test the influence of non-natural substrates containing multiple heteroatoms, while substrate **2.246** may provide information regarding the importance of the location of the heteroatom. Substrate **2.248** is also of interest, as it would require RebP to perform an aryl-aryl coupling of two indole benzenoid rings (in contrast to the more facile hetAr-hetAr coupling in the natural substrate **2.1**), without the additional stabilization of the Glu-396 interactions with the indole NH units.

Indolocarbazole biosynthesis pathways are particularly well suited to combinatorial biosynthesis applications: key enzymes have the ability to incorporate unnatural substrates into the biosynthetic pathway, and they have evolved to stabilize reactive intermediates and convert them rapidly to product through coupled enzyme chemistry. We anticipate that in addition to enhancing mechanistic studies, the analogues described herein have the potential to generate diverse libraries of indolocarbazoles using combinatorial biosynthesis.

2.4.5 Conversion of CPA Analogues 2.230 and 2.244 to Indolocarbazole Derivatives 2.266 and 2.267

With the aim of preparing new indolocarbazole analogues, a study of oxidative cyclization of 3,4-diheteroaryl substituted pyrroles **2.230**, **2.236 and 2.244** was undertaken, and the results are summarized in Table 2.4. The reaction conditions (stoichiometric $Pd(OAc)_2$ in refluxing HOAc) were chosen based on their successful application in the intra- or intermolecular oxidative coupling of a variety of heterocycles including indole (arcyriaflavin A synthesis),[205] and furans.[206] These conditions were most effective when applied to the oxidative coupling of **2.244**, resulting in the formation of **2.266** in 80% yield (entry 1). However, application of these conditions to the oxidative coupling of **2.230** and **2.236** afforded **2.267** in low yield (entry 2) or resulted in no conversion (entries 3-4).

In order to rationalize the ineffective oxidative coupling of **2.230** and **2.236** under the Pd-catalyzed reaction conditions, the following issues were considered: i) competition between intra- and intermolecular coupling reactions, and ii) the stability of the furan and thiophene rings towards the oxidizing conditions. Although ceric ammonium nitrate (CAN) gave a negative result

(entry 4), exploration of alternative reaction conditions (using different oxidants, and testing the requirement of different additives) remains as future work.

Table 2.4. Oxidative cyclization of bis-heteroarylpyrroles **2.224 and 2.230** to indolocarbazole derivatives **2.266** and **2.267**

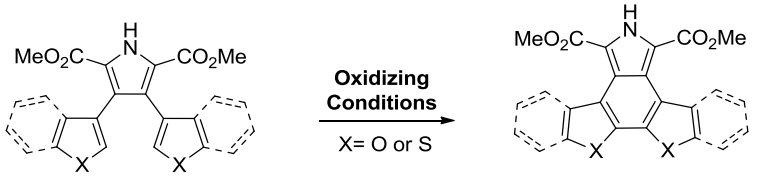

2.224, 2.230, 2.236 → **2.266, 2.267**

Entry	Substrate	Oxidant	Solvent	Temp. (° C)	Time (h)	Product	Yield
1	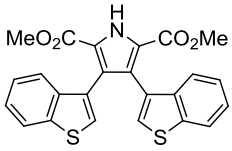 **2.244**	$Pd(OAc)_2$ (1.12 eq)	HOAc	70	15	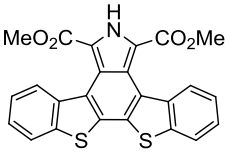 **2.266**	80%
2	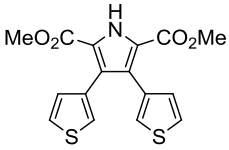 **2.230**	$Pd(OAc)_2$ (1.12 eq)	HOAc	70	17	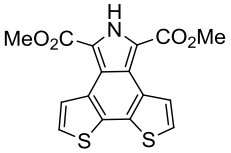 **2.267**	22%
3	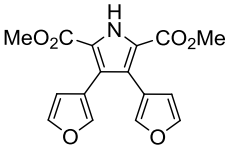 **2.236**	$Pd(OAc)_2$ (1.12 eq)	HOAc	70	17	------	------
4		CAN (2.5 eq)	H_2O, CH_3CN	-20	1	------	------

2.5 Conclusions

This thesis chapter has described the development of a modular synthetic method which allowed the generation of a small library of stable heterocyclic analogues of chromopyrrolic acid (**2.1**), shown in Tables 2.2 and 2.3. In stark contrast with the diverse family of natural and synthetic di(het)arylmaleimides, and polyoxygenated 3,4-diarylpyrroles described previously

(including lamellarins, ningalins, storniamides, polycitrins, polycitones and lycogarubins (Figure 2.1)), development of the 3,4-bis(heteroaryl)pyrrole family of natural products has been largely limited to synthesis of known biologically active compounds (e.g. lycogarubin C (**2.5**), shown in Schemes 2.2, 2.6, 2.7 and 2.8), combinatorial biosynthesis, or isolation and structural elucidation work. Therefore, the preparation of these CPA derivatives according to the established methodology has contributed to the development of an underexplored area of 3,4-diheteroarylpyrrole chemical space. Screening of reaction conditions for the efficient preparation of **2.230**, our initial analogue of interest, revealed that conditions developed by Buchwald (Pd_2dba_3/S-Phos/K_3PO_4/*t*-BuOH), effective for Suzuki couplings involving heteroaromatic boronic acids of low reactivity or limited stability, performed well in the cross-coupling of **2.31** with **2.229** to afford **2.230**, and reactivity trends were established upon application of the reaction conditions to couplings of **2.31** with a variety of other heteroaromatic boronic acids (Tables 2.2 and 2.3). The results showed that efficient coupling occurred with π-excessive heterocyclic boronic acids (thiophene, furan and benzothiophene 3-boronic acids), although lower yields were obtained from Suzuki-Miyaura coupling reactions involving the π-deficient cross-coupling partner *N*-methylpyrazine-3-boropinacolate, as well as heteroaryl boronic acids more susceptible to protodeboronation (*N*-TIPS pyrrole-3-boronic acid and thiophene-2-boronic acid). Initial results comparing the reactivity of pyrrole cross-coupling partners **2.31** and **2.260** in Suzuki-Miyaura couplings revealed that **2.260** engaged in high yielding reactions with heteroaromatic boronic acids **2.229** and **2.245** to give products **2.261** and **2.262** (Table 2.3), when appropriate conditions were employed.

In addition to providing a synthetic route to new molecules related to chromopyrrolic acid **(2.1)**, intramolecular cyclization of **2.230** and **2.244** to form either tetra- or hexacyclic derivatives **2.266**, **2.267** (Table 2.4), which are constructed around a central fused benzene / pyrrole ring junction, provides access to new compounds related to the heterocyclic indolocarbazoles described in Section 2.2.3, and these compounds may possess significant biological activities.

2.6 Future Work

As the main objective of this project was to achieve the synthesis of analogues of the CPA dimethyl ester (shown in Table 2.2), we propose that the ground state CPA analogues may be useful in studying our hypothesized role of specific amino acid residues in the active site, in accordance with our proposed mechanisms of the RebC and the RebCF216VR239N catalytic cycles described in Chapter 1, Section 1.6. The substrate flexibility of the indolocarbazole biosynthetic enzymes (described in detail in Chapter 1) is expected to be advantageous in this study. Consequently, it would be of interest to monitor *in vivo* indolocarbazole production from heterologous expression of *rebPC* in *E. Coli* (using the pET-Duet-*rebPC* construct described in chapter 1) in a culture broth enriched with CPA derivatives such as **2.230** or **2.244** (or their respective bis-carboxylic acids). Furthermore, the synthesis and testing of amide analogues of the esters would be of interest. This latter series of compounds would be tested as inhibitors of RebC, as they are not able to undergo oxidative decarboxylation.

Although a modular synthetic approach for accessing heterocyclic CPA analogues has been developed, its value and utility would be significantly enhanced with generalization for efficient coupling of pyrrole dibromo ester **2.31** (Scheme 2.28) with a variety of heterocyclic boronic acids. Use of surrogates of heteroaromatic boronic acids (including thermally stable boropinacolate esters of **2.237**[207] or the MIDA boronate of **2.242**)[208] may provide a solution to problems of low reactivity/stability. Extension of the synthetic methodology to include the synthesis of unsymmetrical analogues of CPA by sequential Suzuki coupling of **2.31** with different boronic acids similar to the studies of Iwao[126a] may generate new compounds with significant biological activities. Synthesis of such molecules may be achieved from **2.31** using the representative sequence of reactions shown in Scheme 2.35, affording **2.269**. Subsequent $Pd(OAc)_2$ oxidative cyclization would generate new heterocyclic compounds of type **2.270**, related to indolocarbazoles.

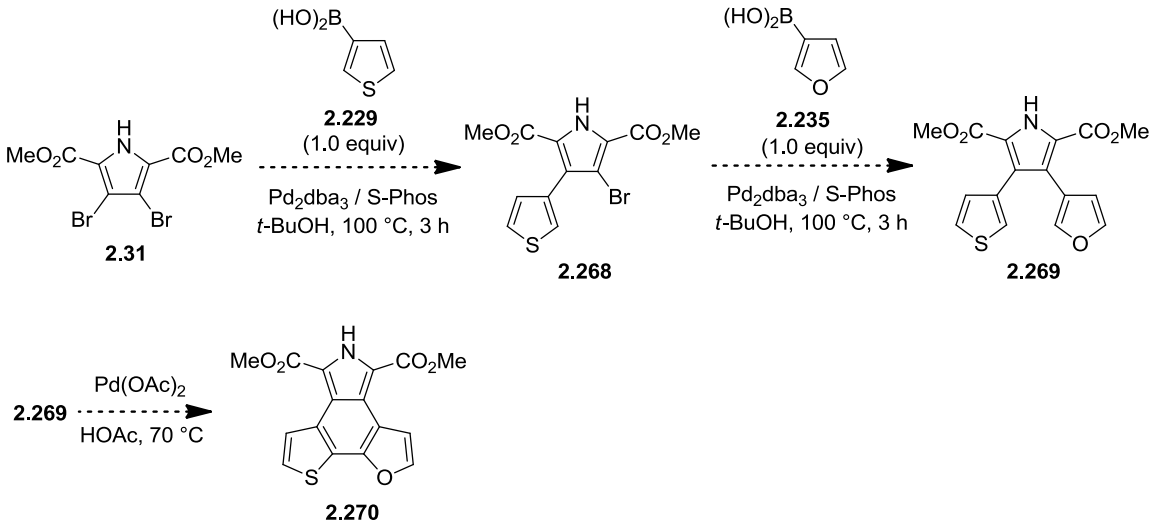

Scheme 2.35. Proposed Suzuki-Miyaura cross-coupling methodology for the synthesis of unsymmetrical compound **2.270** related to indolocarbazoles

Unrelated applications may also been envisaged for molecules of type **2.230** or **2.252** in the synthesis of curved molecules shown in Scheme 2.36. Construction of a pentacyclic [5,5,5,5,5] ring system containing heterocyclic fluorenones using Directed remote Metalation (D*re*M) chemistry may be achieved by deprotonation of the most acidic C-2 and C-2' hydrogens (in thiophene, $pK_a = 33$) using the ester group as a directed metalation group (DMG),[209] affording **2.271** (Scheme 2.36a). Furthermore, D*re*M-cyclization of **2.252** would provide access to an interesting [6,6,5,6,6] phenanthrol ring system **2.272** (Scheme 2.36b). Cross-coupling of **2.31** with 4-methylthiophene-3-boronic acid to afford **2.273**, followed by D*re*M cyclization may provide the interesting [5,6,5,6,5] ring system corresponding to **2.274** (Scheme 2.36c). According to literature review of these ring systems, **2.271** and **2.274** are unknown. The core pentacyclic ring system of **2.272** (7H-dibenzo[c,g]carbazole) is known,[210] and a suspected human carcinogen. Mono-hydroxylated variants are typical metabolic products, with the hydroxyl group often located on one of the fused benzene rings A or E in **2.272** (without B or D ring hydroxylation).

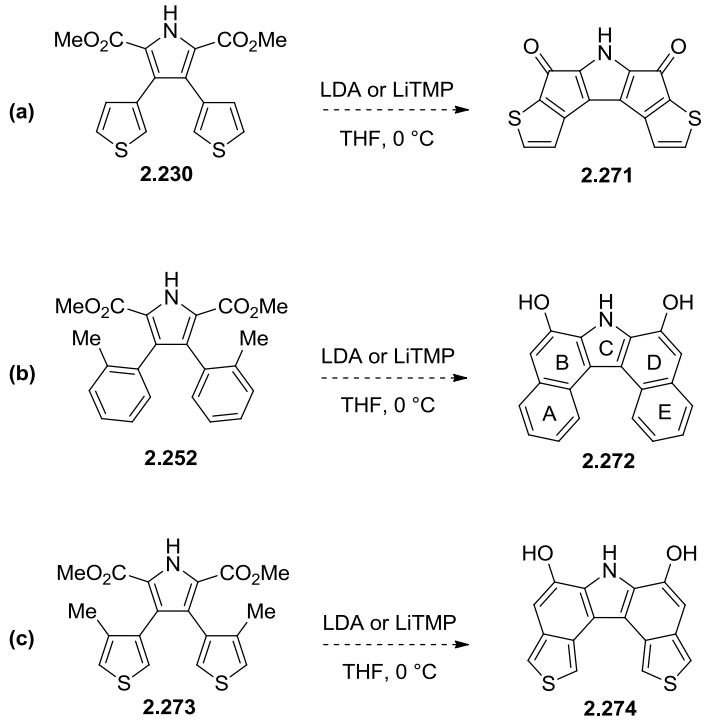

Scheme 2.36. Potential marriage of Suzuki-coupling / D*re*M cyclization for the construction of diverse polyaromatic and polyheteroaromatic ring systems **2.271**, **2.272**, and **2.274**

2.7 Experimental Section

Materials and Methods

Melting points were obtained on recrystallized materials using a Fisher Scientific Melting Point Apparatus or Mel-Temp apparatus and are uncorrected. IR spectra were recorded as films or KBR pellets on a BOMEM FT-IR or Varian 1000 FT-IR spectrometer. ^{1}H NMR and ^{13}C NMR spectra were obtained on Bruker Avance-300, 400, 500 or 600 MHz spectrometers. The chemical shifts of ^{1}H NMR and ^{13}C NMR signals are recorded relative to internal C*H*Cl$_3$ (δ = 7.26 ppm) and *C*DCl$_3$ (δ = 77.0). ^{1}H NMR data is reported as follows: chemical shift in ppm value (δ), multiplicity (ie. s = singlet, d = doublet, t = triplet, q = quartet, m = multiplet, br s = broad singlet), coupling constant (Hz) and integration. ^{13}C NMR data is reported according to chemical shift values (δ). High resolution mass spectra were obtained using a GCT Mass Spectrometer (Waters, Micromass) and a QSTAR XL hybrid mass spectrometer (Applied Biosystems/MDS Sciex). Boronic acids were purchased from Frontier Scientific and stored in the refrigerator.

Pd_2dba_3 and $Pd(OAc)_2$ were purchased from Aldrich, and S-Phos from Frontier Scientific. 3-Coumaranone was purchased from Frontier Scientific. Anhydrous *t*-BuOH was purchased from Sigma-Aldrich, and was used without further purification in most cases. Additional drying was carried out by filtration over $MgSO_4$, followed by stirring in the presence of iodine activated magnesium turnings for several hours prior to distillation. Anhydrous solvents (dioxane, *t*-BuOH) and water were vigorously degassed through prolonged Ar bubbling (15-30 min), and added to the vessel using syringe-septum technique prior to immersion in a pre-heated oil bath. The K_3PO_4 base was dried at 150 ℃ for 4 h using the Kugelrohr distillation apparatus, and stored in a dessicator prior to the reaction. Flash column chromatography was carried out using Silicycle Silia-P silica gel (particle size: 40-60 μM, 60A).

General Procedures

A. Suzuki-Miyaura cross-coupling reactions of 2.31. A mixture of dimethyl 3,4-dibromopyrrole-2,5-dicarboxylate **2.31** (1.0 equiv), an aromatic or heteroaromatic boronic acid (3.0-5.0 equiv), Pd_2dba_3 (5 mol%), S-Phos (20 mol%) and anhydrous K_3PO_4 (4 equiv, weighed in the glove bag) in a flame dried vial was charged with degassed, anhydrous *t*-BuOH (2 mL/mmol halide). The vial was sealed and heated either by conventional heating at 100 ˚C (oil bath temperature) for 4 h to 2.5 d or microwave heating at 120 ˚C or 150 ˚C for 5 h under an argon atmosphere. The reaction progress under thermal heating conditions was monitored by thin-layer chromatography (TLC) analysis. The reaction mixture was cooled to rt, diluted with EtOAc, the whole was subjected to filtration and the filtrate was concentrated *in vacuo*. The resulting residue was subjected to flash column chromatography (SiO_2) using either hexane/EtOAc or CH_2Cl_2/MeOH as the eluent to yield the product.

B. Suzuki-Miyaura cross-coupling reactions of 2.259 or 2.260. A mixture of dimethyl 3,4-bis(trifluoromethanesulfonyl)pyrrole-2,5-dicarboxylate **2.259** (1.0 equiv) or dimethyl (*N*-benzyl)-3,4-bis-(trifluoromethanesulfonyl)pyrrole-2,5-dicarboxylate **2.260** (1.0 equiv), a heteroaromatic boronic acid (3.0 equiv), Na_2CO_3 (4.0 equiv) and $Pd(PPh_3)_4$ (4 mol%, weighed in the glove bag) in a vial was charged with degassed water (0.35 mL) and degassed THF (3.5 mL). The vial was sealed and immersed in a 100 ˚C oil bath for 20 h, under an argon atmosphere. The reaction progress under thermal heating conditions was monitored by thin-layer chromatography (TLC)

analysis. The reaction mixture was cooled to rt, diluted with EtOAc, the whole was subjected to filtration and the filtrate was concentrated *in vacuo*. The resulting residue was subjected to flash column chromatography (SiO_2) using hexane/EtOAc as eluent to yield the product.

Experimental Procedures and Data

2-trichloroacetylpyrrole[211] (2.218)

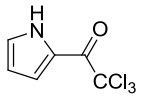

A solution of freshly distilled pyrrole (17 mL, 250 mmol, 1.0 equiv) in Et_2O (140 mL, 1.8 M) was prepared and added slowly from an addition funnel over 1.5 h to a solution of trichloroacetyl chloride (31 mL, 275 mmol, 1.1 equiv) in Et_2O (42 mL, 6.5 M), in a flame dried 500 mL flask under argon. The initially clear solution of trichloroacetyl chloride changed from colourless to deep violet over the course of pyrrole addition, and began to reflux slightly during the addition. Refluxing (at 60 ˚C) was continued for 1.5 h, and upon cooling to rt, the reaction mixture was quenched by slow addition of aq. 3 M Na_2CO_3 solution until no further evolution of CO_2 was observed. Following separation of the aqueous and organic phases, the red ether layer was washed with water, brine, and dried over $MgSO_4$. The red organic layer was treated with Norite and filtered through Celite, to afford **2.218** as a colourless solid (50.0 g, 90%); mp 73-74˚C (hexanes), lit[212] mp 73-75˚C; ^{1}H NMR (400 MHz, $CDCl_3$): δ 6.37-6.41 (m, 1 H), 7.16-7.19 (m, 1 H), 7.38-7.41 (m, 1 H), 9.62 (br s, NH) ppm; ^{13}C NMR (100 MHz, $CDCl_3$): δ 111.8, 121.2, 122.9, 127.2, 173.2 ppm. With the exception of the tri-chlorinated carbon signal (not detected in the ^{13}C NMR spectrum), the physical and spectral data were consistent with those previously reported,[211,212] and the material was used in the next reaction without purification.

Methyl pyrrole-2-carboxylate[211] (2.219)

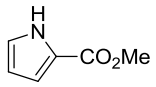

In a flask containing anhydrous MeOH (461 mL) was dissolved Na metal (2.7 g, 115 mmol, 0.5 equiv). Trichloroacetyl pyrrole (49 g, 231 mmol, 1.0 equiv) was added portionwise at rt, and the reaction mixture was stirred for 15 h under argon, and evaporated to dryness. The resulting residue was dissolved in Et_2O (200 mL), washed with aq. 3 M HCl (100 mL) and sat. aq. $NaHCO_3$ (150 mL), dried over $MgSO_4$, and concentrated to half the volume. The solution was treated with Norite and subjected to filtration through a bed of Celite. The filtrate was concentrated to dryness, affording **2.219** as a colourless solid (26.0 g, 90%). mp 72-73˚C

(hexanes), lit[211] mp 73˚C; ^{1}H NMR (300 MHz, $CDCl_3$): δ 3.86 (s, 3H), 6.25-6.29 (m, 1H), 6.90–6.94 (m, 1H), 6.95-6.99 (m, 1H), 9.23 (br s, N-H) ppm; ^{13}C NMR (100 MHz, $CDCl_3$): δ 51.4, 110.4, 115.3, 122.6, 122.9, 161.7 ppm. The physical and spectral data were consistent with those previously reported,[211] and the material was used in the next reaction without purification.

Methyl 5-formyl-pyrrole-2-carboxylate[213] (2.220)

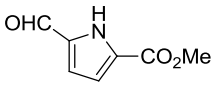

Phosphorus(V) oxychloride (0.37 mL, 4.0 mmol, 1.0 equiv) was added dropwise to a flask containing DMF (0.31 mL, 4.0 mmol, 1.0 equiv) at 5-10 ˚C in order to prepare the Vilsmeier reagent. The reaction mixture was brought to rt and diluted with CH_2Cl_2 (2 mL), then re-cooled to 0 ˚C. A solution of methyl pyrrole-2-carboxylate **2.217** (500 mg, 4.0 mmol, 1.0 equiv) dissolved in dichloromethane (2.2 mL) was added dropwise over 10 minutes at 0 ˚C. The reaction was then refluxed with vigorous stirring for 1 h, cooled to 10 ˚C (approximately), and hydrolyzed with a solution of aq. NaOAc (164 mg, 2.0 mmol) in water (0.5 mL). The aqueous and organic phases were separated, and the aqueous phase was extracted with Et_2O in order to ensure all product was in the organic phase. The combined Et_2O layers were washed with sat. aq. Na_2CO_3 solution until evolution of CO_2 ceased, and the organics were dried with $MgSO_4$ and subjected to filtration. The filtrate was concentrated to dryness, resulting in an oily orange residue that was purified by flash column chromatography (2:1 hexane:EtOAc) and afforded **2.220** (259 mg, 52%) and **2.221** (136 mg, 27%) both as slightly yellow solids.

2.220: mp 94-95 ˚C (hexanes): lit[211] mp 96 ˚C; ^{1}H NMR (300 MHz, $CDCl_3$): δ 3.94 (s, 3H), 6.96 (d, 2H, J = 2.5 Hz), 9.69 (s, 1H, CH), 9.99 (br s, NH); ^{13}C NMR (100 MHz, $CDCl_3$): δ 52.2, 115.7, 119.7, 128.1, 134.5, 160.8, 180.3 ppm. The physical and spectral data were consistent with those previously reported.[211]

2.221: mp 98-99 ˚C (hexanes): lit[214] mp 98-99 ˚C; ^{1}H NMR (300 MHz, $CDCl_3$): δ 3.90 (s, 3H), 7.30-7.33 (m, 1H), 7.58-7.60 (m, 1H), 9.85 (s, 1H), 10.06 (br s, NH) ppm; ^{13}C NMR (100 MHz, $CDCl_3$): δ 52.0, 114.3, 124.8, 127.6, 128.5, 161.3, 185.6 ppm. The physical and spectral data were consistent with those previously reported.[211,213]

Methyl 5-carboxy-pyrrole-2-carboxylate[215] **(2.222)**

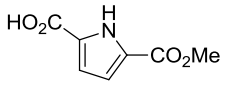

To a solution of aldehyde **2.214** (500 mg, 3.3 mmol, 1.0 equiv) in acetonitrile (25 mL, 0.13 M) was added a solution of NaH_2PO_4 (2.04 g, 13.1 mmol, 4.0 equiv) in water (5 mL, 2.6 M), followed by sodium chlorite (591 mg, 6.5 mmol, 4.0 equiv) and a solution of aq 30 wt% H_2O_2 (3.3 mL, 6.5 mmol, 10.0 equiv) at 0˚C. The reaction mixture was stirred at rt for 15 h, and adjusted to basic pH by treatment with sat. aq. Na_2CO_3. The acetonitrile was removed under reduced pressure on a rotary evaporator, and the resulting aqueous layer was acidified with aq. 3M HCl solution and the whole was extracted with copious amounts of Et_2O affording **2.222** as a colourless solid (480 mg, 87%) upon concentration *in vacuo*. mp 253-255 ˚C (anhydrous EtOH): lit[215] mp 241 - 242 ˚C and lit[216] mp 270 ˚C; ^{1}H NMR (400 MHz, d_6-DMSO): δ 3.78 (s, 3 H), 6.76 (1H, dd, J = 3.8 Hz, 2.4 Hz), 6.80 (1H, dd, ^1J = 3.8 Hz, ^2J = 2.4 Hz), 12.47 (s, 1 H, NH) ppm; ^{13}C NMR (100 MHz, $CDCl_3$): δ 51.4, 115.0, 115.2, 125.9, 127.7, 160.1, 161.1 ppm. The physical and ^{1}H NMR spectral data were consistent with those previously reported,[213] and the material was used in the next reaction without purification.

Dimethyl pyrrole-2,5-dicarboxylate[215] **(2.223)**

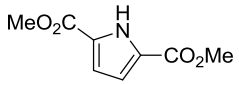

Thionyl chloride (0.33 mL, 4.5 mmol, 4.0 equiv) was added dropwise to a solution of **2.215** (190 mg, 1.1 mmol, 1.0 equiv) in anhydrous MeOH (1.0 mL) at 0 ˚C. The reaction mixture was heated at 70 ˚C for 16 h, cooled, and neutralized with sat. aq. Na_2CO_3. The organic phase obtained after extraction with EtOAc was dried over $MgSO_4$, subjected to filtration, and concentrated *in vacuo* affording **2.223** as a colourless solid (162 mg, 80%). mp 123-124 ˚C (anhydrous EtOH): lit[215] mp 126-127.5 ˚C; ^{1}H NMR (400 MHz, $CDCl_3$): δ 3.89 (s, 6H), 6.87 (d, 2H, J = 2.3 Hz), 9.50-9.90 (br s, NH) ppm; ^{13}C NMR (100 MHz, $CDCl_3$): δ 52.0, 115.5, 126.0, 160.7 ppm. The physical and spectral data were consistent with those previously reported, [215] and the material was used in the next reaction without purification. The following Table 2.5 shows the results of optimization experiments.

Table 2.5. Determination of optimal conditions for esterification of **2.223**

Entry	Starting Material	Reagents	Solvent	Temp (°C)	Time (h)	Product	Yield
1	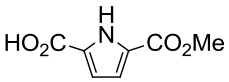 **2.222**	H_2SO_4 (5 mol%)	MeOH	75	2.5	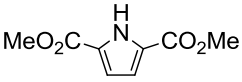 **2.223**	26%
2	**2.222**	EDCI (1.1 equiv), DMAP (5 mol%	MeOH / CH_2Cl_2	r.t.	20	**2.223**	33%
3	**2.222**	$TMSCH_2N_2$ (5.0 equiv)	MeOH	r.t.	22	**2.223**	48%
4	**2.222**	$LiOH•H_2O$ Me2SO4 (1.0 equiv) (1.0 equiv)	THF	65	18	**2.223**	56%
5	**2.222**	TMSCl	MeOH	r.t.	20	**2.223**	68%
6	**2.222**	(10.0 equiv)	MeOH	60	17		81%
7	**2.222**	$SOCl_2$ (4 equiv)	MeOH	70	16	**2.223**	80%

Dimethyl 3,4-dibromopyrrole-2,5-dicarboxylate[116] **(2.31**)

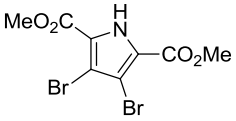

Bromine (1.0 mL, 20.2 mmol, 10.0 equiv) was added to a suspension of pyrrole **2.223** (466 mg, 2.02 mmol, 1.0 equiv) in water (20 mL) at 0 ˚C, and the reaction mixture was stirred for 1 h at rt. Sat. aq. Na_2SO_3 was introduced, and the reaction stirred until complete reduction of excess bromine was achieved, as indicated by a colour change from deep red to a very pale yellow. Extraction with CH_2Cl_2, drying of the combined organic phases over $MgSO_4$, filtration and evaporation of the filtrate to dryness *in vacuo* gave a solid which upon flash column chromatography (2:1 hex:EtOAc) afforded **2.31** as a colourless solid (2.5 g, 80%). mp 224-225 ˚C (EtOAc): lit[17] mp 220-222 ˚C; ^{1}H NMR (400 MHz, $CDCl_3$): δ 3.95 (s, 6H), 9.96 (br s, NH) ppm; ^{13}C NMR (100 MHz, $CDCl_3$): δ 52.5, 107.8, 123.0, 159.0 ppm. The physical and spectral data were consistent with those previously reported.[115]

Dimethyl iminodiacetate[217] (2.257)

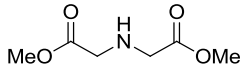

To a suspension of iminodiacetic acid (4.0 g, 30.1 mmol, 1.0 equiv) in anhydrous MeOH (19 mL) was added BF_3•MeOH (7.8 mL, 50%). The resulting brown solution was heated at reflux (80 ˚C) for 15 h. The reaction mixture was cooled to rt, partitioned between a 2:1 mixture of $CHCl_3$ and a saturated solution of $NaHCO_3$ (120 mL:60 mL), and the slight basicity of the aqueous solution was confirmed by pH paper. The $CHCl_3$ layer was separated, and the aqueous layer extracted with $CHCl_3$. The combined organics were dried over $MgSO_4$, subjected to filtration and evaporated to dryness *in vacuo* to afford afford **2.257** as a viscous brown oil (4.06 g, 84%). ^{1}H NMR (400 MHz, $CDCl_3$): δ 3.36 (s, 4H), 3.61 (s, 6H) ppm; ^{13}C NMR (100 MHz, $CDCl_3$): δ 49.7, 51.5, 171.9 ppm. The ^{1}H NMR spectral data was consistent with that previously reported,[217] and the material was used in the next reaction without purification.

Dimethyl 3,4-dihydroxypyrrole-2,5-dicarboxylate[203] (2.258)

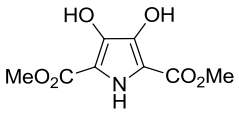

To a solution of NaOMe prepared by dissolving Na metal (1.1 g, 47 mmol, 2.2 equiv) in anhydrous MeOH (7 mL) was added dimethyl oxalate (2.5 g, 21 mmol, 1.0 equiv) and dimethyl iminodiacetate **2.234** (3.4 g, 21 mmol, 1.0 equiv). The reaction mixture was heated at reflux (80 ˚C) for 17 h, cooled to rt and acidified to approximately pH = 5 using glacial acetic acid. The MeOH was removed under reduced pressure, and the acidic aqueous layer was poured into ice-water (40 mL). The resulting precipitate was collected by vacuum filtration using a PIAB pump, and further dried using the high vacuum, to afford **2.258** as an orange solid (1.86 g, 34%). mp 208-209 ˚C (H_2O): lit[125] mp 180-210 ˚C (MeOH, decomp); ^{1}H NMR (400 MHz, $CDCl_3$): δ 3.93 (s, 6H), 6.81 (br s, 2H), 8.07 (br s, 1H (NH)) ppm; ^{13}C NMR (100 MHz, $CDCl_3$): δ 51.9, 108.4, 137.9, 161.9 ppm. The physical and spectral data (^{1}H-NMR) were consistent with those previously reported,[203] and the material was used in the next reaction without purification.

Dimethyl 3,4-(bis-trifluoromethanesulfonyl)pyrrole-2,5-dicarboxylate[204] (2.259)

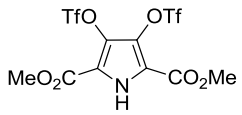

To a solution of compound **2.235** (494 mg, 2.3 mmol, 1.0 equiv) in anhydrous pyridine (3.5 mL, 0.65 M) at 0 ˚C was added neat triflic anhydride (1.43 g, 5.1 mmol, 2.2 equiv). The reaction mixture was stirred at 0 ˚C for 2 h, quenched with water (10 mL) and the mixture was warmed to rt, and extracted with CH_2Cl_2 (4 x 10 mL). The combined organic layers were washed with aq. 2 M HCl solution (10 mL), water (2 x 10 mL), brine (2 x 15 mL), dried over $MgSO_4$ and subjected to filtration. The filtrate was evaporated to dryness *in vacuo* resulting in a solid that was purified by flash column chromatography (2:1 hexane:EtOAc) and afforded **2.259** as a colourless solid (506 mg, 45%). mp 118-120 ˚C (hexanes): lit[204] mp 122-122.5 ˚C (Et_2O-hexane); ^{1}H NMR (400 MHz, $CDCl_3$): δ 4.00 (s, 6H), 9.0-10.5 (br s, NH) ppm; ^{13}C NMR (100 MHz, $CDCl_3$): δ 52.8, 116.1, 118.4 (q, J = 321Hz), 127.4, 158.2 ppm. The physical and spectral data were consistent with those previously reported.[204]

Dimethyl (*N*-benzyl)3,4-dihydroxypyrrole-2,5-dicarboxylate[204] (2.260)

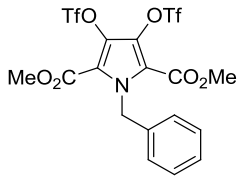

To a suspension of 60% NaH in mineral oil (38 mg, 0.95 mmol, 1.1 equiv) in anhydrous DMF (1.0 M, 0.95 mL) at 0 ˚C was added a solution of **2.236** (414 mg, 0.86 mmol, 1.0 equiv) in DMF (1.73 mL, 0.5 M). The reaction mixture was stirred at rt for 0.5 h, followed by addition of benzyl bromide (0.1 mL, 0.86 mmol, 1.0 equiv) at 0 ˚C. The reaction mixture was stirred at rt for 24 h, treated with H_2O, extracted with EtOAc, and dried over $MgSO_4$. The filtrate was evaporated to dryness in *vacuo*, resulting in a residue that upon flash column chromatography (4:1 CH_2Cl_2:hexane) afforded **2.260** as a colourless solid (277 mg, 58%). mp 72-74 ˚C (hexanes): lit[204] mp 70.5-71 ˚C (Et_2O-hexane); ^{1}H NMR (400 MHz, $CDCl_3$): δ 3.89 (s, 6H), 6.19 (s, 2H), 6.97-7.02 (m, 2H), 7.22-7.36 (m, 3H) ppm; ^{13}C NMR (100 MHz, $CDCl_3$): δ 49.8, 52.4, 117.7, 118.4 (J = 321 Hz), 126.1, 127.8, 128.4, 128.8, 136.4, 158.1 ppm. The physical and spectral data were consistent with those previously reported.[204]

3-bromo-*N*-(*tert*-butyldimethylsilyl)indole[190,218] **(2.32)**

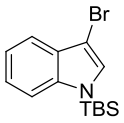

To a solution of indole (1.5 g, 12.8 mmol, 1.0 equiv) in anhydrous THF (46 mL, 0.28 M) at -78 ˚C was added a solution of *n*-BuLi (6 mL, 2.32 M in hexanes, 1.1 equiv) dropwise over 15 mins. The temperature of the solution was raised to -10 ˚C, maintained for 15 mins, and brought back to -78 ˚C. A solution of TBDMSCl (2.2 g, 14.3 mmol, 1.12 equiv) in THF (11 mL, 1.3 M) was added at a steady rate over 10 mins, and the solution was stirred at 0 ˚C for 3 h. The reaction mixture was then cooled to -78 ˚C and NBS (12.8 mmol, 2.3 g, 1.0 equiv) was added in one portion prior to stirring for a further 2 h at -78 ˚C. The reaction mixture was treated with a hexane / pyridine solution (50 mL / 0.5 mL), and the whole was subjected to filtration through a bed of celite. Evaporation to dryness *in vacuo* gave a solid which was subjected to flash column chromatography (6:1 hex:CH_2Cl_2) and afforded **2.32** (3.34 g, 84%) as a colourless solid (which was observed to turn purple in the freezer over time, as described).[218] The reported decomposition of **2.32** upon heating in solution[218] prevented recystallization in order to obtain a melting point. ^{1}H NMR (400 MHz, $CDCl_3$): δ 0.60 (s, 6H), 0.93 (s, 9H), 7.17 (s, 1H), 7.18-7.22 (m, 2H), 7.46-7.50 (m, 1H), 7.55-7.58 (m, 1H) ppm; ^{13}C NMR (100 MHz, $CDCl_3$): δ -4.0, 19.4, 26.2, 93.6, 114.1, 119.1, 120.5, 122.5, 129.7, 129.9, 140.3 ppm. The spectral data were consistent with those previously reported.[218]

***N*-(*p*-toluenesulfonyl)indole**[193c] **(2.226)**

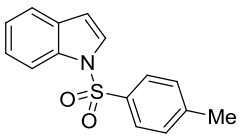

To a solution of indole (4.0 g, 34 mmol, 1.0 equiv) in toluene (75 mL, 0.45 M) at 0 ˚C containing tetrabutylammonium hydrogen sulphate (TBAHS) (1.7 g, 5.1 mmol, 15 mol%) was added sequentially 50% aqueous sodium hydroxide (75 mL) and *p*-toluenesulfonyl chloride (9.78 g, 51 mmol, 1.5 equiv). The reaction mixture was stirred at 0 ˚C for 45 mins, and then at rt overnight (18 h). The organic layer was separated, and washed with aq. 1 M HCl, sat. aq. $NaHCO_3$, water and brine. The combined organics were dried over $MgSO_4$, subjected to filtration and evaporated to dryness *in vacuo* to afford **2.226** (7.5 g, 81%) as a pink solid, which was used in subsequent reactions without further purification. mp 82-84 ˚C (hexanes): lit[194c] mp 87-88 ˚C; ^{1}H NMR (400 MHz, $CDCl_3$): δ 2.31 (s, 3 H), 6.64 (d, 1H, J = 3.7 Hz), 7.16-7.33 (m, 4H), 7.51 (d, 1H, J = 7.8 Hz), 7.55 (d, 1H, J = 3.7 Hz), 7.75 (d, 2H, J = 8.4 Hz), 7.98 (dd, 1H, ^1J = 8.3 Hz, ^2J = 0.6 Hz) ppm; ^{13}C NMR (100 MHz,

$CDCl_3$): δ 21.5, 109.0, 113.5, 121.3, 123.2, 124.5, 126.3, 126.8, 129.8, 130.7, 134.8, 135.3, 144.9 ppm. The physical and spectral data were consistent with those previously reported.[193c]

3-bromo-*N*-(*p*-toluenesulfonyl)indole[219] (2.227)

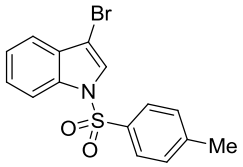

N-bromosuccinimide (1.3 g, 7.4 mmol, 1.0 equiv) was added to a solution of *N*-Ts indole **2.226** (2.0 g, 7.4 mmol, 1.0 equiv) in anhydrous THF (100 mL) at 0 ˚C, warmed to rt and stirred for 2 d. The reaction mixture was quenched with water, and the organic layer was separated and washed with sat. aq. NaCl and water. The combined organics were dried over $MgSO_4$, subjected to filtration and evaporated to dryness *in vacuo*. Flash column chromatography (x 2, 9:1 hex:EtOAc) afforded **2.227** as a colourless solid (709 mg, 27%). The low yield results from the difficulty encountered with separation of the product from unreacted starting material. mp 120-122 ˚C (hexane): lit[219] mp 120-123 ˚C (hexane); ^{1}H NMR (400 MHz, $CDCl_3$): δ 2.30 (s, 3H), 7.22 (d, 2H, *J* = 8.0 Hz), 7.31 (t, 1H, *J* = 7.5 Hz), 7.38 (t, 1H, *J* = 7.4 Hz), 7.49 (d, 1H, *J* = 7.7 Hz), 7.64 (s, 1H), 7.78 (d, 2H, *J* = 8.1 Hz), 8.01 (d, 1H, *J* = 8.2 Hz) ppm; ^{13}C NMR (100 MHz, $CDCl_3$): δ 21.5, 99.5, 113.5, 120.0, 123.8, 124.7, 125.7, 126.8, 129.7, 129.9, 134.2, 134.7, 145.3 ppm. The physical and spectral data were consistent with those previously reported.[219]

3-(4,4,5,5-tetramethyl-1,3,2-dioxaborolan-2-yl)-benzofuran (2.249)[220]

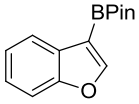

To a solution of benzofuran-3-one (400 mg, 2.98 mmol, 1.0 equiv) in CH_2Cl_2 (25 mL) in a salt-ice bath (approx. -14˚C) was added Et_3N (1.25 mL, 8.95 mmol, 3.0 equiv) followed by a solution of triflic anhydride (1.26 g, 4.47 mmol, 1.5 equiv) as a solution in CH_2Cl_2 (1.1 M, 4.1 mL). The mixture was stirred between -10 ˚C to -15 ˚C for 1 h, and quenched with an aq. 8% solution of $NaHCO_3$. The organic phase was separated, dried over $MgSO_4$, and subjected to filtration. The solvent was removed by rotary evaporation, taking caution to maintain the temperature below 30 ˚C. The isolated 3-trifluoromethanesulfonylbenzofuran was added to a microwave vial containing a solution of distilled Et_3N (1.25 mL, 8.95 mmol, 3.0 equiv), distilled HBPin (611 mg, 4.77 mmol, 1.6 equiv) and $PdCl_2$dppf•CH_2Cl_2 (109 mg, 0.15 mmol, 5 mol%) in anhydrous THF (4.8 mL). The reaction mixture was subjected to microwave irradiation (3 min, 150 ˚C), cooled, and evaporated to dryness. Flash column chromatography (9:1 hexane:EtOAc) afforded **2.249** (325 mg, 41%) as a

brown solid. mp > 55 ˚C (hexanes, decomp.); IR (KBr disc) ν_{max} = 2978, 2932, 1560, 1476, 1452, 1382, 1326, 1292, 1240, 1143, 1090, 1017, 855, 747, 676, 426 cm^{-1}; ^1H NMR (400 MHz, $CDCl_3$): δ 1.37 (s, 12 H), 7.24-7.32 (m, 2H), 7.51 (dd, ^1J = 6.4 Hz, ^2J = 2.0 Hz), 7.91-7.95 (m, 1H), 7.96 (s, 1H) ppm; ^{13}C NMR (400 MHz, $CDCl_3$): δ 24.9, 83.5, 111.0, 122.9, 122.87, 122.94, 124.2, 130.0, 153.7, 155.5 ppm; HRMS calcd for $C_{14}H_{17}BO_3$ 244.1271, found 244.1279.

Dimethyl 3,4-bis(thien-3-yl)pyrrole-2,5-dicarboxylate (2.230)

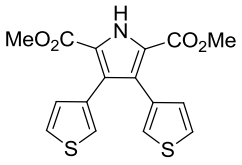

The reaction was performed according to General Procedure A using the following materials in refluxing *t*-BuOH for 4 h: dimethyl 3,4-dibromopyrrole-2,5-dicarboxylate **2.31** (51 mg, 0.15 mmol, 1.0 equiv), thiophene-3-boronic acid **2.229** (58 mg, 0.45 mmol, 3.0 equiv), $Pd_2(dba)_3$ (7 mg, 7.5 µmol, 5.0 mol%), S-Phos (12 mg, 0.03 mmol, 20.0 mol%), and anhydrous K_3PO_4 (127 mg, 0.6 mmol, 4.0 equiv) in anhydrous *t*-BuOH (0.6 mL). Flash column chromatography (5:1 hexane:EtOAc) afforded **2.230** (43 mg, 83%) as a yellow solid. mp 187 ˚C (Et_2O, decomp); IR (KBr disc) ν_{max} = 3298, 1713 cm^{-1}; ^1H NMR (400 MHz, $CDCl_3$): δ 3.82 (s, 6H), 6.88 (d, 2H, *J* = 4.7 Hz), 7.07 (m, 2H), 7.19 (dd, 2H, ^1J = 4.8 Hz, ^2J = 3.0 Hz), 9.80 (br s, NH), ^{13}C NMR (400 MHz, $CDCl_3$): δ 51.9 (2 x CH_3), 121.4 (2 x C_q), 123.7 (2 x CH), 125.0 (2 x CH), 126.3 (2 x C_q), 129.7 (2 x CH), 132.4 (2 x Cq), 160.5 (2 x C(O)) ppm; HRMS calcd for $C_{16}H_{13}NO_4S_2$ 347.0286, found 347.0291.

Dimethyl (*N*-benzyl)-3,4-bis(thien-3-yl)pyrrole-2,5-dicarboxylate (2.261)

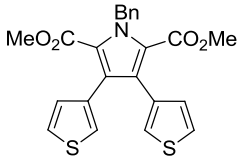

The reaction was performed according to General Procedure B using the following materials in refluxing THF/H_2O for 20 h: dimethyl (*N*-benzyl)-3,4-bis(trifluoromethylsulfonyloxy)pyrrole-2,5-dicarboxylate **2.260** (100 mg, 0.18 mmol, 1.0 equiv), thiophene-3-boronic acid **2.229** (67 mg, 0.53 mmol, 3.0 equiv), $Pd(PPh_3)_4$ (8.1 mg, 7.0 µmol, 4.0 mol%), and Na_2CO_3 (123 mg, 1.16 mmol, 6.6 equiv) in THF (3.5 mL)/H_2O (0.35 mL). Flash column chromatography (6:1 hex:EtOAc) afforded **2.261** (69 mg, 89%) as a yellow solid. mp 128.4-129.5 ˚C (hexanes); IR (KBr disc) ν_{max} = 3110, 3087, 3029, 2949, 1719, 1697, 1494, 1436, 1327, 1287, 1209, 1171, 1034, 797, 733 cm^{-1}; ^1H NMR (400 MHz, $CDCl_3$): δ 3.60 (s, 6H), 6.00 (s, 2H), 6.81 (dd, 2H, ^1J = 4.9 Hz, ^2J = 0.8 Hz), 6.90 (dd, 2H, ^1J = 2.8 Hz, ^2J = 0.9 Hz), 7.09 (d, 2H, *J* = 7.1 Hz), 7.16 (dd, 2H, ^1J = 4.9 Hz, ^2J =

3.0 Hz), 7.23 (t, 1H, J = 7.2 Hz), 7.31 (m, 2H) ppm; ^{13}C NMR (400 MHz, $CDCl_3$): δ 49.8 (CH_2), 51.7 (2 x CH_3), 123.7 (2 x CH), 123.9 (2 x CH), 124.8 (2 x C_q), 126.1 (2 x C_q), 126.4 (2 x CH), 127.2 (2 x Cq), 128.5 (2 x CH), 129.7 (2 x CH), 133.7 (2 x C_q), 138.5 (2 x Cq), 161.9 (2 x C(O)) ppm; HRMS calcd for $C_{23}H_{19}NO_4S_2$ 437.0756, found 437.0745.

Dimethyl (*N*-benzyl)-3,4-bis(thien-2-yl)pyrrole-2,5-dicarboxylate (2.262)

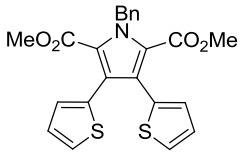

The reaction was performed according to General Procedure B using the following materials in refluxing THF/H_2O for 15 h: dimethyl (*N*-benzyl)-3,4-bis(trifluoromethylsulfonyloxy)pyrrole-2,5-dicarboxylate **2.260** (100 mg, 0.18 mmol, 1.0 equiv), thiophene-2-boronic acid **2.245** (67 mg, 0.53 mmol, 3.0 equiv), $Pd(PPh_3)_4$ (8.1 mg, 7.0 µmol, 4.0 mol%), and Na_2CO_3 (123 mg, 1.16 mmol, 6.6 equiv) were weighed into a microwave vial and degassed THF (3.5 mL) and degassed water (0.35 mL) were added. Flash chromatography (6:1 hex:EtOAc) afforded **2.262** (60 mg, 80%) as a colourless solid. mp 139.5-140.8 ˚C (EtOAc); IR (KBr disc) ν_{max} = 3121, 3097, 3067, 3027, 2991, 2954, 1717, 1604, 1562, 1496, 1458, 1439, 1413, 1349, 1273, 1250, 1229, 1202, 1168, 1079, 1058, 1011, 947, 925, 855, 837, 698, 657, 515 cm^{-1}; ^{1}H NMR (400 MHz, $CDCl_3$): δ 3.60 (s, 6H), 5.99 (s, 2H), 6.81 (dd, 2H, ^1J = 3.5 Hz, ^2J = 1.1 Hz), 6.91 (dd, 2H, ^1J = 5.1 Hz, ^2J = 3.5 Hz), 7.10 (d, 2H, J = 7.4 Hz), 7.21-7.27 (m, 3H), 7.31 (2H, t, J = 7.4 Hz) ppm; ^{13}C NMR (400 MHz, $CDCl_3$): δ 49.9 (CH_2), 51.8 (2 x CH_3), 124.1 (2 x C_q), 125.5 (2 x C_q), 125.9 (2 x CH), 126.2 (2 x CH), 126.4 (2 x CH), 127.3 (CH), 128.3 (2 x CH), 128.6 (2 x CH), 134.1 (2 x C_q), 138.0 (2 x C_q), 161.6 (2 x C(O)) ppm; HRMS calcd for $C_{23}H_{19}NO_4S_2$ 437.0755, found 437.0743.

Dimethyl 3,4-bis(furan-3-yl)pyrrole-2,5-dicarboxylate (2.236)

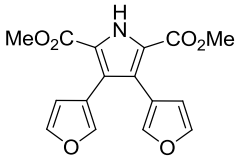

The reaction was performed according to General Procedure A using the following materials in refluxing *t*-BuOH for 38 h: dimethyl 3,4-dibromo-pyrrole-2,5-dicarboxylate **2.31** (100 mg, 0.29 mmol, 1.0 equiv), furan-3-boronic acid **2.235** (99 mg, 0.88 mmol, 3.0 equiv), $Pd_2(dba)_3$ (14 mg, 15 µmol, 5.0 mol%), S-Phos (24 mg, 60 µmol, 20.0 mol%) and anhydrous K_3PO_4 (249 mg, 1.2 mmol, 4.0 equiv) in anhydrous *t*-BuOH (1.2 mL). Flash column chromatography (6:1 hex:EtOAc to 1:1 hex:EtOAc gradient) afforded **2.236** (71 mg, 77%) as a colourless solid. mp 142-145 ˚C (CH_2Cl_2 / hexane); IR (KBr disc) ν_{max} = 3300, 1706, 1433, 1309, 1261 cm^{-1}; ^{1}H NMR (400 MHz,

$CDCl_3$): δ 3.85 (s, 6 H), 6.33-6.35 (m, 2H), 7.37-7.39 (m, 2H), 7.40-7.42 (m, 2H), 9.82 (br s, NH) ppm; ^{13}C NMR (100 MHz, $CDCl_3$): δ 51.9 (2 x CH_3), 112.4 (2 x CH), 116.5 (2 x C_q), 121.7 (2 x C_q), 122.2 (2 x C_q), 141.9 (2 x CH), 142.0 (2 x CH), 160.4 (2 x C(O)) ppm; HRMS calcd for $C_{16}H_{13}NO_6$ 315.0743, found 315.0749.

Dimethyl 3,4-bis(*N*-(triisopropylsilyl)pyrrol-3-yl)pyrrole-2,5-dicarboxylate (2.238)

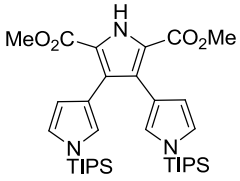

The reaction was performed according to General Procedure A using the following materials in refluxing *t*-BuOH for 38 h: dimethyl 3,4-dibromo-pyrrole-2,5-dicarboxylate **2.31** (100 mg, 0.29 mmol, 1.0 equiv), *N*-(tri-isopropylsilyl)pyrrole-3-boronic acid **2.237** (235 mg, 0.88 mmol, 3.0 equiv), $Pd_2(dba)_3$ (14 mg, 15 μmol, 5.0 mol%), S-Phos (24 mg, 60 μmol, 20.0 mol%) and anhydrous K_3PO_4 (249 mg, 1.2 mmol, 4.0 equiv) in anhydrous *t*-BuOH (1.2 mL). Flash column chromatography (8:1 hex:EtOAc to 6:1 hex:EtOAc gradient) afforded **2.238** (55 mg, 30%) as a colourless solid. mp 151-152 ˚C (hexanes); IR (KBr disc) ν_{max} = 3315, 2948, 2866, 1701, 1267, 1091 cm^{-1}; ^1H NMR (400 MHz, $CDCl_3$): δ 1.08 (d, 36 H, *J* = 7.5 Hz), 1.39 (septet, 6H, *J* = 7.5 Hz), 3.78 (s, 6 H), 6.21-6.24 (m, 2H), 6.62-6.65 (m, 2H), 6.74-6.77 (m, 2H) ppm; ^{13}C NMR (100 MHz, $CDCl_3$): δ 11.7 (6 x CH), 17.8 (12 x CH_3), 51.5 (2 x CH_3), 112.8 (2 x CH), 117.3 (2 x C_q), 121.0 (2 x C_q), 122.7 (2 x CH), 124.8 (2 x CH), 126.2 (2 x C_q), 161.4 (2 x C(O)) ppm; HRMS calcd for $C_{34}H_{55}N_3O_4Si_2$ 625.3731, found 625.3746.

Dimethyl 3,4-bis(*N*-methyl-3-pyrazolyl)pyrrole-2,5-dicarboxylate (2.241)

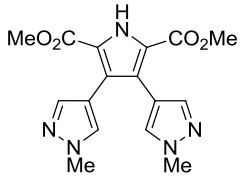

The reaction was performed according to General Procedure A using the following materials in refluxing *t*-BuOH/H_2O for 17 h: dimethyl 3,4-dibromo- pyrrole-2,5-dicarboxylate **2.31** (100 mg, 0.29 mmol, 1.0 equiv), *N*-methylpyrazolyl-3-boropinacolate ester **2.239** (183.1 mg, 0.88 mmol, 3.0 equiv), $Pd_2(dba)_3$ (14 mg, 15 μmol, 5.0 mol%), S-Phos (24 mg, 60 μmol, 20.0 mol%) and anhydrous K_3PO_4 (249 mg, 1.2 mmol, 4.0 equiv) in degassed *t*-BuOH (1.2 mL) and water (0.48 mL). Flash column chromatography (100% CH_2Cl_2 → 1:1 CH_2Cl_2:Et_2O → 5% MeOH in CH_2Cl_2 gradient) afforded **2.241** (23.2 mg, 23%) as a tan solid. mp.: > 270 ˚C decomp (MeCN); IR (KBr disc) ν_{max} = 3124, 2951, 1702, 1635, 1537, 1434, 1270, 1220, 1121, 1068, 987, 781 cm^{-1}; ^1H NMR (400 MHz, $CDCl_3$): δ 3.84 (s, 6 H), 3.88 (s, 6 H), 7.35 (s, 2H), 7.36 (s, 2H), 9.73 (br s, NH)

ppm; ^{13}C NMR (100 MHz, $CDCl_3$): δ 38.9 (2 x *N*-CH_3), 51.8 (2 x CH_3), 112.7 (2 x C_q), 121.3 (2 x C_q), 122.2 (2 x C_q), 130.5 (2 x CH), 140.3 (2 x CH), 160.5 (2 x C(O)) ppm; HRMS calcd for $C_{16}H_{17}N_5O_4$ 343.1281, found 343.1293.

Dimethyl 3,4-bis(benzothien-3-yl)pyrrole-2,5-dicarboxylate (2.244)

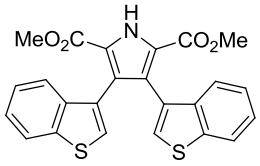

The reaction was performed according to General Procedure A using the following materials in refluxing *t*-BuOH for 17 h: dimethyl 3,4-dibromo-pyrrole-2,5-dicarboxylate **2.31** (100 mg, 0.29 mmol, 1.0 equiv), benzothiophene-3-boronic acid **2.243** (418 mg, 2.3 mmol, 8.0 equiv), $Pd_2(dba)_3$ (14 mg, 15 µmol, 5.0 mol%), S-Phos (24 mg, 60 µmol, 20.0 mol%) and anhydrous K_3PO_4 (249 mg, 1.2 mmol, 4.0 equiv) in degassed *t*-BuOH (1.2 mL). The standard work-up procedure (including removal of solvent under reduced pressure) was followed by washing of the crude residue with hexane in order to remove benzothiophene resulting from protodeboronation of **2.243** and afforded **2.244** (117.3 mg, 89%) as a colourless solid. mp > 243 ˚C (CH_2Cl_2/hexane, decomp.); IR (KBr disc) ν_{max} = 3307, 1725, 1678, 1280, 762, 735 cm^{-1}; ^{1}H NMR (600 MHz, $CDCl_3$, T = 283 K): δ 3.67 (s, 3H), 3.72 (s, 3H), 6.88 (s, 1H (H-9)), 7.09 (t, 1H (H-5 or H-6), *J* = 7.4 Hz), 7.23 (t, 1H (H-5 or H-6), *J* = 7.5 Hz), 7.26 (s, 1H (H-1)), 7.30-7.33 (m, 1H (H-4 or H-7)), 7.34-7.40 (m, 2H (H-13 and H-14)), 7.56-7.61 (m, 1H (H-12 or H-15)), 7.76 (d, 1H (H-4 or H-7), *J* = 8.0 Hz), 7.82-7.87 (m, 1H (H-12 or H-15)), 10.24 (br s, NH), 10.25 (br s, NH) ppm; ^{13}C NMR (100 MHz, $CDCl_3$): δ 52.0 (CH_3), 52.5 (CH_3), 122.2 (CH), 122.5 (2 x CH), 122.7 (CH), 122.85 (C_q), 122.9 (C_q), 123.6 (CH), 123.8 (2 x CH), 124.0 (CH), 125.1 (C_q), 125.4 (CH), 125.5 (C_q), 126.2 (CH), 128.2 (C_q), 128.3 (C_q), 138.3 (C_q), 138.9 (C_q), 139.2 (C_q), 139.4 (C_q), 160.5 (C(O)), 160.6 (C(O)) ppm; HRMS calcd for $C_{24}H_{17}NO_4S_2$ 447.0599, found 447.0591.

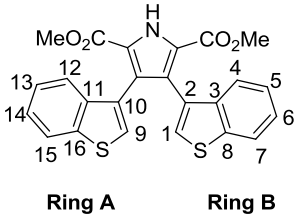

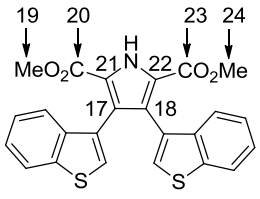

Dimethyl 3,4-bis(thien-2-yl)pyrrole-2,5-dicarboxylate (2.246)

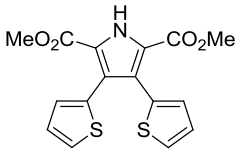

The reaction was performed according to a modified General Procedure A using the following materials with microwave heating at 150 ˚C in *t*-BuOH for 5 h: dimethyl 3,4-dibromo-pyrrole-2,5-dicarboxylate **2.31** (100 mg, 0.29 mmol, 1.0 equiv), thiophene-2-boronic acid **2.245** (188 mg, 1.5 mmol, 5.0 equiv), $Pd_2(dba)_3$ (14 mg, 15 µmol, 5.0 mol%), S-Phos (24 mg, 60 µmol, 20 mol%) and anhydrous K_3PO_4 (374 mg,1.8 mmol, 6.0 equiv) in degassed *t*-BuOH (1.2 mL). Flash column chromatography (5:1 hexane:EtOAc) afforded **2.246** (39 mg, 38%) as a yellow solid. mp 205-208 ˚C (MeOH); IR (KBr disc) ν_{max} = 3298, 1708, 1282, 1237, 706 cm^{-1}; ^1H NMR (400 MHz, $CDCl_3$): δ 3.82 (s, 6 H), 6.95-6.99 (m, 4H), 7.27-7.32 (m, 2H), 9.92 (br s, NH); ^{13}C NMR (100 MHz, $CDCl_3$): δ 52.0, 122.1, 124.6, 126.3, 126.5, 129.1, 132.8, 160.2 ppm; HRMS calcd for $C_{16}H_{13}NO_4S_2$ 347.0286, found 347.0293.

Dimethyl 3,4-bis(indol-5-yl)pyrrole-2,5-dicarboxylate (2.248)

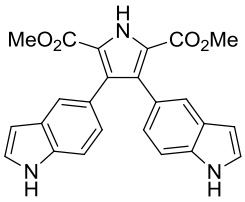

The reaction was performed according to General Procedure A using the following materials in refluxing *t*-BuOH for 16 h: dimethyl 3,4-dibromo-pyrrole-2,5-dicarboxylate **2.31** (100 mg, 0.29 mmol, 1.0 equiv), indole-5-boronic acid **2.247** (142 mg, 0.88 mmol, 3.0 equiv), $Pd_2(dba)_3$ (14 mg,15 µmol, 5.0 mol%), S-Phos (24 mg, 60 µmol, 20 mol%) and anhydrous K_3PO_4 (249 mg, 1.2 mmol, 4.0 equiv) in degassed *t*-BuOH (1.2 mL). Flash column chromatography (5:1 hexane:EtOAc) afforded **2.248** (97.4 mg, 80%) as a brown solid. mp 262-263.5 ˚C (MeCN); IR (KBr disc) ν_{max} = 3425, 3381, 3340, 2954, 1699, 1689, 1454, 1314, 1269, 1250, 1228, 1135, 1092, 1027, 893, 772, 737, 581 cm^{-1}; ^1H NMR (400 MHz, d_6-acetone): δ 3.67 (s, 6H), 6.29-6.33 (m, 2H), 6.88 (d, 2H, *J* = 8.4 Hz), 7.16 (d, 2H, *J* = 8.4 Hz), 7.19-7.22 (m, 2H), 7.41 (s, 2H), 10.08 (br s, 2 NH), 10.89 (br s, NH); ^{13}C NMR (100 MHz, d_6-acetone): δ 52.5 (2 x CH_3), 103.5 (2 x CH), 111.7 (2 x CH), 124.6 (2 x CH), 126.3 (2 x CH), 126.7 (2 x CH), 129.4 (2 x C_q), 134.7 (2 x Cq), 137.2 (2 x C_q), 162.5 (2 x C(O)) ppm; HRMS calcd for $C_{24}H_{19}N_3O_4$ 413.1376, found 413.1385.

Dimethyl 3,4-bis(benzofuran-3-yl)pyrrole-2,5-dicarboxylate (2.250)

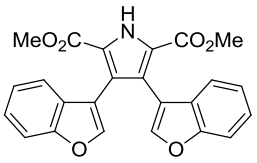

The reaction was performed according to General Procedure A using the following materials in refluxing *t*-BuOH/H_2O for 17 h: dimethyl 3,4-dibromo- pyrrole-2,5-dicarboxylate **2.31** (100 mg, 0.29 mmol, 1.0 equiv), 3-(4,4,5,5-tetramethyl-1,3,2-dioxaborolan-2-yl)-benzofuran **2.249** (215 mg, 0.88 mmol, 3.0 equiv), $Pd_2(dba)_3$ (14 mg, 15 µmol, 5.0 mol%), S-Phos (24 mg, 60 µmol, 20.0 mol%) and anhydrous K_3PO_4 (249 mg, 1.2 mmol, 4.0 equiv) in anhydrous *t*-BuOH (1.2 mL) and water (0.48 mL). Flash column chromatography (10:1 hex:EtOAc to 8:1 hex:EtOAc) afforded **2.250** (25.3 mg, 21%) as a yellow solid. mp 232-234 ˚C (EtOAc); IR (KBr disc) v_{max} = 3326, 3145, 2958, 1711, 1529, 1449, 1297, 1268, 1217, 1097, 993, 970, 927, 859, 786, 745 cm^{-1}; ^1H NMR (400 MHz, d_6-acetone): δ 3.64 (s, 6H), 6.98-7.04 (t, 2H, *J* = 7.5 Hz), 7.12-7.22 (m, 4H), 7.37 (d, 2H, *J* = 8.2 Hz), 7.68 (s, 2H), 11.72 (br s, NH) ppm; ^{13}C NMR (100 MHz, d_6-acetone): δ 52.8 (2 x CH_3), 112.9 (2 x CH), 115.4 (2 x C_q), 122.3 (2 x C_q), 122.4 (2 x CH), 124.2 (2 x CH), 125.5 (2 x C_q), 125.8 (2 x CH), 129.9 (2 x C_q), 146.1 (2 x CH), 156.5 (2 x C_q), 161.8 (2 x C(O)) ppm; HRMS calcd for $C_{24}H_{17}NO_6$ 415.1056, found 415.1053.

Dimethyl 3,4-bis(2-(methylphenyl))pyrrole-2,5-dicarboxylate (2.252)

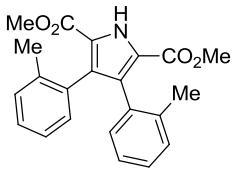

The reaction was performed according to General Procedure A using the following materials in refluxing *t*-BuOH for 22 h: dimethyl 3,4-dibromo-pyrrole-2,5-dicarboxylate **2.31** (100 mg, 0.29 mmol, 1.0 equiv), 2-methylphenylboronic acid **2.251** (118 mg , 0.88 mmol, 3.0 equiv), $Pd_2(dba)_3$ (14 mg, 15 µmol, 5.0 mol%), S-Phos (24 mg, 60 µmol, 20.0 mol%) and anhydrous K_3PO_4 (249 mg, 1.2 mmol, 4.0 equiv) in degassed *t*-BuOH (1.2 mL). Flash column chromatography (8:1 hex:EtOAc) afforded **2.252** (56 mg, 53%) as a yellow solid. mp 185-187 ˚C (EtOAc/hex); IR (KBr disc) v_{max} = 3302, 3012, 2955, 2923, 1710, 1549, 1463, 1431, 1299, 1279, 1242, 1155, 1116, 1016, 951, 787, 771, 732 cm^{-1}; ^1H NMR (400 MHz, $CDCl_3$): δ 2.03 (s, 3H, CH_3), 2.14 (s, 3H, CH_3), 3.73 (s, 6H), 6.82-6.88 (m, 1H), 6.94-7.00 (m, 1H), 7.14-7.20 (m, 6H), 9.92 (br s, NH) ppm; ^{13}C NMR (100 MHz, $CDCl_3$): δ 19.8 (CH_3), 20.2 (CH_3), 51.8 (2 x CH_3), 121.86 (C_q), 121.92 (C_q), 124.6 (CH), 124.8 (CH), 127.28 (CH), 127.3 (CH), 129.2 (CH), 129.3 (CH), 129.8 (CH), 131.07 (C_q), 131.1 (C_q), 131.2 (CH), 132.6 (C_q), 133.0 (C_q), 136.7 (C_q), 137.0 (C_q), 160.65 (C(O)), 160.67 (C(O)) ppm; HRMS calcd for $C_{22}H_{21}NO_4$ 363.1471, found 363.1482.

Dimethyl 3,4-bis(quinolin-3-yl)pyrrole-2,5-dicarboxylate (2.254)

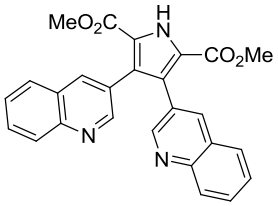

The reaction was performed according to General Procedure A using the following materials in refluxing *t*-BuOH for 32 h: 3,4-dibromo pyrrole-2,5-dicarboxylate **2.31** (200 mg, 0.59 mmol, 1.0 equiv), quinoline-3-boronic acid **2.253** (304 mg, 1.76 mmol, 3.0 equiv), $Pd_2(dba)_3$ (27 mg, 30 µmol, 5.0 mol%), S-Phos (48 mg, 0.12 mmol, 20.0 mol%), and anhydrous K_3PO_4 (498 mg, 2.4 mmol, 4.0 equiv). Flash column chromatography (CH_2Cl_2 → 4% MeOH in CH_2Cl_2) afforded **2.254** (33 mg,13%) as a yellow solid. mp > 250 ˚C (EtOAc, decomp.); IR (KBr disc) ν_{max} = 3044, 2931, 2852, 1713, 1590, 1494, 1471, 1450, 1431, 1354, 1322, 1249, 1111, 1076, 1035, 1001, 942, 927, 827, 784, 756, 567, 538 cm^{-1}; ^1H NMR (400 MHz, d_6-DMSO): δ 3.69 (s, 6H), 7.51 (m, 2H), 7.69 (m, 2H), 7.80 (d, 2H, *J* = 7.8 Hz), 7.91 (d, 2H, *J* = 8.4 Hz), 8.13 (d, 2H, *J* = 1.7 Hz), 8.64 (d, 2H, *J* = 2.1 Hz) ppm; ^{13}C NMR (400 MHz, d_6-DMSO): δ 51.6, 122.2 (2 x C_q), 126.6 (2 x CH), 126.8 (2 x C_q), 127.2 (2 x C_q), 127.9 (2 x CH), 128.4 (2 x CH), 129.4 (2 x CH), 136.8 (2 x CH), 146.0 (2 x C_q), 152.1 (2 x CH), 160.0 (2 x C(O)) ppm; HRMS calcd for $C_{26}H_{19}N_3O_4$ 437.1376, found 437.1366.

Dimethyl 2*H*-Dibenzothieno[3,2-*e*:2',3'-*g*]isoindole-5,5'-dicarboxylate (2.266)

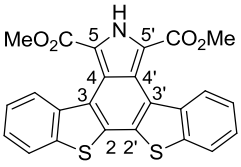

A solution of dimethyl 3,4-bis(thien-3-yl)pyrrole-2,5-dicarboxylate **2.244** (50 mg, 0.11 mmol, 1.0 equiv) in HOAc (0.01 M) containing $Pd(OAc)_2$ (28 mg, 0.13 mmol, 1.12 equiv) was heated at 70 ˚C for 48 h. Flash column chromatography (5:1 hex:EtOAc) afforded **2.239c** (39.7 mg, 80%) as a yellow solid. mp > 260 ˚C (decomp); IR (KBr disc) ν_{max} = 3275, 3060, 2959, 1716, 1687, 1498, 1466, 1447, 1275, 1259, 1233, 1209, 1077, 749, 726 cm^{-1}; ^1H NMR (400 MHz, d_6-DMSO): δ 3.96 (s, 6H), 7.52-7.62 (m, 4H), 7.84-7.89 (m, 2H), 8.17-8.22 (m, 2H), 14.03 (br s, NH) ppm; ^{13}C NMR (100 MHz, d_6-DMSO): δ 52.0 (2 x CH_3), 118.3 (2 x C_q), 119.2 (2 x C_q), 123.1 (2 x CH), 124.3 (2 x CH), 124.7 (2 x C_q), 125.8 (2 x CH), 125.9 (2 x CH), 131.7 (2 x C_q), 135.0 (2 x C_q), 137.9 (2 x C_q), 161.8 (2 x C(O)) ppm; HRMS calcd for $C_{24}H_{15}NO_4S_2$ 445.0442, found 445.0443.

Dimethyl 2*H*-Dithieno[3,2-*e*:2',3'-*g*]isoindole-5,5'-dicarboxylate (2.267)

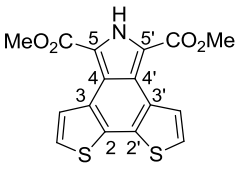

A solution of dimethyl 3,4-bis(thien-3-yl)pyrrole-2,5-dicarboxylate **2.230** (100 mg, 0.29 mmol, 1.0 equiv) in HOAc (0.01 M) containing $Pd(OAc)_2$ (72 mg, 0.32 mmol, 1.1 equiv) was heated at 70 ˚C for 15 h. Flash column chromatography (CH_2Cl_2) afforded **2.267** (22 mg, 22%) as a yellow solid. mp > 200 ˚C (EtOAc); IR (KBr disc) ν_{max} = 3458, 3089, 2952, 1708, 1463, 1436, 1416, 1282, 1226, 1163, 1137, 1111, 1054, 874, 745, 638, 612 cm^{-1}; ^1H NMR (400 MHz, $CDCl_3$): δ 4.06 (s, 6H), 7.43 (d, 2H, *J* = 5.3 Hz), 8.73 (d, 2H, *J* = 5.3 Hz), 10.5 (br s, NH) ppm; ^{13}C NMR (100 MHz, $CDCl_3$): δ 52.2 (2 x CH_3), 115.7 (2 x C_q), 122.4 (2 x C_q), 122.7 (2 x CH), 127.2 (2 x CH), 128.6 (2 x C_q), 133.9 (2 x C_q), 160.1 (2 x C(O)) ppm; HRMS calcd for $C_{16}H_{12}NO_4S_2$ $[M+H]^+$ 346.0208, found 346.0207.

2.8 Appendix

Table 1. Crystal data and structure refinement for 2.246

Empirical formula	C16 H13 N O4 S2	
Formula weight	347.39	
Temperature	180(2) K	
Wavelength	0.71073 Å	
Crystal system	Triclinic	
Space group	P-1	
Unit cell dimensions	a = 9.0559(3) Å	α= 83.706(2)°.
	b = 9.6955(3) Å	β= 77.089(2)°.
	c = 9.7020(3) Å	γ= 73.135(2)°.
Volume	793.69(4) $Å^3$	
Z	2	
Density (calculated)	1.454 Mg/m^3	
Absorption coefficient	0.354 mm^{-1}	
F(000)	360	
Crystal size	0.20 x 0.15 x 0.08 mm^3	
Theta range for data collection	2.20 to 26.00°.	
Index ranges	-11<=h<=11, -11<=k<=11, -11<=l<=11	
Reflections collected	6959	
Independent reflections	3078 [R(int) = 0.0210]	
Completeness to theta = 26.00°	99.2 %	
Absorption correction	Semi-empirical from equivalents	
Max. and min. transmission	0.9722 and 0.9325	
Refinement method	Full-matrix least-squares on F^2	
Data / restraints / parameters	3078 / 36 / 206	
Goodness-of-fit on F^2	1.043	
Final R indices [I>2sigma(I)]	R1 = 0.0479, wR2 = 0.1208	
R indices (all data)	R1 = 0.0585, wR2 = 0.1289	
Largest diff. peak and hole	0.631 and -0.493 $e.Å^{-3}$	

Table 2. Atomic coordinates (x 10^4) and equivalent isotropic displacement parameters ($Å^2$x 10^3) for 2.246. U(eq) is defined as one third of the trace of the orthogonalized U^{ij} tensor.

	x	y	z	U(eq)
N(1)	2196(2)	8269(2)	5702(2)	27(1)
O(1)	866(2)	9660(2)	3388(2)	42(1)
O(2)	3290(2)	9179(2)	2015(2)	36(1)
O(3)	1067(2)	7482(2)	8525(2)	47(1)
O(4)	3556(2)	6676(2)	8852(2)	35(1)
C(1)	3068(3)	8431(2)	4389(2)	27(1)
C(2)	4651(3)	7826(2)	4442(2)	25(1)
C(3)	4712(2)	7288(2)	5852(2)	25(1)
C(4)	3160(3)	7584(2)	6603(2)	26(1)
C(5)	2273(3)	9161(2)	3240(2)	30(1)
C(6)	2631(3)	9934(3)	823(3)	42(1)
C(7)	2465(3)	7256(2)	8081(2)	29(1)
C(8)	2989(3)	6224(3)	10295(3)	41(1)
C(9)	6056(3)	7758(2)	3316(2)	28(1)
S(1A)	6657(2)	6576(2)	2024(2)	40(1)
C(10A)	8339(5)	7145(6)	1347(6)	36(1)
C(11A)	8413(7)	8208(6)	2100(5)	36(1)
C(12A)	7261(8)	8512(8)	3122(7)	40(1)
S(1B)	7217(4)	8732(4)	3342(3)	40(1)
C(10B)	8558(15)	7880(14)	1788(10)	36(1)
C(11B)	8025(11)	6870(15)	1356(13)	36(1)
C(12B)	6702(18)	6850(19)	2154(18)	40(1)
C(13)	6191(3)	6549(3)	6328(2)	29(1)
S(2A)	7025(2)	7333(2)	7257(2)	42(1)
C(14A)	8704(5)	5848(5)	7113(5)	42(1)
C(15A)	8594(5)	4784(5)	6422(5)	42(1)
C(16A)	7381(9)	5178(8)	5935(9)	42(1)
S(2B)	7224(4)	5023(4)	5822(4)	42(1)
C(14B)	8775(10)	5172(9)	6630(9)	42(1)
C(15B)	8467(10)	6382(9)	7300(9)	42(1)

C(16B)	7349(15)	7244(15)	6991(15)	42(1)

Table 3. Bond lengths [Å] and angles [°] for 2.246

N(1)-C(4)	1.358(3)
N(1)-C(1)	1.360(3)
N(1)-H(1A)	0.8800
O(1)-C(5)	1.206(3)
O(2)-C(5)	1.332(3)
O(2)-C(6)	1.449(3)
O(3)-C(7)	1.205(3)
O(4)-C(7)	1.330(3)
O(4)-C(8)	1.445(3)
C(1)-C(2)	1.393(3)
C(1)-C(5)	1.467(3)
C(2)-C(3)	1.417(3)
C(2)-C(9)	1.471(3)
C(3)-C(4)	1.394(3)
C(3)-C(13)	1.472(3)
C(4)-C(7)	1.471(3)
C(6)-H(6A)	0.9800
C(6)-H(6B)	0.9800
C(6)-H(6C)	0.9800
C(8)-H(8A)	0.9800
C(8)-H(8B)	0.9800
C(8)-H(8C)	0.9800
C(9)-C(12B)	1.418(15)
C(9)-C(12A)	1.451(7)
C(9)-S(1B)	1.610(4)
C(9)-S(1A)	1.681(3)
S(1A)-C(10A)	1.737(4)
C(10A)-C(11A)	1.351(6)
C(10A)-H(10A)	0.9500

C(11A)-C(12A)	1.258(7)
C(11A)-H(11A)	0.9500
C(12A)-H(12A)	0.9500
S(1B)-C(10B)	1.817(8)
C(10B)-C(11B)	1.350(11)
C(10B)-H(10B)	0.9500
C(11B)-C(12B)	1.276(14)
C(11B)-H(11B)	0.9500
C(12B)-H(12B)	0.9500
C(13)-C(16A)	1.474(8)
C(13)-S(2B)	1.568(4)
C(13)-C(16B)	1.666(16)
C(13)-S(2A)	1.658(3)
S(2A)-C(14A)	1.756(5)
C(14A)-C(15A)	1.329(6)
C(14A)-H(14A)	0.9500
C(15A)-C(16A)	1.234(8)
C(15A)-H(15A)	0.9500
C(16A)-H(16A)	0.9500
S(2B)-C(14B)	1.801(8)
C(14B)-C(15B)	1.332(10)
C(14B)-H(14B)	0.9500
C(15B)-C(16B)	1.184(12)
C(15B)-H(15B)	0.9500
C(16B)-H(16B)	0.9500

C(4)-N(1)-C(1)	109.85(18)
C(4)-N(1)-H(1A)	125.1
C(1)-N(1)-H(1A)	125.1
C(5)-O(2)-C(6)	116.24(19)
C(7)-O(4)-C(8)	116.10(18)
N(1)-C(1)-C(2)	108.13(19)
N(1)-C(1)-C(5)	119.5(2)
C(2)-C(1)-C(5)	132.4(2)

C(1)-C(2)-C(3)	107.00(19)
C(1)-C(2)-C(9)	129.3(2)
C(3)-C(2)-C(9)	123.7(2)
C(4)-C(3)-C(2)	106.70(19)
C(4)-C(3)-C(13)	129.9(2)
C(2)-C(3)-C(13)	123.36(19)
N(1)-C(4)-C(3)	108.32(19)
N(1)-C(4)-C(7)	119.28(19)
C(3)-C(4)-C(7)	132.4(2)
O(1)-C(5)-O(2)	124.4(2)
O(1)-C(5)-C(1)	123.8(2)
O(2)-C(5)-C(1)	111.84(19)
O(2)-C(6)-H(6A)	109.5
O(2)-C(6)-H(6B)	109.5
H(6A)-C(6)-H(6B)	109.5
O(2)-C(6)-H(6C)	109.5
H(6A)-C(6)-H(6C)	109.5
H(6B)-C(6)-H(6C)	109.5
O(3)-C(7)-O(4)	124.4(2)
O(3)-C(7)-C(4)	123.4(2)
O(4)-C(7)-C(4)	112.17(19)
O(4)-C(8)-H(8A)	109.5
O(4)-C(8)-H(8B)	109.5
H(8A)-C(8)-H(8B)	109.5
O(4)-C(8)-H(8C)	109.5
H(8A)-C(8)-H(8C)	109.5
H(8B)-C(8)-H(8C)	109.5
C(12B)-C(9)-C(12A)	98.9(6)
C(12B)-C(9)-C(2)	130.3(6)
C(12A)-C(9)-C(2)	130.6(3)
C(12B)-C(9)-S(1B)	108.7(6)
C(12A)-C(9)-S(1B)	9.8(3)
C(2)-C(9)-S(1B)	120.85(19)
C(12B)-C(9)-S(1A)	6.9(6)

C(12A)-C(9)-S(1A)	105.7(3)
C(2)-C(9)-S(1A)	123.42(18)
S(1B)-C(9)-S(1A)	115.49(16)
C(9)-S(1A)-C(10A)	92.0(2)
C(11A)-C(10A)-S(1A)	111.6(5)
C(11A)-C(10A)-H(10A)	124.2
S(1A)-C(10A)-H(10A)	124.2
C(12A)-C(11A)-C(10A)	111.9(7)
C(12A)-C(11A)-H(11A)	124.1
C(10A)-C(11A)-H(11A)	124.1
C(11A)-C(12A)-C(9)	118.8(5)
C(11A)-C(12A)-H(12A)	120.6
C(9)-C(12A)-H(12A)	120.6
C(9)-S(1B)-C(10B)	90.7(6)
C(11B)-C(10B)-S(1B)	110.8(12)
C(11B)-C(10B)-H(10B)	124.6
S(1B)-C(10B)-H(10B)	124.6
C(12B)-C(11B)-C(10B)	109.0(14)
C(12B)-C(11B)-H(11B)	125.5
C(10B)-C(11B)-H(11B)	125.5
C(11B)-C(12B)-C(9)	120.7(12)
C(11B)-C(12B)-H(12B)	119.7
C(9)-C(12B)-H(12B)	119.7
C(16A)-C(13)-C(3)	131.6(3)
C(16A)-C(13)-S(2B)	9.9(3)
C(3)-C(13)-S(2B)	122.2(2)
C(16A)-C(13)-C(16B)	96.1(5)
C(3)-C(13)-C(16B)	129.1(5)
S(2B)-C(13)-C(16B)	106.0(4)
C(16A)-C(13)-S(2A)	104.3(3)
C(3)-C(13)-S(2A)	123.24(19)
S(2B)-C(13)-S(2A)	114.08(17)
C(16B)-C(13)-S(2A)	11.8(5)
C(13)-S(2A)-C(14A)	91.53(19)

C(15A)-C(14A)-S(2A)	113.0(3)
C(15A)-C(14A)-H(14A)	123.5
S(2A)-C(14A)-H(14A)	123.5
C(16A)-C(15A)-C(14A)	109.6(5)
C(16A)-C(15A)-H(15A)	125.2
C(14A)-C(15A)-H(15A)	125.2
C(15A)-C(16A)-C(13)	121.0(6)
C(15A)-C(16A)-H(16A)	119.5
C(13)-C(16A)-H(16A)	119.5
C(13)-S(2B)-C(14B)	90.5(3)
C(15B)-C(14B)-S(2B)	115.1(6)
C(15B)-C(14B)-H(14B)	122.4
S(2B)-C(14B)-H(14B)	122.4
C(16B)-C(15B)-C(14B)	110.4(11)
C(16B)-C(15B)-H(15B)	124.8
C(14B)-C(15B)-H(15B)	124.8
C(15B)-C(16B)-C(13)	114.4(11)
C(15B)-C(16B)-H(16B)	122.8
C(13)-C(16B)-H(16B)	122.8

Symmetry transformations used to generate equivalent atoms:

Table 4. Anisotropic displacement parameters ($Å^2 x\ 10^3$) for 2.246. The anisotropic displacement factor exponent takes the form: $-2\pi^2[\ h^2\ a^{*2}U^{11} + ... + 2\ h\ k\ a^*\ b^*\ U^{12}\ ]$

	U^{11}	U^{22}	U^{33}	U^{23}	U^{13}	U^{12}
N(1)	20(1)	31(1)	26(1)	0(1)	0(1)	-3(1)
O(1)	27(1)	55(1)	34(1)	2(1)	-6(1)	1(1)
O(2)	32(1)	44(1)	24(1)	7(1)	-4(1)	-1(1)
O(3)	27(1)	68(1)	34(1)	10(1)	3(1)	-6(1)
O(4)	30(1)	49(1)	22(1)	4(1)	-1(1)	-7(1)
C(1)	27(1)	27(1)	25(1)	-2(1)	-4(1)	-5(1)
C(2)	26(1)	26(1)	23(1)	-2(1)	-2(1)	-6(1)
C(3)	24(1)	26(1)	24(1)	-1(1)	-3(1)	-6(1)

C(4)	27(1)	26(1)	24(1)	0(1)	-3(1)	-6(1)
C(5)	28(1)	29(1)	28(1)	-1(1)	-5(1)	-4(1)
C(6)	48(2)	48(2)	25(1)	9(1)	-12(1)	-8(1)
C(7)	29(1)	30(1)	25(1)	-1(1)	-1(1)	-5(1)
C(8)	43(2)	50(2)	22(1)	5(1)	-1(1)	-8(1)
C(9)	26(1)	32(1)	22(1)	4(1)	-5(1)	-5(1)
S(1A)	40(1)	42(1)	33(1)	-12(1)	4(1)	-12(1)
C(10A)	24(1)	50(2)	30(1)	5(1)	1(1)	-9(1)
C(11A)	24(1)	50(2)	30(1)	5(1)	1(1)	-9(1)
C(12A)	40(1)	42(1)	33(1)	-12(1)	4(1)	-12(1)
S(1B)	40(1)	42(1)	33(1)	-12(1)	4(1)	-12(1)
C(10B)	24(1)	50(2)	30(1)	5(1)	1(1)	-9(1)
C(11B)	24(1)	50(2)	30(1)	5(1)	1(1)	-9(1)
C(12B)	40(1)	42(1)	33(1)	-12(1)	4(1)	-12(1)
C(13)	27(1)	38(1)	21(1)	5(1)	-2(1)	-11(1)
S(2A)	42(1)	46(1)	42(1)	0(1)	-16(1)	-14(1)
C(14A)	42(1)	46(1)	42(1)	0(1)	-16(1)	-14(1)
C(15A)	42(1)	46(1)	42(1)	0(1)	-16(1)	-14(1)
C(16A)	42(1)	46(1)	42(1)	0(1)	-16(1)	-14(1)
S(2B)	42(1)	46(1)	42(1)	0(1)	-16(1)	-14(1)
C(14B)	42(1)	46(1)	42(1)	0(1)	-16(1)	-14(1)
C(15B)	42(1)	46(1)	42(1)	0(1)	-16(1)	-14(1)
C(16B)	42(1)	46(1)	42(1)	0(1)	-16(1)	-14(1)

Table 5. Hydrogen coordinates (x 10^4) and isotropic displacement parameters ($Å^2$x 10^3) for 2.246.

	x	y	z	U(eq)
H(1A)	1161	8563	5933	33
H(6A)	3484	9941	-1	63
H(6B)	2051	10929	1062	63
H(6C)	1913	9443	600	63
H(8A)	3829	6042	10832	62
H(8B)	2672	5339	10300	62

H(8C)	2081	6986	10730	62
H(10A)	9112	6758	546	44
H(11A)	9235	8670	1882	44
H(12A)	7183	9223	3755	47
H(10B)	9506	8115	1339	44
H(11B)	8549	6269	584	44
H(12B)	6145	6221	1967	47
H(14A)	9598	5810	7490	51
H(15A)	9335	3861	6318	51
H(16A)	7213	4588	5298	51
H(14B)	9744	4440	6581	51
H(15B)	9059	6533	7936	51
H(16B)	7132	8248	7111	51

Table 6. Torsion angles [°] for 2.246.

C(4)-N(1)-C(1)-C(2)	0.2(3)
C(4)-N(1)-C(1)-C(5)	-179.4(2)
N(1)-C(1)-C(2)-C(3)	-0.2(2)
C(5)-C(1)-C(2)-C(3)	179.3(2)
N(1)-C(1)-C(2)-C(9)	-178.3(2)
C(5)-C(1)-C(2)-C(9)	1.2(4)
C(1)-C(2)-C(3)-C(4)	0.1(2)
C(9)-C(2)-C(3)-C(4)	178.4(2)
C(1)-C(2)-C(3)-C(13)	179.3(2)
C(9)-C(2)-C(3)-C(13)	-2.5(3)
C(1)-N(1)-C(4)-C(3)	-0.1(3)
C(1)-N(1)-C(4)-C(7)	-178.4(2)
C(2)-C(3)-C(4)-N(1)	0.0(2)
C(13)-C(3)-C(4)-N(1)	-179.1(2)
C(2)-C(3)-C(4)-C(7)	177.9(2)
C(13)-C(3)-C(4)-C(7)	-1.2(4)
C(6)-O(2)-C(5)-O(1)	3.8(4)

C(6)-O(2)-C(5)-C(1)	-177.3(2)
N(1)-C(1)-C(5)-O(1)	1.4(4)
C(2)-C(1)-C(5)-O(1)	-178.1(2)
N(1)-C(1)-C(5)-O(2)	-177.6(2)
C(2)-C(1)-C(5)-O(2)	3.0(4)
C(8)-O(4)-C(7)-O(3)	3.6(4)
C(8)-O(4)-C(7)-C(4)	-175.8(2)
N(1)-C(4)-C(7)-O(3)	4.8(4)
C(3)-C(4)-C(7)-O(3)	-172.9(2)
N(1)-C(4)-C(7)-O(4)	-175.72(19)
C(3)-C(4)-C(7)-O(4)	6.6(4)
C(1)-C(2)-C(9)-C(12B)	-76.9(12)
C(3)-C(2)-C(9)-C(12B)	105.2(12)
C(1)-C(2)-C(9)-C(12A)	108.7(5)
C(3)-C(2)-C(9)-C(12A)	-69.2(5)
C(1)-C(2)-C(9)-S(1B)	108.1(3)
C(3)-C(2)-C(9)-S(1B)	-69.7(3)
C(1)-C(2)-C(9)-S(1A)	-77.9(3)
C(3)-C(2)-C(9)-S(1A)	104.3(3)
C(12B)-C(9)-S(1A)-C(10A)	10(8)
C(12A)-C(9)-S(1A)-C(10A)	-0.7(4)
C(2)-C(9)-S(1A)-C(10A)	-175.6(2)
S(1B)-C(9)-S(1A)-C(10A)	-1.3(3)
C(9)-S(1A)-C(10A)-C(11A)	-0.1(4)
S(1A)-C(10A)-C(11A)-C(12A)	1.1(6)
C(10A)-C(11A)-C(12A)-C(9)	-1.9(9)
C(12B)-C(9)-C(12A)-C(11A)	0.4(8)
C(2)-C(9)-C(12A)-C(11A)	176.0(5)
S(1B)-C(9)-C(12A)-C(11A)	179(3)
S(1A)-C(9)-C(12A)-C(11A)	1.7(8)
C(12B)-C(9)-S(1B)-C(10B)	-0.4(11)
C(12A)-C(9)-S(1B)-C(10B)	-2(2)
C(2)-C(9)-S(1B)-C(10B)	175.5(4)
S(1A)-C(9)-S(1B)-C(10B)	1.1(4)

C(9)-S(1B)-C(10B)-C(11B)	-0.9(8)
S(1B)-C(10B)-C(11B)-C(12B)	2.0(14)
C(10B)-C(11B)-C(12B)-C(9)	-3(2)
C(12A)-C(9)-C(12B)-C(11B)	2.2(18)
C(2)-C(9)-C(12B)-C(11B)	-173.6(11)
S(1B)-C(9)-C(12B)-C(11B)	2(2)
S(1A)-C(9)-C(12B)-C(11B)	-167(9)
C(4)-C(3)-C(13)-C(16A)	114.6(5)
C(2)-C(3)-C(13)-C(16A)	-64.3(5)
C(4)-C(3)-C(13)-S(2B)	110.5(3)
C(2)-C(3)-C(13)-S(2B)	-68.4(3)
C(4)-C(3)-C(13)-C(16B)	-90.7(7)
C(2)-C(3)-C(13)-C(16B)	90.4(7)
C(4)-C(3)-C(13)-S(2A)	-78.0(3)
C(2)-C(3)-C(13)-S(2A)	103.1(2)
C(16A)-C(13)-S(2A)-C(14A)	-2.3(4)
C(3)-C(13)-S(2A)-C(14A)	-172.6(2)
S(2B)-C(13)-S(2A)-C(14A)	-0.4(3)
C(16B)-C(13)-S(2A)-C(14A)	-49(2)
C(13)-S(2A)-C(14A)-C(15A)	-2.0(4)
S(2A)-C(14A)-C(15A)-C(16A)	6.4(7)
C(14A)-C(15A)-C(16A)-C(13)	-9.1(9)
C(3)-C(13)-C(16A)-C(15A)	176.5(5)
S(2B)-C(13)-C(16A)-C(15A)	-163(3)
C(16B)-C(13)-C(16A)-C(15A)	16.0(9)
S(2A)-C(13)-C(16A)-C(15A)	7.4(8)
C(16A)-C(13)-S(2B)-C(14B)	9(2)
C(3)-C(13)-S(2B)-C(14B)	171.1(3)
C(16B)-C(13)-S(2B)-C(14B)	8.0(6)
S(2A)-C(13)-S(2B)-C(14B)	-1.1(4)
C(13)-S(2B)-C(14B)-C(15B)	1.2(7)
S(2B)-C(14B)-C(15B)-C(16B)	-13.8(13)
C(14B)-C(15B)-C(16B)-C(13)	20.0(14)
C(16A)-C(13)-C(16B)-C(15B)	-19.5(12)

C(3)-C(13)-C(16B)-C(15B)	179.2(8)
S(2B)-C(13)-C(16B)-C(15B)	-19.3(12)
S(2A)-C(13)-C(16B)-C(15B)	115(3)

Symmetry transformations used to generate equivalent atoms:

Chapter 3

Benzenoid Ring Functionalization of Indoles via the Directed *ortho* Metalation (D*o*M) Reaction

3.1 Introduction

3.1.1 Directed *ortho* Metalation (D*o*M): Mechanism, Development and Application

Discovery of the Directed *ortho* Metalation (D*o*M) reaction originates from the independent work of Wittig[221] (1938) and Gilman[222] (1939), who demonstrated that anisole (**3.1**) undergoes *ortho*-deprotonation upon treatment with *n*-BuLi (Scheme 3.1a,b). Subsequent electrophilic quench of the intermediate lithiated species **3.2** with benzophenone (Wittig) or CO_2 (Gilman) resulted in regioselective formation of **3.3** (68% yield) or 2-methoxybenzoic acid **3.4** (19% yield). Excellent reviews describing the development, mechanistic studies, and industrial applications of the D*o*M reaction are available,[223] and the following sections will discuss directed metalation groups (DMGs), current understanding of mechanistic paradigms, and its combination with cross-coupling chemistry (the D*o*M-XCoupl nexus).

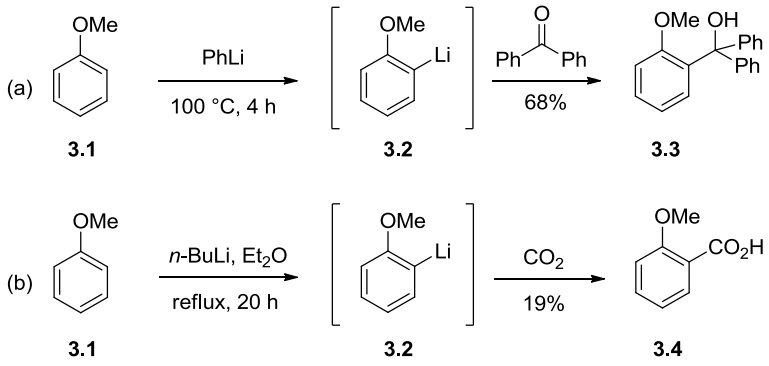

Scheme 3.1. Discovery of the Directed *ortho* Metalation (D*o*M) reaction[222,223]

3.1.2 Directed *ortho* Metalation Groups (DMGs)

Two criteria have been established in order to determine whether a given functional group has potential to be an effective directed metalation group (DMG): the ability to undergo coordination with a base (facilitated by the presence of a heteroatom), and resistance towards nucleophilic attack by a strong base (by decreased electrophilicity resulting from steric hindrance or anionic charge repulsion or both factors). Directed metalation groups are classified as being carbon-based or heteroatom-based, and the most widely used DMGs are shown in Table 3.1.[224a-t] A comparative assessment of directing group power is provided by the generally applicable hierarchy of DMGs (Figure 3.1), determined through intra- and intermolecular competition studies.[223c]

Table 3.1. Representative Directed Metalation Groups

Carbon-based DMGs	Discoverer	Ref.	Heteroatom-based DMGs	Discoverer	Ref.
CON^-R	Hauser (1964)	224a	SO_2N^-R	Hauser (1968)	224h
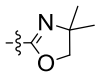	Meyers (1975) Gschwend (1975)	224b 224c	SO_2NR_2	Hauser (1969)	224i
			OMOM	Christensen (1975)	224j
$CONEt_2$	Beak (1977)	224d	NHBoc	Gschwend (1979)	224k
	Comins (1982)*	224e	NHPiv	Muchowski (1980)	224l
			$OCONEt_2$	Snieckus (1983)	224m
CO_2H	Mortier (1994)	224f	$OP(O)(NMe_2)_2$	Watanabe (1989)	224n,o
			$P(O)t\text{-}Bu_2$	Snieckus (1998)	224p
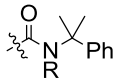	Snieckus (1999)	224g	OSO_2NR_2	Snieckus (2003)	224q
			OC(O)N(TMS)(*i*-Pr)	Hoppe (2006)*	224r,s
			$OP(O)(NEt_2)_2$	Snieckus (2008)	224t

* Generated *in situ*.

The ability to convert DMGs to other functional groups after metalation enhances the synthetic utility of the D*o*M reaction. For example, the OMOM,[225] NHBoc[225] and oxazoline[226] DMGs may be hydrolyzed to the corresponding alcohols, amines and carboxylic acids, and cumyl amides may be decumylated.[224g] DMG manipulation can also be achieved through Kumada-Corriu or Suzuki-Miyaura cross-coupling with Grignard reagents or boronic acids, as demonstrated for the *N*,*N*-diethyl sulfonamides,[227] sulfamates,[224q,228] and carbamates.[228,229,230]

Furthermore, SO_2NEt_2 and $OCONEt_2$ DMGs participate in Ni(0)-catalyzed reductive cleavage with *i*-PrMgBr, enhancing the synthetic utility of these latent directed metalation groups.[227,230] Metalation reactions in the presence of *in situ* generated DMGs have also been described, and include α-amino alkoxides[231] and *N*-TMS-*N*-isopropyl carbamates,[224r,s] which are readily hydrolyzed to the corresponding respective benzaldehydes and phenols. Recently, the Schwartz reagent has been shown to reduce aryl amides[232a-c] and aryl carbamates[232c-d] to the corresponding aryl aldehydes and phenols respectively, and a process for *in situ* generation of the Schwartz reagent was recently developed and patented in the Snieckus research group.[232c] A recent addition to the heteroatom based DMGs, the *N*,*N*,*N′*,*N′*-tetraethylphosphorodiamidate, $OPO(NEt_2)_2$, has excellent directing power and synthetic potential for biaryl construction.[233]

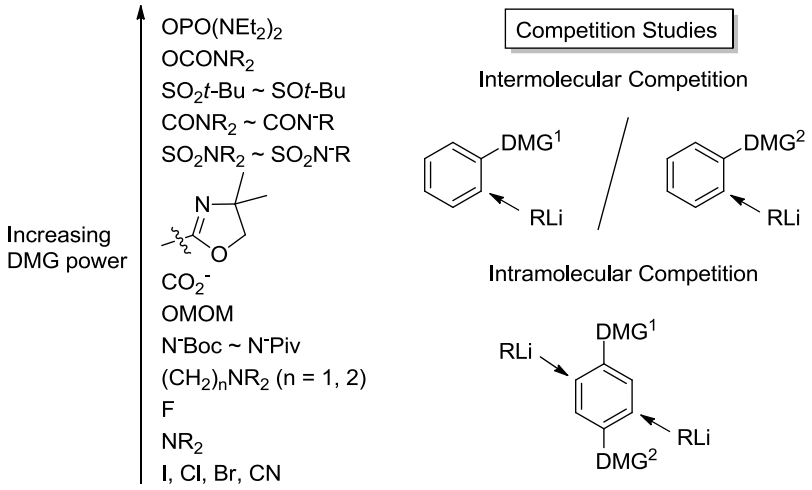

Figure 3.1. Hierarchy of DMGs[223c]

Alkyllithium bases are frequently used in D*o*M procedures, and their performance is enhanced by addition of a chelating, bidentate ligand (commonly TMEDA) to the reaction media that serves to break down higher order aggregates (hexamers in hydrocarbon solvents, and tetramers/dimers in coordinating solvents) into lower aggregates (dimers and monomers) of higher kinetic basicity.[234] Lithium amide bases such as lithium tetramethylpiperidine (LTMP) and lithium diisopropylamide (LDA) also find routine use in D*o*M chemistry for a variety of reasons: (i) they are more compatible with electrophilic functional groups and reagents than alkyllithium

bases (as they are less nucleophilic);[235] (ii) they are compatible with *in situ* electrophilic trapping experiments;[235] and (iii) they are effective in the metalation of more acidic π-deficient heteroaromatics.[236] Recently, Knochel developed the use of mixed Li/Mg amide bases TMPMgCl•LiCl[237] and $(TMP)_2Mg•2LiCl$[238] which are highly soluble in THF, have high kinetic basicity (presumably due to the ability of LiCl to break up aggregates of Mg amides), and excellent functional group tolerance. Historically, development of these mixed Li/Mg amide bases follows from Eaton's study of the magnesium bases R_2NMgCl, R_2NMgR' and $(R_2N)_2Mg$,[239] which suffered from low solubility and were required in large excess. Use of mild mixed aluminum ate $^{i}Bu_3Al(TMP)Li$[240,241] or TMP-zincate TMP-$Zn^{t}Bu_2Li$[242] complexes as bases for D*o*M permit *ortho*-alumination or zincation of functionalized aromatics and heteroaromatics bearing sensitive ester, nitrile and halogen functionalities (which are often incompatible with other bases commonly used in D*o*M).

3.1.3 Mechanism

Two schools of thought exist with regards to the mechanism of the D*o*M reaction, although no single mechanistic picture provides a sufficient rationalization of the process for all arene-DMG systems. The most widely accepted mechanism is based on the concept of the *Complex-Induced Proximity Effect* (CIPE) proposed by Beak and Meyers in 1985,[243] and subsequently by Klumpp,[244] as shown in Scheme 3.2. The CIPE sequence begins with the establishment of a rapid equilibrium involving coordination of the heteroatom of the DMG to the alkyllithium aggregate (**3.6**), followed by slow, irreversible deprotonation to **3.7** to form the coordinated, *ortho*-lithiated species **3.8**. Finally, electrophilic quench of **3.8** results in formation of the 1,2-disubstituted aromatic product **3.9**. The CIPE is based on the premise that pre-lithiation complex **3.6** brings the reactive lithiating base into close proximity with the acidic *ortho* hydrogen, resulting in the observed regioselective deprotonation.

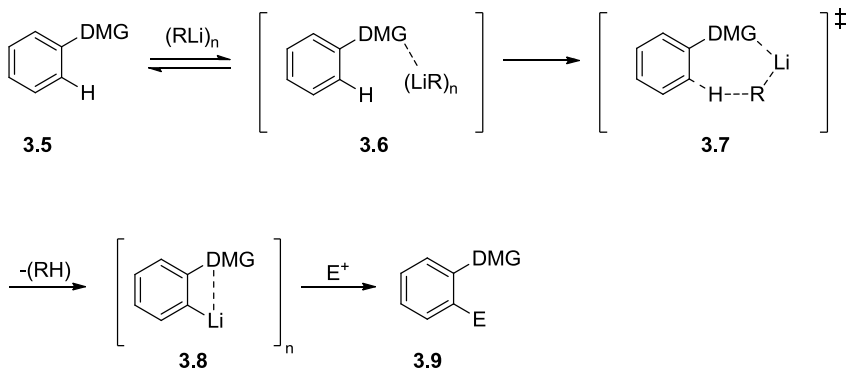

Scheme 3.2. Mechanism of D*o*M reaction according to the Complex-Induced Proximity Effect (CIPE) analysis[243,244]

The alternative mechanistic picture proposed by Schleyer,[245] termed "kinetically enhanced metalation (KEM)" requires that proton transfer is the only step between reactant and lithiated product. The theoretical basis of the KEM model (Figure 3.2) states that directing and accelerating effects of DMGs arise from transition state stabilization, rather than involvement of a prelithiation complex, as in the CIPE theory. Schleyer argues that formation of such a complex would increase the energy barrier to deprotonation and render D*o*M an unlikely event. The transition state associated with the KEM pathway (Figure 3.2) is proposed to involve simultaneous coordination between the DMG and base and deprotonation, and can be stabilized in the presence of electronegative substituents in two ways: (i) by providing an electrostatically favourable arrangement of charges, and (ii) by strong coordination of electron rich atoms, such as oxygen and fluorine, to the lithium centre. The high inductive effect and poor complexation ability of F, Cl, and CF_3 have been exploited in metalation studies which presumably are in accordance with an operative KEM model.[246]

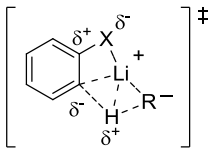

Figure 3.2. Kinetically Enhanced Metalation (KEM) transition state[245,246]

3.1.3.1 Kinetics

A variety of kinetic studies have been performed in order to gain insight into the mechanism of the D*o*M reaction. Beak reported the direct observation of a pre-lithiation complex formed during the *s*-BuLi mediated α-lithiation of *N*,*N*-dialkylbenzamides (in hydrocarbon solvent), using kinetics and stopped-flow FT infrared spectroscopy.[247] In this study, a reaction scheme consistent with the experimental data involved multiple coordination equilibria generating three *s*-BuLi/TMEDA tetrameric complexes in the form $(amide)_x(TMEDA)_y(s\text{-}BuLi)_4$. The most reactive of these complexes towards *ortho*-lithiation, $(amide)_1(TMEDA)_2(s\text{-}BuLi)_4$, was the most destabilized aggregate by virtue of the three-fold ligand association, favouring reaction between the carbanion and the α-hydrogen of the *N*,*N*-dialkylbenzamide. Subsequent measurements of large primary kinetic isotope effects (KIEs) reported by Beak for both intra- and intermolecular *ortho*-lithiation of secondary and tertiary benzamides indicate that proton transfer is the rate determining step,[248] and it may be interpreted that the D*o*M reaction proceeds through a fast, reversible complexation of the amide DMG with the organolithium base, followed by slow deprotonation.

Results of kinetic studies described by Stratkis[249] and Collum[250] are in direct opposition to CIPE theory. Stratkis determined that intramolecular and intermolecular KIEs for D*o*M of anisole in diethyl ether, in the absence or presence of the bidentate chelating ligand TMEDA, are small and identical within experimental error, suggesting that D*o*M occurs via a single rate determining deprotonation (without the formation of a pre-lithiation complex). In kinetic studies of *n*-BuLi/TMEDA lithiation of alkoxy substituted arenes (benzene, $MeOC_6H_5$, 1,3-$(MeO)_2C_6H_5$, $MeOCH_2OC_6H_5$, and $Me_2N(CH_2)_2OC_6H_5$),[251] Collum observed that deprotonation events were governed by substituent-dependent rate laws but one substrate-independent mechanistic picture consistent with a rate limiting transition state of stoichiometry $[(n\text{-}BuLi)_2(TMEDA)_2(Ar\text{-}H)]^{‡}$. A common transition state for *ortho*-lithiation of substrates with variable coordinating abilities precludes involvement of CIPE, and computational investigation supports the notion that regioselectivity of the lithiation event is governed by inductive effects associated with the ring substituent(s). Collum advises that caution must be taken in extrapolation of the results to stronger DMGs (such as carboxamides), due to differences in inductive and coordinative properties.

Indeed, Collum's subsequent investigation of the anionic Snieckus-Fries rearrangement of aryl carbamates revealed rate constants consistent with complex, solvent-influenced reaction pathways proceeding through ArLi monomers, or LDA-aryllithium mixed dimers or trimers.[252] Evidence for these types of intermediates has been provided by React-IR studies, as well as ^{6}Li, ^{15}N and ^{13}C NMR spectroscopy. The complexity of LDA-mediated lithiations of aryl carbamates is further demonstrated by postulated involvement of an autocatalytic pathway,[253] involving LDA-aryllithium mixed dimer intermediates.

3.1.3.2 NMR and Computational Studies

Structural studies have also been performed which provide inferential evidence that a CIPE effect is operative. Schleyer and Hauser studied the metalation of anisole **3.1** with *n*-BuLi in toluene at -64 ˚C (Scheme 3.3) and observed prelithiation complex **3.10** using a combination of 1D (^{1}H, ^{13}C, ^{6}Li) and 2D (^{6}Li-^{1}H HOESY) NMR.[254] Despite the proximity of lithium to the *ortho* hydrogen atoms of anisole, this complex was found to be unproductive and underwent deaggregation to **3.11** upon addition of one equivalent of TMEDA.[255] At this stage, hypothetical prelithiation complex **3.12** is proposed to achieve *ortho* lithiation of anisole **3.1** via agostic complex **3.13** having an agostic C-H interaction with the Li metal,[256] that forms **3.2** via an *ortho*-lithiation reaction. Although transition state **3.13** is presumably present in significantly low concentration as to avoid detection using NMR spectroscopy, MNDO calculations of proposed complex **3.13** show agostic Li hydrogen interactions. Additional indirect evidence is provided by an NMR investigation of the lithiation of 1-naphthol, in which close contacts between 1-naphthol peri-hydrogens and lithium atoms (of the lithium aggregate cluster) are observed by ^{7}Li-^{1}H HOESY.[257]

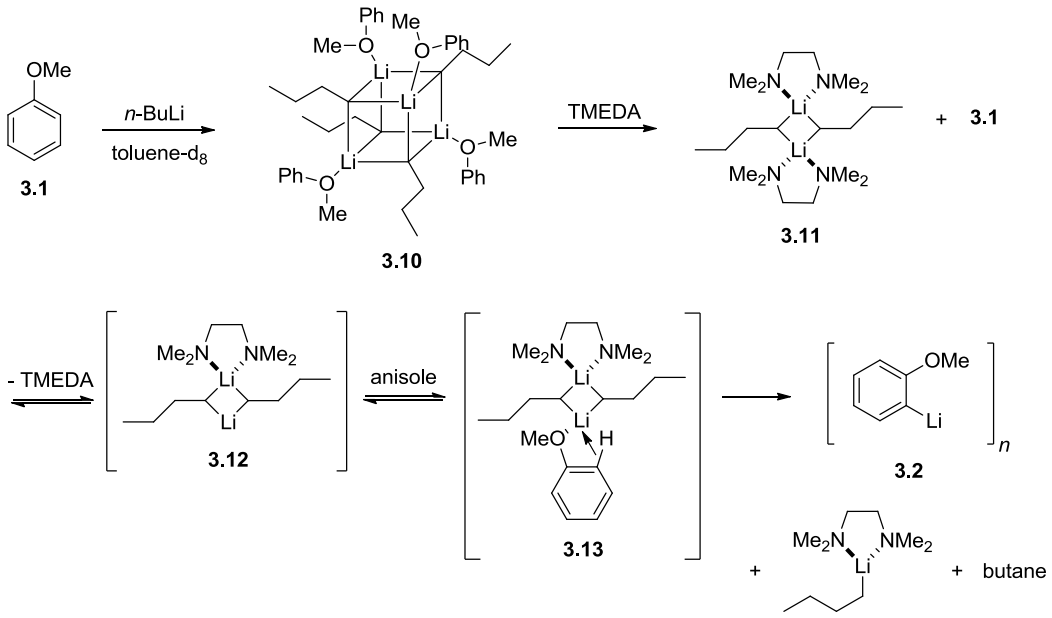

Scheme 3.3. Role of TMEDA as a deaggregation agent during D*o*M of anisole (**3.1**)[254]

In a study of competitive efficiencies of *ortho*-lithiation in a series of structurally related amides, including 2-isopropylisoquinolin-1-(*2H*)-one **3.14**, *N*,*N*-diisopropylbenzamide **3.15**, and 2-trimethylsilyl-*N*,*N*-diisopropylbenzamide **3.16** (Figure 3.3),[258] the indicated values for competitive efficiency suggest a correlation between increasing DMG efficiency and planarity between the DMG carbonyl oxygen and *ortho* hydrogen atom. These results suggest a strong geometrical dependence on planarity in the DoM process, and were considered to be indirect evidence in support of CIPE.

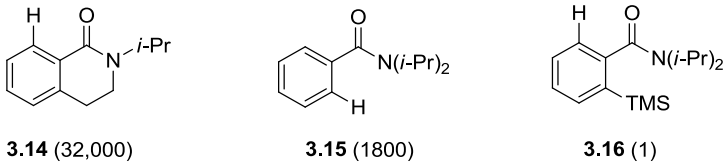

Figure 3.3. Competitive efficiencies of lithiation among structurally related amides[258]

3.1.3.3 Solvent Effects and Additives

Slocum and co-workers have made significant contributions towards understanding the influence of additives and solvent coordination versus substrate dependent electronic effects in D*o*M reactions of methoxy substituted aromatics. Slocum observed that the presence of TMEDA in anisole D*o*M reactions, as first described by Langer,[259] results in substantial rate enhancements.[260] This effect was also observed upon incremental addition of TMEDA to D*o*M reactions of anisole,[261] *p*-fluoroanisole,[262] *p*-methylanisole,[263] and *p*-dimethoxybenzene.[264] Slocum postulated a predictive model in accordance with the kinetic data, which is in opposition to CIPE: (i) in the absence of TMEDA, anisole/*n*-BuLi complexation occurs in the rate-limiting step, followed by rapid deprotonation, (ii) the presence of TMEDA eliminates the slow step through an "overriding base" effect that allows rapid deprotonation without prior pre-complexation. During studies of "uncatalyzed" *ortho*-lithiations of 1,2-di, 1,3-di, and 1,2,4-trimethoxybenzenes in hydrocarbon solvents (performed without added TMEDA or ether),[265] Slocum found that the aromatic methoxy substituents act both as DMGs and deoligomerization agents through dimeric complexes of stoichiometry $(n\text{-BuLi})_2$ $(C_6H_x(OMe)_y)_2$, and coined the term "substrate-promoted *ortho* lithiation." In more recent studies, Slocum observed that addition of increasing increments of THF or TMEDA increases the basicity of *n*-BuLi in cyclohexane,[266] through manipulation of the oligomeric equilibrium of *n*-BuLi (predominantly a hexamer in hydrocarbons), in favour of more basic tetrameric and dimeric complexes $[(n\text{-BuLi})_6(\text{TMEDA})_X \leftrightarrow (n\text{-BuLi})_4(\text{TMEDA})_X \leftrightarrow (n\text{-BuLi})_2(\text{TMEDA})_X]$, where x = 1-4. A similar equilibrium can be written for THF coordination. Some evidence exists in support of "substrate-promoted *ortho* lithiation" for DoM reactions performed in diethyl ether.[267]

3.1.3.4 Current Mechanistic Picture

The current mechanistic understanding of the D*o*M reaction is such that neither CIPE nor KEM models adequately explain every reaction, and the application of either model is dependent upon the particular arene-DMG system. As previously discussed, the CIPE model effectively describes D*o*M reactions involving strongly coordinating DMGs (e.g. $CONR_2$), which are most efficient when either co-planarity or a very small dihedral angle between the carbonyl oxygen and the *ortho* hydrogen is achieved. The KEM pathway is believed operative with weakly

coordinating DMGs, in which coordination is electronically or geometrically impossible. In this case, inductive effects predominate and are thereby proposed to increase the acidity of the *ortho* hydrogen.

3.1.4 The D*o*M-Cross Coupling Nexus

Although it could be argued that C-H activation (see section 3.2.2) chemistry is both complementary and competitive with D*o*M, and ultimately may surpass D*o*M since the need for pre-functionalized reactants is avoided in transition-metal catalyzed processes, the D*o*M reaction occupies its own niche in transition-metal catalyzed chemistry. Efficient generation of transmetalated species **3.18** (Met = B, Mg, Zn, Sn, and Si) resulting from D*o*M reaction of **3.17** have allowed the marriage of D*o*M chemistry with Suzuki-Miyaura, Kumada-Corriu, Negishi, Stille and Hiyama couplings (Table 3.2), providing ready regioselective access to biaryl and heterobiaryl compounds **3.20**.[268] Biaryls **3.20** are synthetically valuable in their own right, due to potential further manipulation *via* D*o*M or Directed remote Metalation (DreM) chemistries.

Table 3.2. The D*o*M / Cross-Coupling Nexus

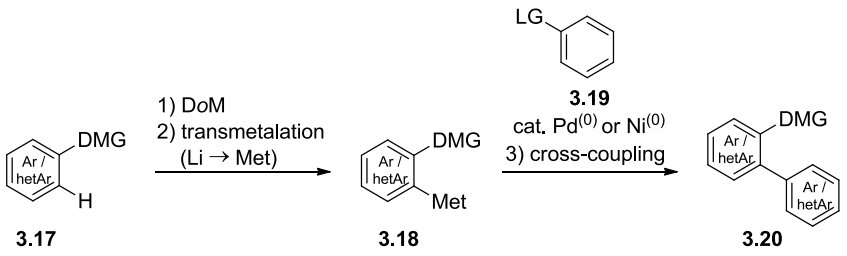

Met	LG	Cat.	Cross-coupling
$B(OR)_2$	I > Br > OTf	Pd	Suzuki-Miyaura
MgX	Hal, OTf	Ni	Kumada-Corriu
ZnX	Hal, OTf	Ni	Negishi
SnR_3	Hal, OTf	Pd	Stille-Migita
$Si(OR)_3$	Hal, OTf	Pd	Hiyama

3.2 Synthesis and Functionalization of Indoles

3.2.1 Classical methods of indole synthesis involving heteroannulation processes

The multitude of classical syntheses of indoles has been comprehensively discussed in numerous reviews.[269] A classification system has been developed in which indole syntheses are defined in accordance with the fundamental chemistry involved, and includes sigmatropic rearrangements (e.g. Fischer,[270] Gassman,[271] and Bartoli[272] syntheses), reductive cyclization (e.g. Leimgruber-Batcho,[273] and Reissert[274] syntheses), and nucleophilic cyclization (e.g. Madelung[275] and Nenitzescu[276] syntheses). These synthetic methods are detailed in Scheme 3.4 alongside the corresponding disconnections of the indole heteroaromatic framework, however this is far from a complete list of all the classical methods developed for indole synthesis.[277] The intention of this introduction is to present a retrosynthetic analysis scheme of the most well-known indole syntheses (Scheme 3.4).

Similiarities between the Fischer, Gassman and Bartoli indole syntheses arise because all methods involve construction of bonds between N1-C2 and C3-C4a (disconnection A, Scheme 3.4) *via* sigmatropic rearrangements, and commence from reactions of aniline or nitrobenzene derivatives. Specifically, the Fischer indole synthesis is extremely effective for the synthesis of 2,3-disubstituted indoles, and proceeds via initial reaction of arylhydrazines, **3.21**, with aldehydes or ketones to form intermediate arylhydrazones under acidic reaction conditions. Subsequent steps involving hydrazone tautomerization and [3,3]-sigmatropic rearrangement lead to indoles. An advantageous feature of this reaction is the facile preparation of the required arylhydrazones via the Japp-Klingemann reaction.[278] The Gassman indole synthesis, first described in 1974,[271] commences with initial *N*-chlorination of aniline **3.24** followed by reaction of the resulting *N*-chloroaniline with β-ketosulfides **3.25**. The resulting intermediate azasulfonium ylide undergoes a Sommelet-Hauser rearrangement[279] to form an *ortho* substituted aniline, which undergoes cyclization and dethiomethylation to afford 2-substituted indole **3.26**. In comparison with the Fischer indole synthesis, advantages of the Gassman method include the availability and cost-effectiveness of starting materials, mild reaction conditions, better functional group tolerance, diminished problems associated with regioselectivity control, as well as comparable or improved yields. However, a major limitation of the method arises from the inability to prepare specific indoles from anilines bearing a cation stabilizing group (*o*-OMe or *p*-OMe). The Bartoli synthesis

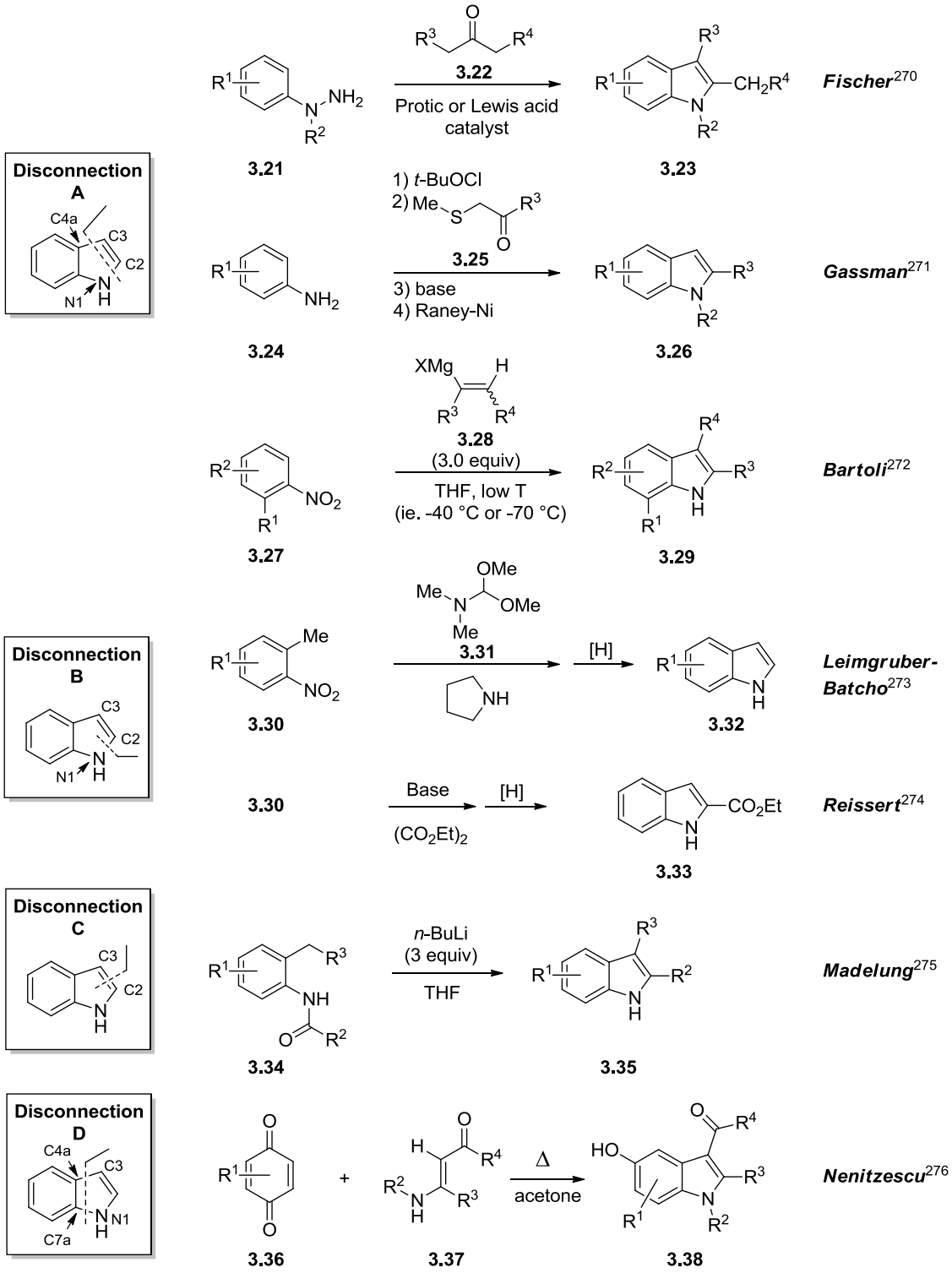

Scheme 3.4. Classical indole synthesis involving heteroannulation processes[269]

provides an alternative synthetic route to 2,3-substituted indoles, and involves the reaction of *ortho*-substituted nitrobenzenes **3.27** with excess Grignard reagent **3.28**, to form 2,3,7-trisubstituted indoles of type **3.29**. The lack of an *ortho* substituent to the nitro group tends to result in the formation of very low yield of product.

A number of methods for indole syntheses involve formation of the N1-C2 bond via a reductive cyclization of nitro aromatics but are dependent on the availability of 1,2-disubstituted systems (disconnection B). The Leimgruber-Batcho indole synthesis involves reaction of *ortho*-nitrotoluene **3.30** with dimethylformamide dimethylacetal (**3.31**) to form an intermediate β-dialkylamino-*o*-nitrostyrene, and subsequent reductive cyclization to give indole **3.32**. Owing to the final reduction step (Pd/C catalyst, or Raney Nickel), particular OBn and halogen substituents, among others, in **3.30** are not tolerated. The related classical Reissert indole synthesis involves reaction of *ortho*-nitrotoluene **3.30** with diethyloxalate, followed by reductive cyclization of the resulting ethyl *ortho*-nitrophenylpyruvate to produce 2-substituted indole **3.33**.

The Houlihan modification[280] of the Madelung indole synthesis (disconnection C) is based on formation of the C2-C3 bond via a nucleophilic cyclization reaction of an *N*-acyl-*o*-toluidine **3.34**. Use of LDA or *n*-BuLi as the base[280] allows the reaction to proceed under milder conditions than the original Madelung conditions, which typically required strong alkoxide bases (such as NaOEt) and reaction temperatures at or exceeding 250 ˚C. Additionally, activation of the *ortho*-methyl hydrogens by anion stabilizing groups (such as $R^3 = CO_2Me$) also allows the use of milder conditions to affect the cyclization to substituted indoles **3.35**.[281] Lastly, the Nenitzescu indole synthesis involves formation of 5-hydroxyindoles **3.38** upon reaction of 1,4-benzoquinone **3.36** with enamines **3.37**. A variety of benzoquinone substituents are tolerated (e.g. alkyl, aryl, esters, halogens), but certain substitution patterns dictate the regioselective outcome of the reaction. Structural diversity in the enamine component of the reaction is also well tolerated (with R^2, R^3 = alkyl, cycloalkyl, aryl, benzyl, *O*-alkyl, CO_2-alkyl, and R^4 = alkyl, aryl, *O*-alkyl, NH_2, and NR_2).

The value of this established chemistry remains apparent and relevant, as new variations and mechanistic studies involving these classical methods are appearing in the current literature, with a large proportion of the research involving advancements in Fischer indolization. Recent variations have focused on development of reagents which circumvent the use of arylhydrazines. Moody reported an efficient two-step synthetic method involving metal-halogen exchange of

haloarenes followed by quenching with di-*tert*-butylazodicarboxylates and reaction with aldehydes or ketones under acidic conditions to furnish 2,3-disubstituted indoles.[282] Successful use of *N*-arylhydrazones[283] and benzyne[284] in place of arylhydrazines has also been described. Recent applications of Fischer indole synthesis in the realm of natural products chemistry are evident. For example, Garg reported an interrupted Fischer indole synthesis in the preparation of the tetracyclic indoline core found in communesins and perophoramidine,[285] (±)-aspidophylline A,[286] and (+)-phenserine.[287] Smith and co-workers also recently employed a Fischer indolization in the first total synthesis of (+)-scholarisine A.[288]

The Bartoli and Nenitzescu indole syntheses have also appeared recently in the preparation of specifically substituted indoles (Scheme 3.5). New methodology for the preparation of 4,7-disubstituted or 3,4,7-trisubstituted indoles was developed (Scheme 3.5a),[289] using a key Bartoli reaction, while the Nenitzescu reaction has been used as a key step in the preparation of 2-methyl-4-(trifluoromethyl)-1H-indole-5-carbonitrile **3.46** (Scheme 3.5b).[290]

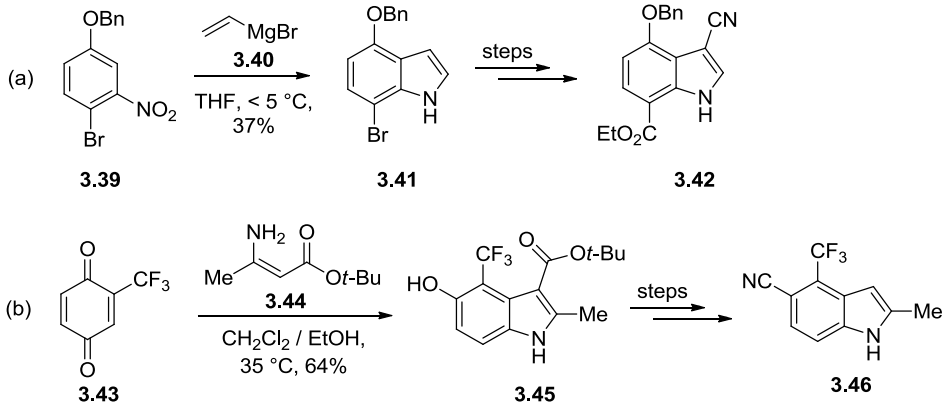

Scheme 3.5. Applications of Bartoli and Nenitzescu indole synthesis in the preparation of densely functionalized indoles **3.42** and **3.46**[289,290]

3.2.2 Synthesis of indoles via Pd-catalyzed reactions

Palladium catalyzed synthesis of indoles is a well developed science, and has been the subject of comprehensive reviews.[291,292,293] These types of reactions are categorized either as pyrrole ring heteroannulation reactions onto benzenoid scaffolds, for which a comprehensive retrosynthetic analysis of alkene and alkyne-based heteroannulation methods is available,[291b] or reactions which functionalize preformed indole rings. This section highlights advances in indole

synthesis achieved through transition-metal catalyzed heteroannulations and C-H bond activation chemistry, whereas Section 3.2.3 addresses current methodologies used for indole functionalization.

Perhaps one of the most extensively studied Pd-catalyzed indole forming reactions is the Larock indole synthesis (first described in 1991),[294] which involves the intermolecular Pd-catalyzed heteroannulation of *o*-haloanilines **3.47** with internal alkynes **3.48** (in which R^S and R^L correspond to small and large alkyne substituents, respectively), affording 2,3-disubstituted indoles **3.49** (Scheme 3.6). In general, the C-2 and C-3 positions of **3.49** are substituted with R^L and R^S, respectively, although regiocontrol is less straightforward when unsymmetrical alkyne **3.48** bears similarly sized substituents.

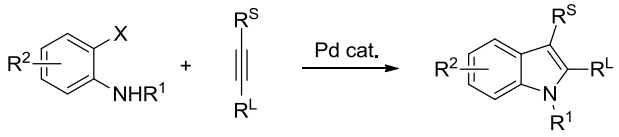

3.47 **3.48** **3.49**

X = I, Br, Cl

Scheme 3.6. Larock indole synthesis: heteroannulation of *o*-haloanilines with internal alkynes[294]

Intramolecular versions of the Larock indole synthesis give rise to regioselectively substituted indoles, and this strategy was employed by Boger and co-workers in the preparation of key intermediate **3.51** from **3.50** (Scheme 3.7), required for the total synthesis of complestatin.[295] Notably, this macrocyclization proceeded in high atropodiastereoselectivity and excellent yield.

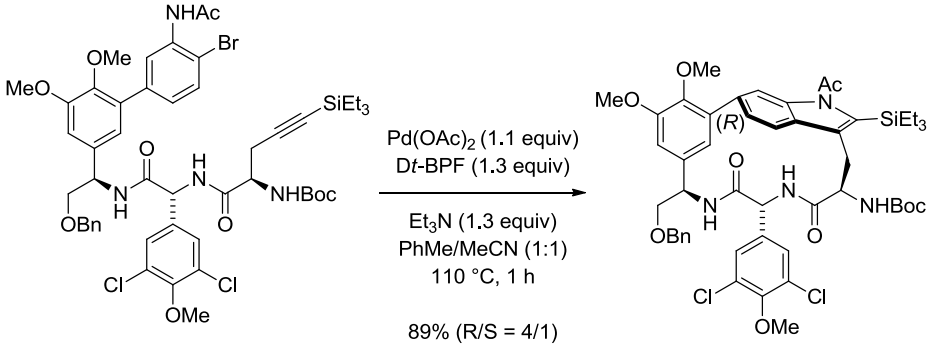

3.50 **3.51**

Scheme 3.7. Boger's use of an intramolecular Larock indole heteroannulation to prepare **3.51**[295]

Recent attention to *o*-alkynylhaloarenes or *o*-dihaloarenes as substrates for the synthesis of indoles[291] is due in large part to the development of efficient transition-metal catalyzed C-N bond forming reactions using Buchwald-Hartwig or Ullman-Goldberg type couplings.

Incorporation of C-H activation strategies into the repertoire of indole synthesis methodologies comprises an active and rapidly advancing area of modern organic synthesis. In 2012, Zhu and co-workers described a new Pd-catalyzed process incorporating isocyanide insertion and C-H activation chemistry[296] which resulted in the preparation of indole-3-carboxamides. Successful application of Zhu's finding to the synthesis of 2-substituted indole-3-carboxamides **3.54** was reported[297] (Scheme 3.8a), and involved Pd-catalyzed intramolecular cyclization of *o*-alkynyltrifluoroacetamide **3.52** and subsequent isocyanide insertion into the intermediate 3-indolylpalladium complex. Recently, Takemoto and co-workers reported a Pd-catalyzed cascade process involving isocyanide insertion and benzylic C-H activation (Scheme 3.8b).[298] This chemistry represents the first example of Pd-catalyzed heterocycle synthesis involving sequential isocyanide insertion and C(sp^3)-H activation processes, although Pd-catalyzed heterocycle synthesis through isocyanide insertion and C(sp^2)-H activation had been previously established.[299] Furthermore, a double insertion / benzylic C(sp^3)-H activation process has been described by Takemoto and co-workers, allowing efficient construction of tetracyclic carbazoles.[298]

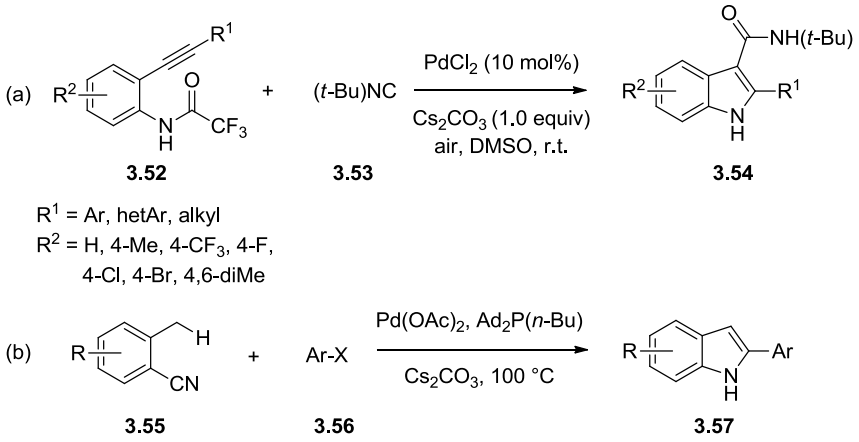

Scheme 3.8. Pd-catalyzed processes in indole synthesis[298,299]

Recently, Glorius and co-workers disclosed an efficient method for the synthesis of indoles **3.59** involving an intramolecular oxidative cyclization of *N*-aryl enamines **3.58** (Scheme 3.9a),[300] which were readily prepared from reactions of anilines with β-dicarbonyl compounds. This theme was further applied to the synthesis of indoles **3.61** involving oxidative cyclization of *N*-aryl imines **3.60** (Scheme 3.9b).[301] Interestingly, this chemistry was a serendipitous discovery, as the initial intention was to achieve imine-directed cyclopalladation (in order to oxidatively functionalize the *ortho* C-H bond of the phenyl ring). Fundamental mechanistic questions remain due to experimental results which show that Glorius' catalytic system is ineffective in achieving the transformation shown in Scheme 3.9b, as well as the uncertain role of the tetraalkylammonium salt.

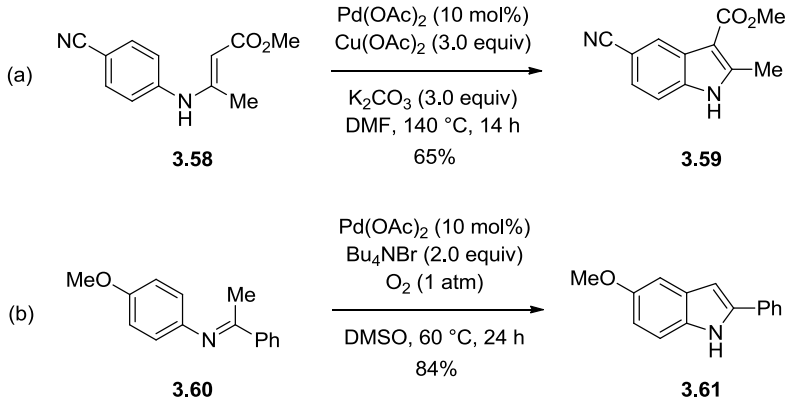

Scheme 3.9. Indole synthesis using intramolecular oxidative cyclization of a) of *N*-aryl enamines and b) of *N*-aryl imines[300,301]

In an alternative approach, Hartwig has developed synthesis of indoles **3.66** from β-aryl oxime ester derivatives **3.62**,[302] involving C-N bond formation via intramolecular amination of an aryl C-H bond (Scheme 3.10).

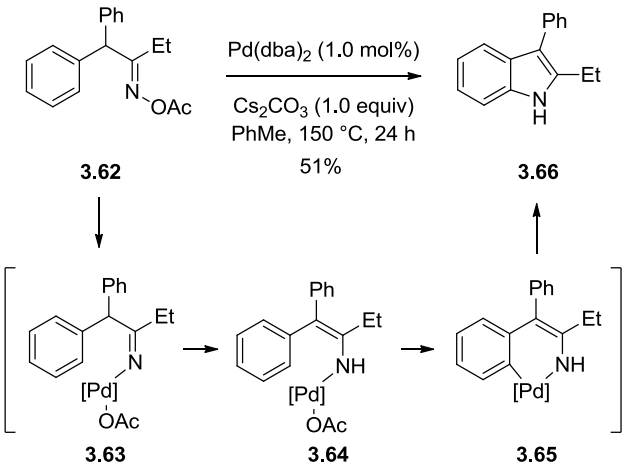

Scheme 3.10. Indole synthesis via intramolecular C-H amination of β-aryl oxime ester **3.62**[302]

In addition to Pd, other metals have also found recent application in C-H activation chemistry as it pertains to the synthesis of indoles (and other heterocycles). Ackermann used cationic Ru(II) complexes in the synthesis of 2,3-disubstituted indoles (Scheme 3.11),[303] similar to the Larock indole synthesis but obviating the need for *ortho* pre-functionalization of the starting aniline. Important aspects regarding scope, chemoselectivity, solvent, cost economics, and mechanism were part of this study.[304]

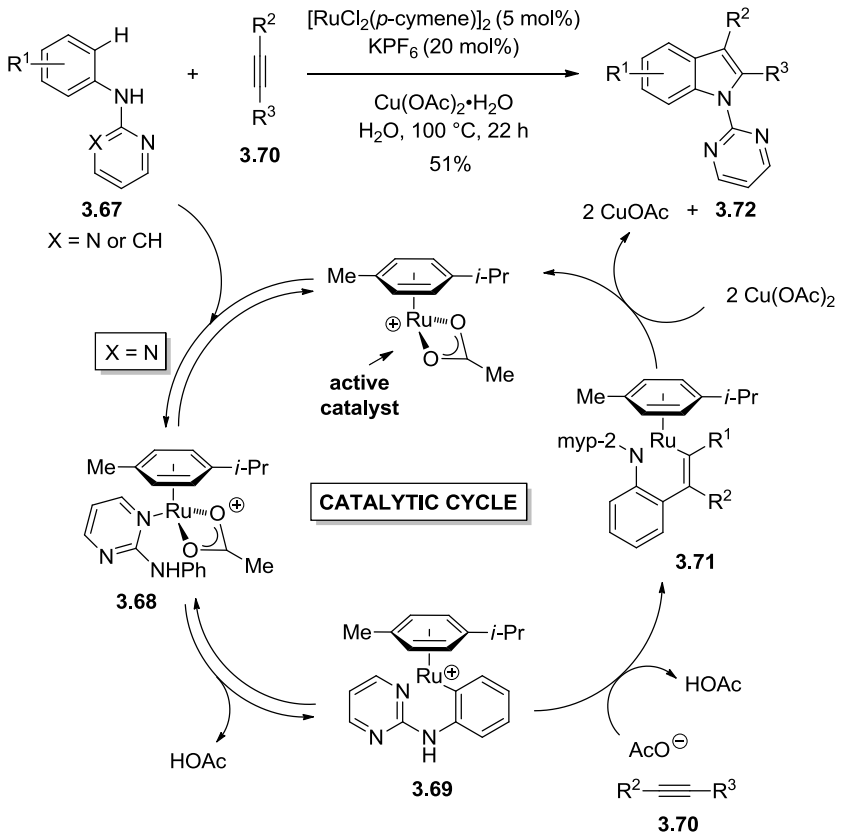

Scheme 3.11. Indole synthesis via aniline C-H activation[303]

The late Keith Fagnou addressed the complications of regioselectivity associated with the preparation of unsymmetrical 2,3-aliphatic substituted indoles (as mentioned previously in context of the Larock indole synthesis) by using a vinyl group as a regiocontrol element in Rh-catalyzed heteroannulations of anilides (Scheme 3.12),[305] an area of chemistry in which the Fagnou group has made significant contributions.[306] Use of a vinyl group in this manner was precedented by regioselective heteroannulations of anilides with alkynes bearing an sp^2 hybridized substituent (eg. aryl) that was installed at the indole C-2 position.[307]

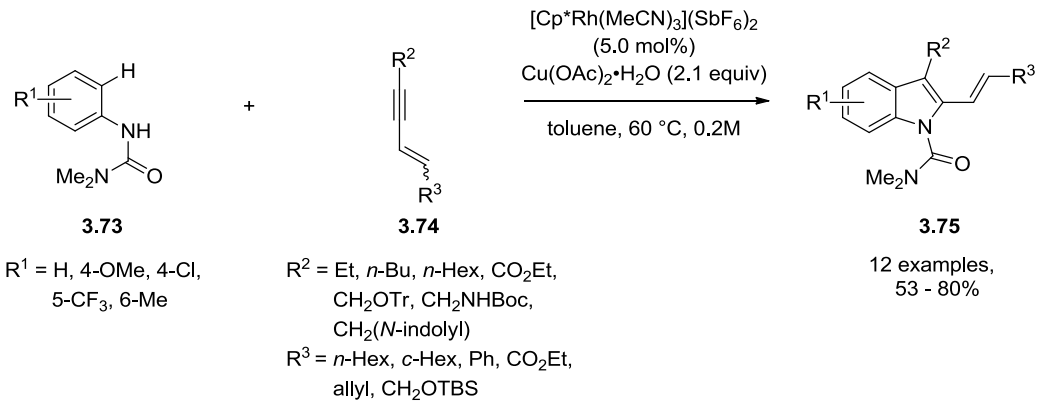

Scheme 3.12. Fagnou's regioselective synthesis of C-2 substituted indoles via Rh(III) catalyzed heteroannulation[305]

In addition to the metal-catalyzed heteroannulation routes described above, a plethora of methods exist based on functionalization of indoles, including metalation chemistry,[308] oxidative coupling reactions, transition-metal catalyzed direct arylation chemistry and C-H activation strategies.[309] These topics are elaborated further in Sections 3.2.3 and 3.3.

3.2.3 Functionalization of indole

3.2.3.1 Electrophilic aromatic substitution (S_EAr)

The rich S_EAr chemistry of the indole heteroaromatic framework has been recently reviewed,[310] and the following discussion will be limited to a few recent examples involving the use of indole S_EAr chemistry as it pertains to C-3 indole functionalization.

A new procedure for the regioselective C-3 trifluoromethanesulfanylation of indoles **3.76** has recently been described,[311] and gives rise to products of type **3.78** (Scheme 3.13). The method uses trifluoromethanesulfanyl amide **3.77** as a surrogate of CF_3S^+, generated *in situ* by acidic activation. In an interesting new methodology, Si-H bond activation is paired with regioselective indole silylation at the C-3 position, catalyzed by a cationic ruthenium(II) complex.[312] Two key intermediates in the catalytic cycle (**3.80** and **3.81**) are shown in Scheme 3.14, which results in

formation of products of type **3.82**. As shown in intermediate **3.80**, the Si-H bond is heterolytically split by the Ru-S bond of the coordinately unsaturated cationic Ru(II) complex, forming a sulfur-stabilized silicon electrophile.

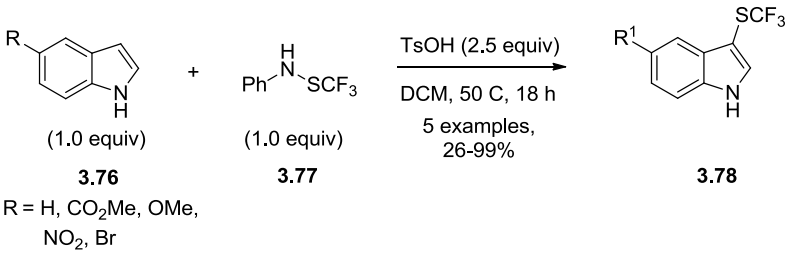

Scheme 3.13. C-3 introduction of SCF_3 group into indoles using S_EAr chemistry[311]

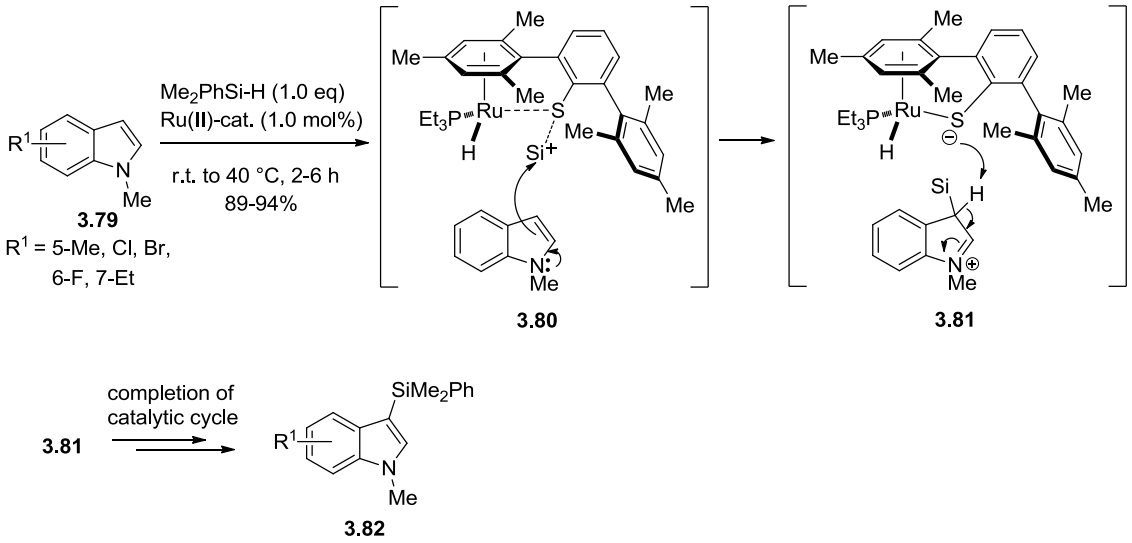

Scheme 3.14. Indole C-3 functionalization via a paired Si-H bond activation / electrophilic silylation strategy in the presence of a cationic Ru(II) complex[312]

3.2.3.2 Functionalization of indoles using oxidative coupling chemistry

Indole functionalization using oxidative coupling chemistry, as well as metal-catalyzed methods have been extensively reviewed.[291-293] Consequently, the following discussion is limited to recent developments which have culminated in the currently established chemistry, and is not intended to be a comprehensive review.

The first example of C-2 arylation of indole using an oxidative coupling approach was reported by Itahara in 1981,[313] and despite the harsh reaction conditions (substoichiometric quantities of $Pd(OAc)_2$ in refluxing HOAc), the value of this chemistry was recognized, and was followed by the development of regioselective, catalytic variants. In 2007, Fagnou reported a very significant result (Scheme 3.15):[314] the catalytic, regioselective arene oxidative C-3 arylation of *N*-acetylindoles **3.83** to **3.85** using $Pd(TFA)_2$ with $Cu(OAc)_2$ as terminal co-oxidant and additives 3-nitropyridine and cesium pivalate. Regioselective C-2 arylation of *N*-pivalyl protected indole **3.84** to **3.86** was achieved by tuning the reaction conditions (Scheme 3.15).[315] Pd-catalyzed direct arylation of a diverse array of heterocycles (e.g. thiophene, pyrrole, indolizine, imidazole, benzothiophene, benzofuran, and thiazole) with aryl bromides was subsequently developed by the Fagnou group,[316] highlighting the broad synthetic utility and application of Pd-catalyzed arylation in heterocycle functionalization. Although De Boef also encountered oxidant controlled regioselectivity in the directed arylation of *N*-acetyl indoles,[317] limited substrate scope,[318] modest yields, and requirement of high catalyst loadings were significant drawbacks of the methodology.

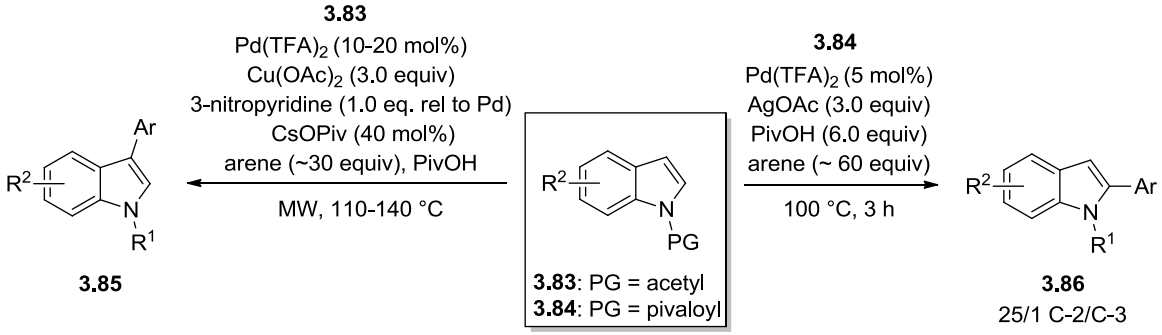

Scheme 3.15. Oxidative regioselective coupling route to C-2 or C-3 arylated indoles[314,315]

Despite the methods available for direct arylation of indoles, harsh reaction conditions or lack of control over C-2/C-3 regioselectivity have posed a problem for oxidative coupling reactions involving challenging substrates. De Boef overcame the propensity for decomposition of electron-rich *N*-alkyl indoles under typical oxidative coupling conditions, and established regioselective C-2 arylation of sensitive indole substrates in buffered media (Scheme 3.16).[319]

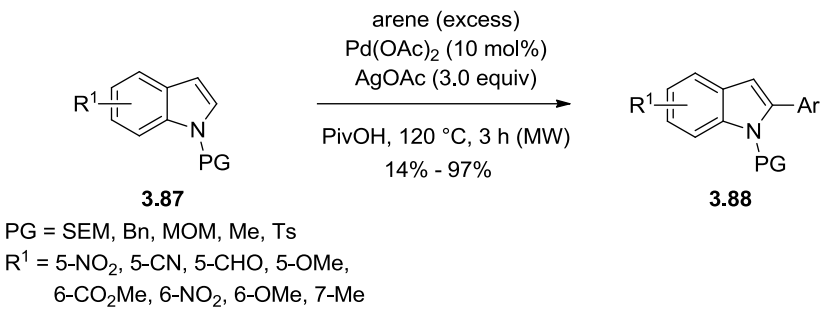

Scheme 3.16. C-2 arylation of *N*-alkyl indoles by oxidative coupling[319]

3.2.3.3 Transition-metal catalyzed, regioselective C-2 and C-3 arylation of indoles

In addition to oxidative coupling chemistry, regioselective C-2 and C-3 arylation of indoles has been achieved using Pd, Rh, and Cu-catalyzed procedures, and developed from the seminal work of Ohta in the 1980's which established an initial set of conditions for Pd-catalyzed regioselective C-2 or C-3 arylation of *N*-H or *N*-substituted indoles with aryl or heteroaryl halides.[320,321]

Extensive research efforts have focused on the development of Pd-catalyst/ligand systems, typically incorporating phosphines and/or NHCs, in order to improve Pd-catalyzed direct C-2 arylations. Notably, Sames described the use of Pd(OAc)/PPh_3 and Pd/NHC complexes with phosphines for the regioselective catalytic arylation of *N*-Me indoles[322] and *N*-SEM indoles,[323] respectively, with aryl iodides, and extended the latter methodology to direct arylation of other heterocycles. Bhanage circumvented the necessity of phosphine ligands in C-2 arylation of *N*-methyl indoles by using the air-stable catalyst $Pd(TMHD)_2$.[324] More recently, Daugulis employed a biarylmonophosphine ligand in the Pd-catalyzed direct arylation of indoles, pyrroles and furans using aryl chlorides.[325] In comparison with the use of phosphines as ligands in Pd-catalyzed C-H activation chemistry, use of bidentate nitrogen ligands is considerably less common, although recent work by Shibahari[326] and Itami[327] have demonstrated the use of 1,10-phen and 2,2'-bipy as ligands for Pd in direct C-2 arylation of a diverse series of heterocycles.

Similarly, a variety of catalyst/ligand combinations have been developed in order to achieve improvements in direct C-3 arylation chemistry of indoles. The first report of the direct Pd-catalyzed C-3 arylation of free *N*-H indoles with ArBr in 2007 employed the air-stable Pd /

phosphinous acid complex $[(t\text{-Bu})_2P(OH)]_2PdCl_2$,[328] and, with the exception of electron-deficient indoles, afforded arylated products in respectable yields. A similar trend in indole reactivity was apparent in the subsequent investigation of ligandless, Pd-catalyzed C-3 arylation of *N*-H indoles by Bellina and co-workers.[329] More recently, Djakovitch and co-workers described a versatile catalyst system [$Pd(OAc)_2$/dppm] that can be tuned to give site-selective C-H functionalization of indoles at the C-2 or C-3 positions in water as solvent,[330] without the requirement of protecting or directing groups (Scheme 3.17). Intriguingly, the regioselectivity is determined by specific base/ArX combinations, and mechanistic studies are reportedly in progress.

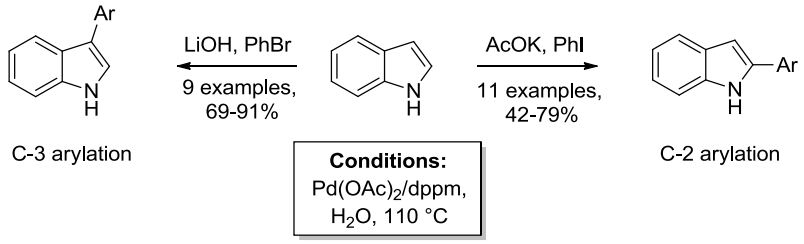

Scheme 3.17. Protecting group free, site-selective indole arylation in water[330]

Use of aryliodonium salts **3.90** in direct arylation chemistry has become an immensely popular field of research, owing to Sanford's initial description of the effectiveness of **3.90** in mild regioselective C-2 indole arylation of indoles **3.89** + **3.90** → **3.91** (Scheme 3.18a), through a proposed Pd(II)/Pd(IV) catalytic cycle.[331]

Although the reaction proceeded using catalytic $Pd(OAc)_2$, superior yields were obtained using $IMesPd(OAc)_2$. Subsequently, Ackermann demonstrated a reversal in selectivity favouring C-3 arylation **3.92** + **3.93** → **3.94** (Scheme 3.18b) using diaryliodinium salts in the absence of a transition metal catalyst,[332] and both synthetic methods have recently been applied to the direct arylation of pyrroles.[333,334] Notably, free *N*-H or *N*-alkylated indoles appear to exhibit comparable reactivity in these types of transformations, the I^{III} arylating reagents can be prepared *in situ* from simple precursors, and significant substrate scope in terms of both the indole and diaryliodonium reagents is evident. Cu-catalyzed direct arylation of indoles using symmetrical and unsymmetrical diaryliodonium salts has also recently been established by Gaunt,[335] in which C-2 vs. C-3 site selectivity could be achieved by judicious choice of indole protecting group (*N*-H or *N*-Ac), and control of the reaction temperature.

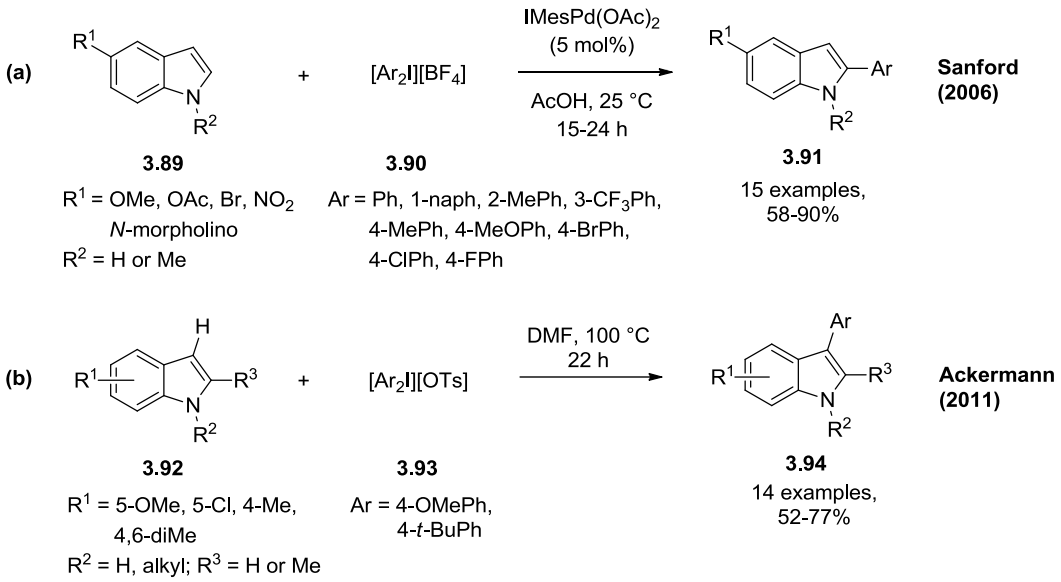

Scheme 3.18. Diaryliodonium salts for the direct arylation of indoles[331,332]

In recent adventures into Pd-catalyzed direct arylation of indoles, the Fagnou group recently described use of a C-Cl bond as a handle for enhancing reactivity and influencing site selectivity in challenging substrate combinations, as demonstrated for *N*-alkyl indoles **3.95** and **3.96** (Scheme 3.19).[336] In addition to indoles, the methodology was also applied to the regioselective functionalization of thiophenes, thiazoles, benzofurans, pyrroles and imidazoles, and detailed mechanistic and computational studies revealed the involvement of a concerted metalation-deprotonation (CMD) pathway.[337]

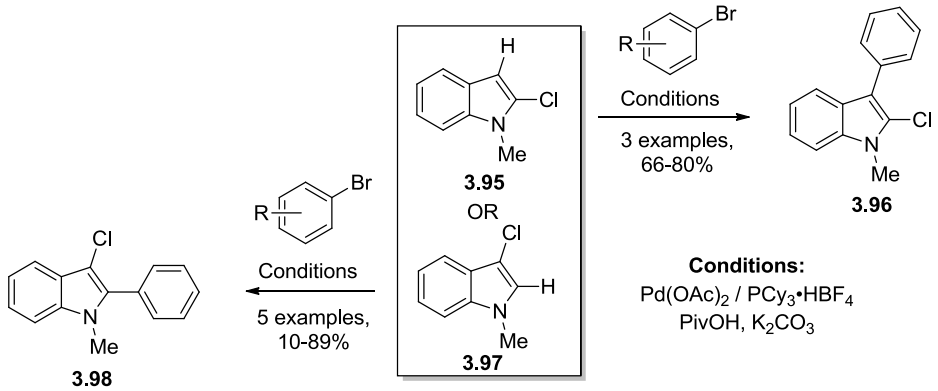

Scheme 3.19. Regioselective C-2 and C-3 arylation of chloroindoles **3.95** and **3.96**[336]

In contrast to its Pd-catalyzed counterparts, application of Rh metal in direct indole C-2 and C-3 arylation chemistry has received less attention. In 2005, Sames described the first Rh-catalyzed procedure allowing direct C-2 arylation of indoles and pyrroles,[338] involving *in situ* generation of the active catalyst, $ArRh(OPiv)_2(L_2)$, where L corresponds to $P[p\text{-}CF_3C_6H_4]_3$. The reaction was optimal when electron-rich indoles or pyrroles were reacted with electron-deficient ArI, and high regioselectivities (> 50:1) were reported. Subsequently, the Itami group devised a readily prepared, air and moisture stable catalyst system $L_2Rh(CO)Cl$ (L = $P[OCH(CF_3)_2]_3$) that effectively catalyzed the C-H arylation of nucleophilic arenes with ArI in the presence of stoichiometric Ag_2CO_3.[339] The same electronic effects of the substrates were observed as reported by Sames, although the regioselectivity was observed to follow that of S_EAr.

As evident from the discussion of direct arylation of indoles, the most reactive positions towards C-H activation are, unsurprisingly, C-2 and C-3. However, C-H activation at C-2 and C-7 of the 1-isoquinolyl indole **3.99** via directed oxidative Heck chemistry to give sequentially **3.100** and **3.101** (Scheme 3.20), has been described.[340] The 1-isoquinolyl group was crucial to the success of this reaction, as use of other directing groups (2-pyridylmethyl, methylquinoline or phenanthridine) afforded poor to moderate yields of the 2-alkenylated product and small amounts of bis-alkenylated product.

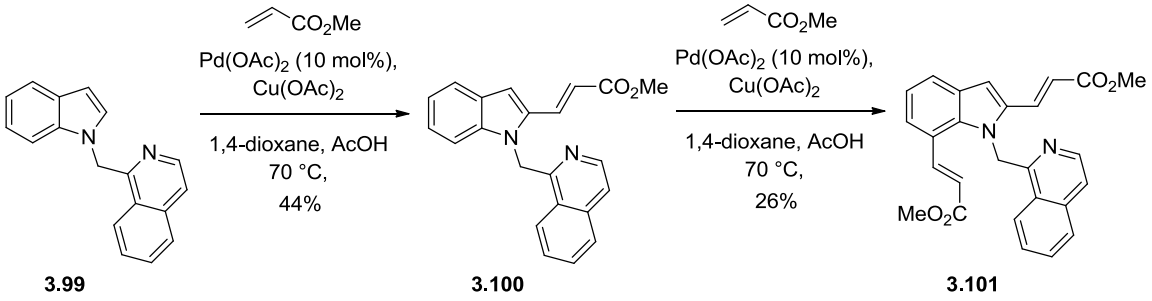

Scheme 3.20. Sequential C-2 and C-7 indole alkenylation via oxidative Heck coupling[340]

The functionalization of molecules using C-H activation is a very significant and continuously developing branch of chemistry, driven by the advantages associated with atom economy, convenience, and environmental considerations. Furthermore, the reactions proceed

under milder conditions than those used in traditional substitution chemistry. The most reactive positions of indole towards C-H activation (N1, C2 and C3) have traditionally relinquished the task of benzenoid ring functionalization to classical S_EAr reactions. Development of benzenoid ring substitution by C-H activation methods would be welcome.

3.3 Metalation of DMG-Bearing Indole Systems

3.3.1 Historical Development

The widespread occurrence of indole in biology (tryptophan, melatonin, serotonin), drug molecules,[341] natural products (e.g. rebeccamycin and ellipticine) and complex synthetic targets has resulted in the development of a rich field of indole metalation chemistry. As a testament to the deep and fascinating history of this chemistry, Gilman had described the first selective lithiation of the indole-containing ring systems carbazole and *N*-ethyl carbazole at the C-4 position by 1936,[342] several years before the independent discoveries of the directed *ortho*-deprotonation of anisole by Wittig[222] and Gilman.[223] The initial example of Gilman, combined with the impact of the directed *ortho* metalation reaction, led to significant advancements in the selective metalation of indoles throughout the following decades, and continues to remain an active area of research in present times. In 1953, Shirley and Roussell demonstrated that *N*-methylindole is selectively C-2 deprotonated by *n*-butyllithium.[343] The inability to *N*-demethylate has been a recognized limitation of this chemistry. Consequently, the development of removable *N*-protecting groups also capable of directing C-2 deprotonation was of fundamental importance for enhancing the synthetic utility of this reaction. In 1973, Sundberg described the C-2 selective metalation of indole using the *N*-benzenesulfonyl group as a DMG,[344] and found that it could be readily removed under mild basic conditions. In 1981 Fowler and Levy used the acid-labile *N*-Boc group in order to achieve the same result,[345] although use of this DMG has not been investigated as systematically as its *N*-SO_2Ph counterpart. Katritzky developed a metalation strategy which obliviated the need for prior *N*-functionalization, and demonstrated that efficient C-2 deprotonation could be achieved through the use of the *N*-carboxylate as a transient *N*-protecting / directing group.[346] Gribble reported the first example of C-3 indole metal-halogen exchange in 1982,[347] and Rapaport subsequently described the use of this reaction for the

benzenoid ring functionalization of bromoindoles.[348] This marked the beginning of a period of time where functionalization of the indole benzenoid ring using metalation tactics became increasingly prominent. In 1993, Iwao demonstrated the first example of C4-selective lithiation of *N*-TIPS gramine upon treatment with *t*-BuLi.[349] About the same time, Snieckus reported a method for the regioselective lithiation of *N*-TBS indole-5-*O*-carbamate at the 4- and 6-positions.[350] Snieckus also developed powerful strategies to achieve regioselective indole C-7 functionalization, which could be accomplished through the use of the di-(*tert*-butyl)phosphine oxide DMG,[351] or by metalation of *N*-carbamoyl-2-TMS indoles (silicon protection strategy).[351] Iwao demonstrated that CIPE theory (Scheme 3.2) could be used to explain the ability of *N*-DEB (DEB = 2,2-diethylbutanoyl) protected indoles to undergo C-7 metalation (although the C-2/C-7 selectivity was an issue).[352] The historical timeline summarizing achievement of these milestones is shown in Figure 3.4 (page 203).

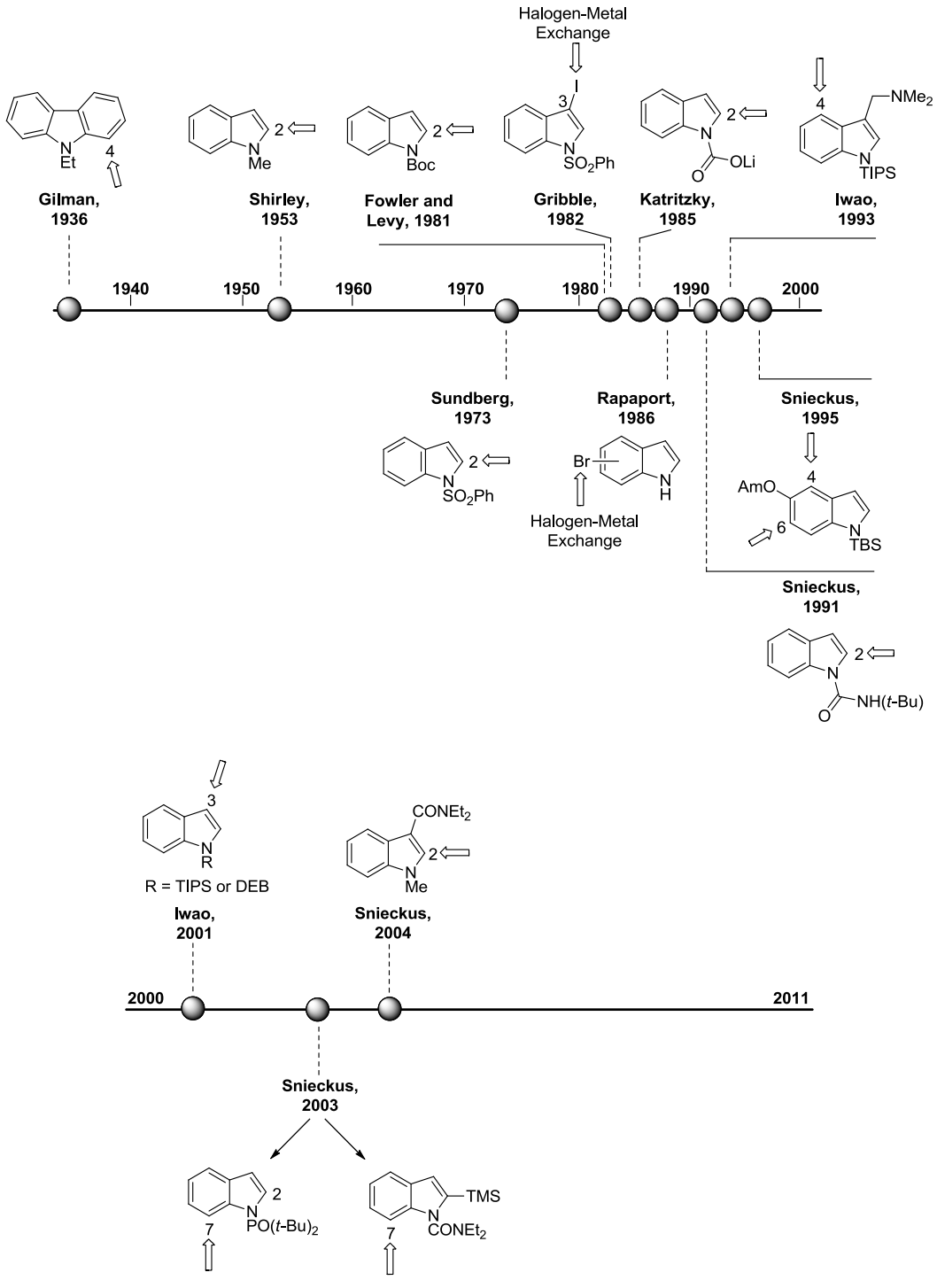

Figure 3.4. Historical Development of Indole Metalation Chemistry

3.3.2 Metalation Tactics Specific for Benzenoid Ring Functionalization

Selective lithiation of *N*-DMG (or *N*-substituted) bearing indoles can lead to selective deprotonation at positions C-2, C-3 or C-7. However, most substitution patterns give rise to C-2 selective metalation, as demonstrated by the plethora of *N*-DMG examples shown in Figure 3.4. An illustrative example involves the use of the *N*-*tert*-butylcarbamoyl DMG CON(*t*-Bu)Li (Scheme 3.21),[353] which achieves C-2 selective deprotonation of **3.102** and subsequent electrophile introduction to form **3.103** which, upon treatment with LiOH, affords **3.104**. Introduction of E = $CONMe_2$, $CONEt_2$, COPh or CO_2H results in spontaneous decarbamoylation, most likely due to anchimeric assistance.

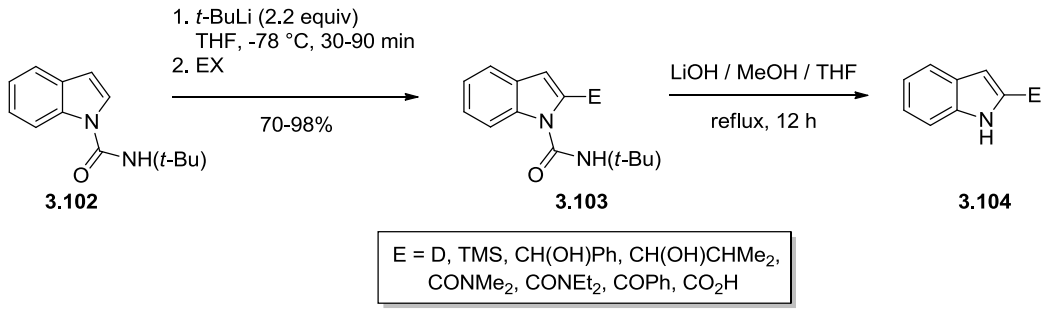

Scheme 3.21. Regioselective indole C-2 metalation with *N*-*tert*-butylcarbamoyl as DMG[353]

Several strategies have been developed in order to achieve regioselective metalation of indoles at the C-7 position which involve either the use of specific DMGs, or masking the reactivity of the C-2 hydrogen prior to the metalation event. Iwao demonstrated the effectiveness of the DEB group (2,2-diethylbutanoyl) in achieving selective lithiation at C-7 of indole, without requiring functionalization of the 2-position prior to metalation (Scheme 3.22).[352]

In the conformational equilibrium due to amide bond restricted rotation, two extreme conformers, *(E)*-**3.105** and *(Z)*-**3.106**, are accessible to the *N*-DEB substituted indole. The repulsive interaction with the *peri*-hydrogen in the (*E*)-conformer shifts the equilibrium towards the (*Z*)-conformer. Regioselective kinetic deprotonation at C-7 is expected as long as the

orientation of the carbonyl group is maintained during the transition state **3.109** of the deprotonation (CIPE).

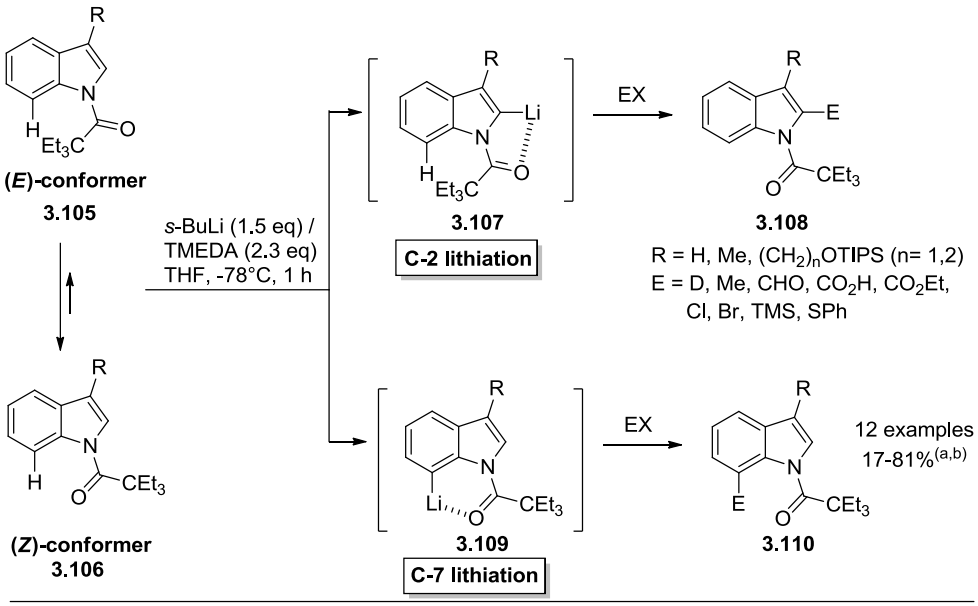

(a) In the case when R = H and E = D, the isolated yield of 81% corresponds to 2 products with 52% D-incorp. at C-7 and 49% D-incorp. at C-2; (b) in most reactions with 3-substituted indoles, the product from C-2 lithiation is isolated in low amounts (6-13%)

Scheme 3.22. Regioselective kinetic and thermodynamic lithiation of *N*-DEB indoles **3.105** and **3.106**[352]

Results of metalation and quench with a variety of electrophiles demonstrated the effectiveness of this methodology in the regioselective preparation of 3,7-disubstituted indoles not easily accessible by conventional methods. An additional advantage is the ease of removal of the DEB group upon treatment with *t*-BuOK in aqueous MeOH.

Indole C-7 D*o*M chemistry was further developed by Snieckus with the introduction of the *N*-di-*tert*-butylphosphinoyl group into the arsenal of DMGs. The use of phosphorous-based DMGs in carbanionic synthetic chemistry lacks development in comparison with commonly used carbon-based DMGs (amides, tertiary aryl-*O*-carbamates, and oxazolines) and heteroatom-based DMGs (OMOM, NHBoc, sulfones, sulfonamides). Initial studies on the $P(O)(R)_2$ DMG focused on ferrocene-D*o*M reactions using diarylphosphine oxide as DMG, and although the results

demonstrated the potential for effective metalation,[354] limitations of poor solubility of the metalation substrate, low yields, and formation of interfering by-products from aryl deprotonation of the DMG were encountered. The di-*tert*-butyl phosphine oxide was considered a potential alternative for the following reasons: a) the bulky alkyl groups would increase the solubility, particularly in hydrocarbon solvents, b) the lack of aromatic hydrogens would eliminate side-product formation, and c) steric shielding of the phosphorous would hinder reaction with nucleophilic bases. Synthesis and the optimized metalation conditions for the ferrocenyl phosphinyl derivative **3.112,** prepared from the corresponding stanylated ferrocene **3.111** are shown in Scheme 3.23.[354] The best results were obtained when *t*-BuLi was used as the base and, in the case of TMSCl quench, led to product **3.113** in high yield.

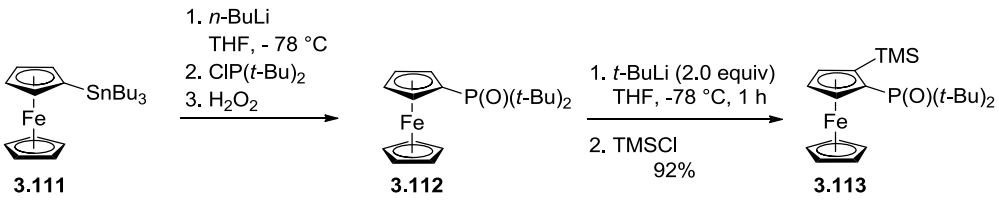

Scheme 3.23. Synthesis and D*o*M reaction of di-(*tert*-butyl)phosphinoferrocene **3.130**[354]

Following promising preliminary studies of the di-*tert*-butyl phosphinyl DMG in D*o*M reactions in the benzene series,[355] which included X-ray crystallography and MM2 calculations, it was a logical progression to test the potential of this DMG in indole metalation chemistry in the Snieckus laboratories, using indole **3.114** as the starting material (Scheme 3.24).[351] The results of systematic studies[354] using TMSCl as the electrophile led to the establishment of the following optimized conditions: use of *n*-BuLi at -40˚C for 2 h gave products **3.115:3.116** in > 99:1 ratio while using LDA at 0 ˚C for 15 min led to complete reversal of regioselectivity to give **3.115:3.116** in > 1:99 ratio.

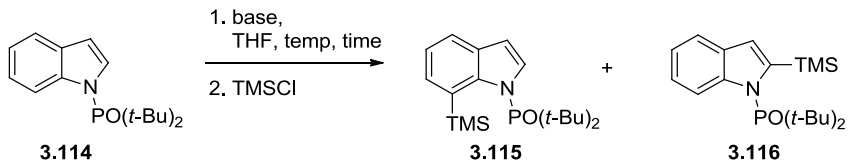

Scheme 3.24. D*o*M reaction of *N*-di-*tert*-butylphosphinoyl indole **3.114**[354]

Although this finding was exploited in the regioselective synthesis of a variety of C-7 functionalized indoles,[351] the harsh conditions for cleavage of the di-(*tert*-butylphosphinoyl) DMG to achieve a useful route to such difficultly accessed systems prompted the consideration of alternative *N*-DMG indoles for this purpose.

In accordance with this objective, Snieckus and co-workers developed a regioselective C-7 indole functionalization method using a D*o*M - latent silicon protection strategy (Scheme 3.25).[351] Thus metalation – silylation of *N*-$CONEt_2$ indole provided **3.117** which upon a second D*o*M reaction using 2.5 equiv of *s*-BuLi/TMEDA followed by electrophile quench led to products **3.118**. This proved to be a general strategy for the convenient synthesis of 7–substituted indoles which heretofore had not been achieved, and allowed further D*o*M and cross coupling chemistry. This chemistry is most relevant to the thesis work (see Results and Discussion).

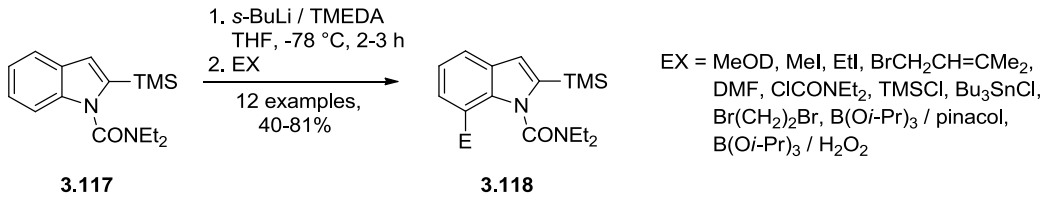

3.117 **3.118**

Scheme 3.25. Silicon protection strategy for the regioselective synthesis of C-7 functionalized indoles **3.118**[351]

In another study, Snieckus developed a combined directed *ortho* metalation (D*o*M)-cross coupling methodology for the regioselective C-4 and C-6 functionalization of indoles using the C-5 aryl-*O*-carbamate DMG.[350] This synthetic strategy was used to achieve the regiospecific construction of 4,5,6-substituted indoles and tryptophols from **3.119** (Scheme 3.26). Thus, metalation of **3.119** using standard conditions (*s*-BuLi/TMEDA) followed by electrophile quench affords 4,5-disubstituted indoles **3.120**. Subsequent lithiation with s-BuLi/TMEDA results in anionic *ortho*-Fries and trapping of the phenoxide with Ac_2O according to transformation **3.120** → **3.121**, whereas metalation at lower temperature (-90 ˚C) suppresses the anionic *ortho*-Fries rearrangement and affords products **3.122** upon electrophile quench. Further synthetic manipulation involves the D*o*M-Negishi XCoupl nexus, in which Li → Zn transmetalation of C-4 deprotonated **3.120** permits cross-coupling with 3-bromopyridine. Also of synthetic utility is the

ease of manipulation of the C-5 aryl-*O*-carbamate DMG, owing to its ability to undergo Ni-catalyzed cross-coupling with RMgX reagents. This methodology offers a convenient alternative to classical S_EAr chemistry, as well as the introduction of substituents prior to indole ring construction.

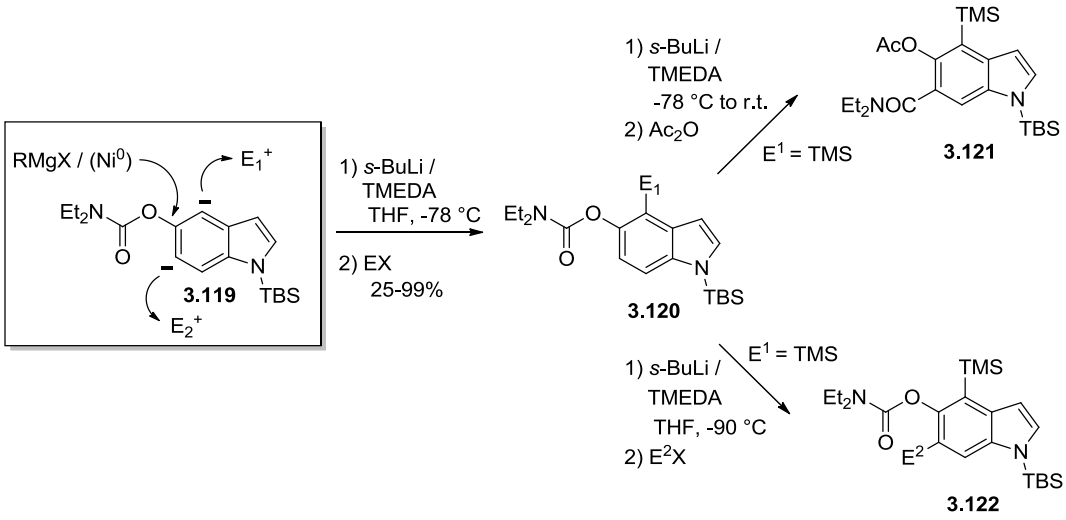

Scheme 3.26. D*o*M chemistry for C-4 and C-6 functionalization of indole 5-aryl-O-carbamate **3.119**[350]

3.4 Aims of Research

The aim of the research described in this thesis was to establish new fundamental directed *ortho* metalation (D*o*M) chemistry pertaining to indole-6-carboxylic acid **3.123**, a compound synthesized in large quantities in the Boehringer-Ingelheim drug discovery program.[356] The synthesis of **3.123** using the Leimgruber-Batcho indole synthesis has been reported.[357]

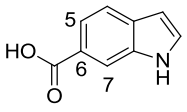

3.123

We envisaged that the powerful *N*,*N*-diethyl amide of **3.123** would be opportunistic for the development of new regioselective functionalization of the C-5 or C-7 positions of indole, establishing D*o*M chemistry of synthetic value. Four possible strategies were initially considered in order to achieve regioselective metalation (Figure 3.5).

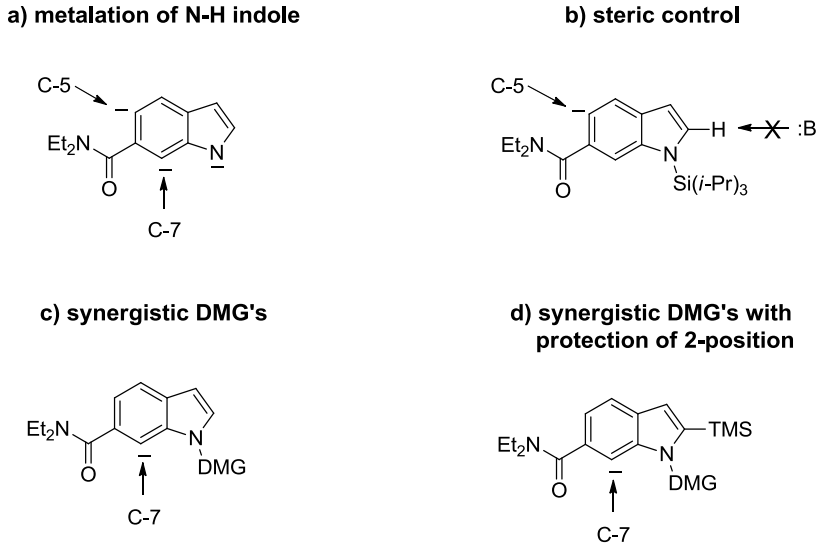

Figure 3.5. Strategies for regioselective C-5 or C-7 D*o*M chemistry of appropriately functionalized indole-6-carboxamide derivatives

Strategy a) corresponds to the most direct route for potentially achieving C-5 and/or C-7 metalation, as it does not require initial introduction of an indole *N*-DMG. Schlosser used a similar strategy in order to achieve regioselective C-7 carboxylation of 6-fluoroindole,[358] in which he relied on *N*-Li neighbouring group participation to outweigh the deactivating electron donation of the *N*-Li centre. The concept of anionic shielding of the reactive C-2 position, as recently demonstrated in the regioselective (*peri*) metalation of appropriately functionalized *N*-H 7-azaindole,[359] is also a relevant consideration in this analysis. Strategy b) is based on the original findings of Sundberg[344] and, subsequently, of Iwao[349] and Snieckus,[350] that bulky *N*-silicon substituents modulate C-2 reactivity by steric shielding. In this scenario, approach of the base towards the C-2 or C-7 protons may be hindered, increasing the likelihood of favourable C-5 deprotonation. Strategy c) invokes the concept of "synergistic DMGs" in metalation

chemistry,[223c] which invariably results in "in-between" metalation at C-7. Finally, Strategy d) involves a combination of synergistic DMGs and C-2 silicon protection strategy, although occurrence of D*o*M chemistry at the indole C-5 position in Strategies c) and d), especially by bulky bases such as LDA or LiTMP, may not be discounted. The specific aim of the research described in this thesis has been to explore the strategies shown in Figure 3.5, and establish a set of metalation conditions which allows regioselective introduction of electrophiles at the C-5 and/or C-7 positions.

Development of the D*o*M chemistry of **3.123** was pursued with the consideration that it could ultimately be used in the synthesis of new regioisomeric polyaromatic pyrrolofluorenones **3.124**-**3.125** and pyrrolophenanthrols **3.126**-**3.127** (Figure 3.6), a largely unknown class of compounds.[360]

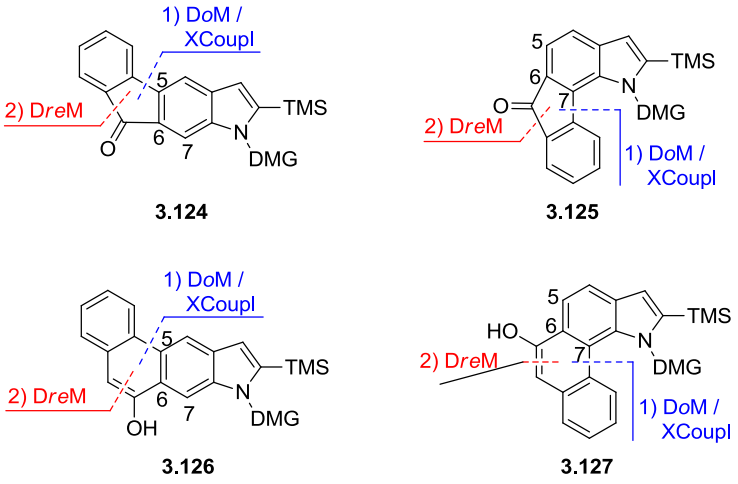

Figure 3.6. Retrosynthetic analysis of regioisomeric pyrrolofluorenones (a) and pyrrolophenanthrols (b) using a D*o*M - Xcoupl - DreM reaction sequence

3.5 Results and Discussion

Initial experiments testing Strategy a) (Figure 3.5a) were based on the previously described results obtained by Schlosser, who demonstrated that metalation of 6-fluoroindole **3.128** led reasonably efficiently to 6-fluoroindole-7-carboxylic acid **3.130**, via the presumed *N*-

lithiated intermediate **3.129** (Scheme 3.27).[358] Although chemistry involving the Lochmann-Schlosser base (*n*-BuLi / KO*t*-Bu) is arguably governed by KIE and not CIPE (see Section 3.1.3), the concept of anionic shielding of the C-2 hydrogen by anion repulsion is relevant. Consequently, selective deprotonation of the the C-7 proton having enhanced kinetic acidity is a reasonable expectation.

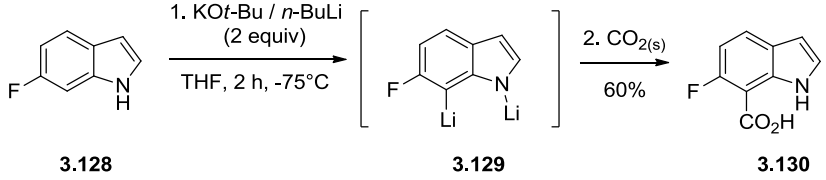

Scheme 3.27. Metalation of 6-fluoroindole **3.128** using Lochmann-Schlosser base[358]

In order to carry out initial metalation studies, *N*,*N*-diethyl indole-6-carboxamide **3.131** was prepared by standard EDC coupling of **3.123** with diethylamine, as shown in Scheme 3.28 (see Experimental Section). Several conditions for metalation were explored, and the results are presented in Table 3.4.

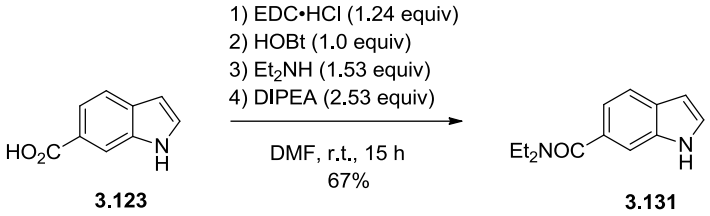

Scheme 3.28. Synthesis of indole metalation substrate **3.131**

Treatment of **3.131** using 2.0 equiv of Lochmann-Schlosser base was first tested (Table 3.3, entry 1), followed by MeOD quench and aqueous work-up, which resulted in isolation of **3.123**, but not products **3.132** or **3.133** arising from deuterium incorporation. However, a minor contaminant was identified in the recovered **3.131**, likely corresponding to the product of nucleophilic attack of *n*-BuLi on the amide DMG. Standard conditions used for *ortho*-metalation of amides (*s*-BuLi/TMEDA, and *s*-BuLi alone) also failed to show, by MeOD quench experiments, C-5 or C-7 deprotonation (entries 2 and 3). Finally, the same negative result was

observed using 2.2 equiv of LDA as the base (entry 4). These results may suggest that the indole *N*-anion of **3.123** is too electron-rich for metalation to occur.

Table 3.3. Metalation of *N*,*N*-diethyl indole-6-carboxamide **3.131**

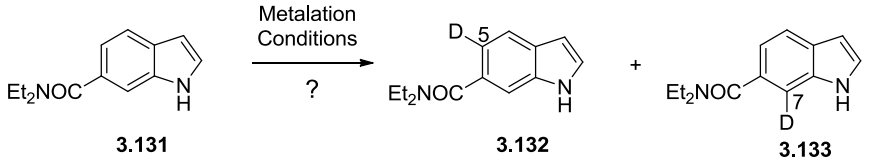

Entry	Base	Time (h)	Temp. (° C)	EX (10 equiv)	Result
1	*n*-BuLi / KOt-Bu (2.0 equiv)	1	-78	MeOD	**3.157** recovery, No d_1 incorporation
2	*s*-BuLi / TMEDA (2.2 equiv)	1	-78	MeOD	- - -(a)
3	*s*-BuLi (2.2 equiv)	1	-78	MeOD	- - -(a)
4	LDA (2.2 equiv)	1	-78	MeOD	- - -(a)

(a) Same result as in Entry 1.

In order to explore whether the electron-richness of the *N*-indole anion of **3.131** plays a significant role in preventing any C-deprotonation, a sterically encumbered *N*-TIPS protecting group was introduced into **3.131** to afford metalation substrate **3.134** (Scheme 3.29). Additionally, this modification invoked a steric effect of the C-2 and C-7 positions, corresponding to strategy b) (Figure 3.5) and therefore the possible expectation that selective C-5 deprotonation may occur.

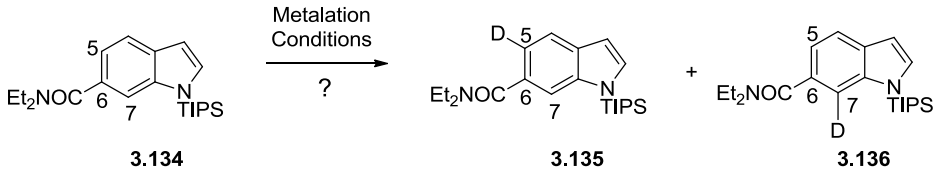

Scheme 3.29. Metalation studies of *N*-TIPS indole-6-carboxamide **3.134**

Based on the previous NMR identification of a minor ketone contaminant arising from the reaction of **3.131** with Lochmann-Schlosser base (Table 3.4, entry 1), and the anticipated reactivity of such an aromatic amide with *n*-BuLi, use of *s*-BuLi/TMEDA was pursued. Analysis of the GC/MS obtained of the crude reaction mixture indicated the formation of several products, which could be traced to the reaction of *s*-BuLi with the amide. Consequently, metalation of **3.134** was attempted using the more sterically hindered LiTMP and resulted in isolation of unreacted starting material. Based on these results, it was decided not to pursue metalation according to Strategy b).

Application of the indole-*N*-(di-*tert*-butylphosphinyl) DMG, previously successful in C-7 metalation (Section 3.3.2, Scheme 3.24) was then pursued, to take advantage of the synergistic effect of two DMGs **3.137** (Scheme 3.30). Compound **3.137** was easily prepared from **3.131** (as described in the Experimental Section).

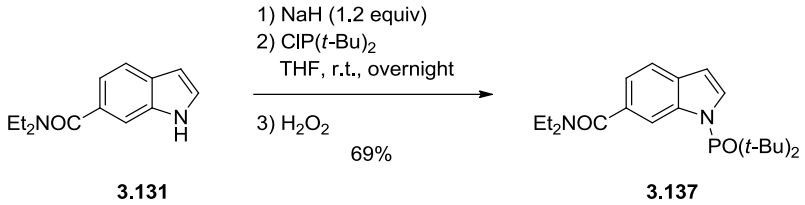

Scheme 3.30. Synthesis of synergistic metalation substrate **3.137**

The conditions optimized for C-7 metalation of **3.114** (*n*-BuLi (2.2 equiv)/THF/-40 ˚C/2 h) were not ideal for **3.137**, as they would likely result in undesired ketone formation (due to reaction of *n*-BuLi with the amide DMG). In fact, metalation of **3.137** with *n*-BuLi at -40 ˚C and -78 ˚C (and subsequent MeOD quench) resulted in nucleophilic attack, as evidenced by ^{1}H and

^{13}C NMR analysis of the crude reaction product. Treatment of **3.137** with the less nucleophilic but also less basic LDA followed by MeOD quench only resulted in insignificant C-2 deprotonation of the C-2 position (approximately 10% d_1-incorporation as determined by ^{1}H-NMR).

In order to pursue synergistic metalation efforts in conjunction with a C-2 silicon protection strategy (Strategy D, Figure 3.5), substrate **3.139** was synthesized (Scheme 3.31). Starting amide **3.131** (Scheme 3.28) was converted into *N*-carbamoyl derivative **3.138** in 77% yield, and metalation-silylation of the latter gave **3.139** in 40-77% yield. An attempt to telescope the sequence of reactions through to **3.139** without intermediate flash column chromatography steps resulted in a decreased yield of **3.139** (40%), accompanied by the formation of two side products **3.140**, resulting from apparent nucleophilic reaction between *t*-BuLi and **3.139**, and **3.141** (Scheme 3.31). Formation of 2,7-bisTMS product **3.141** is a promising result, and leads to several possible scenarios for C-5/C-7 functionalization using DoM chemistry (see Future Work).

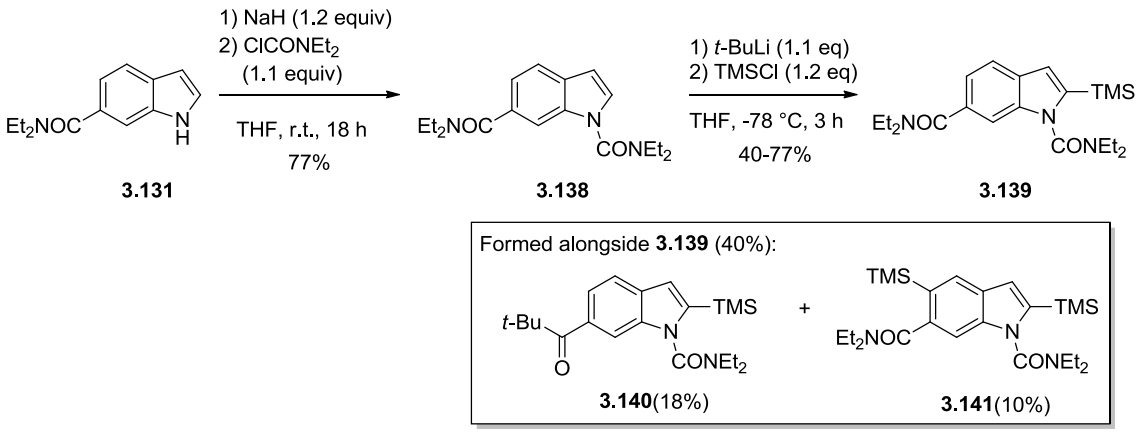

Scheme 3.31. Synthesis of indole metalation substrate **3.139**

In order to explore further DoM chemistry of **3.139**, standard tertiary amide metalation conditions (*s*-BuLi/TMEDA) were initially adopted, and the results are presented in Table 3.4. Unless specified otherwise, the reactions described were performed using "standard-addition," meaning that the base was added to the mixture of starting material and TMEDA.

Use of MeI as electrophile (entry 1) resulted in the isolation of a co-eluted mixture of unreacted starting material **3.139** (12%) and C-5 methylated product **3.142** (21%) following flash chromatography, and isolated yields were determined on the basis of NMR ratios of **3.139** and

3.142. In order to avoid these difficulties with purification, use of hexachloroethane as electrophile was pursued, due to the expected larger difference in polarity between starting material and product. Additionally, the identification of chlorine-containing compounds by GC/MS would be unambiguous due to the distinct isotope pattern. As indicated in entry 2, metalation and quench with hexachloroethane resulted in isolation of unreacted starting material **3.139** and self condensation product **3.143** both in low yield. The observed formation of the self-condensation product prompted a change in experimental conditions. Use of inverse addition and higher dilution (0.05 M) was anticipated to decrease the formation of **3.143**. However, experiment (entry 3) indicated that this was not the case. NMR analysis of the crude reaction mixture indicated the formation of an approximately 3:2 ratio of **3.143**:**3.139**. Based on the observation of C-5 TMS incorporation in the synthesis of **3.139**, the reaction using *t*-BuLi was next attempted (entry 4).

Table 3.4. Metalation studies of substrate **3.139**

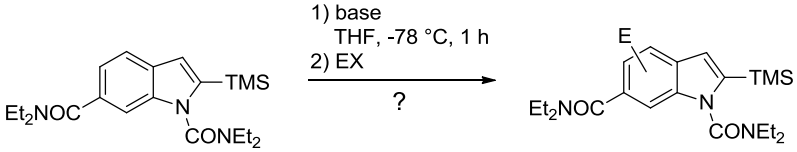

3.139

Entry	Base	Time (h)	Temp. (° C)	EX	Result
1	*s*-BuLi / TMEDA (2.2 equiv)	1	-78	MeI (10 equiv)	1.0 : 2.1 (36 mg) **3.139** : **3.142**(a)
2	*s*-BuLi / TMEDA (1.2 equiv)	1	-78	C_2Cl_6 (1.6 equiv)	15% **3.139** 10% **3.143**
3	*s*-BuLi / TMEDA (2.2 equiv)	1	-78	MeOD (10 equiv)	60%: 40% **3.143** : **3.139**(b)
4	*t*-BuLi (2.2 equiv)	1	-78	C_2Cl_6 (2.5 equiv)	6% **3.144** 8% **3.143** 17% **3.145** 18% **3.146**

(a) By NMR of an inseparable mixture (b) Inverse addition at a concentration of 0.05 M. NMR analysis of the crude reaction product.

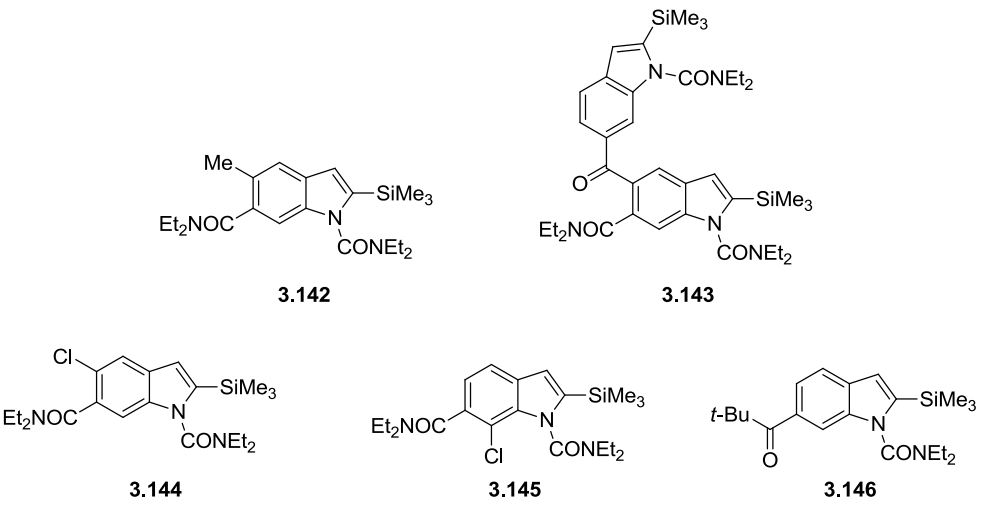

Figure 3.7. Products resulting from metalation of **3.139** with *s*-BuLi / TMEDA (**3.142**) or *t*-BuLi (**3.143 - 3.146**)

Treatment of **3.139** using excess *t*-BuLi (2.2 equiv) and subsequent quench with hexachloroethane (2.5 equiv) afforded the four products shown in Figure 3.7. Importantly, C-5 and C-7 chlorinated products **3.144** and **3.145** were isolated in a 1:2.8 ratio (6% and 17%, respectively). Despite this success, nucleophilic reaction of *t*-BuLi with the C-6 amide remained problematic, as 18% of ketone **3.146** was isolated, in addition to the self-condensation product **3.143** (8%).

Significant information was obtained as a result of these studies: i) material balance was not obtained after the reactions (even using 1.2 equiv of base), which implies the formation of unknown decomposition products, ii) formation of self-condensation product **3.143** was observed in several experiments, regardless of whether normal or inverse addition was used, and iii) although evidence for C-7 and C-5 deprotonation was obtained using *t*-BuLi, nucleophilic attack on the amide was also observed.

In an effort to overcome the reactivity of the *N*,*N*-diethylamide DMG towards nucleophilic attack by strong bases and increase the likelihood of metalation, the more sterically hindered *N*,*N*-diisopropylamide **3.149** was prepared (Scheme 3.32). Initial *N*-functionalization was achieved by reaction of indole-6-carboxylic acid **3.123** with *in situ* prepared LDA (2.1 equiv), followed by selective quench of the nitrogen based anion with *N*,*N*-diethylcarbamoyl chloride to afford **3.147** in 86% yield. Standard amide formation via EDC coupling of **3.123** with

diisopropylamine gave a lower yield of **3.147** (in comparison to **3.131**). Standard conditions for the installation of the C-6 *N*,*N*-diisopropylamide afforded **3.148**, and subsequent TMS introduction *via* the D*o*M reaction furnished **3.149** in 44% yield.

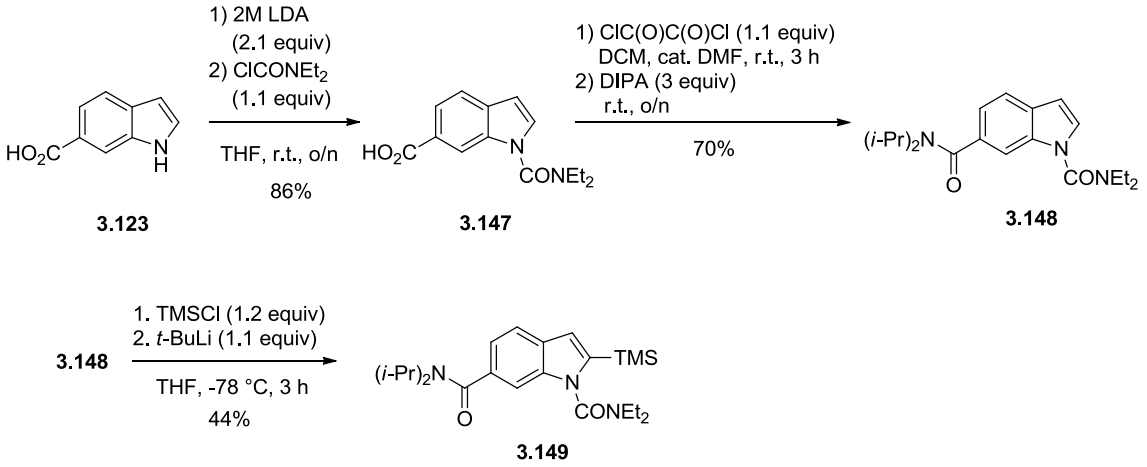

Scheme 3.32. Synthesis of indole metalation substrate **3.149**

Initial metalation of **3.149** was tested using the standard conditions shown in Scheme 3.33. Based on previous identification of undesired product **3.143** (Table 3.4, entries 2,3), the reaction was performed under conditions of high dilution (0.05 M) and using inverse addition to ensure that the starting material would always be exposed to excess base, and undergo deprotonation at a faster rate than the competing intermolecular self-condensation process.

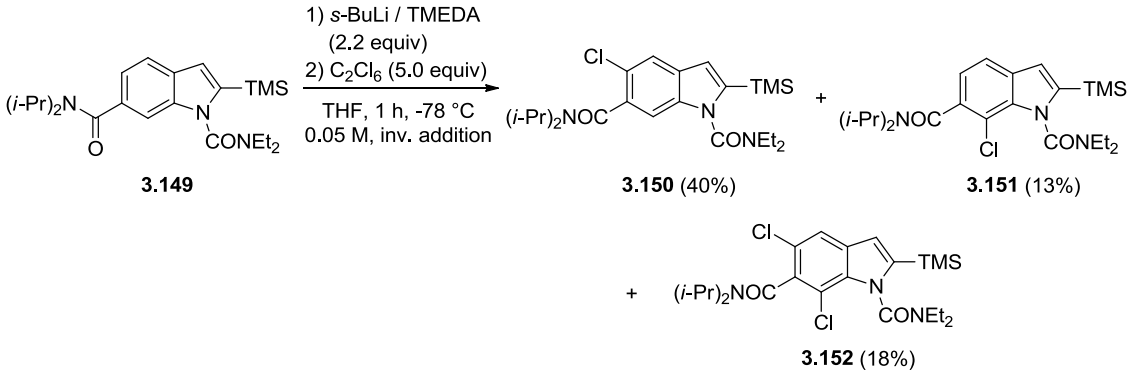

Scheme 3.33. Results of initial metalation studies of **3.149**

To our delight, metalation using 2.2 equiv of *s*-BuLi and TMEDA afforded the products of C-5 and C-7 chlorination (**3.150** and **3.151**) in 40% and 13% yield, respectively. The C-5/C-7 bis-chlorinated product **3.152** was also isolated in 18% yield, whose formation may be attributed to the rate of addition of the electrophile (over a period of 5 mins). The formation of the bis-chlorinated product **3.152** may arise via double chlorination of the dilithiated species or by sequential chlorination of the C-5 and C-7 chloro derivative (or vice versa).

The results suggest that when *s*-BuLi is used as the base, a synergistic effect between the two DMG groups is overridden by C-7 steric crowding, and consequently, C-5 deprotonation is favoured (with low C-5 over C-7 selectivity). Comparison with results of *t*-BuLi metalation-chlorination experiments of **3.139** (Table 3.4, entry 4) reveals a higher C-7 over C-5 regioselectivity in the former case. Metalation of **3.139** using 1.2 equiv of *s*-BuLi and MeOD quench (Table 3.4, entry 2), did not afford product(s) with d_1-incorporation, indicating that at least 2 equivalents of base are necessary for substantial metalation to occur.

3.6 Conclusions

The purpose of the research described in this chapter was to develop new D*o*M chemistry of *N*,*N*-diethyl indole 6-carboxamide **3.123** which would lead to regioselective functionalization at either the C-5 or C-7 positions of the ring. The apparent low D*o*M reactivity of **3.123**, and corresponding high electrophilic reactivity of the diethylamide towards strong alkyllithiums or lithium dialkylamide prohibited the desired metalation from occurring. This trend was observed among the variety of metalation tactics tested, including synergistic metalation of *N*-PO(*t*-Bu)$_2$ **3.137** and *N*-CONEt$_2$ **3.138** functionalized indoles, and 2-silicon protection strategies (**3.139**). Although C-5 and C-7 chlorinated products **3.144** and **3.145** were obtained (Table 3.7, entry 4), the problem of the alkyllithium addition to the amide was not completely overcome. However, metalation-chlorination of the bulkier diisopropylamide under inverse addition and high dilution conditions led to C-5 and C-7 chlorinated products **3.150** and **3.151** which, in addition to dichlorinated **3.152**, provided good material balance in product formation. Although promising initial results have been demonstrated here, this project is still in early stages of development and requires further investigation.

3.7 Future Work

The establishment of C-5 and C-7 metalation of **3.149** using the conditions shown in Scheme 3.33 is a valuable starting point from which efforts to improve the regioselectivity of this reaction may be initiated. The selection of base to ensure stoichiometic metalation of **3.149** needs detailed study. In the case of metalation of **3.149**, use of *t*-BuLi must be attempted according to the conditions shown in Scheme 3.33, which were successful for the corresponding reaction of **3.139**. Use of electrophiles which are compatible with the dialkyl amide bases (TMSCl and B(O*i*-Pr)$_3$)[15, 142] could be advantageous. Improvement in the C-5/C-7 selectivity of metalation of **3.149** is anticipated upon further optimization of the reaction conditions, and in particular, the metalation time. The following experiments (Scheme 3.34) are expected to be informative regarding conditions governing kinetic and thermodynamic metalation of **3.149**. It is hypothesized that C-5 lithiation arises from kinetic deprotonation (low temperature, short reaction time), avoiding the steric environment surrounding the C-7 position. In contrast, the presence of the *N*- and C-6 DMGs suggest thermodynamic stability of the anion resulting from C-7 lithiation.

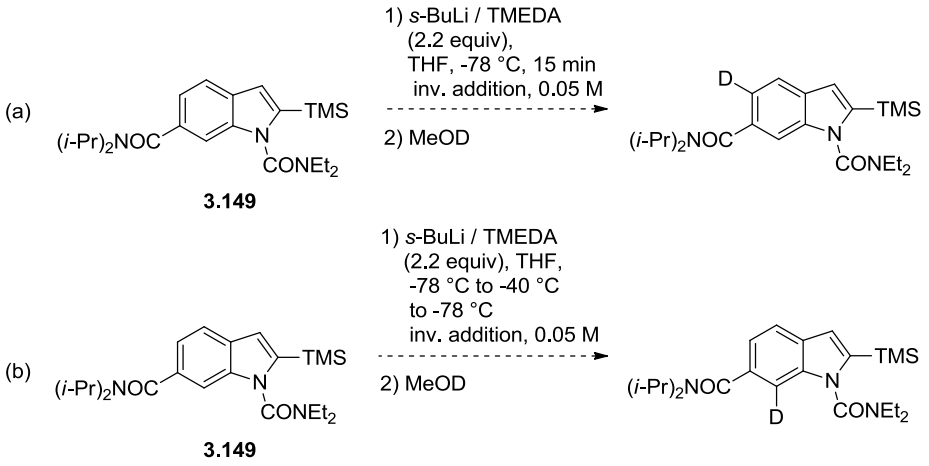

Scheme 3.34. Experiments designed to distinguish kinetic vs. thermodynamic deprotonation of **3.149**

In addition to establishing kinetic and thermodynamic metalation parameters for **3.149**, C-5 vs C-7 regioselective deprotonation may be approached by variation in the *N*-functional group, and a variety of indole *N*-DMGs are available for exploration. Thus it may be expected

that the smaller MOM DMG would be more favourable for C-7 deprotonation (Scheme 3.35). As always, exploration of the appropriate base (*s*-BuLi, *t*-BuLi or lithium amide bases), as well as optimization of the reaction conditions would be required.

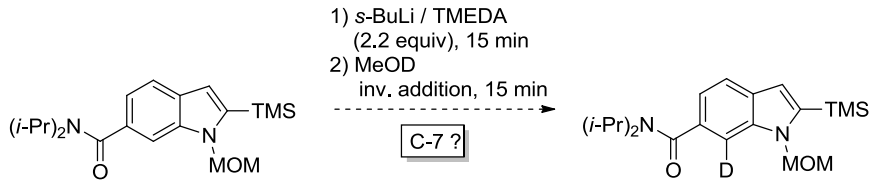

Scheme 3.35. Experiments designed to test the relationship between indole *N*-substituent and metalation outcome.

Achievement of regioselective C-5 and C-7 metalation has potential application in the synthesis of pyrrolofluorenones and pyrrolophenanthrols. The synthetic methodology to pyrrolofluorenones **3.124** and pyrrolophenanthrols **3.126** following C-5 functionalization of **3.149** is shown in Scheme 3.36, and regioisomeric compounds are anticipated to arise from an XCoupl-DreM sequence initiated from the related C-7 functionalized reagent (Figure 3.6).

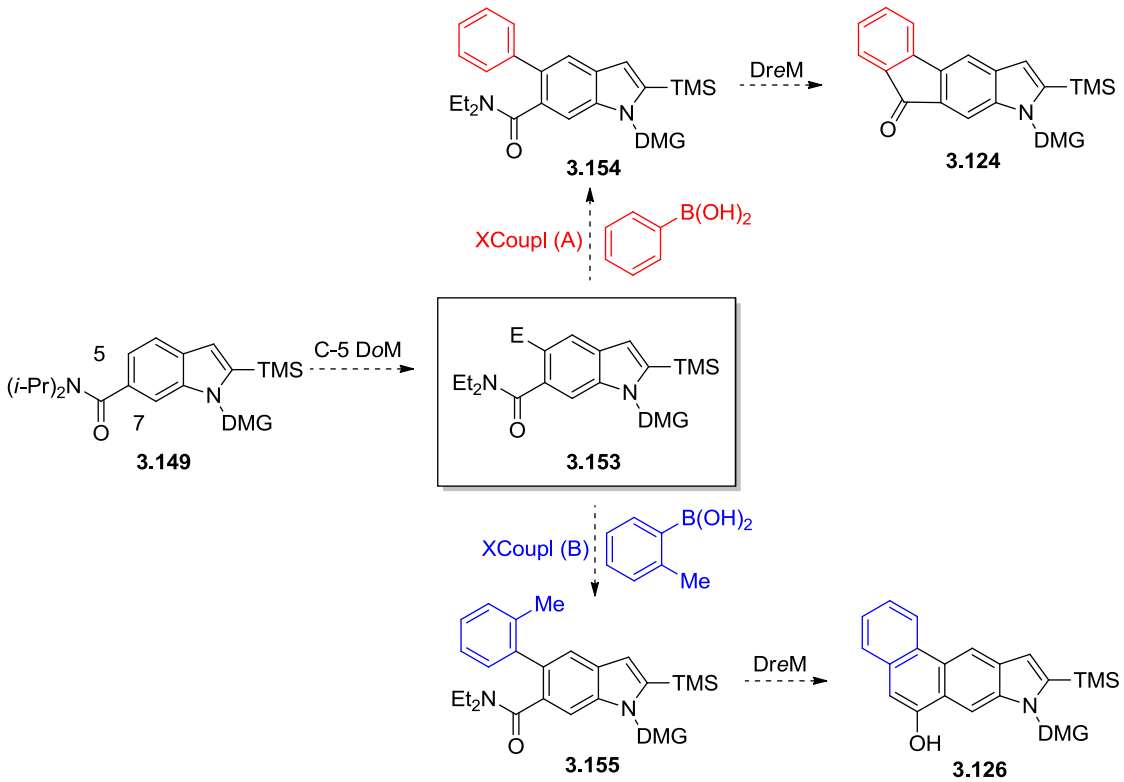

Scheme 3.36. Proposed synthetic routes to pyrrolofluorenones **3.124** and pyrrolophenanthrols **3.126**

3.8 Experimental Section

Materials and Methods.

See Chapter 2 Experimental Section for General Materials and Methods. Alkyllithiums were purchased from Sigma-Aldrich and were titrated bi-weekly (or as needed) against *s*-butanol using 1,10-phenanthroline as indicator or through reaction with *N*-benzylbenzamide to a blue endpoint. Anhydrous TMEDA, diisopropylamine and triethylamine were distilled over KOH and stored under argon and over KOH in a flame dried bottle. TMSCl was distilled over CaH_2 and stored in a flame dried bottle under argon. Indole-6-carboxylic acid was received as a gift from Boehringer-Ingelheim. The reaction temperature values refer to actual reaction mixtures as

measured through a thermocouple thermometer (Barnant 600-1040) equipped with a type J temperature probe.

***N,N*-diethyl indole-6-carboxamide (3.131)**

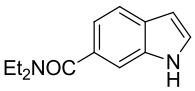

Indole-6-carboxylic acid **3.123** (1.83 g, 11.4 mmol, 1.0 equiv) was added to a flask containing DMF (57 mL), followed by EDC•HCl (2.7 g, 14.1 mmol, 1.24 equiv), HOBt (1.5 g, 11.4 mmol, 1.0 equiv), Et_2NH (1.8 mL, 17.4 mmol, 1.53 equiv), and DIPEA (5.0 mL, 28.7 mmol, 2.53 equiv). The reaction mixture was stirred at rt for 15 h, and the DMF was removed by Kugelrohr distillation. Flash column chromatography (100% EtOAc) afforded **3.131** (1.66 g, 67%) as a colourless solid. mp 126-128˚C (EtOAc); IR (KBr disc) ν_{max} = 3201, 3136, 2976, 1590, 1516, 1452, 1316, 1211, 1167, 897, 871, 831, 788, 734 cm^{-1}; ^1H NMR (400 MHz, $CDCl_3$): δ 1.18 (br s, 6H), 3.20-3.70 (apparent doublet, 4H), 6.51 (m, 1H), 7.09 (dd, 1H, ^1J = 8.1 Hz, ^2J = 1.3 Hz), 7.21 (m, 1H), 7.45 (s, 1H), 7.60 (d, 1H, J = 8.1 Hz) ppm; ^{13}C NMR (100 MHz, $CDCl_3$): δ 102.2, 110.1, 117.9, 120.3, 126.0, 128.5, 130.5, 135.4, 172.7 ppm; ^1H NMR (400 MHz, d_6-DMSO, 353 K): δ 1.13 (t, 6 H, J = 7.1 Hz), 3.38 (q, 4H), 6.45-6.48 (m, 1H), 6.99 (dd, 1H, ^1J = 8.1 Hz, ^2J = 1.4 Hz), 7.57 (d, 1 H, J = 8.1 Hz), 7.37-7.42 (m, 2H), 11.0 (s, NH) ppm; ^{13}C NMR (100 MHz, d_6-DMSO, 353 K): δ 13.0 (2 x CH_3), 40.4 (2 x CH_2), 100.7, 109.2, 116.9, 119.2, 126.1, 127.7, 129.7, 134.8, 170.8 ppm; HRMS calcd for $C_{13}H_{16}N_2O$ 216.1263, found 216.1257.

***N,N*-diethyl (*N'*-triisopropylsilyl)indole-6-carboxamide (3.134)**

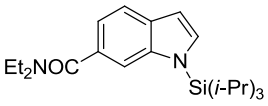

A 60% dispersion of NaH in mineral oil (269 mg, 6.7 mmol, 5.0 equiv) was washed with anhydrous hexanes in a flame dried flask under argon and cooled to 0 ˚C. A solution of **3.131** (500 mg, 1.34 mmol, 1.0 equiv) in THF (8 mL) was added slowly, with vigorous generation of H_2 gas. The reaction mixture was stirred for 15 min at 0 ˚C, followed by addition of TIPSCl (0.71 mL, 3.35 mmol, 2.5 equiv), and stirring was continued at rt for 24 h. The reaction mixture was quenched with H_2O (6 mL) at 0 ˚C, and the organic layer was washed with 1 M HCl, brine, and dried over $MgSO_4$. Filtration and evaporation to dryness *in vacuo* gave a solid which was subjected to flash column chromatography (4:1 hex:EtOAc) and afforded **3.134** (461 mg, 92%) as a colourless solid. mp 79-81 ˚C (hexane); IR (KBr disc) ν_{max} = 2947, 2868, 1631 cm^{-1}; ^1H NMR (400 MHz, $CDCl_3$): δ 1.14

(d, 18 H, J = 7.6 Hz), 1.10-1.24 (br s, 6 H), 1.70 (septet, 3H, J = 7.5 Hz), 3.30-3.64 (br s, 4H), 6.63 (m, 1H), 7.12 (dd, 1H, ^1J = 8.1 Hz, ^2J = 0.9 Hz), 7.31 (d, 1H, J = 3.2 Hz), 7.54 (s, 1H), 7.61 (d, 1H, J = 8.0 Hz) ppm; ^{13}C NMR (100 MHz, $CDCl_3$): δ 12.8 (2 x CH_3), 18.1 (6 x CH_3), 104.7, 112.2, 118.6, 120.3, 130.3, 132.1, 132.6, 140.1, 172.5 ppm; HRMS calcd for $C_{22}H_{36}N_2OSi$ 372.2597, found 372.2604.

_N,N_-diethyl 1-(diethylcarbamoyl)indole-6-carboxamide[351] (3.138)

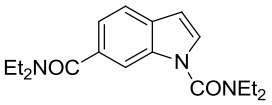

To a 60% dispersion of NaH in mineral oil (222 mg, 5.6 mmol, 1.2 equiv) in anhydrous THF (10 mL) at 0 ˚C was added a solution of indole-6-carboxamide **3.134** (1.0 g, 4.6 mmol, 1.0 equiv) in anhydrous THF (8 mL). Upon stirring for 15 min at 0 ˚C, *N*,*N*-diethylcarbamoyl chloride (0.64 mL, 5.1 mmol, 1.1 equiv) was added and the reaction mixture was stirred at rt for 18 h, quenched with sat. aq. NH_4Cl and extracted with CH_2Cl_2. Filtration and concentration to dryness *in vacuo* afforded 810 mg of **3.138** (77%) as a colourless solid. mp 119-121 ˚C (EtOAc); IR (KBr disc) ν_{max} = 3004, 2979, 2946, 2898, 1673, 1617, 1422, 1310, 1263, 1214 cm^{-1}; ^{1}H NMR (400 MHz, d_6-DMSO, 353 K): δ 1.13 (t, 6H, ^1J = 7.1 Hz), 1.17 (t, 6H, J = 7.1 Hz), 3.37 (q, 4H, J = 7.4 Hz), 3.42 (q, 4H, J = 7.1 Hz), 6.67-6.70 (m, 1H), 7.14 (dd, 1H, ^1J = 8.1 Hz, ^2J = 1.3 Hz), 7.54 (s, 1H), 7.56 (d, 1H, J = 3.4 Hz), 7.65 (d, 1H, J = 8.0 Hz) ppm; ^{13}C NMR (100 MHz, $CDCl_3$, 353 K): δ 12.7 (2 x CH_3), 12.9 (2 x CH_3), 40.4 (2 x CH_2), 41.8 (2 x CH_2), 104.2, 110.3, 119.2, 120.1, 127.3, 128.6, 131.8, 134.2, 152.7, 170.1 ppm; HRMS calcd for $C_{18}H_{25}N_3O_2$ 315.1947, found 315.1939. The material was used in the next reaction without purification.

_N,N_-diethyl (_N′_-diethylcarbamoyl)-2-trimethylsilylindole-6-carboxamide[351] (3.139)

A solution of *N*,*N*-diethyl (*N′*-diethylcarbamoyl)indole-6-carboxamide **3.138** (810 mg, 2.6 mmol, 1.0 equiv) and TMSCl (0.39 mL, 3.1 mmol, 1.2 equiv) in anhydrous THF (17 mL) was cooled to -78 ˚C, and treated by dropwise addition of freshly titrated *t*-BuLi (2.26 mL, 2.8 mmol, 1.1 equiv). The resulting yellow solution was stirred for 3 h at -78 ˚C and quenched with sat. aq. NH_4Cl before warming to rt. The combined organic layers resulting from EtOAc extraction were dried over $MgSO_4$, filtered, and concentrated *in vacuo* prior to purification by flash column chromatography (10:1 hexane:EtOAc to 1:1 hexane:EtOAc) which afforded products **3.139**, **3.140** and **3.141** in order of elution.

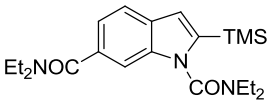

Product **3.139**: (401 mg, 40% yield), as a yellow oil. IR (KBr disc) ν_{max} 3426, 2973, 2940, 2899, 1678, 1620 cm^{-1} ; ^1H NMR (400 MHz, $CDCl_3$): δ 0.36 (s, 9H), 1.10-1.30 (br s, 6H), 1.21 (t, 6H, J = 7.1 Hz), 3.42 (m, 4 H), 3.20-3.66 (m, 4H), 6.81 (s, 1H), 7.14 (dd, 1H, ^1J = 8.1 Hz, ^2J = 1.1 Hz), 7.30 (s, 1H), 7.58 (d, 1H, J = 8.1 Hz) ppm; ^{13}C NMR (100 MHz, $CDCl_3$): δ -0.5, 13.6, 42.9, 109.6, 115.2, 119.5, 120.8, 129.8, 132.3, 137.1, 143.1, 154.7, 171.9 ppm; ^1H NMR (400 MHz, $CDCl_3$, 353 K): δ 0.34 (s, 9H), 1.08-1.16 (m, 12 H), 3.37 (q, 8 H, J = 6.9 Hz), 6.89 (s, 1H), 7.09-7.13 (m, 1H), 7.24 (s, 1H), 7.64 (d, 1H, J = 8.1 Hz) ppm; ^{13}C NMR (100 MHz, d_6-DMSO, 353 K): δ -1.1, 12.7 (2 x CH_3), 12.9 (2 x CH_3), 40.3 (2 x CH_2), 41.8 (2 x CH_2), 108.3, 114.3, 118.8, 120.2, 128.4, 132.1, 136.2, 141.7, 153.3, 169.9 ppm; HRMS calcd for $C_{21}H_{33}N_3O_2Si$ 387.2342, found 387.2354.

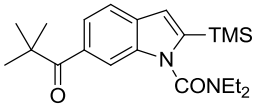

Product **3.140**: (171 mg, 18% yield), as a yellow oil which solidified upon standing. mp 91-92 ˚C (hexanes); IR (KBr) ν_{max} 2973, 2950, 2900, 1680, 1478, 1431, 1414, 1311, 1267, 1244, 1209, 1179, 1167, 1128, 1091, 920, 845, 829 cm^{-1}; ^1H NMR (400 MHz, $CDCl_3$): δ 0.37 (s, 9H), 1.23 (t, 6H, ^1J = 7.1 Hz), 1.40 (s, 9H), 3.40 (m, 2H), 3.51 (m, 2H), 6.82 (m, 1H), 7.57 (d, 1H, ^1J = 8.3 Hz), 7.63 (dd, 1 H, ^1J = 8.3 Hz, ^2J = 1.4 Hz), 7.79 (s, 1H) ppm; ^{13}C NMR (100 MHz, $CDCl_3$): δ -0.6, 13.6, 15.3, 28.5 (3 x CH_3), 42.7, 44.1, 65.9, 112.2, 115.1, 120.1, 121.5, 131.3, 132.8, 137.0, 145.1, 154.5, 208.1 ppm; HRMS calcd for $C_{21}H_{32}N_2O_2Si$ 372.2233, found 372.2228.

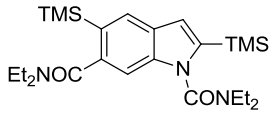

Product **3.141**: (113 mg, 10% yield), as a colourless solid. mp > 160 ˚C (hexanes, sublimation); IR (KBr) ν_{max} 2974, 2955, 2900, 1673, 1626, 1428, 1319, 1275, 840 cm^{-1}; ^1H NMR (400 MHz, $CDCl_3$): δ 0.30 (s, 9H), 0.36 (s, 9H), 1.00-1.08 (m, 3H), 1.19 (t, 6H, J = 7.1 Hz), 1.24-1.32 (m, 3H), 3.10-3.18 (m, 2H), 3.33-3.44 (m, 2H), 3.45-3.53 (m, 2H), 3.53-3.63 (m, 2H), 6.81 (s, 1H), 7.09 (s, 1H), 7.82 (s, 1H) ppm; ^{13}C NMR (100 MHz, $CDCl_3$): δ -0.4, 0.2, 12.8, 13.7, 13.9, 38.9, 43.0, 43.5, 108.7, 115.6, 128.5, 129.0, 129.2, 137.2, 137.8, 142.7, 154.7, 172.9 ppm; HRMS calcd for $C_{24}H_{41}N_3O_2Si_2$ 459.2737, found 459.2729.

***N*,*N*-diethyl 1-(di-*t*-butylphosphinoyl)indole-6-carboxamide**[351] **(3.137)**

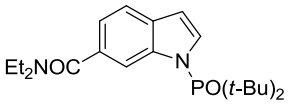

To a 60% dispersion of NaH in mineral oil (111 mg, 4.6 mmol, 1.2 equiv) in THF (2 mL) at 0 ˚C, washed with anhydrous hexane, was added a solution of *N*,*N*-diethyl indole-6-carboxamide **3.131** (500 mg, 2.3 mmol, 1.0 equiv) in anhydrous THF (6 mL, 0.4 M) and the resulting suspension was stirred at rt for 10 min. The reaction was cooled to 0 ˚C and di-*t*-butyl chlorophosphine (0.53 mL, 2.8 mmol, 1.2 equiv) was added as a solution in THF (0.56 mL, 5.0 M). After stirring for 18 h at rt, the reaction mixture was diluted with MeOH (5 mL) and most of the solvents were removed under reduced pressure. The residue was re-suspended in MeOH (10 mL), and the whole was cooled to 0 ˚C before treatment with excess 30 wt% H_2O_2 (0.38 mL, 12.3 mmol, 1.6 equiv). The reaction mixture was stirred for 45 mins at 0 ˚C, treated with sat. aq. $Na_2S_2O_3$ (5 mL) and stirred for a further 2 h at 0 ˚C. Then the reaction mixture was treated with 12 mL of HCl (10% v/v) and stirred 1.5 h at rt. The reaction was concentrated to remove most of the MeOH, and the remaining material was poured into water (50 mL) and the whole was extracted with CH_2Cl_2. Flash column chromatography (2% MeOH in CH_2Cl_2) afforded **3.137** (600 mg, 69%) as a colourless solid. mp 182-184 ˚C (EtOAc); IR (KBr) ν_{max} = 3106, 2973, 2935, 2872, 1631, 1427, 1135, 669, 608 cm^{-1}; ^{1}H NMR (400 MHz, $CDCl_3$): δ 1.14 (br s, 2 CH_3, 6H), 1.32 (s, 9H), 1.35 (s, 9H), 3.29 (br s, CH_2, 2H), 3.53 (br s, CH_2, 2H), 6.69 (m, 1H), 7.25 (m, 1 H, ovlp with residual C*H*Cl_3), 7.29 (dd, 1H, ^1J = 3.3 Hz, ^2J = 1.2 Hz), 7.59 (d, 1H, J = 8.0 Hz), 8.61 (s, 1H) ppm; ^{13}C NMR (100 MHz, $CDCl_3$): δ 26.6, 38.6 (d, J = 68.9 Hz), 107.1 (d, J = 4.8 Hz), 114.2, 120.5, 120.6, 127.6 (d, J = 4.6 Hz), 129.7 (d, J = 5.3 Hz), 132.3, 140.7, 172.2 ppm; ^{31}P NMR (162 MHz, $CDCl_3$): δ 63.6 ppm; ^{1}H NMR (400 MHz, d_6-DMSO, 353K): δ 1.13 (t, 6H, J = 7.0 Hz), 1.26 (s, 9H), 1.30 (s, 9H), 3.35 (q, 4H, J = 6.9 Hz), 6.76-6.81 (m, 1H), 7.11 (dd, 1H, ^1J = 8.0 Hz, ^2J = 1.3 Hz), 7.56-7.59 (m, 1H), 7.60-7.63 (d, 1H, J = 8.0 Hz),8.50 (s, 1H) ppm; ^{13}C NMR (100 MHz, d_6-DMSO, 353K): δ 12.9 (2 x CH_3), 25.6 (6 x CH_3), 37.6 (d, 2 x C_q, $J_{C\text{-}P}$ = 68.6 Hz), 40.5 (2 x CH_2), 106.3 (d, $J_{C\text{-}P}$ = 4.6 Hz), 113.3, 119.2, 119.6, 128.5 (d, $J_{C\text{-}P}$ = 4.3 Hz), 129.0 (d, $J_{C\text{-}P}$ = 5.1 Hz), 131.3, 140.0, 170.4 ppm; ^{31}P NMR (162 MHz, d_6-DMSO, 353K): δ 65.1 ppm; HRMS calcd for $C_{21}H_{33}N_2O_2P$ 376.2280, found 376.2271.

***N*,*N*-diethyl 5-chloro-1-(diethylcarbamoyl)-2-trimethylsilylindole-6-carboxamide (3.144)**

To a solution of indole **3.137** (93 mg, 0.24 mmol, 1.0 equiv) in THF (0.05 M, 4.8 mL) was cooled to -78 ˚C, and freshly titrated *t*-BuLi (0.42 mL, 0.53 mmol, 2.2 equiv) was slowly added dropwise, accompanied by a colour change from yellow to deep red. After 1 h, a solution of C_2Cl_6 (142 mg, 0.6 mmol, 2.5 equiv) dissolved in a minimum amount of anhydrous THF was added all at once, and the reaction mixture was allowed to warm to rt. Water (5 mL) was added and the whole was extracted with EtOAc. The combined organic layers were dried over $MgSO_4$, filtered and concentrated to give a crude residue, which, upon flash column chromatography (5:1 hexane:EtOAc → 1:1 hexane:EtOAc) afforded, in order of elution, products **3.144**, **3.145**, **3.146** and **3.143**.

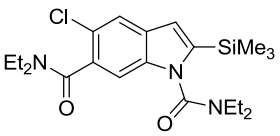

Product **3.144**: (6 mg, 6% yield), as a yellow oil. IR (KBr) ν_{max} = 3448, 2975, 2936, 1690, 1637, 1429, 1316, 1289, 1265, 1240, 1141, 983, 871, 842 cm^{-1}; ^1H NMR (400 MHz, $CDCl_3$): δ 0.36 (s, 9H), 1.01 (t, 3H, *J* = 7.1 Hz), 1.09 (t, 3H, *J* = 7.1 Hz), 1.24-1.33 (m, 6H), 3.09-3.18 (m, 2H), 3.28-3.38 (m, 2H), 3.39-3.49 (m, 2H), 3.56-3.68 (m, 1H), 3.82-3.92 (m, 1H), 6.73 (s, 1H), 7.14 (s, 1H), 7.58 (s, 1H) ppm; ^{13}C NMR (100 MHz, $CDCl_3$): δ -0.6, 12.5, 13.3, 13.88, 13.94, 38.8, 42.1, 42.6, 43.7, 109.7, 114.5, 121.4, 122.9, 130.3, 131.4, 135.8, 144.4, 154.3, 168.3 ppm; HRMS calcd for $C_{21}H_{32}ClN_3O_2Si$ 421.1952, found 421.1941.

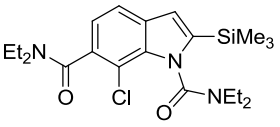

Product **3.145**: (17 mg, 17% yield), as an orange oil. IR (KBr) ν_{max} = 2973, 2937, 2899, 2877, 1682, 1632, 1486, 1456, 1426, 1416, 1381, 1348, 1314, 1266, 1208, 1167, 1125, 1092, 1056, 959, 844, 762 cm^{-1}; ^1H NMR (400 MHz, $CDCl_3$): δ 0.36 (s, 9H), 0.93 (t, 3H, *J* = 7.2 Hz), 1.01 (t, 3H, *J* = 7.1 Hz), 1.27 (t, 3H, *J* = 7.1 Hz), 1.34 (t, 3H, *J* = 7.2 Hz), 2.82 (q, 2H, *J* = 7.4 Hz), 3.10 (q, 2H, *J* = 7.1 Hz), 3.37 (dq, 1H, ^1J = 14.0 Hz, ^2J = 7.1 Hz), 3.49 (dq, 1H, ^1J = 14.2 Hz, ^2J = 7.2 Hz), 3.68 (dq, 1H, ^1J = 14.2 Hz, ^2J = 7.2 Hz), 3.82 (dq, 1H, ^1J = 14.2 Hz, ^2J = 7.1 Hz), 6.80 (s, 1H), 7.01 (d, 1H, *J* = 8.0 Hz), 7.52 (1H, d, *J* = 8.0 Hz) ppm; ^{13}C NMR (100 MHz, $CDCl_3$): δ -0.7, 12.0, 12.7, 13.3, 13.9, 38.9, 42.1, 42.8, 43.6, 114.6, 119.6, 120.0, 130.5, 131.9, 134.0, 142.7, 154.2, 168.5 ppm; HRMS calcd for $C_{21}H_{32}ClN_3O_2Si$ 421.1952, found 421.1943.

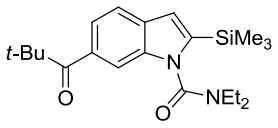

Product **3.146**: (16 mg, 18% yield), as a yellow oil whose physical and spectral data are consistent with those of the previously identified side product **3.140**.

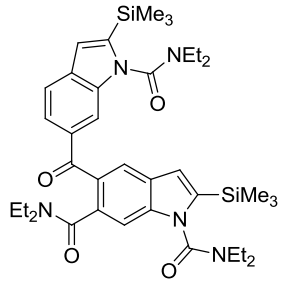

Product **3.143**: (13 mg, 8% yield), as a yellow solid. mp > 200 ˚C (Et_2O); IR (KBr) ν_{max} = 2972, 2899, 1685, 1635, 1605, 1555, 1476, 1413, 1380, 1315, 1235, 1211, 1169, 1124, 1082, 1042, 855, 783, 763, 697, 634 cm^{-1}; ^{1}H-NMR (400 MHz, $CDCl_3$): δ 0.365 (s, 9H), 0.372 (s, 9H), 1.02-1.10 (m, 9H), 1.15 (t, 3H, *J* = 6.8 Hz), 1.23 (t, 6H, *J* = 7.2 Hz), 3.22-3.58 (m, 12 H), 6.79 (d, 1H, *J* = 0.6 Hz), 6.84 (d, 1H, *J* = 0.7 Hz), 7.24 (s, 1H), 7.60 (d, 1H, *J* = 8.2 Hz), 7.65 (dd, 1H, ^1J = 8.2 Hz, ^2J = 1.3 Hz), 7.75 (s, 1H), 7.76 (s, 1H) ppm; ^{13}C-NMR (100 MHz, $CDCl_3$): δ -0.6, 12.1, 13.4, 13.7, 13.8, 109.5, 114.4, 115.3, 116.0, 120.3, 123.3, 124.5, 127.9, 130.8, 132.5, 133.3, 134.3, 137.0, 137.8, 144.4, 145.8, 154.2, 154.4, 170.8, 196.3 ppm; HRMS calcd for $C_{38}H_{56}N_4O_3Si_2$ 701.3793, found 701.3782.

1-(diethylcarbamoyl)indole-6-carboxylic acid (3.147)

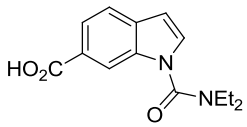

Procedure A: To a solution of indole-6-carboxylic acid **3.123** (450 mg, 2.8 mmol, 1.0 equiv) in anhydrous THF (0.4 M, 6.5 mL) at 0 ˚C was added 2M LDA (2.9 mL, 5.8 mmol, 2.1 equiv) over 10 min. The reaction mixture was stirred an additional 10 min at 0 ˚C, and freshly distilled $ClCONEt_2$ (0.4 mL, 3.1 mmol, 1.1 equiv) was added neat. The reaction mixture was allowed to warm to rt by removal from the cooling bath, and stirred for an additional 15 h. The reaction mixture was quenched with water, acidified with concentrated HCl and extracted with EtOAc, affording **3.147** (621mg, 86%) as a brown solid. mp 166.5 – 167.1 ˚C (MeOH); IR (KBr disc) ν_{max} 3110, 2944, 1686, 1425, 1314, 1261, 1217, 1103, 785 cm^{-1}; ^{1}H NMR (400 MHz, d_6-DMSO): δ 1.16 (t, 6H, *J* = 7.1 Hz), 3.40 (q, 4 H, *J* = 7.0 Hz), 6.74 (d, 1H, *J* = 3.3 Hz), 7.69 (d, 1H, *J* = 8.2 Hz), 7.73 (d, 1H, *J* = 3.4 Hz), 7.76 (dd, 1H, ^1J = 8.3, ^2J = 1.3 Hz), 8.19 (s, 1H); ^{13}C NMR (100 MHz, d_6-DMSO): δ 13.1 (2 x CH_3), 43.1 (2 x CH_2), 104.8, 114.3, 120.5, 122.1, 125.3, 129.6, 132.1, 134.6, 152.7, 167.7 ppm; HRMS calcd for $C_{14}H_{16}N_2O_3$ 260.1161, found 260.1164.

Procedure B: A solution of LDA (6.5 mL, 0.5M) was prepared by dropwise addition of a solution of 2.32M *n*-BuLi in hexanes (1.4 mL, 3.26 mmol, 2.1 equiv) over 15 min to a solution of freshly distilled diisopropylamine (0.55 mL, 3.91 mmol, 2.5 equiv) in anhydrous THF (4.6 mL) at -10 ˚C. The slightly yellow solution was stirred at -10 ˚C for 10 min before use. In a separate flask, a solution of indole-6-carboxylic acid (250 mg, 1.55 mmol, 1.0 equiv) in THF (0.43 M, 3.6 mL) was prepared and cooled to -10 ˚C. The freshly prepared LDA solution was added slowly over 30 mins to the THF solution of indole-6-carboxylic acid, monitoring the internal temperature of the reaction to remain within a range of 0-5 ˚C. The initial translucent brown solution became cloudy and then clear again during the addition of the LDA solution. The reaction mixture was stirred for 15 min at -10 ˚C and neat, freshly distilled $ClCONEt_2$ (0.22 mL, 1.7 mmol, 1.1 equiv) was added at that temperature. The reaction was stirred for 1 h and then allowed to warm to rt overnight. The reaction mixture was quenched with water (5 mL), acidified with concentrated HCl and extracted with EtOAc, affording 318 mg (80%) of **3.170** as a reddish-brown solid. The physical and spectral data matched that described for the material isolated according to Procedure A.

***N*,*N*-di-isopropyl 1-(diethylcarbamoyl)indole-6-carboxamide (3.148)**

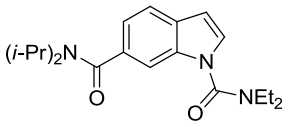

A solution of 1-(diethylcarbamoyl)indole-6-carboxylic acid **3.147** (400 mg, 1.54 mmol, 1.0 equiv) in anhydrous CH_2Cl_2 (0.1 M, 15 mL) at 0 ˚C was treated with oxalyl chloride (215 mg, 1.7 mmol, 1.1 equiv) and DMF (a few drops). The reaction mixture was stirred at rt for 1 h, followed by the addition of freshly distilled DIPA (0.74 mL, 4.6 mmol, 3.0 equiv). The reaction mixture was stirred at rt for 16 h, quenched with water, extracted with EtOAc, and dried using $MgSO_4$. Flash column chromatography (2:1 hexane:EtOAc) of the residue obtained upon concentration *in vacuo* afforded **3.148** (114 mg, 65%) as an orange oil which solidified upon standing. mp 106-107 ˚C (hexane); IR (KBr disc) ν_{max} 2973, 2936, 2874, 1680, 1623, 1422, 1341, 1312, 1266, 1214, 1036, 611 cm^{-1}; ^1H NMR (400 MHz, $CDCl_3$): δ 1.10-1.65 (m, 18H), 3.46 (q, 4H, J = 7.1 Hz), 3.50-4.00 (br s, 2H), 6.59 (dd, 1H, ^1J = 3.4 Hz, ^2J = 0.5 Hz), 7.13 (dd, 1H, ^1J = 8.0 Hz, ^2J = 1.4 Hz), 7.30 (d, 1H, J = 3.5 Hz), 7.58 (d, 1H, J = 8.0 Hz), 7.63-7.66 (m, 1H); ^{13}C NMR (100 MHz, $CDCl_3$, carbon corresponding to isopropyl CH groups not observed): δ 13.4 (2 x

CH_3), 20.8 (4 x CH_3), 42.5 (2 x CH_2), 105.2, 110.7, 119.4, 120.9, 126.8, 129.3, 134.3, 135.2, 154.2, 171.6 ppm; HRMS calcd for $C_{20}H_{29}N_3O_2$ 343.2260, found 343.2253.

***N*,*N*-di-isopropyl 1-(diethylcarbamoyl)-2-trimethylsilylindole-6-carboxamide (3.149)**

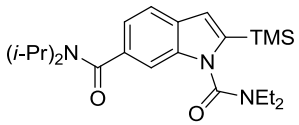

To a solution of *N*,*N*-di-isopropyl 1-(diethylcarbamoyl)indole-6-carboxamide **3.148** (2.43 g, 7.08 mmol, 1.0 equiv) and TMSCl (1.1 mL, 8.49 mmol, 1.2 equiv) in anhydrous THF (0.2 M, 35 mL) at -78˚C was added *t*-BuLi (5.3 mL, 7.78 mmol, 1.1 equiv) dropwise. The reaction mixture was stirred for 3 h at -78˚C, quenched with sat. aq. NH_4Cl (20 mL) and brought to rt. The whole was extracted with EtOAc, dried using $MgSO_4$ and concentrated *in vacuo*. Flash column chromatography (5:1 hexane:EtOAc) afforded **3.149** (1.26 g, 44%) as a colourless solid. mp 120-122˚C (hexane); IR (KBr disc) ν_{max} = 2994, 2972, 2940, 2877, 1685, 1621, 1438, 1369, 1335, 1312, 851, 823 cm^{-1}; ^1H NMR (400 MHz, $CDCl_3$): δ 0.36 (s, 9H), 1.20 (t, 6 H, *J* = 7.1 Hz), 1.20-1.60 (br s, 12H), 3.36-3.52 (m, 4H), 3.50-3.80 (br s, 2H), 6.80 (d, 1H, *J* = 0.6 Hz), 7.07 (dd, 1H, ^1J = 8.0 Hz, ^2J = 1.3 Hz), 7.23 (s, 1H), 7.56 (d, 1H, *J* = 8.0 Hz) ppm; ^{13}C NMR (100 MHz, $CDCl_3$, carbon corresponding to isopropyl CH groups not observed): δ -0.49, 13.6 (2 x CH_3), 20.8 (4 x CH_3), 42.9 (2 x CH_2), 108.9, 115.2, 118.9, 120.8, 129.9, 134.6, 137.7, 143.1, 155.2, 172.1 ppm; HRMS calcd for $C_{23}H_{37}N_3O_2Si$ 415.2655, found 415.2652.

***N*,*N*-di-isopropyl-5-chloro-1-(diethylcarbamoyl)-2-trimethylsilylindole-6-carboxamide (3.150)**

To solution of *s*-BuLi (0.79 mL, 0.79 mmol, 2.2 equiv) and TMEDA (0.12 mL, 0.79 mmol, 2.2 equiv) in anhydrous THF (6.2 mL) at -78˚C was added a solution of **3.149** (150 mg, 0.36 mmol, 1.0 equiv) in THF (1 mL) over 5 min. The reaction mixture was stirred for 1 h at -78˚C, and treated with a solution of Cl_6C_2 (428 mg, 1.8 mmol, 5.0 equiv) as a solution in THF (1 mL) over 5 mins. The reaction mixture was stirred for 0.5 h at -78˚C, allowed to warm to rt, and the whole was treated with water (5 mL), extracted with EtOAc, dried using $MgSO_4$ and concentrated. Flash column chromatography (8:1 hexane:EtOAc to 4:1 hexane:EtOAc) afforded products **3.150** and **3.151**, in order of elution.

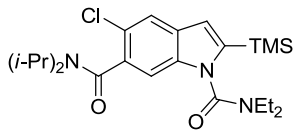

Product **3.150**: (64 mg, 40% yield), as a colourless solid. mp 167-169 ˚C (hexanes); IR (KBr disc) ν_{max} = 3106, 3055, 2973, 2934, 2899, 1683, 1628, 1554, 1470, 1436, 1404, 1339, 1304, 1264, 1250, 1203, 1163, 1127, 1100, 1060, 1043, 993, 905, 877, 840, 759, 695, 656, 634, 610, 539, 485, 421 cm^{-1}; ^1H NMR (400 MHz, $CDCl_3$): δ 0.35 (s, 9H), 1.01 (d, 3H, *J* = 6.7 Hz), 1.10 (t, 3H, *J* = 7.1 Hz), 1.19 (d, 3H, *J* = 6.7 Hz), 1.28 (t, 3H, *J* = 7.1 Hz), 1.58 (d, 3H, *J* = 6.7 Hz), 1.58 (d, 3H, *J* = 6.7 Hz), 3.20-3.70 (m, 5H), 6.73 (s, 1H), 7.05 (s, 1H), 7.57 (s, 1H) ppm; ^{13}C NMR (100 MHz, $CDCl_3$): δ -0.6, 13.4, 13.9, 20.0, 20.4, 20.9, 21.0, 42.1, 43.6, 45.9, 51.1, 108.9, 114.6, 121.5, 122.8, 130.0, 132.9, 135.9, 144.1, 154.4, 167.9 ppm; HRMS calcd for $C_{23}H_{36}ClN_3O_2Si$ 449.2265, found 449.2273.

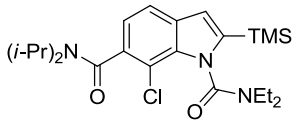

Product **3.151**: (21 mg, 14% yield), as a colourless solid. mp 120-122˚C (hexane); IR (KBr disc) ν_{max} = 2970, 2935, 2360, 2340, 1688, 1633, 1468, 1434, 1410, 1370, 1341, 1311, 1265, 1242, 1217, 1160, 906, 865, 840, 730 cm^{-1}; ^1H NMR (400 MHz, $CDCl_3$): δ 0.36 (s, 9H), 0.91 (t, 3H, *J* = 7.2 Hz), 1.03 (d, 3H, *J* = 6.6 Hz), 1.14 (d, 3H, *J* = 6.6 Hz), 1.35 (t, 3H, J = 7.2 Hz), 1.56-1.62 (m, 6H), 2.75-2.85 (m, 2H), 3.45-3.72 (m, 4H), 6.79 (s, 1H), 6.94 (d, 1H, *J* = 7.9 Hz), 7.49 (d, 1H, *J* = 8.0 Hz) ppm; ^{13}C NMR (100 MHz, $CDCl_3$): δ -0.7, 12.1, 13.3, 20.4, 20.6, 20.7, 20.8, 42.1, 43.5, 45.9, 51.2, 112.9, 114.6, 118.9, 119.9, 130.1, 133.4, 134.1, 142.5, 168.1 ppm; HRMS calcd for $C_{23}H_{36}ClN_3O_2Si$ 449.2265, found 449.2257.

References

[1] Sánchez, C.; Méndez, C.; Salas, J. A. *Nat. Prod. Rep.* **2006**, *23*, 1007.

[2] Nakano, H.; Omura, S. *J. Antibiot*. **2009**, *62*, 17.

[3] Sánchez, C.; Butovich, I. A.; Braña, A. F.; Rohr, J.; Méndez, C.; Salas, J. A. *Chemistry & Biology* **2002**, *9*, 519.

[4] Bush, J. A.; Long, B. H.; Catino, J. J.; Bradner, W. T. *J. Antibiot.*, **1987**, *40*, 668.

[5] a) Staker B. L.; Feese M. D.; Cushman, M.; Pommier, Y.; Zembower, D.; Stewart, L.; Burgin, A. B. *J. Med. Chem*. **2005**, *48*, 2336. b) Prudhomme, M. *Eur. J. Med. Chem.* **2003**, *38*, 123. c) Moreau, P.; Anizon, F.; Sancelme, M.; Prudhomme, M.; Bailly, C.; Severe, D.; Riou, J.-F.; Fabbro, D.; Meyer, T.; Aubertin, A.-M. *J. Med. Chem.***1999**, *42*, 584.

[6] a) Matson, J. A.; Claridge, C.; Bush, J. A.; Titus, J.; Bradner, W. T.; Doyle, T. W.; Horan, A. C.; Patel, M. *J. Antibiot*. **1989**, *42*, 1547. b) Golik, J.; Doyle, T. W.; Krishnan, B.; Dubay, G.; Matson, J. A. *J. Antibiot*. **1989**, *42*, 1784.

[7] Facompre, M.; Carrasco, C.; Colson, P.; Houssier, C.; Chisholm, J. D; Van Vranken, D. L; Bailly, C. *Mol. Pharmacol*. **2002**, *62*, 1215.

[8] Onaka, H.; Taniguchi, S.; Igarashi, Y.; Furumai, T. *J. Antibiot*. **2002**, *55*, 1063.

[9] Chiu, H-T.; Chen, Y-L.; Chen, C-Y.; Jin, C.; Lee, M-N.; Lin, Y-C. *Mol. BioSyst*. **2009**, *5*, 1180.

[10] Tamaoki, T.; Nomoto, H.; Takahashi, I.; Kato, Y.; Morimoto, M.; Tomita, F. *Biochem. Biophys. Res. Commun.* **1986**, *135*, 397.

[11] Pommier, Y.; Leo, E.; Zhang, H.; Marchand, C. *Chemistry & Biology* **2010**, *17*, 421.

[12] Prudhomme, M. *Curr. Med. Chem*. **2000**, *7*, 1189.

[13] Kase, H.; Iwahashi, K.; Matsuda, Y. *J. Antibiot.* **1986**, *39*, 1059.

[14] Sánchez, C.; Butovich, I. A.; Braña, A. F.; Rohr, J.; Méndez, C.; Salas, J. A. *Chemistry & Biology* **2002**, *9*, 519.

[15] Ohuchi, T.; Ikeda-Araki, T. A.; Watanabe-Sakomoto, A.; Kjiri, K.; Nagashima, M.; Okanishi, M.; Suha, H. *J. Antibiot*. **2000**, *53*, 393.

[16] Meksuriyen, D.; Cordell, G. A. *J. Nat. Prod.* **1988**, *51*, 893.

[17] Pearce, C. J.; Doyle, T. W.; Forenza, S.; Lam, K. S.; Shroeder, D. R. *J. Nat. Prod*. **1988**, *51*, 937.

[18] Hoshino, T.; Kondo, T.; Uchiyama, T.; Ogasawara, N. *Agric. Biol. Chem.* **1987**, *51*, 965.

[19] Lam, K.S.; Forenza, S.; Doyle, T. W.; Pearce, C. J. *J. Ind. Biochem*. **1990**, *6*, 291.

[20] Onaka, H.; Taniguchi, S-I.; Igarashi, Y.; Furumai, T. *Biosci. Biotechnol. Biochem*. **2003**, *67*, 127.

[21] Balibar, C. J.; Walsh, C. T. *Biochemistry* **2006**, *45*, 15444.

[22] August, P. R.; Grossman, T. H.; Minor, C.; Draper, M. P.; MacNeil, I. A.; Pemberton, J. M.; Call, K. M.; Holt, D.; Osburne, M. S. *J. Mol. Microbiol. Biotechnol*. **2000**, *2*, 513.

[23] Hirano, S.; Asamizu, S.; Onaka, H.; Shiro, Y.; Nagano, S. *J Biol. Chem*. **2008**, *283*, 6459.

[24] Yeh, E.; Garneau, S.; Walsh, C. T. *Proc. Natl. Acad. Sci.* **2005**, *102*, 3960.

[25] Keller, S.; Wage, T.; Hohaus, K.; Holzer, M.; Eichhorn, E.; van Pée, K. H. *Angew. Chem. Int. Ed*. **2000**, *39*, 2300.

[26] Holzer, M.; Burd, W.; Reissig, H. U.; van Pee, K. H. *Adv. Synth. Cat*. **2001**, *343*, 591.

[27] a) Yeh, E.; Garneau, S.; Walsh, C. T. *Proc. Natl. Acad. Sci. U.S.A*. **2005**, *102*, 3960. b) Keller, S.; Wage, T.; Hohaus, K.; Holzer, M.; Eichhorn, E.; van Pee, K. H. *Angew. Chem. Int. Ed*. **2000**, *39*, 2300. c) Dong, C.; Flecks, S.; Unversucht, S.; Haupt, C.; van Pée, K. H.; Naismith, J. H. *Science* **2005**, *309*, 2216.

[28] Palfey, B. A.; McDonald, C. A. *Arch. Biochem. Biophys*. **2010**, *493*, 26.

[29] Sucharitakul, J.; Prongjit, M.; Haltrich, D.; Chaiyen, P. *Biochemistry* **2008**, *47*, 8485.

[30] Yeh , E.; Blasiak, l. C.; Koglin, A.; Drennan, K. A.; Walsh, C. T. *Biochemistry* **2007**, *46*, 1284.

[31] Blasiak, L. C.; Drennan, C. L. *Acc. Chem. Res*. **2009**, *42*, 147.

[32] Nishiza, T.; Aldrich, C. C.; Sherman, D. H. *J. Bacteriol*. **2005**, *187*, 2084.

[33] Howard-Jones, A. R.; Walsh, C. T. *Biochemistry* **2005**, *44*, 15652.

[34] Baldwin, J. E. *J. Chem. Soc. Chem. Comm.* **1976**, 734.

[35] Asamizu, S.; Kato, Y.; Igarashi, Y.; Furumai, T.; Onaka, H. *Tetrahedron Lett*. **2006**, *47*, 473.

[36] Asamizu, S.; Hirano, S.; Onaka, H.; Koshino, H.; Shiro, Y.; Nagano, S. *ChemBioChem*. **2012**, *13*, 2495.

[37] Dunford, H. B. *Heme Peroxidases;* Wiley-VCH: New York, **1999**.

[38] Howard-Jones, A. R.; Walsh, C. T. *J. Am. Chem. Soc*. **2006**, *128*, 12289.

[39] Funa, N.; Funabashi, M.; Ohnishi, Y.; Horinouchi, S. *J. Bacteriol.* **2005**, *187*, 8149.

[40] Zhao, B.; Guengerich, P. F.; Bellamine, A.; Lamb, D. C.; Izumikawa, M.; Lei, L.; Podust, L. M.; Sundaramoorthy, M.; Kalaitzis, J. A.; Reddy, M. L.; Kelly, S. L.; Moore, B. S.; Stec, D.; Voehler, M.; Falck, J. R.; Shimada, T.; Waterman, M. R. *J. Biol. Chem*. **2005**, *280*, 11599.

[41] Howard-Jones, A. R.; Walsh, C. T. *J. Am. Chem. Soc*. **2007**, *129*, 11016.

[42] Makino, M.; Sugimoto, H.; Shiro, Y.; Asamizu, S.; Onaka, H.; Nagano, S. *Proc. Natl. Acad. Sci*. **2007**, *104*, 11591.

[43] a) Poulos, T. L. *Nat. Prod. Rep*. **2007**, 24, 504. b) Poulos, T. L. in *The Porphyrin Handbook*, Kadish, K. M., Smith, K. M., Guilard, R. Eds.; Academic Press: New York, **2000**; Vol. 4, pp. 189-218. c) Colas, C.; Ortiz de Montellano, P. R. *Chem. Rev*. **2003**, *103*, 2305. d) Dunford, H. B. *Heme Peroxidases*; Wiley-VCH: New York, **1999**.

[44] Derat, E.; Shaik, S. *J. Am. Chem. Soc.* **2006**, *128*, 13940.

[45] Barrows, T. P.; Bhaskar, B.; Poulos, T. L. *Biochemistry* **2004**, *43*, 8826.

[46] de Visser, S. P.; Shaik, S.; Sharma, P. K.; Kumar, D.; Thiel, W. *J. Am. Chem. Soc*. **2003**, *125*, 15779.

[47] Wang, Y.; Hirao, H.; Chen, H.; Onaka, H.; Nagano, S.; Shaik, S. *J. Am. Chem. Soc*. **2008**, *130*, 7170.

[48] Derat, E.; Shaik, S. *J. Phys. Chem. B* **2006**, *110*, 10526.

[49] Derat, E.; Shaik, S. *J. Am. Chem. Soc.* **2006**, *128*, 940.

[50] Wang, Y.; Chen, H.; Makino, M.; Yoshitsugu, S.; Nagano, S.; Asamizu, S.; Onaka, H.; Shaik, S. *J. Am. Chem. Soc.* **2009**, *131*, 6748.

[51] Staalduinen, L. M.; Bhattacharya, A.; Groom, K.; Zechel, D.L.; Zongchao, J. *Acta Cryst*. **2007**, *F63*, 980.

[52] Ryan, K. S.; Howard-Jones, A. R.; Hamill, M. J.; Elliott, S. J.; Walsh, C. T.; Drennan, C. L. *Proc. Natl. Acad. Sci*. **2007**, *104*, 15311.

[53] Martin, J. L. *Structure (London)* **1995**, *3*, 245.

[54] Gatti, D. L.; Palfey, B. A.; Lah, M. S.; Entsch, B.; Massey, V.; Ballou, D. P.; Ludwig, M. L. *Science* **1994**, *266*, 110.

[55] Enroth, C. *Acta Crystallogr. D*. **2003**, *59*, 1597.

[56] Ryan, K. S.; Chakraborty, S.; Howard-Jones, A. R.; Walsh, C. T.; Ballou, D. P.; and Drennan, C. L. *Biochemistry.* **2008**, *47*, 13506.

[57] Zhang, C.; Albermann, C.; Fu, X.; Peters, N. R.; Chisholm, J. D.; Zhang, G.; Gilbert, E. J.; Wang, P. G.; Van Vranken, D. L.; Thorson, J. *ChemBioChem*. **2006**, *7*, 795.

[58] Singh, S.; McCoy, J. G.; Zhang, C.; Bingman, C. A.; Phillips, G. N. Jr.; Thorson, J. S. *J. Biol. Chem.* **2008**, *283*, 22628.

[59] Prade, L.; Engh, R. A.; Girod, A.; Kinzel, V.; Huber, R.; Bossemeyer, R. *Structure* **1997**, *5*, 1627.

[60] Tamaoki, T.; Nomoto, H.; Takahashi, I.; Kato, Y.; Morimoto, M.; Tomita, F. *Biochem. Biophys. Res. Commun*. **1986**, *135*, 397.

[61] Onaka, H.; Taniguchi, S.; Igarashi, Y.; Furumai, T. *J. Antibiot*. **2002**, *55*, 1063.

[62] Madduri, K.; Hutchinson, C. R. *J Bacteriol*. **1995**, *177*, 1208.

[63] Chiu, H-T.; Chen, Y-L.; Chen, C-Y.; Jin, C.; Lee, M-N.; Lin, Y-C. *Mol. BioSyst*. **2009**, *5*, 1180.

[64] Chiu, H-T.; Lin, Y-C.; Lee, M-N.; Chen, Y-L.;Wang, M-S.; Lai, C-C. *Mol. BioSyst*. **2009**, *5*, 1191.

[65] Fang-Yuan, C. ; Brady, S. F. *J. Am. Chem. Soc*. **2011**, *133*, 9996.

[66] Salas, J. A.; Mendez, C. *Curr. Opin. Chem. Biol*. **2009**, *13*, 152.

[67] Sánchez, C.; Zhu, L.; Braña, A. F.; Salas, A. P.; Rohr, J.; Méndez, C.; Salas, J. A. *Proc. Natl. Acad. Sci*. **2005**, *104*, 461.

[68] Zehner, S.; Kotzsch, A.; Bister, B.; Süssmuth, R. D.; Méndez, C.; Salas, J. A.; van Pée, K.-H. *ChemBiol*. **2005**, *12*, 445.

[69] van Pée, K.-H. *Arch. Microbiol.* **2001**, *175*, 250.

[70] Sánchez, C.; Méndez, C.; Salas, J. A. *J Ind. Microbiol. Biotechnol*. **2006**, *33*, 560.

[71] Salas, J. A.; Méndez, C. *Curr. Opin. Chem. Biol*. **2009**, *13*, 152.

[72] Sánchez, C.; Salas, A. P.; Braña, A. F.; Palomino, M.; Pineda-Lucena, A.; Carbajo, R. J.; Méndez, C.; Moris, F.; Salas, J. A. *Chem. Commun*. **2009**, *27*, 4118.

[73] Knölker, H.J.; Reddy, K. R. *Chem. Rev*. **2002**, *102*, 4303.

[74] Bhide, G. V.; Tikotkar, N. L.; Tilak, B. D. *Chem. Ind. (London)* **1957**, 363.

[75] Mann, F. G.; Willcox, T. J. *J. Chem. Soc*. **1958**, 1525.

[76] Royer, H.; Joseph, D.; Prim, D.; Kirsch, G. *Synth. Commun*. **1998**, *28*, 1239.

[77] Bergman, J.; Pelcman, B. *J. Org. Chem.* **1989**, *54*, 824.

[78] Merlic, C. A.; McInnis, D. M. *Tetrahedron Lett*. **1997**, *38*, 7661.

[79] Bergman, J.; Venemalm, L. *J. Org. Chem*. **1992**, *57*, 2495.

[80] Bocchi, V.; Palla, G. *Synthesis* **1982**, 1096.

[81] Rajeshwaran, G. G.; Mohanakrishnan, A. K. *Org. Lett.* **2011**, *13*, 1418.

[82] Reddy, G. M.; Chen, S.Y.; Uang, B.-J. *Synthesis* **2003**, *4*, 497. b) Bergman, J.; Koch, E.; Pelcman, B. *Perkin 1*, **2000**, *16*, 2609. c) Harris, W.; Hill, C. H.; Keech, E.; Malsher, P. *Tetrahedron Lett*. **1993**, *34*, 8361. d) Wang, K.; Liu, Z. *Synth. Comm*. **2010**, *40*, 144. e) Nakazono, M.; Nanbu, S.; Uesaki, A.; Kuwano, R.; Kashiwabara, M.; Zaitsu, K. *Org. Lett*. **2007**, *9*, 3583.

[83] Wilson, L. J.; Malaviya, R.; Yang, C.; Argentieri, R.; Wang, B.; Chen, X.; Murray, W.V.; Cavender, D. *Bioorg. Med. Chem. Lett*. **2009**, *19*, 3333. b) Wilson, L. J.; Murray, W. V.; Yang, S.-M.; Yang, C.; Wang, B. U.S. Pat. Appl. Publ., 20070249590, 2007. c) Yang, S.-M.; Malaviya, R.; Wilson, L. J.; Argentieri, R.; Chen, X.; Yang, C.; Wang, B.; Cavender, D.; Murray, W.V. *Bioorg. Med. Chem. Lett*. **2007**, *17*, 326.

[84] Gallant, M.; Link, J. T.; Danishefsky, S. J. *J. Org. Chem*. **1993**, *58*, 343.

[85] a) Wood, J. L.; Stoltz, B. M.; Dietrich, H.-J. *J. Am. Chem. Soc*. **1995**, *117*, 10413. b) Wood, J. L.; Stoltz, B. M.; Dietrich, H.-J.; Pflum, D. A.; Petsch, D. T. *J. Am. Chem. Soc.* **1997**, *119*, 9641.

[86] Bergman, J.; Koch, E.; Pelcman, B. *Tetrahedron* **1995**, *51*, 5631.

[87] McCombie, S. W.; Bishop, R. W.; Carr, D.; Dobek, E.; Kirkup, M. P.; Kirschmeier, P.; Lin, S. I.; Petrin, J.; Rosinski, K.; Shankar, B. B.; Wilson, O. *Bioorg. Med. Chem.* **1993**, *3*, 1537.

[88] Weygand, F.; Steglich, W.; Bjarnason, J.; Akhtar, R.; Khan, N. M. *Tetrahedron Lett*. **1966**,

29, 3483.

[89] Link, J. T.; Raghavan, S.; Gallant, M.; Danishefsky, S. J.; Chou, T. C.; Ballas, L. M. *J. Am. Chem. Soc*. **1996**, *118*, 2825.

[90] Wood, J. L.; Stoltz, B. M.; Goodman, S. N. *J. Am. Chem. Soc*. **1996**, *118*, 10656.

[91] Wood, J. L.; Stoltz, B. M.; Goodman, S. N; Onwueme, K. *J. Am. Chem. Soc*. **1997**, *119*, 9652.

[92] Chang-Gu, H.; Bililign, T.; Liao, J.; Thorson, J. S. *ChemBioChem*. **2003**, *4*, 114.

[93] Cole, L. J., Entsch, B., Ortiz-Maldonado, M., Ballou, D. P. *Biochemistry* **2005**, *44*, 14807.

[94] Enroth, C., Neujahr, H., Schneider, G., Lindqvist, Y. *Structure* **1998**, *6*, 605.

[95] Asamizu, S.; Shiro, Y.; Igarashi, Y.; Nagano, S.; Onaka, H. *Biosci. Biotechnol. Biochem*. **2011**, *75*, 2184.

[96] Goldman,P. J.; Ryan, K. S.; Hamill, M. J.; Howard-Jones, A. R.; Walsh, C. T.; Elliott, S. J.; Drennan, C. L. *Chemistry & Biology* **2012**, *19*, 855.

[97] a) Groom, K.; Bhattacharya, A.; Zechel, D. L. *Chem. Bio. Chem*. **2011**, *12*, 396.

[98] Sambrook, J.; Russell, D. W. in *Molecular Cloning:A Laboratory Manual* (3rd ed.). Cold Spring Harbor Laboratory Press: New York, 2001

[99] a) Howard-Jones, A. R.; Walsh, C. T. *J. Am. Chem. Soc*. **2006**, *128*, 12289. b) Yong, W., Hajime, H., Hui, C., Hiroyasu, O., Shingo, N., Sason, S. *J. Am. Chem. Soc*. **2008**, *130*, 7170. c) Yong, W., Hui, C., Masatomo, M., Yoshitsugu, S., Shingo, N., Shumpei, A., Onaka, H., Sason, S. *J. Am. Chem. Soc*. **2009**, *131*, 6748.

[100] a) Funa, N.; Funabashi, M.; Ohnishi, Y.; Horinouchi, S. *J. Bacteriol*. **2005**, *187*, 8149. b) Zhao, B. et al. *J. Biol. Chem*. **2005**, *280*, 11599. c) Zerbe, K.; Woithe, K.; Li, D. B.; Vitali, F.; Bigler, L.; Robinson, J. A. *Angew. Chem. Int. Ed*. **2004**, *43*, 6709. d) Woithe, K.; Geib, N.; Zerbe, K.; Li, D.B.; Heck, M.; Fournier-Rousset, S.; Meyer, O.; Vitali, F.; Matoba, N.; Abou-Hadeed, K.; Robinson, J. A. *J. Am. Chem. Soc*. **2007**, *129*, 6887.

[101] Nishizawa, T.; Grüschow, S.; Jayamaha, D.-H. E.; Nishizawa-Harada, C.; Sherman, D. H. *J. Am. Chem. Soc*. **2006**, *3*, 724.

[102] Mundle, S. O. C.; Lacrampe-Couloume, G.; Sherwood, L. B.; Kluger, R. *J. Am. Chem. Soc*. **2010**, *132*, 2430.

[103] Fröde, R.; Hinze, C.; Josten, I.; Schmidt, B.; Steffan, B.; Steglich, W. *Tetrahedron Lett*. **1994**, *35*, 1689.

[104] Hinze, C.; Kreipl, A.; Terpin, A.; Steglich, W. *Synthesis* **2007**, *4*, 608.

[105] Liangfeng, F.; Gribble, G. W. *Tetrahedron Lett*. **2010**, *51*, 537.

[106] (a) Huang, Q.; Larock, R. C. *J. Org. Chem*. **2003**, *68*, 7342. (naphthalenes and carbazoles) (b) Zhang, H.; Larock, R. C. *Org. Lett*. **2001**, *3*, 3083. (carbolines) (c) Roesch, K. R.; Zhang, H.; Larock, R. C. *J. Org. Chem*. **2001**, *66*, 8042. (isoquinolines and pyridines) (d) Larock, R. C.; Doty, M. J.; Han, X. *J. Org. Chem*. **1999**, *64*, 8770. (isocoumarins and pyrones) (e) Zeni, G.; Larock, R. C. *Chem. Rev*. **2004**, *104*, 2285, and the references cited therein.

[107] Kamenskii, A. B.; Smushkevich, Y. I.; Livshits, A. I.; Suvorov, N. N. *Chem. Heterocycl. Compd. (Engl. Transl.)* **1980**, *16*, 741.

[108] Roy, S.; Gribble, G. W. *Synth. Commun.* **2007**, *37*, 829.

[109] Han, X., in *Name Reactions for Homologations*, Li, J. J. Ed.; Wiley: New Jersey, **2009**; Part 1, pp. 393.

[110] Gribble, G. W.; Jiang, J.; Liu, Y. *J. Org. Chem*. **2002**, *67*, 1001.

[111] Oakdale, J. S.; Boger, D. L. *Org. Lett*. **2010**, *12*, 1132.

[112] Sakamoto, T.; Funami, N.; Kondo, Y.; Yamanaka, H. *Heterocycles* **1991**, *32*, 1387.

[113] Heldmann, D. K.; Sauer, J. *Tetrahedron Lett*. **1997**, *38*, 5791.

[114] Sauer, J.; Heldmann, D. K.; Hetzenegger, J.; Sichert, H.; Schuster, J. *Eur. J. Org. Chem*. **1998**, 2885.

[115] Han, X.; Stolz, B. M.; Corey, E. J. *J. Am. Chem. Soc.* **1999**, *121*, 7600.

[116] Fürstner, A.; Krause, H.; Thiel, O. R. *Tetrahedron* **2002**, *58*, 6373.

[117] Yang, C.-G.; Liu, G.; Jiang, B. *J. Org. Chem*. **2002**, *67*, 9392.

[118] Howard-Jones, A. R.; Walsh, C. T. *Biochemistry* **2005**, *44*, 15652.

[119] Asamizu, S.; Kato, Y.; Igarashi, Y.; Furumai, T.; Onaka, H. *Tetrahedron Lett*. **2006**, *47*, 473.

[120] Chae, C.-S.; Park, J-S.; Chung, S.-C.; Kim, T.-I.; Lee, S.-H.; Yoon, K.-M.; Shin, J.; Oh, K.-B. *Bioorg. Med. Chem. Lett*. **2009**, *19*, 1581.

[121] Chiu, H-T.; Lin, Y-C.; Meng-Na, L.; Chen, Y-L.; Wang, M-S.; Lai, C-C. *Mol. BioSyst*., **2009**, *5*, 1192.

[122] Sánchez, C.; Zhu, L.; Braña, A. F.; Salas, A. P.; Rohr, J.; Méndez, C.; Salas, J. A. *Proc. Natl. Acad. Sci. U.S.A.* **2005**, *102*, 461.

[123] Andersen, R. J.; Faulkner, D. J.; He, C.-H.; Van, Duyne, G. D.; Clardy, J. *J. Am. Chem. Soc.* **1985**, *107*, 5492.

[124] a) Pla, D.; Albericio, F.; Alvarez, M. *MedChemComm.* **2011**, *2*, 689. b) Fukuda, T.; Ishibashi, F.; Iwao, M. *Heterocycles* **2011**, *83*, 491. c) Fan, A-L.; Lin, W-H.; Jia, Y.-X. *J. Chin. Pharm. Sci*. **2011**, *20*, 425. d) Fan, H.; Peng, J.; Hamann, M. T.; Hu, J.-F. *Chem. Rev.*, **2008**, *108*, 264. e) Kluza, J.; Marchetti, P.; Bailly, C. in *Modern Alkaloids*, Fattorusso, E., Taglialatela-Scafati, O. Eds.; Wiley-VCH: Weinheim, **2008**; pp. 171-187. f) Handy, S. T.; Zhang, Y. *Org. Prep. Proc. Int.* **2005**, *37*, 411. g) Cironi, P.; Albericio, F.; Álvarez, M. in *Progress in Heterocyclic Chemistry*, Gribble, G. W., Joule, J. A. Eds.; Pergamon: Oxford, U.K., **2004**; Vol. 16, pp. 1-26.

[125] a) Carroll, A. R.; Bowden, B. F.; Coll, J. C. *Australian J. Chem.* **1993**, *46*, 489. b) A. R. Quesada, A. R.; Gravalos, M. D. G.; Puentes, J. L. F. *Brit. J. Cancer* **1996**, 74, 675.

[126] Hwang, Y.; Rhodes, D.; Bushman, F. *Nucleic Acids Res.* **2000**, *28*, 4884.

[127] a) Fürstner, A.; Krause, H.; Thiel, O. R. *Tetrahedron* **2002**, *58*, 6373. b) Boger, D. L.; Soenen, D. R.; Boyce, C. W.; Hedrick, M. P.; Jin, Q. *J. Org. Chem.*, **2000**, *65*, 2479. c) Gupton, J. T.; Clough, S. C.; Miller, R. B.; Lukens, J. R.; Henry, C. A.; Kanters, R. P. F.; Sikorski, J. A. *Tetrahedron* **2003**, *59*, 207. d) Hamasaki, A.; Zimpleman, J. M.; Hwang, I.; Boger, D. L. *J. Am. Chem. Soc*. **2005**, *127*, 10767. e) Chou, T.-C.; Guan, Y. B.; Soenen, D. R.; Danishefsky, S. J.; Boger, D. L. *Cancer Chemother. Pharmacol.* **2005**, *56*, 379.

[128] For biomimetic total syntheses of lamellarins and related natural products, see; (a) Heim, A.; Terpin, A.; Steglich, W. *Angew. Chem., Int. Ed.* **1997**, *36*, 155. (b) Peschko, C.; Winklhofer, C.; Steglich, W. *Chem. Eur. J.* **2000**, *6*, 1147. (c) Peschko, C.; Winklhofer, C.; Terpin, A.; Steglich,W. *Synthesis* **2006**, 3048. (d) Winklhofer, C.; Terpin, A.; Peschko, C.; Steglich, W. *Synthesis* **2006**, *18*, 3043. (d) Kreipl, A. T.; Reid, C.; Steglich, W. *Org. Lett.* **2002**, *4*, 3287. (e) Hinze, C.; Kreipl, A.; Terpin, A.; Steglich, W. *Synthesis* **2007**, 608. (f) Terpin, A.; Polborn, K.; Steglich, W. *Tetrahedron* **1995**, *51*, 9941. (g) Li, Q.; Jiang, J.; Fan, A.; Cui, Y.; Jia, Y. *Org. Lett*. **2011**, *13*, 312.

[129] For lamellarin synthesis using intramolecular cyclizations of isoquinoline ylides, see; (a) Ishibashi, F.; Miyazaki, Y.; Iwao, M. *Tetrahedron* **1997**, *53*, 5951. (b) Banwell, M.; Flynn, B.; Hockless, D. *Chem. Commun.* **1997**, 2259. (c) Flynn, B.; Banwell, M. *Heterocycles* **2012**, *84*,

1141. (d) Cironi, P.; Manzanares, I.; Albericio, F.; Álvarez, M. *Org. Lett*. **2003**, *5*, 2959. (e) Liermann, J. C.; Opatz, T. *J. Org. Chem*. **2008**, *73*, 4526.

[130] For synthesis of lamellarins and related natural products using Suzuki-Miyaura cross-coupling, see; (a) Iwao, M.; Takeuchi, T.; Fujikawa, N.; Fukuda, T.; Ishibashi, F. *Tetrahedron Lett*. **2003**, *44*, 4443. (b) Fujikawa, N.; Ohta, T.; Yamaguchi, T.; Fukuda, T.; Ishibashi, F.; Iwao, M. *Tetrahedron* **2006**, *62*, 594. (c) Ohta, T.; Fukuda, T.; Ishibashi, F.; Iwao, M. *J. Org. Chem.* **2009**, *74*, 8143. (d) Yamaguchi, T.; Fukuda, T.; Ishibashi, F.; Iwao, M. *Tetrahedron Lett*. **2006**, *47*, 3755. (e) Fukuda, T.; Ohta, T.; Saeki, S.; Iwao, M. *Heterocycles* **2010**, *80*, 841. (f) Kamiyama, H.; Kubo, Y.; Sato, H.; Yamamoto, N.; Fukuda, T.; Ishibashi, F.; Iwao, M. *Bioorg. Med. Chem*. **2011**, 7541. (g) Fukuda, T.; Sudo, E-i.; Shimokawa, K.; Iwao, M. *Tetrahedron* **2008**, *64*, 328. (h) Handy, S. T.; Zhang, Y.; Bregman, H. *J. Org. Chem.* **2004**, 69, 2362. (i) Pla, D.; Marchal, A.; Olsen, C. A.; Albericio, F.; Álvarez, M. *J. Org. Chem*. **2005**, *70*, 8231. (j) Hasse, K.; Willis, A. C.; Banwell, M. G. *Eur. J. Org. Chem*. **2011**, 88.

[131] Belanger, P. *Tetrahedron Lett.* **1979**, *27*, 2505.

[132] Boger, D. L.; Soenen, D. R.; Boyce, C. W.; Hedrick, M. P.; Jin, Q. *J. Org. Chem.* **2000**, *65*, 2479.

[133] For synthesis of lamellarins and related natural products using vinylogous iminium salts and microwave-accelerated Vilsmeier-Haack formylations, see; (a) Gupton, J.; Banner, E.; Scharf, A.; Norwood, B.; Kanters, R.; Dominey, R.; Hempel, J.; Kharlamova, A.; Bluhn-Chertudi, I.; Hickenboth, C.; Little, B.; Coppock, M.; Krumpe, K.; Burnham, B.; Holt, H.; Du, K.; Keertikar, K.; Diebes, A.; Ghassemi, S.; Sikorski, J. *Tetrahedron* **2006**, *62*, 8243. (b) Gupton, J.; Miller, R.; Clough, S.; Krumpe, K.; Banner, E.; Kanters, R.; Du, K.; Keertikar, K.; Lauerman, N.; Solano, J.; Adams, B.; Callahan, D.; Little, B.; Scharf, A.; Sikorski, J. *Tetrahedron* **2005**, *61*, 1845. (c) Gupton, J.; Clough, S.; Miller, R.; Lukens, J.; Henry, C.; Kanters, R.; Sikorski, J. *Tetrahedron* **2003**, *59*, 207. (d) Gupton, J.; Giglio, B.; Eaton, J.; Rieck, E.; Smith, K.; Keough, M.; Barelli, P.; Firich, L.; Hempel, J.; Smith, T.; Kanters, R. *Tetrahedron* **2009**, *65*, 4283; (e) Gupton, J.; Giglio, B.; Eaton, J.; Rieck, E.; Smith, K.; Keough, M.; Barelli, P.; Firich, L.; Hempel, J.; Smith, T.; Kanters, R. *Tetrahedron* **1999**, *55*, 14515.

[134] Gupton, J. T.; Banner, E. J.; Sartin, M. D.; Coppock, M. B.; Hempel, J. E.; Kharlamova, A.; Fisher, D. C.; Giglio, B. C.; Smith, K. L.; Keough, M. J.; Smith, T. M.; Kanters, R. P. F.; Dominey, R. N.; Sikorski, J. A. *Tetrahedron* **2008**, *64*, 5246.

[135] Knölker, H-J.; Reddy, K. R. *Chem. Rev*. **2002**, *102*, 4303.

[136] Sánchez, C.; Méndez, C.; Salas, J. A. *Nat. Prod. Rep*. **2006**, *23*, 1007.

[137] Bailly, C.; Riou, J-F.; Colson, P.; Houssier, C.; Rodrigues-Pereira, E.; Prudhomme, M. *Biochemistry* **1997**, *36*, 3197.

[138] a) Kaneko, T.; Wong, H.; Utzig, H.; Schurig, J.; Doyle, T. *J. Antibiot*. **1990**, *43*, 125. b) Long, B. H.; Rose, W. C.; Vyas, D. M.; Matson, J. A.; Forenza, S. *Curr. Med. Chem.: Anti-Cancer Agents* **2002**, *2*, 255. c) Rewcastle, G. W. *IDrugs* **2005**, *8*, 838. d) Bailly, C.; Qu, X.; Chaires, J. B.; Colson, P.; Houssier, C.; Ohkubo, M., Nishimura, S., Yoshinari, T. *J. Med. Chem.* **1999**, *42*, 2927. e) Ohkubo, M.; Nishimura, T.; Honma, T.; Nishimura, I.; Ito, S.; Yoshinari, T.; Arakawa, H.; Suda, H.; Morishima, H.; Nishimura, S. *Bioorg. Med. Chem. Lett.*, **1999**, *9*, 3307. f) Goosens, J. F.; Kluza, J.; Vezin, H.; Kouach, M.; Briand, G.; Baldeyrou, B.; Wattez, N.; Bailly, C. *Biochem. Pharmacol.*, **2003**, *65*, 25. g) Pereira, E. R.; Belin, L.; Sancelme, M.; Prudhomme, M.; Ollier, M.; Rapp, M.; Sevère, D.; Riou, J-F.; Fabbro, D.; Meyer, T. *J. Med. Chem.* **1996**, *39*, 4471.

[139] a) Anizon, F.; Belin, L.; Moreau, P.; Sancelme, M.; Voldoire, A.; Prudhomme, M.; Ollier, M.; Sevère, D.; Riou, J-F.; Bailly, C.; Fabbro, D.; Meyer, T. *J. Med. Chem*. **1997**, *40*, 3456. b) Ohkubo, M.; Nishimura, T.; Kawamoto, H.; Nakano, M.; Honma, T. et al. *Bioorg. Med. Chem. Lett*. **2000**, *10*, 419. c) Bailly, C.; Qu, X.; Anizon, F.; Prudhomme, M.; Riou, J.-F.; Chaires, J. B. *Mol. Pharm*. **1999**, *55*, 377. d) Anizon, F.; Moreau, P.; Sancelme, M.; Laine, W.; Bailly, C; Prudhomme, M. *Bioorg. Med. Chem*. **2003**, *11*, 3709. e) Animati, F.; Berettoni, M.; Bigioni, M.; Binaschi, M.; Felicetti, P.; Gontrani, L.; Incani, O.; Madami, A.; Monteagudo, E.; Olivieri, L.; Resta, S.; Rossi, C.; Cipollone, A. *ChemMedChem*. **2008**, *3*, 266. f) Marminon, C.; Anizon, F.; Moreau, P.; Léonce, S.; Pierré, A.; Pfeiffer, B.; Renard, P. and Prudhomme, M. *J. Med. Chem*. **2002**, *45*, 1330. g) Moreau, P.; Gaillard, N.; Marminon, C.; Anizon, F; Dias, N.; Baldeyrou, B.; Bailly, C.; Pierré, A.; Hickman, J.; Pfeiffer, B.; Renard, P.; Prudhomme, M. *Bioorg. Med. Chem*. **2003**, *11*, 4871. h) Zhang, G.; Shen, J.; Cheng, H.; Zhu, L.; Fang, L.; Luo, S.; Muller, M. T.; Lee, G. E.; Wei, L.; Du, Y.; Sun, D.; Wang, P. G. *J. Med. Chem*. **2005**, *48*, 2600.

[140] a) Mahboobi, S.; Burgemeister, T.; Dove, S.; Kuhr, S.; Popp, A. *J. Org. Chem.* **1999**, *64*, 8130. b) Brenner, M.; Mayer, G.; Terpin, A.; Steglich, W. *Chem. Eur. J.* **1997**, *3*, 70. c) Bourderioux, A.; Ouach, A.; Bénéteau, V.; Mérour, J.-Y.; Routier, S. *Synthesis* **2010**, *7*, 783.

[141] Gadbois, D. M.; Hamaguchi, J. R.; Swank, R. A.; Bradbury, E. M. *Biochem. Biophys. Res. Commun.* **1992**, *184*, 80.

[142] Kawakami, K.; Futami, H.; Takahara, J.; Yamaguchi, K. *Biochem. Biophys. Res. Commun.* **1996**, *219*, 778.

[143] a) Meijer, L.; Kim, S. H. *Methods Enzymol*. **1997**, *283*, 113; b) Webster, K. R.; Kimball, S. D. *Emerg. Drugs* **2000**, *5*, 45.

[144] Long, B. H.; Rose, W. C.; Vyas, D. M.; Matson, J. A.; Forenza S. *Curr. Med. Chem.: Anti-Cancer Agents* **2002**, *2*, 255.

[145] Balasubramanian, B. N.; St. Laurent, D. R.; Saulnier, M. G.; Long, B. H.; Bachand, C.; Beaulieu, F.; Clarke, W.; Deshpande, M.; Eummer, J.; Fairchild, C. R.; Frennesson, D. B.; Kramer, R.; Lee, F. Y.; Mahler, M.; Martel, A.; Naidu, B. N.; Rose, W. C.; Russell, J. *J. Med. Chem.* **2004**, *47*, 1609.

[146] Saulnier, M. G.; Balasubramanian, B. N.; Long, B. H.; Frennesson, D. B.; Ruediger, E.; Zimmermann, K.; Eummer, J. T.; St. Laurent, D. R.; Stoffan, K. M.; Naidu, B. N.; Mahler, M.; Beaulieu, F.; Bachand, C.; Lee, F. Y.; Fairchild, C. R.; Stadnick, L. K.; Rose, W. C.; Solomon, C.; Wong, H.; Martel, A.; Wright, J. J.; Kramer, R.; Langley, D. R.; Vyas, D. M. *J. Med. Chem.* **2005**, *48*, 2258.

[147] Badenock, J. C.; Barden, T. C.; Berthel, S. J.; Firooznia, F.; Fu, L.; Gribble, G. W.; Kester, R. F.; Kishbaugh, T. L. S.; Li, J. J.; Pelkey, E. T.; Russel, J. S.; Sundberg, R. J.; Wu, Y.-J. in *Topics in Heterocyclic Chemistry*; *Heterocyclic scaffolds II: Reactions and Applications of Indole*, Maes, Bert. U. W. Ed.; Springer: Heidelberg, **2010**; Vol. 26, pg. 23.

[148] Moreau, P.; Gaillard, N.; Marminon, C.; Anizon, F; Dias, N.; Baldeyrou, B.; Bailly, C.; Pierré, A.; Hickman, J.; Pfeiffer, B.; Renard, P.; Prudhomme, M. *Bioorg. Med. Chem*. **2003**, 4871.

[149] a) Faul, M. M.; Winneroski, L. L.; Kumrich, C. A. *Tetrahedron Lett*. **1999**, *40*, 1109. b) Sanchez-Martinez, C.; Faul, M. M.; Chuan, S.; Sullivan, K. A.; Grutsch, J. L.; Cooper, J. T.; Kolis. S. P. *J. Org. Chem*. **2003**, *68*, 8008. c) Peifer, C.; Stoiber, T.; Unger, E.; Totzke, F.; Schächtele, C.; Marmé, D.; Brenk, R.; Klebe, G.; Schollmeyer, D.; Dannhardt. G. *J. Med. Chem*. **2006**, *49*, 1271.

[150] Zhu, G.; Conner, S. E.; Zhou, X.; Shih, C.; Li, T.; Anderson, B. D.; Brooks, H. B.; Morris, R.; Campbell, E. C.; Dempsey, J. A.; Faul, M, M.; Ogg, C.; Patel, B.; Schultz, R. M.; Spencer, C. D.; Teicher, B.; Watkins, S. A. *J. Med. Chem.* **2003**, *46*, 2027.

[151] Sanchez-Martinez, C.; Shih, C.; Faul, M. M.; Zhu, G.; Paal, M.; Somoza, C.; Li, T.; Kumrich, C. A.; Winneroski, L. L.; Xun, Z.; Brooks, H. B.; Patel, B. K. R.; Schultz, R. M.; DeHahn, T. B.; Spencer, C. D.; Watkins, S. A.; Considine, E.; Dempsey, J. A.; Ogg, C. A.; Campbell, R. M.; Anderson, B. A.; Wagner, J. *Bioorg. Med. Chem. Lett*. **2003**, *13*, 3835.

[152] Sanchez-Martinez, C.; Faul, M. M.; Shih, C.; Sullivan, K. A.; Grutsch, J. L.; Cooper, J. T.; Kolis, S. P. *J. Org. Chem*. **2003**, *68*, 8009.

[153] Routier, S.; Peixoto, P.; Mérour, J-Y.; Coudert, G.; Dias, N.; Bailly, C.; Pierré, A.; Léonce, S.; Caignard, D-H. *J. Med. Chem.* **2005**, *48*, 1401.

[154] Hudkins, R. L.; Johnson, N. W.; Angeles, T. S.; Gessner, G. W.; Mallamo, J. P. *J. Med. Chem*. **2007**, *50*, 433.

[155] Routier, S.; Mérour, J-Y.; Dias, N.; Lansiaux, A.; Bailly, C.; Lozach, O.; Meijer, L. *J. Med. Chem*. **2006**, *49*, 789.

[156] Routier, S.; Coudert, G.; Mérour, J-Y.; Caignard, D-H. *Tetrahedron Lett*. **2002**, *43*, 2561.

[157] Arimondo, P. B.; Baldeyrou, B.; Laine, W.; Bal, C.; Alphonse, F. A.; Routier, S.; Coudert, G.; Mérour, J. Y.; Colson, P.; Houssier, C.; Bailly, C. *Chem. Biol. Int*. **2001**, 138, 59.

[158] Routier, S.; Ayerbe, N.; Mérour, J-Y.; Coudert, G.; Bailly, C.; Pierre, A.; Pfeiffer, B.; Caignard, D-H.; Renard, P. *Tetrahedron* **2002**, *58*, 6621.

[159] Marminon, C.; Pierré, A.; Pfeiffer, B.; Pérez, V.; Léonce, S.; Joubert, A.; Bailly, C.; Renard, P.; Hickman, J.; Prudhomme, M. *J. Med. Chem*. **2003**, *46*, 609.

[160] Messaoudi, S.; Anizon, F.; Léonce, S.; Pierré, A.; Pfeiffer, B.; Prudhomme, M. *Eur. J. Med. Chem*. **2005**, *40*, 961.

[161] Messaoudi, S.; Anizon, F.; Pfeiffer, B.; Prudhomme, M. *Tetrahedron* **2005**, *61*, 7304.

[162] Messaoudi, S.; Anizon, F.; Pfeiffer, B.; Golsteyn, R.; Prudhomme, M. *Tetrahedron Lett*. **2004**, *45*, 4643.

[163] Marminon, C.; Pierré, A.; Pfeiffer, B.; Pérez, V.; Léonce, S.; Renard, P.; Prudhomme, M. *Bioorg. Med. Chem*. **2003**, *11*, 679.

[164] Lefoix, M.; Coudert, G.; Routier, S.; Pfeiffer, B.; Caignard, D.-H.; Hickman, J.; Pierré, A.; Golsteyn, R. M.; Léonce, S.; Bossard, C.; Mérour. J.-Y. *Bioorg. Med. Chem*. **2008**, *16*, 5303.

[165] Jiang, X.; Zhao, B.; Britton, R.; Lim, L.Y.; Leong, D.; Sanghera, J. S.; Zhou, B-B. S.; Piers, E.; Andersen, R. J.; Roberge, M. *Mol. Cancer Ther*. **2004**, 1221.

[166] For reviews, see: a) Henon, H.; Conchon, E.; Hugon, B.; Messaoudi, S.; Golsteyn, R. M. *Anticancer Agents Med. Chem*. **2008**, *8*, 577. b) Deslandes, S.; Chassaing, S.; Delfourne, E. *Mar. Drugs* **2009**, *7*, 754.

[167] Bregman, H.; Williams, D. S.; Atilla, E.; Carroll, P. J.; Meggers, E. *J. Am. Chem. Soc*. **2004**, *126*, 13594.

[168] Cohen, P.; Goedert, M. *Nat. Rev. Drug Discov.* **2004**, *3*, 479.

[169] Atilla-Gokcumen, G.E.; Williams, D.S.; Bregman, H.; Pagano, N.; Meggers, E. *ChemBioChem* **2006**, *7*, 1443.

[170] Bregman, H.; Meggers, E. *Org. Lett*. **2006**, *8*, 5465.

[171] Atilla-Gokcumen, G.E.; Pagano, N.; Streu, C.; Maksimoska, J.; Filippakopoulos, P.; Knapp, S.; Meggers, E. *ChemBioChem* **2008**, *9*, 2933.

[172] Hugon, B.; Anizon, F.; Bailly, C.; Golsteyn, R. M.; Pierre, A.; Leonce, S.; Hickman, J.; Pfeiffer, B.; Prudhomme, M. *Bioorg. Med. Chem*. **2007**, *15*, 5965.

[173] Conchon, E.; Anizon, F.; Aboab, B.; Golsteyn, R. M.; Leonce, S.; Pfeiffer, B.; Prudhomme, M. *Bioorg. Med. Chem*. **2008**, *16*, 4419.

[174] Deslandes, S.; Chassaing, S.; Delfourne, E. *Tetrahedron Lett*. **2010**, *51*, 5640.

[175] Deslandes, S.; Lamoral-Theys, D.; Frongia, C.; Chassaing, S.; Bruyère, C.; Lozach, O.; Meijer, L.; Ducommun, B.; Kiss, R.; Delfourne, E. *Eur. J. Med. Chem*. **2012**, *54*, 626.

[176] Zhu, G.; Conner, S.; Zhou, X.; Shih, C.; Brooks, H.B.; Considine, E.; Dempsey, J.A.; Ogg, C.; Patel, B.; Schultz, R.M.; Spencer, C.D.; Teicher, B.; Watkins, S.A. *Bioorg. Med. Chem. Lett.* **2003**, *13*, 1231.

[177] Wang, J.; Soundarajan, N.; Liu, N.; Zimmermann, K.; Naidu, B. N. *Tetrahedron Lett*. **2005**, *46*, 907.

[178] Ayerbe, N.; Routier, S.; Gillaizeau, I.; Maiereanu, C.; Caignard, D.-H., Pierré, A.; Léonce, S.; Coudert, G. *Bioorg. Med. Chem. Lett*. **2010**, *20*, 4670.

[179] Sánchez, C.; Butovich, I. A.; Braña, A. F.; Rohr, J.; Méndez, C.; Salas, J. A. *Chemistry & Biology* **2002**, *9*, 519.

[180] a) Yeh, E.; Garneau, S.; Walsh, C. T. *PNAS* **2005**, *102*, 3960. b) Yeh , E.; Blasiak, l. C.; Koglin, A.; Drennan, K. A.; Walsh, C. T. *Biochemistry* **2007**, *46*, 1284. c) Nishiza, T.; Aldrich, C. C.; Sherman, D. H. *J. Bacteriol*. **2005**, *187*, 2084. d) Howard-Jones, A. R.; Walsh, C. T. *Biochemistry* **2005**, *44*, 15652. e) Howard-Jones, A. R.; Walsh, C. T. *J. Am. Chem. Soc*. **2006**, *128*, 12289.

[181] a) Green, L.; Chauder, B.; Snieckus, V. *J. Heterocycl. Chem*. **1999**, *36*,1453. B) Anctil, E. J.-G.; Snieckus, V. *J. Organomet. Chem*. **2002**, *653*, 150. c) Johansson Seechurn, C. C. C.; Kitching, M. O.; Thomas J. Colacot, T. J.; Snieckus, V. *Angew. Chem. Int. Ed*. **2012**, *51*, 5062. d) Schneider, C.; Broda, E.; Snieckus, V. *Org. Lett*. **2011**, *13*, 3588.

[182] a) Toshihiro, H.; Akiyo, Y.; Kyoko, A.; Shigeru, T.; Motoo, T.; Yoshinori, A. *Tetrahedron Lett.* **1994**, *35*, 2559. b) McArthur, K. A.; Mitchell, S. S.; Tsueng, G.; Rheingold, A.; White, D. J.; Grodberg, J.; Lam, K. S.; Potts, B. C. M. *J. Nat. Prod*. **2008**, *71*, 1732. c) Zhang, W.; Liu, Z.; Li, S.; Yang, T.; Zhang, Q.; Ma, L.; Tian, X.; Zhang, H.; Huang, C.; Zhang, S.; Ju, J.; Shen, Y.; Zhang, C. *Org. Lett*. **2012**, *14*, 3364.

[183] Mitchell, S, S.; Lam, K, S.; Potts, B. C.; Tsueng, G.; Grodberg, J.; White, D. J.; Reed, K. A. WO 2005070922 A2 20050804, **2005**.

[184] Donohoe T. J.; Thomas R. E. *Nat. Protoc.* **2007**, *2*, 1888.

[185] Schmuck, C. *Tetrahedron* **2001**, *57*, 3063.

[186] Chakraborty, T. K.; Udawant, S. P.; Roy, S.; Mohan, B. K.; Rao, K. S.; Dutta, S. K.; Kunwar, A. C. *Tetrahedron Lett*. **2006**, *47*, 4631.

[187] Kandil, S.; Biondaro, S.; Vlachakis, D.; Cummins, A-C.; Coluccia, A.; Berry, C.; Leyssen, P.; Johan, N.; Brancale, A. *Bioorg. Med. Chem. Lett*. **2009**, *19*, 2935.

[188] Muchowski, J. M.; Hess, P. *Tetrahedron Lett*. **1988**, *29*, 777.

[189] Khusnutdinov, R. I.; Baiguzina, A. R.; Mukminov, R. R.; Akhmetov, I. V.; Gubaidullin, I. M.; Spivak, S. I.; Dzhemilev, U. M. *Russ. J. Org. Chem.* **2010**, *46*, 1053.

[190] Davidsen, S. K.; Summers, J. B.; Michaelides, M. R.; Florjancic, A. S.; Guo, Y.; Sheppard, G. S.; Xu, L.; Holms, J. H.; Steinman; D. H. U.S. Patent 5,952,320 A1, **1999**.

[191] Yang, C.-G.; Liu, G.; Jiang, B. *J. Org. Chem*. **2002**, *67*, 9392.

[192] Personal communication with Prof. Alois Fürstner.

[193] For the synthesis of *N*-Ts indole using tetrabutylammonium hydrogen sulfate as phase-transfer catalyst, see: a) Berry, J. M.; Bradshaw, T. D.; Fichtner, I.; Ren, R.; Schwalbe, C. H.; Wells, G.; Chew, E.-H.; Stevens, M. F. G.; Westwell, A. D. *J. Med. Chem*. **2005**, *48*, 639. b) Simon, G.; Couthon-Gourves, H.; Haelters, J.P.; Corbel, B.; Kervarec, N.; Michaud, F.; Meijer, L. *J. Heterocycl. Chem*. **2007**, *4*, 793. c) Ramalingan, C.; Lee, I.-S.; Kwak, Y.-W. *Chem. & Pharm. Bull*. **2009**, *57*, 591. d) Wang, K.; Li, X.Y.; Chen, X. G.; Liu, Z.Z. *J. Asian Nat. Prod. Res*. **2010**, *12*, 36. e) Wang, K.; Liu, Z. *Synth. Commun*. **2010**, *40*, 144.

[194] For syntheses of *N*-Ts indole using triethylbenzylammonium chloride (TEBAC) as phase-transfer catalyst, see: a) Xu, H.; Wang, Y.-Y. *Bioorg. Med. Chem. Lett*. **2010**, *20*, 7274. b) Ran, J.-Q.; Huang, N.; Xu, H.; Yang, L.-M.; Lv, M.; Zheng, Y.-T. *Bioorg. Med. Chem. Lett*. **2010**, *20*, 3534. c) Fan, L.-L.; Liu, W.-Q.; Xu, H.; Yang, L.-M.; Lv, M.; Zheng, Y.-T. *Chem. Pharm. Bull*. **2009**, *57*, 797; for synthesis of *N*-Ts indole via direct deprotonation reactions, see: d) Potavathri, S.; Pereira, K. C.; Gorelsky, S.I.; Pike, A.; LeBris, A. P.; DeBoef, B. *J. Am. Chem. Soc*. **2010**, *132*, 14676; for synthesis of *N*-Ts indole via Pd-catalyzed *de novo* ring construction strategies, see: e) Nair, R. N.; Lee, P. J.; Reingold, A. R.; Grotjahn, D. B. *Chem.-Eur. J*. **2010**, *16*, 7992.

[195] Conway, S. C.; Gribble, G. *Heterocycles* **1990**, *30*, 627.

[196] Brown, R. D.; Buchanan, A. S.; Humffray, A. *Aust. J. Chem.* **1965**, *18*, 1521.

[197] Billingsley, K., Buchwald, S. L. *J. Am. Chem. Soc*. **2007**, *129*, 3358.

[198] a) Johnson, C. N.; Stempa, G.; Anandb, N.; Stephen, S. C.; Gallagher, T. *Synlett* **1998**, 1025. b) Tyrrell, E.; Brookes, P. *Synthesis* **2004**, *4*, 469.

[199] Larhed, M.; Hallberg, A. *J. Org. Chem*. **1996**, *61*, 9582.

[200] Barder, T. E.; Walker, S. D.; Martinelli, J. R.; Buchwald, S. L. *J. Am. Chem. Soc.* **2005**, *127*, 4685.

[201] Sandström, J. *Dynamic NMR Spectroscopy;* Academic Press: London, 1982.

[202] Killoran, J.; Gallagher, J.; Murphy, P. V.; O'Shea, D. *New. J. Chem*. **2005**, *29*, 1258.

[203] Merz, A.; Shropp, R.; Dötterl, E. *Synthesis* **1995**, 795.

[204] Fukuda, T.; Hayashida, Y.; Iwao, M. *Heterocycles* **2009**, *2*, 1105.

[205] Wang, K.; Liu, Z. *Synth. Comm*. **2010**, *40*, 144.

[206] Kozhevnikov, I. V. *React. Kinet. Catal. Lett*. **1976**, *5*, 415.

[207] a) Billingsley, K. L.; Anderson, K. W.; Buchwald, S. L. *Angew. Chem. Int. Ed*. **2006**, *45*, 484. b) Takagi, J.; Sato, K.; Hartwig, J. F.; Ishiyama, T., Miyaura, N. *Tetrahedron Lett*. **2002**, *43*, 649.c) Ayats, C.; Soley, R.; Albericio, F.; Alvarez, M. *Org. Biomol. Chem*. **2009**, *7*, 860. d) Del Grosso, A.; Singleton, P.J.; Muryn, C.A.; Ingleson, M. J. *Angew. Chem. Int. Ed*. **2011**, *50*, 2102.

[208] Knapp, D. M.; Gillis, E. P.; Burke, M. D. *J. Am. Chem. Soc*. **2009**, *131*, 6961.

[209] Kalinin, A. V.; Reed, M. A.; Norman, B. H.; Snieckus, V. *J. Org. Chem*. **2003**, *68*, 5992.

[210] Shertzer, H. G.; Genter, M. B.; Talaska, G.; Curran, C. P.; Nebert, D. W.; Dalton, T. P. *Carcinogenesis* **2007**, *28*, 1371.

[211] Schmuck, C.; Bickert, V.; Merschky, M.; Geiger, L.; Rupprecht, D.; Dudaczek, J.; Wich, P.; Rehm, T.; Machon, U. *Eur. J. Org. Chem*. **2008**, *2*, 324.

[212] Dubis,A. T.; Domagała, M.; Grabowski, S. J. *New. J. Chem*. **2010**, *34*, 556.

[213] Schmuck, C. *Tetrahedron* **2001**, *57*, 3063.

[214] Muchowski, J. M.; Hess, P. *Tetrahedron Lett.* **1988**, *29*, 777.

[215] Barker, P.; Gendler, P.; Rapoport, H. *J. Org. Chem*. **1978**, *43*, 4849.

[216] Hodge, P.; Rickards, R. W. *J. Chem. Soc*. **1965**, 459.

[217] Holme, K. R.; Hall, L. D. *Can. J. Chem*. **1991**, *69*, 585.

[218] Amat, M.; Hadida, S.; Sathyanarayana, S.; Bosch, J. *J. Org. Chem*. **1994**, *59*, 10

[219] Harrington, P. J.; Hegedus, L. S. *J. Org. Chem*. **1984**, *49*, 2658

[220] Neubert, A.; Barnes, D.; Kwak, Y.-S.; Nakajima, K.; Bebernitz, G. R.; Pola, G. M.; Kirman, L.; Serrano-Wu, M. H.; Stams, T. WO2007115058 A2, **2007**.

[221] Wittig, G.; Pockels, U.; Droge, H. *Chem. Ber*. **1938**, *71B*, 1903.

[222] Gilman, G.; Bebb, R.L. *J. Am. Chem. Soc*. **1939**, *61*, 109.

[223] a) Gschwend, H. W.; Rodriguez, H. R. in *Organic Reactions*; Dauben, W. G., Ed.; Robert E. Krieger Publishing Company: Malabar, FL, 1979; Vol. 26, p 1-360. b) Beak, P.; Snieckus, V. *Acc. Chem. Res*. **1982**, *15*, 306. c) Snieckus, V. *Chem. Rev*. **1990**, *90*, 879. d) Whisler, M. C.; MacNeil, S.; Snieckus, V.; Beak, P. *Angew. Chem. Int. Ed*. **2004**, *43*, 2206. e) Macklin, T. K.; Snieckus, V. in *Handbook of C-H Transformations*, Dyker, G. Ed.; Wiley-VCH: Weinheim, **2005**; Vol. 1, pp. 106-118.

[224] a) Puterbaugh, W. H.; Hauser, C. R. *J. Org. Chem*. **1964**, *29*, 853. b) Meyers, A. I.; Mihelich, E. D. *Tetrahedron* **1975**, *40*, 3158. c) Gschwend, H. W.; Hamden, A. *J. Org.Chem*. **1975**, *40*, 2008. d) Beak, P.; Brown, R. A. *J. Org. Chem*. **1977**, *42*, 1823. e) Comins, D. L.; Brown, J. D.; Mantlo, N. B. *Tetrahedron Lett*. **1982**, *23*, 3979. f) Mortier, J.; Moyroud, J.; Bennetau, B.; Cain, P. A. *J. Org. Chem*. **1994**, *59*, 4042. g) Metallinos, C.; Nerdinger, S.; Snieckus, V. *Org. Lett*. **1999**, *1*, 1183. h) Watanabe, H.; Gay, R. L.; Hauser, C. R. *J. Org. Chem*. **1968**, *33*, 900. i) Watanabe, H.; Schwarz, R. A.; Hauser, C. R.; Lewis, J.; Slocum, D. W. *Can. J. Chem*. **1969**, *47*, 1543. j) Christensen, H. *Synth. Commun*. **1975**, *5*, 65. k) Fuhrer, W.; Gschwend, H. W. *J. Org. Chem*. **1979**, *44*, 1133. l) Muchowski, J. M.; Venuti, M. C. *J. Org. Chem*. **1980**, *45*, 4798. m) Sibi, M. P.; Snieckus, V. *J. Org. Chem*. **1983**, *48*, 1935. n) Watanabe, M.; Date, M.; Kawanishi, K.; Hori, T.; Furukawa, S. *Chem. Pharm. Bull*. **1990**, *38*, 2637. o) Watanabe, M.; Date, M.; Kawanishi, K.; Tsukazaki, M.; Furukawa, S. *Chem.Pharm. Bull*. **1989**, *37*, 2564. p) Gray, M.; Chapell, B. J.; Felding, J.; Taylor, N. J.; Snieckus, V. *Synlett* **1998**, 422. q) Macklin, T. K.; Snieckus, V. *Org. Lett*. **2005**, *7*, 2519. r) Kaush, M.; Hoppe, D. *Synthesis* **2006**, *10*, 1575; s) Kaush, M.; Hoppe, D. *Synthesis* **2006**, 1578. t) Alessi, M., Ph.D. Thesis, Queen's University, Kingston, ON, Canada, 2008.

[225] Greene, T. W.; Wuts, P. G. M. *Protective Groups in Organic Synthesis*, 4th ed.; Wiley: Hoboken, 2007.

[226] Meyers, A. I.; Gabel, R.; Mihelich, E. D. *J. Org. Chem*. **1978**, *43*, 1372.

[227] Milburn, R. R.; Snieckus, V. *Angew. Chem. Int. Ed*. **2004**, *43*, 888.

[228] Quasdorf, K. W.; Antoft-Finch, A.; Liu, P.; Silberstein, A. L.; Komaromi, A.; Blackburn, T.; Ramgren, S. D.; Houk, K. M.; Snieckus, V.; Garg, N. K. *J. Am. Chem. Soc*. **2011**, *133*, 6352.

[229] Sengupta, S.; Leite, M.; Raslan, D. S.; Quesnelle, C.; Snieckus, V. *J. Org. Chem*. **1992**, *57*, 4066.

[230] Antoft-Finch, A., Blackburn, T.; Snieckus, V. *J. Am. Chem. Soc*. **2009**, *131*, 17750.

[231] a) Comins, D. L. *Synlett* **1992**, 615 (and references therein); b) Comins, D. L.; Brown, J. D. *J. Org. Chem*. **1989**, *54*, 3730.

[232] a) Spletstoser, J. T.; White, J. M.; Tunnori, A. R.; Georg, G. I. *J. Am. Chem. Soc*. **2007**, *129*, 3408. b) White, J. M.; Tunoori, A. R.; Georg, G. I. *J. Am. Chem. Soc*. **2000**, *122*,11995. c) Zhao, Y.; Snieckus, V. U.S. Patent US2010145060 A1, 2010. d) Morin, J., M.Sc. Thesis, Queen's University, ON, Canada, 2007.

[233] a) Demchuk, O. M.; Yoruk, B.; Blackburn, T.; Snieckus, V. *Synlett* **2006**, 2908. b) Alessi, M.; Snieckus, V. *Unpublished results.*

[234] Clayden, J. in *Chemistry of Organolithium Compounds*; Z. Rappoport, I. M., Ed.; John Wiley & Sons: Chichester, 2004; Vol. 1, p 495-646.

[235] a) Krizan, T. D.; Martin, J. C. *J. Am. Chem. Soc.* **1983**, *105*, 6155. b) Caron, S.; Hawkins, J. M. *J. Org. Chem.* **1998**, *63*, 2054.

[236] Alessi, M.; Larkin, A. L.; Ogilvie, K. A.; Green, L. A.; Lai, S.; Lopez, S.; Snieckus, V. *J. Org. Chem.* **2007**, *72*, 1588.

[237] a) Krasovskiy, A.; Krasovskaya, V.; Knochel, P. *Angew. Chem. Int. Ed.* **2006**, *45*, 2958. b) Lin, W.; Baron, O.; Knochel, P. *Org. Lett.* **2006**, *8*, 5673.

[238] a) Clososki, G.; Rohbogner, C.J.; Knochel, P. *Angew. Chem. Int. Ed.* **2007**, *46*, 7681. b) Rohbogner, C.J.; Clososki, G.; Knochel, P. *Angew. Chem. Int. Ed.* **2008**, *47*, 1503.

[239] a) Eaton, P. .E.; Lee, C.-H.; Xion, Y. *J. Am. Chem. Soc.* **1989**, *111*, 8016. b) Eaton, P. E.; Lukin, K. A. *J. Am. Chem. Soc.* **1993**, *115*, 11370. c) Ooi, T.; Uematsu, Y.; Maruoka, K. *J. Org. Chem.* **2003**, *68*, 4576.

[240] Naka, H.; Uchiyama, M.; Matsumoto, Y.; Wheatley, A. E. H.; McPartlin, M.; Morey, J. V.; Kondo, Y. *J. Am. Chem. Soc.* **2007**, *129*, 1921.

[241] Masanobu, U.; Hiroshi, N.; Yotaro, M.; Tomohiko, O. *J Am. Chem. Soc*. **2004**, *126*, 10526.

[242] Uchiyama, M.; Miyoshi, T.; Kajihara, Y.; Sakamoto, T.; Otani, Y.; Ohwada, T.; Kondo, Y. *J. Am. Chem. Soc.* **2002**, *124*, 8514.

[243] Beak, P.; Meyers, A. I. *Acc. Chem. Res*. **1985**, *19*, 356.

[244] Klumpp, G. *Recl. Trav. Chim. Pays-Bas* **1986**, 105, 1.

[245] a) Hommes, N.; Schleyer, P. von R. *Angew. Chem*. **1992**, *104*, 768. b) Hommes, N.; Schleyer, P. von R. *Angew. Chem. Int. Ed. Engl.* **1992**, *31*, 755. c) Hommes, N.; Schleyer, P. von R.

Tetrahedron **1994**, *50*, 5903.

[246] a) Shirley, D. A.; Johnson, J. R.; Hendrix, J. P. *J. Organomet. Chem.***1968**, 209. b) Gilman, H.; Soddy, T. *J. Org. Chem.* **1957**, *22*, 1716. c) Schlosser, M. *Angew. Chem. Int. Ed.* **1998**, *110*, 1496. d) Mongin, F.; Schlosser, M. *Tetrahedron Lett.* **1996**, *37*, 6551. e) Rausis, T.; Schlosser, M. *Eur. J. Org. Chem.* **2002**, 3351. f) Schlosser, M.; Katsoulos, G.; Takagishi, S. *Synlett* **1990**, 747. g) Schlosser, M. *Angew. Chem. Int. Ed.* **2005**, *44*, 376.

[247] Hay, D. R.; Song, Z.; Smith, S. G.; Beak, P. *J. Am. Chem. Soc*. **1988**, *110*, 8145.

[248] Anderson, D. R.; Faibish, N. C.; Beak, P. *J. Am. Chem. Soc*. **1999**, *121*, 7553.

[249] Stratkis, M. *J. Org. Chem*. **1997**, *62*, 3024.

[250] Rennels, R. A.; Maliakal, A. J.; Collum, D. B. *J. Am. Chem. Soc*. **1998**, *120*, 421.

[251] Chadwick, S. T.; Rennels, R. A.; Rutherford, J. L.; Collum. D. B. *J. Am. Chem. Soc*. **2000**, *122*, 8640.

[252] Riggs, J. C.; Singh, K. J.; Yun, M.; Collum, D. B. *J. Am. Chem. Soc*. **2008**, *130*, 13709.

[253] Kanwal J. Singh, Alexander C. Hoepker, and David B. Collum *J. Am. Chem. Soc*. **2008**, *130*, 18008.

[254] Bauer, W.; von Ragué Schleyer, P. *J. Am. Chem. Soc.* **1989**, *111*, 7191.

[255] McGarrity, J. F.; Ogle, C. A. *J. Am. Chem. Soc.* **1985**, *107*, 1805; McGarrity, J. F.; Ogle, C. A.; Brich, Z.; Loosli, H. R. *J. Am. Chem. Soc.* **1985**, *107*, 1810.

[256] For evidence of the involvement of agostic interactions in lithiation reactions, see a) Saa, J. M.; Martorell, G.; Frontera, A. *J. Org. Chem*. **1996**, *61*, 5194. b) Suner, G. A.; Deya, P. M.; Saa, J. M. *J. Am. Chem. Soc*. **1990**, *112*, 1467. c) Saa, J. M.; Deya, P. M.; Suner, G. A.; Frontera, A. *J. Am. Chem. Soc*. **1992**, *114*, 9093. d) Saa, J. M.; Morey, J.; Frontera, A.; Deya, P. M. *J. Am. Chem. Soc*. **1995**, *117*, 1105.

[257] Saa, J. M.; Martorell, G.; Frontera, A. *J. Org. Chem.* **1996**, *61*, 5194.

[258] Beak, P.; Kerrick, S. T.; Gallagher, D. J. *J. Am. Chem. Soc.* **1993**, *115*, 10628.

[259] Langer, A. W., Jr. *Trans. New York Acad. Sci*. **1965**, *27*, 741.

[260] Slocum, D. W.; Book, G.; Jennings, C. A. *Tetrahedron Lett*. **1970**, 3443.

[261] Slocum, D. W.; Moon, R.; Thompson, J.; Coffey, D. S.; Li, J. D.; Slocum, M. G.; Siegel, A.; Gayton-Garcia, R. *Tetrahedron Lett.* **1994**, *35*, 385.

[262] Slocum, D. W.; Coffey, D. S.; Siegel, A.; Grimes, P. *Tetrahedron Lett.* **1994**, *35*, 389.

[263] Slocum, D. W.; Thompson, J.; Friesen, C. *Tetrahedron Lett.* **1995**, *36*, 8171.

[264] Slocum, D. W.; Hayes, G.; Kline, N. *Tetrahedron Lett.* **1995**, *36*, 8175.

[265] Slocum, D. W.; Dumbris, S.; Brown, S.; Jackson, G.; LaMastus, R.; Mullins, E.; Ray, J.; Shelton, P.; Walstrom, A.; Micah Wilcox, J.; Holman, R. W. *Tetrahedron* **2003**, *59*, 8275.

[266] Slocum, D. W.; Carroll, A.; Dietzel, P.; Eilerman, S.; Culver, J. P.; McClure, B.; Brown, S.; Holman, R. W. *Tetrahedron Lett.* **2006**, *47*, 865.

[267] a) Maggi, R.; Schlosser, M. *Tetrahedron Lett.* **1999**, *40*, 8797. b) Napolitano, E.; Fiaschi, R. *Tetrahedron Lett*. **2000**, *41*, 4663.

[268] a) Anctil, E. J.-G.; Snieckus, V. *J Organomet. Chem.* **2002**, *653*, 150. b) Anctil, E. J.-G.; Snieckus, V. in *Metal-Catalyzed Cross-Coupling Reactions (2nd Ed.)*, Diederich, F., De Meijere, A., Eds.; Wiley-VCH: Weinheim, Germany, 2004, pp. 761-813.

[269] a) Humphrey, G. R.; Kuethe, J. T. *Chemical Reviews* **2006**, *106*, 2875. b) Gribble, G. W. *J. Chem. Soc. Perkin Trans*. *1*, **2000**, 1045. c) Taber, D. F.; Pavan, T. K. *Tetrahedron* **2011**, 7195. d) Barluenga, J.; Valdes, C. in *Modern Heterocyclic Chemistry*, Alvarez-Builla, J.; Vaquero, J. J.; Barluenga, J. Eds.Wiley-VCH: Weinheim, 2011; Vol. 1, pp. 377-533.

[270] Robinson, B. in *The Fischer Indole Synthesis*, Wiley-Interscience: New York, 1982.

[271] a) Gassman, P.G. *J. Am. Chem. Soc*. **1974**, *96*, 5495. b) Li, J.; Cook, J. M. in *Name Reactions in Heterocyclic Chemistry*, Li, J. J., Corey, E. J. Eds.; Wiley: Hoboken, 2005; pp. 128-131.

[272] Bartoli, G.; Palmieri, G.; Bosco, M.; Dalpozzo, R. *Tetrahedron Lett*. **1989**, *30*, 2129.

[273] Li, J.; Cook, J. M. in *Name Reactions in Heterocyclic Chemistry*, Li, J. J., Corey, E. J. Eds.; Wiley: Hoboken, 2005; pp. 104-106.

[274] Li, J.; Cook, J. M. in *Name Reactions in Heterocyclic Chemistry*, Li, J. J., Corey, E. J. Eds.; Wiley: Hoboken, 2005; pp. 154-158.

[275] Madelung, W. *Ber*. **1912**, *45*, 1128.

[276] Nenitzescu, C. D. *Bull. Soc. Chim. Romania* **1929**, *11*, 37.

[277] a) Joule, J. A.; Mills, K. *Heterocyclic Chemistry*, 4th ed.; Blackwell Science: Cambridge, 2000; pp. 353-366. b) Joule, J. A. in *Science of Synthesis:Product Class 13 (Knowledge Updates)*, Georg Thieme Verlag: Stuttgart, 2010; pp. 1-486.

[278] Li, Jin. in *Name Reactions for Functional Group Transformations*, Lie, J. J., Corey, E. J. Eds. Wiley: Location, 2007; pp. 630-634.

[279] Zografos, A. L. in *Name Reactions in Heterocyclic Chemistry II*, Li, J. J. Ed. Wiley: Location, 2011; pp. 197-206.

[280] Houlihan, W. J.; Parrino, V. A.; Uike, Y. *J. Org. Chem*. **1981**, *46*, 4511.

[281] Schulenberg, J. W. *J. Am. Chem. Soc*. **1968**, *90*, 7008.

[282] Inman, M.; Carbone, A.; Moody, C. J. *J. Org. Chem*. **2012**, *77*, 1217.

[283] Wagaw, S.; Yang, B. H.; Buchwald, S. L. *J. Am. Chem. Soc*. **1999**, *121*, 10251.

[284] McAusland, D.; Seo, S.; Pintori, D. G.; Finlayson, J.; Greaney, M. F. *Org. Lett*. **2011**, *13*, 3667.

[285] Schammel, A. W.; Chiou, G.; Garg, N. K. *Org. Lett*. **2012**, *14*, 4556.

[286] Zu, L.; Boal, B. W.; Garg, N. K. *J. Am. Chem. Soc*. **2011**, *133*, 8877.

[287] Schammel, A. W.; Chiou, G.; Garg, N. K. *J. Org. Chem*. **2012**, *77*, 725.

[288] Adams, G. L.; Carroll, P. J.; Smith, A. B. III. *J. Am. Chem. Soc*. **2012**, *134*, 4037.

[289] Grant, S. W.; Gallagher, T. F.; Bobko, M. A.; Duquenne, C.; Axten, J. M. *Tetrahedron Lett*. **2011**, *52*, 3376.

[290] Boros, E. E.; Kaldor, I.; Turnbull, P. S. *J. Heterocycl. Chem*. **2011**, *48*, 733.

[291] a) Cacchi, S.; Fabrizi, G. *Chem. Rev*. **2005**, *105*, 2873; b) Cacchi, S.; Fabrizi, G. *Chem. Rev*. **2011**, *111*, pp. PR215-PR283. c) Cacchi, S.; Fabrizi, G.; Goggiamani, A. in *Organic Reactions*, Wiley: Hoboken, 2012; Vol. 76, pp. 281-534. d) Platon, M.; Amardeil, R.; Djakovitch, L.; Hierso, J.-C. *Chem. Soc. Rev*. **2012**, 41, 3929.

[292] Platon, M.; Amardeil, R.; Djakovitch, L.; Hierso, J-C. *Chem. Soc. Rev*. **2012**, *41*, 3929.

[293] Vicente, R. *Org. Biomol. Chem*. **2011**, *9*, 6469.

[294] Larock, R. C.; Yum, E. K. *J. Am. Chem. Soc*. **1991**, *113*, 6689.

[295] Shimamura, H.; Breazzano, S. P.; Garfunkle, J.; Kimball, F. S.; Trzupek, J. D.; Boger, D. L. *J. Am. Chem. Soc*. **2010**, *132*, 7776.

[296] Peng, J.; Liu, L.; Hu, Z.; Huang, J.; Zhu, Q. *Chem. Commun*. **2012**, *48*, 3772.

[297] Hu, Z.; Liang, D.; Zhao, J.; Huang, J.; Zhu, Q. *Chem. Commun*. **2012**, *48*, 7371.

[298] Nanjo, T.; Tsukano, C.; Takemoto, Y. *Org. Lett*. **2012**, *14*, 4270.

[299] Wang, Y.; Wang, H.; Peng, J.; Zhu, Q. *Org. Lett*. **2011**, *13*, 4604; Tobisu, M.; Imoto, S.; Ito, S.; Chatani, N. *J. Org. Chem*. **2010**, *75*, 4835.

[300] Würtz, W.; Rakshit, S.; Neumann, J. J.; Dröge, T.; Glorius, F. *Angew. Chem. Int. Ed*. **2008**, *47*, 7230.

[301] Wei, Y.; Deb, I.; Yoshikai, N. *J. Am. Chem. Soc.* **2012**, *134*, 9098.

[302] Tan, Y.; Hartwig, J. F. *J. Am. Chem. Soc*. **2010**, *132*, 3676.

[303] Ackermann, L.; Lygin, A.V. *Org. Lett.* **2012**, *14*, 764.

[304] a) Ackermann, L.; Lygin, A. V.; Hofmann, N. *Angew. Chem.Int. Ed*. **2011**, *50*, 6379. (b) Ackermann, L.; Lygin, A. V.; Hofmann, N. *Org. Lett*. **2011**, *13*, 3278. (c) Ackermann, L.;Wang, L.; Lygin, A.V. *Chem. Sci*. **2012**, *2*, 177.

[305] Huestis, M. P.; Chan, L.; Stuart, D. R.; Fagnou, K. *Angew. Chem. Int. Ed*. **2011**, *50*, 1338.

[306] a) Stuart, D. R.; Bertrand-Laperle, M.; Burgess, K. M. N.; Fagnou, K. *J. Am. Chem. Soc*. **2008**, *130*, 16474. b) Stuart, D. R.; Alsabeh, P.; Kuhn, M.; Fagnou, K. *J. Am. Chem. Soc*. **2010**, *132*, 18326.

[307] Stuart, D. R.; Bertrand-Laperle, M.; Burgess, K. M. N.; Fagnou, K. *J. Am. Chem. Soc*. **2008**, *130*, 16474.

[308] Pelkey, E. *Top. Heterocycl. Chem*. **2010**, *26*, 141.

[309] a) Joucla, L.; Djakovitch, l. *Adv. Synth. Catal.* **2009**, *351*, 673. b) Bellina, F.; Rossi, B. *Tetrahedron* **2009**, *65*, 10269.

[310] Sundberg, R. J. *Top. Heterocycl. Chem*. **2010**, *26*, 47.

[311] Ferry, A.; Billard, T.; Bacque, E.; Langlois, B. R. *J. Fluor. Chem*. **2012**, *134*, 160.

[312] Klare, H. F. T.; Oestreich, M.; Ito, J.-I.; Nishiyama, H.; Ohki, Y.; Tatsumi, K. *J. Am. Chem. Soc.* **2011**, *133*, 3312.

[313] Itahara, T. *J. Chem. Soc. Chem. Commun*. **1981**, 254.

[314] Stuart, D. R., Fagnou, K. *Science* **2007**, *316*, 1172.

[315] Stuart, D. R.; Villemure, E.; Fagnou, K. *J. Am. Chem. Soc*. **2007**, *129*, 12072.

[316] Liégault, B.; Lapointe, D.; Caron, L.; Vlassova, A.; Fagnou, K. *J. Org. Chem*. **2009**, *74*, 1826.

[317] Potavathri, S.; Dumas, A. S.; Dwight, T. A.; Naumiec, G. R.; Hammann, J. M.; DeBoef, B. *Tetrahedron Lett*. **2008**, *49*, 4050.

[318] Dwight, T. A.; Rue, N. R.; Charyk, D.; Josselyn, R.; DeBoef, B. *Org. Lett*. **2007**, *9*, 3137.

[319] Potavathri, S.; Pereira, K. C.; Gorelsky, S. I.; Pike, A.; LeBris, A. P.; DeBoef, B. *J. Am. Chem. Soc*. **2010**, *132*, 14676.

[320] Akita, Y.; Inoue, A.; Yamamoto, K.; Ohta, A.; Kurihara, T.; Shimizu, M. *Heterocycles* **1985**, *23*, 2327.

[321] Akita, Y.; Itagaki, S.; Takizawa, S. Ohta, A. *Chem. Pharm. Bull*. **1989,** *37*, 1477.

[322] Lane, B. S.; Sames, D. *Org. Lett.* **2004**, *6*, 2897.

[323] Touré, B. B.; Lane, B. S.; Sames, D. *Org. Lett*. **2006**, *8*, 1979.

[324] Nandurkar, N. S.; Bhanushali, M. J.; Bhor, M. D.; Bhanage, B. M. *Tetrahedron Lett*. **2008**, *49*, 1045.

[325] Nadres, E. T.; Lazareva, A.; Daugulis, O. *J. Org. Chem*. **2011**, *76*, 471.

[326] Shibahara, F.; Yamaguchi, E.; Murai, T. *Chem. Commun*. **2010**, 2471.

[327] Yanagisawa, S.; Itami, K. *Tetrahedron* **2011**, *67*, 4425.

[328] Zhang, Z.; Hu, Z.; Yu, Z.; Lei, P.; Chi, H.; Wang, Y.; He, R. *Tetrahedron Lett*. **2007**, *48*, 2415.

[329] Bellina, F.; Calandri, C.; Cauteruccio, S.; Rossi, R. *Eur. J. Org. Chem*. **2007**, *13*, 2147.

[330] Joucla, L.; Batail, N.; Djakovitch, L. *Adv. Synth. Cat*. **2010**, *352*, 2929.

[331] Deprez, N. R.; Kalyani, D.; Krause, A.; Sanford, M. S. *J. Am. Chem. Soc*. **2006**, *128*, 4972.

[332] Ackermann, L.; Acqua, M. D.; Fenner, S.; Vicente, R.; Sandmann, R. *Org. Lett.* **2011**, 13, 2358.

[333] Wagner, A. M.; Sanford, M. S. *Org. Lett*. **2011**, *13*, 288.

[334] Wen, J.; Zhang, R.-Y.; Chen, S.-Y.; Zhang, J.; Yu, X.-Q. *J. Org. Chem*. **2012**, *77*, 766.

[335] Phipps, R. J.; Grimster, N. P.; Gaunt, M. J. *J. Am. Chem. Soc*. **2008**, *130*, 8172.

[336] Benoit, L.; Petrov, I.; Gorelsky, S. I.; Fagnou, K. *J. Org. Chem*. **2010**, *75*, 2047.

[337] Gorelsky, S. I.; Lapointe, D.; Fagnou, K. *J. Org. Chem.*, **2012**, *77*, 658.

[338]Wang, X.; Lane, B. S.; Sames, D. *J. Am. Chem. Soc*. **2005**, *127*, 4996.

[339] a) Yanagisawa S.; Sudo, T.; Noyori, R. ; Itami, K. *J. Am. Chem. Soc.* **2006**, *128*, 11748. b) Yanagisawa S.; Sudo, T.; Noyori, R. ; Itami, K. *Tetrahedron* **2008**, *64*, 6073.

[340] Fanton, G.; Coles, N. M.; Cowley, A. R.; Flemming, J. P.; Brown, J. M. *Heterocycles* **2010**, *80*, 895.

[341] Wu, Y-J. *Top. Heterocycl. Chem*. **2010**, *26*, 1.

[342] Gilman, H.; Kirby, R. H. *J. Org. Chem*. **1936**, *1*, 146.

[343] Shirley, D. A.; Roussel, P. A. *J. Am. Chem. Soc*. **1953**, *75*, 375.

[344] a) Sundberg, R. J.; Russell, H. F. *J. Org. Chem*. **1973**, *38*, 3324; b) Sundberg, R. J.; Parton, R. L. *J. Org. Chem*. **1976**, *41*, 163.

[345] Hasan, I.; Marinelli, E. R.; Lin, L.; Fowler, F. W.; Levy, A. B. *J. Org. Chem*. **1981**, *46*, 157.

[346] a) Katritzky, A.; Akutagawa, K. *Tetrahedron Lett*. **1985**, *26*, 5935; b) Katritzky, A.; Akutagawa, K. *J. Am. Chem. Soc*. **1986**, *108*, 6808

[347] Saulnier, M. G.; Gribble, G. W. *J. Org. Chem*. **1982**, *47*, 757

[348] Moyer, M. P.; Shiurba, J. F.; Rapoport, H. *J. Org. Chem*. **1986**, *51*, 5106

[349] Iwao, M. *Heterocycles* **1993**, *36*, 29

[350] Griffen, E. J.; Roe, D. G.; Snieckus, V. *J. Org. Chem*. **1995**, *60*, 1484

[351] Hartung, C. G.; Fecher, A.; Chapell, B.; Snieckus, V. *Org. Lett*. **2003**, *5*, 1899

[352] Fukuda, T.; Mine, Y.; Iwao, M. *Tetrahedron* **2001**, *57*, 975

[353] Gharpure, M.; Stoller, A.; Bellamy, F.; Firnau, G.; Snieckus, V. *Synthesis* **1991**, 1079

[354] Chapell, B. J., Ph.D. Thesis, Queen's University, Kingston ON, Canada, **2001**.

[355] Gray, M.; Chapell, B. J.; Felding, J.; Taylor, N. J.; Snieckus, V. *Synlett*. **1998**, 422.

[356] We thank Dr. Timothy Stammers for 10 g of **3.123**.

[357] Tischler, A. N.; Lanza, T. J. *Tetrahedron Lett*. **1986**, *27*, 1653.

[358] Manfred, S.; Ginanneschi, A.; Leroux, F. *Eur. J. Org. Chem*. **2006**, *13*, 2956.

[359] Schneider, C.; David, E.; Toutov, A. A.; Snieckus, V. *Angew. Chem. Int. Ed.* **2012**, *51*, 2722.

[360] Akhvlediani, R. N.; Frolova, E. V.; Abesadze, I. G.; Khachidze, M. M.; Kiriakidi, A. V.; Dzhinikashvili, I. V.; Partsvaniya, D. D. *Sakartvelos Mecnierebata Akademiis Macne, Kimiis Seria* **2003**, *29*, 234. b) Frolova, E. P.; Akhvlediani, R. N.; Suvorov, N. N. *Khimiya Geterotsiklicheskikh Soedinenii* **1982**, *10*, 1358. c) Elizbarashvili, E. N.; Razmadze, T. O.; Samsoniya, Sh. A. *Azerbaidzhabskii Khimicheskii Zhurnal* **2006**, *4*, 71. d) Friesen, M.; O' Neill, I. K.; Malaveille, C.; Garren, L.; Hautefeuille, A.; Cabral, J. R. P.; Galendo, D.; Lasne, C.; Sala, M.; Chouroulinkov, I.; Mohr, U.; Turusov, V.; Day, N. E.; Bartsch, H. *Mutation Res*. **1985**, *150*, 77.